ulm university universität ulm

Tracking the elusive function of the regulatory RNA SolB in solventogenesis and its relation to the RNA-binding protein Hfq in *Clostridium acetobutylicum*

Submitted for the fulfillment of the requirements for the

doctoral degree Dr. rer. nat.

at the Faculty of Natural Sciences, Ulm University

Presented by **Elena Riester**

from Augsburg, Germany

Ulm, March 2017

The present study was prepared at the Institute of Microbiology and Biotechnology, Ulm University under the direction of Prof. Dr. Peter Dürre.

Faculty Dean: Prof. Dr. Peter Dürre

First Reviewer: Prof. Dr. Peter Dürre

Second Reviewer: Prof. Dr. Bernhard Eikmanns

Date of the doctoral examination: June 9th, 2017

Content

Abbreviations

A	
A	ampere, adenine, alanine
aa	amino acid
APS	ammonium persulfate
ATCC	American Type Culture Collection (Manassas VA, USA)
ATP	adenosine triphosphate
B	
B	base(s)
BLAST	Basic Local Alignment Search Tool (US National Library of Medicine, Bethesda MD, USA)
bps	base pairs
BSA	bovine serum albumine
C	
C	cytosine
C.	*Clostridum*
©	copyright
°C	degree Celsius
CA	California
cDNA	copy DNA
CG medium	clostridial growth medium
Co.	Compagnie
CoA	coenzyme A
COG	Clusters of Orthologous Groups
Corp.	Corporation
Ct	threshold cycle
D	
Δ	gene deletion
d	day
D	aspartic acid
Da	dalton
DAD	diode array detector
dcDNA	double-stranded cDNA
ddH_2O	double distilled H_2O
DEPC	diethylpyrocarbonate
DNA	deoxyribonucleic acid
DMF	dimethylformamide
DMSO	dimethyl sulfoxide
dNTP	deoxy nucleoside triphosphate
Dr.	Doctor
DSMZ	Deutsche Sammlung von Mikroorganismen und Zellkulturen (Braunschweig, Germany)
DTT	dithiothreitol
E	
E	glutamic acid
E.	*Escherichia*
ECL	enhanced chemoluminescence
ed.	edition
Eds.	editor
EDTA	ethylenediaminetetraacetic acid
EMSA	electrophoretic mobility shift assay
e.g.	exempli gratia, for example
et al.	et alii, and others
EtBr	ethidium bromide
EtOH	ethanol
F	
F	farad, phenylalanine
F.	*Francisella*
FID	flame ionization detector
G	
g	gram, force, guanine
G	giga (10^9), glycine
gDNA	genomic DNA
GC	gas chromatography
GmbH	Gesellschaft mit beschränkter Haftung
H	
H	hour(s), histidine
Hfq-IP	Hfq co-immunoprecipitation

his	polyhistidine
HPLC	high-performance liquid chromatography
HRP	horseradish peroxidase
I	
I	isoleucine
IEP	Intron-encoded protein
Inc.	Incorporation
int::	integration
IL	Illinois
IMG/ER	Integrated Microbial Genomes/Expert Review
IP	incorporation of PlugOligo
IPTG	isopropyl β-D-1-thiogalactopyranoside
J	
J	Joule
K	
K	kilo (10^3), lysine
kbps	kilo base pairs
KEGG	Kyoto Encyclopedia of Genes and Genomes
KG	Kommanditgesellschaft
L	
L	liter, leucine
LB	Luria Bertani
Lsm	like Sm
Ltd.	private limited company
M	
m	meter, milli (10^{-3})
M	molar, mega (10^6), methionine
µ	micro (10^{-6})
MA	Massachusetts
MD	Maryland
MCS	multiple cloning site
MES	2-(N-morpholino)-ethanesulfonic acid
MOPS	3-(N-morpholino) propanesulfonic acid
N	
n	nano (10^{-9})
N	asparagine
NCBI	National Center for Biotechnology Information (US National Library of Medicine, Bethesda MD, USA)
NTP	nucleoside triphosphate
O	
OD_{600}	optical density at 600 nm
ori	origin of replication
P	
p	pico (10^{-12})
P	phosphate, proline, promoter
Pa	Pascal
PAGE	polyacrylamide gel electrophoresis
PBS	phosphate-buffered saline
PCR	polymerase chain reaction
pH	negative logarithm to base 10 of the activity of the hydrogen ion
Prof.	Professor
PTS	phosphotransferase system
Q	
qRT-PCR	quantitative real-time PCR
R	
r	ribosomal
R	arginine
®	registered trade mark
RBS	ribosomal binding site
RID	refraction index detector
RNA	ribonucleic acid
rRNA	ribosomal ribonucleic acid
rpm	round(s) per min
RT-PCR	reverse transcriptase PCR
S	
s	second(s)
S	serine

S.	*Shigella*
SDS	sodium dodecyl sulphate
SEM	scanning electron micrograph/microscopy
SOB	super optimal broth
sRNA	small RNA
T	
T	thymine, threonine
TAE	tris-acetic acid-EDTA
TB	terrific broth
TBE	tris-borate-EDTA
TEM	transmission elctron micrograph/microscopy
TEMED	tetramethylethylenediamine
™	unregistered trade mark
Tris	tris(hydroxymethyl) aminomethane
tRNA	transfer ribonucleic acid
U	
U	unit(s), uracil
UK	United Kingdom
USA	United States of America
UV	ultra violet
V	
V	volt, valine
VA	Virginia
vs.	versus
v/v	volume per volume
W	
W	watt, tryptophane
w/v	weight per volume
X	
x g	multiples of acceleration of standard gravity (9.81 m/s)
X-Gal	5-bromo-4-chloro-3indolyl-β-D-galactopyranoside
Y	
Y	tyrosine
Ω	
Ω	ohm

1 Introduction

1.1 AB fermentation with clostridial strains

The genus *Clostridium* is one of the largest prokaryotic genera, including more than 130 species. In general, the genus is Gram-positive and endospore-forming. Spores are dormant, hardy structures formed to survive in a harmful environment. As spore-forming cells resemble spindles in the microscope, the genus was named *Clostridium* originating from the Greek word *klōstēr* (spindle). When the non-reproductive spores are placed in a habitat that supports growth, the spores will germinate to a vegetative cell. The vegetative cells of the genus *Clostridium* are rod-shaped and grow under obligate anaerobic conditions. The members of this genus can be found in a number of different environments (Finne and Matches, 1974; Matches and Liston, 1974; Smith, 1975; Molongoski and Klug, 1976) and only a handful of pathogenic species were found. Three important representatives of pathogenic clostridia are *Clostridium perfringens, Clostridium botulinum,* and *Clostridium difficile. C. perfringens* provokes food poisoning, *C. botulinum* produces the botulinum toxin, and *C. difficile* causes diarrhoea (Dürre, 2007a). In contrast to the pathogenic strains, species as *Clostridium sporogenes* are applied in cancer therapy (Minton, 2003; Heap et al., 2014). Furthermore, several clostridial strains are used for biotechnological production of chemicals. The acetogenic bacteria, *Clostridium ljungdahlii* and *Clostridium autoethanogenum,* were applied to produce low-carbon fuels by fixation of CO or CO_2 via the Wood-Ljungdahl-pathway (Ljungdahl, 1986; Köpke et al., 2010, 2011; Liew et al., 2017). Saccharolytic clostridia are capable to manufacture organic acids and solvents. In the biotechnological process, saccharolytic clostridia ferment different sugars, mainly for acetone and butanol production (AB fermentation). The fermentation with saccharolytic clostridia has a long history. In 1912, saccharolytic clostridia were used to produce butanol for the production of synthetic rubber as replacement for natural rubber (Jones and Woods, 1986). During the First World War, high amounts of acetone were produced by clostridal fermentation for the fabrication of gun powder (Killeffer, 1927). Since butanol was used for the production of fast-drying lacquers in the rapidly growing automobile industry, the demand for butanol increased further (Gabriel, 1928). For this purpose, additional fermentation plants were built in the US, Canada, Japan, Puerto Rico, the Soviet Union, and South Africa (Ross, 1961; Spivey, 1978; Zverlov et al., 2006; Ndaba et al., 2015). In the 1950s, the AB fermentation

flourished further on and two thirds of the worldwide butanol demand were supplied by biotechnological fermentation processes (Rose, 1961). With an increasing price for the molasses used as fermentation substrate, the fermentation process became unprofitable compared to solvent production from cheap crude oil (Jones and Woods, 1986; Dürre, 2008).

During the last years, the interest in biotechnological production of solvents and fuels increased as the oil price raised and the depletion of fossil resources progressed (Lee et al., 2008; Kumar and Gayen, 2011). Moreover, the world's primary energy supply increased by almost 150 % from 1971 to 2014 and was provided mainly by fossil fuels (International Energy Agency, 2016). This leads to a further problem as combustion of coal, oil, and gas are responsible for 99 % of the CO_2 emission (International Energy Agency, 2016). CO_2 is a greenhouse gas and one of the main reasons for global warming and climate changes. Biofuels are a renewable energy source and can counterbalance this dangerous CO_2 output (Dürre, 2007b). During combustion of biofuels only those CO_2 amounts are released, which were fixed in the renewable biomass before, decreasing the CO_2 emission compared to fossil fuels (Rice et al., 1991; Dürre, 2007b; Elfasakhany and Mahrous, 2016). To reduce CO_2, the European Union passed the directive 2009/28/EC, which states that in 2020, 10 % of the energy used for transportation has to be generated by renewable sources. Thus, the fermentation of clostridial strains regained interest as butanol is an attractive biofuel, which has some advantages compared to bioethanol. The energy content of butanol is higher and it can be used as blend in fossil fuels as well as in pure form in common petrol engines, because of the lower corrosive character (Dürre, 2007b). Furthermore, butanol is safer due to its lower vapour pressure and easier to handle as it is less hygroscopic than ethanol (Dürre, 2007b). Also industries, such as Green Biologics, recognized the potential of butanol produced by saccharolytic clostridia as the global market for butanol is worth $6 billion (Sutcliffe, 2017). Green Biologics already produces butanol and acetone with genetically improved organisms of *C. acetobutylicum, Clostridium beijerinckii,* and *Clostridium saccharobutylicum*.

In order to increase the economical attractiveness of the commercial production of biofuels with saccharolytic clostridia, the regulation of the solventogenesis has to be entirely elucidated. One of the most prominent representatives for saccharolytic clostrida is *Clostridium acetobutylicum* (Figure 1.1) as it naturally produces the solvents butanol, acetone, and ethanol in a ratio of 6:3:1 (Keis et al., 1995, 2001).

C. acetobutylicum was first described in 1915 by Chaim Weitzmann (Gabriel, 1928) and was completely sequenced in 2001 (Nölling et al., 2001). During the last century, *C. acetobutylicum* was recognized as model organism for solventogenic clostridia (Paredes et al., 2005; Thormann et al., 2002). The complete genome of *C. acetobutylicum* comprises two replicons with an overall GC-content of 30.9 %, a chromosome with 3.94 Mbps and a circular megaplasmid with 192 kbps (Nölling et al., 2001). The megaplasmid was termed pSOL1 as it contains most of the genes necessary for solvent production (Cornillot et al., 1997). *C. acetobutylicum* has a biphasic fermentation pathway (Figure 1.2), which is divided into an acidogenic and solventogenic fermentation. During exponential growth, *C. acetobutylicum* produces the acids acetate and butyrate (Jones and Woods, 1986). The production of acids decreases the pH and initializes the endosporulation process during stationary growth phase. To gain time for sporulation *C. acetobutylicum* metabolizes the acids from the medium into the solvents acetone and butanol, characterizing the solventogenic phase (Grupe and Gottschalk, 1992). Moreover, the essential proton-gradient for energy conservation can be maintained (Jones and Woods, 1986; Dürre, 2005).

The regulation of solventogenesis is complex and is not yet completely understood, although several studies were performed concerning the regulation of solventogenesis in *C. acetobutylicum* (Girbal and Soucaille, 1998; Dürre et al., 2002; Sillers et al., 2009; Grimmler et al., 2011; Lütke-Eversloh and Bahl, 2011; Thorn et al., 2013). Several transcription factors are involved in the regulatory network of solvent production. Spo0A (CA_P2071) was identified as master regulator of solvent production. The phosphorylated form of Spo0A (Spo0A-P) activates the transcription of the *sol* operon (CA_P0162-0164, comprising the *adhE, ctfA,* and *ctfB* genes) and of the *adc* operon (CA_P0165) (Harris et al., 2002). The *sol* operon is essential for AB fermentation and Adc catalysis the last step of the acetone formation (Figure 1.2) (Fischer et al., 1993; Gerischer and Dürre, 1990). The REX regulator (CA_C2713) inhibits the transcription

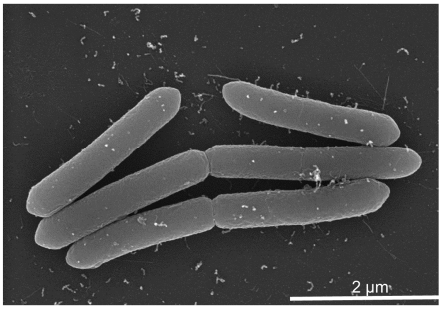

Figure 1.1: Scanning electron microscopy image of *C. acetobutylicum* cells growing in clostridial growth medium in stationary growth phase (scale bar representing 2 µm).

of *thlA* (CA_C2873), *bcs* operon (CA_C2709-2712, comprising the *crt*, *bcd*, *etfA*, *etfB*, and *hbd* gene), and *adhE2* (CA_P0035) in response to the NADH/NAD^+ level (Wietzke and Bahl, 2012; Zhang et al., 2014). Most of the mentioned genes catalyze essential reactions in the metabolic pathways of solvent production (Figure 1.2). Further transcription factors were identified as CodY (CA_C1786) and CA_P0037 in *C. acetobutylicum*. Both transcription factors bind to the 5' region of the *sol* operon (CA_P0162-0164) (Nguyen et al., 2016; Standfest, 2009). CA_P0037 can also interact with the 5' region of the *adc* gene (CA_P0165) and thereby, influences its transcription (Nguyen et al., 2016). Summarizing the findings, all the analyzed regulators of solventogenesis act on the transcriptional level in *C. acetobutylicum*. However, further studies suggest a significant role of posttranscriptional regulators in *C. acetobutylicum*, for example with small RNAs (sRNAs) (Venkataramanan et al., 2013, 2015).

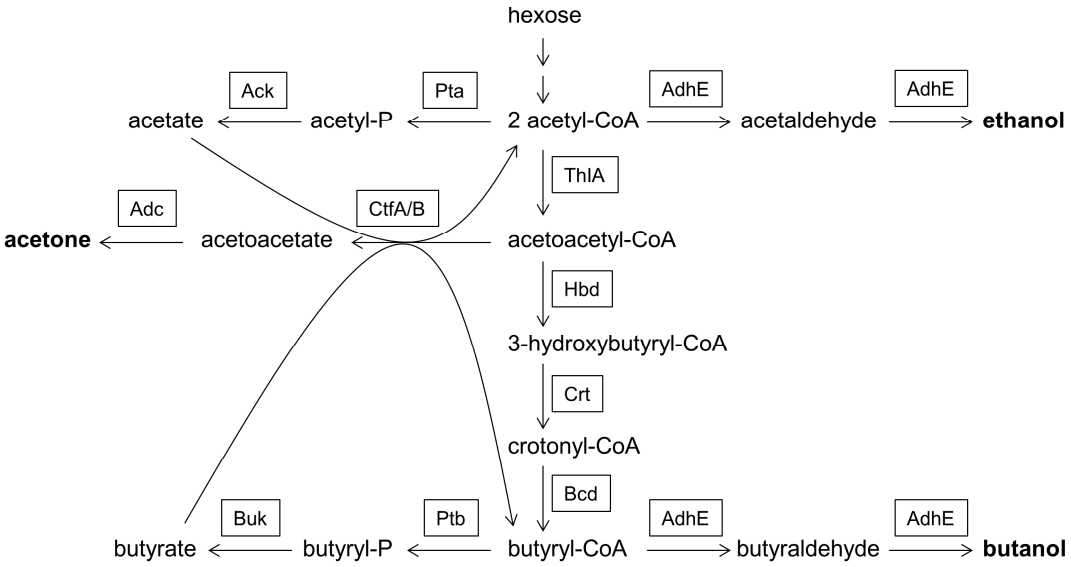

Figure 1.2: Simplified representation of the AB (acetone/butanol) fermentation pathway in *C. acetobutylicum*. During the exponential growth, the acids acetate and butyrate are produced. In the stationary growth phase, *C. acetobutylicum* takes up the acids from the medium and produces the solvents acetone, butanol, and ethanol. Ack, acetate kinase; Adc, acetoacetate decarboxylase; AdhE, alcohol/aldehyde dehydrogenase; Bcd, acyl-CoA dehydrogenase; Buk, butyrate kinase; CtfA/B, acetoacetyl-CoA:acetate/butyrate-CoA-transferase; Crt, crotonase; Hbd, 3-hydroxybutyryl-CoA dehydrogenase; ThlA, acetyl-CoA acetyltransferase; Pta, phosphotransacetylase.

1.2 The world of sRNAs

In recent years, small RNAs (sRNA) have been identified as one of the critical players in bacterial regulation. With the help of new sequence technologies and computational predictions, more and more sRNAs in different organisms have been identified (Sharma and Vogel, 2009). sRNAs have a length between 50 and 500 nt (Gottesman and Storz, 2011). They are mostly encoded in intergenic regions and are usually not used as a template for protein biosynthesis (Gottesman, 2004). Generally, sRNAs act as posttranscriptional regulators interacting with specific mRNA targets, modulating target stability and/or translation initiation (Waters and Storz, 2009). sRNAs can be divded into two groups: cis-acting sRNAs and trans-acting sRNAs. The two groups differ in the complementarity to their target mRNAs. Cis-acting sRNAs are encoded in antisense direction to their target genes and, thus, exhibit an entire complementary sequence to their target mRNA (Wagner et al., 2002). Respective regulation can have a positive (Opdyke et al., 2004; Tramonti et al., 2008; Papenfort and Vanderpool, 2015) or a negative effect (Kawano et al., 2007; Stork et al., 2007; Lu et al., 2014; Cao et al., 2016) for the gene product. In contrast, trans-acting sRNAs are only partly complementary to their target mRNA and the locus of these sRNAs is not in close proximity to its target gene (Delihas, 1995; Altuvia and Wagner, 2000). Several trans-encoded sRNAs are dependent on the RNA-binding protein Hfq (Valentin-Hansen et al., 2004). Bacterial cells use trans-encoded sRNAs for fine tuning of several pathways (Shimoni et al., 2007). So, deletion of trans-encoded sRNAs do rarely exhibit phenotypic effects (Tsui et al., 2010; Postic et al., 2010; Lee and Gottesman, 2016). Interaction of these sRNAs and mRNAs can result in activated translation (Majdalani et al., 1998; Hammer and Bassler, 2007; Prévost et al., 2007) or decreased protein synthesis, either by forced degradation of the complex or blocked ribosomal binding site (RBS) of the target mRNA (Sharma et al., 2007; Vecerek et al., 2007). sRNAs show a wide range of regulatory effects in different metabolic pathways, for example in replication and cell division (Bouché and Bouché, 1989; Balasubramanian et al., 2016), plasmid replication (Stougaard et al., 1981; Chai and Winans, 2005), transcription (Wassarman and Storz, 2000), RNA processing (Kazantsev and Pace, 2006), protein stability (Muto et al., 1998), stress adaptation (Altuvia et al., 1998; Stubben et al., 2014), virulence (Bardill and Hammer, 2012; Tree et al., 2014), or quorum sensing (Lenz et al., 2004). Furthermore, sRNAs often interfere not only with one target mRNA. For example, the sRNAs GcvB and RybB, interact with a number of

different targets in diverse pathways (Massé et al., 2005; Sharma et al., 2007). There are several modes of action postulated and documented. Most frequently, the interaction between the sRNA and the mRNA takes place at the RBS of the target mRNA. Binding of the sRNA at the RBS blocks the translation, while the formation of doublestranded RNA leads to degradation of the whole complex (Desnoyers et al., 2013). Nevertheless, sRNAs can be recycled after the reaction with a mRNA. In this case, the sRNA is not degraded and interaction with further targets is possible (Massé et al., 2003; Overgaard et al., 2009). Activation of translation by sRNAs is mainly achieved by changes in the secondary structure of the mRNAs (Liu and Camilli, 2010; Papenfort and Vanderpool, 2015). For this purpose, the binding of sRNAs at the mRNAs leads to a conformational change in the secondary structure of the mRNAs. If the RBS is initially blocked in a secondary structure, the conformational change induced by the sRNA generates access for the ribosome to the RBS and translation of the mRNA is activated (Beisel and Storz, 2010). Further interactions are described between sRNAs and proteins, but in comparison to sRNA-mRNA interactions, that occurs quite rarely (Babitzke and Romeo, 2007; Wassarman, 2007). Regulation by sRNA provides efficient mode of regulation, which is manifested by fast responses of the target gene to an external stimulus, and also by fast recovery after removal of the stimulus (Guillier et al., 2006). The comparison between transcriptional regulation by proteins and post-transcriptional control by sRNAs showed a faster response for sRNA regulation (Shimoni et al., 2007). Therefore, sRNA were also used as genetic tools for metabolic engineering (Na et al., 2013). This was already successfully performed with a re-targeted sRNA of *E. coli* in *C. acetobutylicum* (Cho and Lee, 2017; Lahiry et al., 2017). The world of sRNAs in Gram-negative bacteria is well elucidated, in contrast, research concerning sRNAs of Gram-positives as for *C. acetobutylicum* is just at the beginning (Vanderpool et al., 2011; Brantl and Brückner, 2014). One well characterized example is a sRNA in *Clostridium saccharobutylicum* that is involved in nitrogen metabolism (Fierro-Monti et al., 1992). Further studies were performed in *C. acetobutylicum* by Chen et al. (2011). They predicted 113 sRNAs in silico and proved the existence of 20 sRNAs by qRT-PCR or by Northern blot experiments. One of these detected sRNAs (sCAC610) seems to be involved in response to the antibiotic clindamycin (Chen et al., 2011). Moreover, the expression pattern of sRNAs was investigated under solvent stress in *C. acetobutylicum* (Venkataramanan et al., 2013). One further identified sRNA of *C. acetobutylicum* is named SolB. This sRNA is involved

in solvent production of *C. acetobutylicum* as it supresses solvent formation in a *C. acetobutylicum solB* overexpression strain (Schiel et al., 2010). SolB is located on the megaplasmid pSOL1 upstream of the *sol* operon (CA_P0163-0165) (Figure 1.3) and was identified as a trans-encoded sRNA. Deletion of *solB* via the ClosTron™ system (Heap et al., 2007) and allelic exchange system revealed no phenotypic changes in *C. acetobutylicum* strains (Schiel et al., 2010; Zimmermann, 2013). In silico analysis revealed putative binding sites for SolB in the 5' untranslated region of the mRNA transcripts of *adhE2* (CA_P0035) and *spo0A* (CA_C2071) genes (Zimmermann, 2013). However, binding motif analysis could neither prove the binding motif nor the direct binding between SolB and the mentioned transcripts (Zimmermann, 2013).

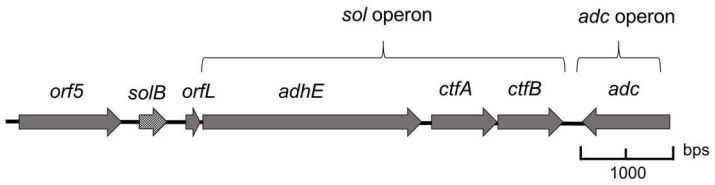

Figure 1.3: Localization of *solB* on the megaplasmid pSOL1 of *C. acetobutylicum.* *orf5* (CA_P0160), cell-adhesion domain-containing protein; *orfL* (CA_P0161), hypothetical protein; *adhE* (CA_P0162), alcohol/aldehyde dehydrogenase; *ctfA/B* (CA_P0163, CA_P0164), acetoacetyl-CoA:acetate/butyrate-CoA-transferase; *adc* (CA_P0165), acetoacetate decarboxylase.

1.3 Aim of this study

The aim of this study was to characterize SolB with regard to its role in solventogenesis in *C. acetobutylicum*. As the mRNAs of *spo0A* (CA_C2071) and *adhE2* (CA_P0035) were predicted as possible binding partners of SolB, different *C. acetobutylicum* mutants were constructed and growth experiments were performed to prove the binding of SolB. In order to identify further targets of SolB, which are responsible for the resulting phenotype of the *solB* overexpression strain, transcriptome data of the *C. acetobutylicum solB* overexpression strain and the *C. acetobutylicum* wild type strain were compared. SolB was identified as a trans-encoded sRNA, which is mainly dependent on the RNA chaperone Hfq. Therefore, the binding capacity of Hfq to SolB was analyzed by pulldown assays and electrophoretic mobility shift assays. Knockdown and knockout approaches for the *hfq* gene were applied in order to investigate the impact of Hfq in the *C. acetobutylicum solB* overexpression strain. Moreover, the Hfq of *C. acetobutylicum* was further characterized by complementation experiments in *hfq* deficient *E. coli* strains and comparison with other *hfq* genes or Hfq proteins regarding the genetic organisation and the amino acid sequence.

At the end, an operating principle of SolB should be predicted to go one step further in understanding the complex regulation network of solventogenesis. The obtained results might help in long-term to improve the solvent production of *C. acetobutylicum*.

2 Material and Methods

2.1 Microorganisms, plasmids and primers

2.1.1 Bacterial strains

All strains used in this study are listed in Table 2.1.

Table 2.1: Bacterial strains

Strain	Relevant characteristics	Reference
Escherichia coli DH5α	F^-, Φ80d*lac*ZΔM15, Δ(*lac*ZYA-*arg*F), U169, *rec*A1, *end*A1, *hsd*R17 (r_k^-, m_k^+), *pho*A, *sup*E44, *λ-, thi-1, gyr*A96, *rel*A	Hanahan, 1983
Escherichia coli XL-1 Blue MRF'	Δ(*mrcA*)183, Δ(*mrcCB-hsdSMR-mrr*)173, *end*A1, *sup*E44, *thi-1, rec*A1, *gyr*A96, *rel*A1, lac, [F' proAB $laqI^q$ ZΔM15 Tn10 (Tet^r)]	Stratagene GmbH; Braunschweig, Germany
Escherichia coli M15 [pREP4]	F^-, Φ80ΔlacM15, *nal*^{s}, *str*^{s}, *rif*^{s}, *thi*$^-$, *lac*$^-$, *ara*$^+$, *gal*$^+$, *mtl*$^-$, F^-, recA, uvr$^+$, lon$^+$, plasmid [pREP4]	Villarejo and Zabin, 1974
Escherichia coli BW25113	F^-, *Δ(araD-araB)567, ΔlacZ4787* (::rrnB-3), *λ-, rph-1, Δ(rhaD-rhaB)568, hsdR514*	Baba et al., 2006
Escherichia coli JW4130	F^-, *Δ(araD-araB)567, ΔlacZ4787*(::rrnB-3), *λ-, rph-1, Δ(rhaD-rhaB)568, hsdR514, Δhfq-722::kan*	Baba et al., 2006
Clostridium acetobutylicum ATCC 824	wild type	DSMZ GmbH, Braunschweig, Germany
Clostridium acetobutylicum Δ*spo0A*	*C. acetobutylicum* ATCC 824, deletion of CA_C2071 (*spo0A*)	Flitsch, unpublished
Clostridium acetobutylicum int::hfq168a	*C. acetobutylicum* ATCC 824; integration at position 168 of CA_C1834 (*hfq*) in antisense direction	This study
Clostridium acetobutylicum int::hfq79s	*Clostridium acetobutylicum* ATCC 824; integration at position 79 of CA_C1834 (*hfq*) in sense direction	This study

2.1.2 Plasmids

Table 2.2 presents all plasmids which were used in this work.

Table 2.2: Plasmids

Plasmid	Size [kbps]	Relevant characteristics	Reference
pIMP1	4.7	pMB1/ColE1 ori (-)(*rep*), pIM13 oriR (+) (*repL*), Ap^R (*bla*), Em^R (*ermC*)	Mermelstein et al., 1992
pIMP1_hfq	5.5	pIMP1 carrying *hfq* from *C. acetobutylicum*	This study
pIMP1_solB	4.9	pIMP1 carrying *solB* from *C. acetobutylicum*	Schiel, unpublished
pIMP1_solB_adhE2	8.3	pIMP1_solB carrying *adhE2* from *C. acetobutylicum*	This study
pIMP1_solB_adhE2_begin	6.0	pIMP1_solB carrying part of *adhE2* from *C. acetobutylicum*	This study
pIMP1_solB_spo0A_begin	5.4	pIMP1_solB carrying part of *spo0A* from *C. acetobutylicum*	This study
pBS77	4.6	pIMP1 carrying the *ptb-buk*-promoter from *C. acetobutylicum*	Schiel, 2006
pBS77_as_hfq	4.2	pBS77 carrying an antisense construct of *C. acetobutylicum hfq*	This study
pBS77_as_hfq_solB	4.4	pBS77_as_hfq carrying *solB* from *C. acetobutylicum*	This study
pGH_solB_runoff	3.1	pGH carrying *solB* from *C. acetobutylicum* for in vitro transcription	ATG:biosynthetics GmbH, Merzhausen, Germany
pQE30_hfq	3.7	ColE1 ori (-) (*rep*), Ap^R (*bla*) T5-promoter	Standfest, 2009
pACYC184	4.2	p15A ori (-) (*rep)*, Cm^R (*catp*), Tc^R (*tetA*)	DMSZ, Braunschweig, Germany
pACYC184_hfq_ec	3.8	pACYC184 carrying promoter and coding region of *E. coli hfq*	This study
pACYC184_hfq_cac	3.8	pACYC184 carrying promoter region of *E. coli hfq* and coding region of *C. acetobutylicum hfq*	This study
pACYC184_pKon	3.5	pACYC184 carrying promoter region of *E. coli hfq*	This study
pDrive	3.9	pMB1/ColE1 ori (-) (*rep*), f1 ori, Ap^R (*bla*), Km^R (*aph*), lacPOZ'	Qiagen GmbH, Hilden, Germany
pJet1.2	3.0	pMB1/ColE1 ori (-) (*rep*), Ap^R (*bla)*, P_{lacUV5}, P_{t7}, *eco47IR*	Thermo Fisher Scientific, Waltham, MA, USA
pANS1	5.9	pACYC148/p15A ori (-) (*rep*), Sp^R (*spcE*), *Φ3T I*	Böhringer, 2002
pIMP1_catp	5.9	pMB1/ColE1 ori (-) (*rep*), pIM13 oriR (+) (*repL*), Ap^R (*bla*), Em^R (*ermC*), Cm^R (*catp*)	Linder, unpublished
pIMP1_catp_solB	6.1	pIMP1_catp carrying *solB* from *C. acetobutylicum*	Zimmermann, 2013
pMTL007C-E2	8.7	ColE1 ori (-) (*rep*), pCB102 ori (+), Cm^R (*catP*), *lacI*, *ltrA*, *oriT*, P_{fdx}	Heap et al., 2012

Table 2: Plasmids (continued)

Plasmid	Size [kbps]	Relevant characteristics	Reference
pMTL007C-E2_79shfq	9.0	Integration plasmid for disruption of *hfq* at position 79	DNA2.0, Manlo Park, CA, USA
pMTL007C-E2_168ahfq	9.0	Integration plasmid for disruption of *hfq* at position 168	DNA2.0, Manlo Park, CA, USA
pIMP1_catp_ptb_hfq	6.4	pIMP1_catp carrying *hfq* from *C. acetobutylicum* with *ptb-buk* promoter	This study
pIMP1_catp_solB_ptb_hfq	6.6	pIMP1_catp_solB carrying *hfq* from *C. acetobutylicum* with *ptb-buk* promoter	This study

2.1.3 Primers and DNA fragments

Table 2.3 provides an overview of primers used in this work for cloning and sequencing. All primers were synthesized by biomers.net GmbH (Ulm, Germany).

Table 2.3: Primers used for cloning work and sequencing reactions

Primer	Sequence (5'→3')	Restriction site (underlined in the sequence)
hfq_fwd_bamHI	GGATCCGACATAATGTTAAGAAATGG	*Bam*HI
hfq_rev_ecoRI	GAATTCCATCATAGTACTTAAATTCC	*Eco*RI
Tobi_primer_fwd_1	ATTAAGCTTGGCTGCAGGTCG	
Tobi_primer_rev	AGGGCGACACGGAAATGTTG	
fD1	AGAGTTTGATCCTGGCTGGCTCAG	
rP2	ACGGCTACCTTGTTACGACTT	
M13 fwd	GTAAAACGACGGCCAGT	
M13 rev	AACAGCTATGACCATG	
PJet_fwd	ACTACTCGATGAGTTTTCGG	
PJet_rev	TGAGGTGGTTAGCATAGTTC	
Kontroll_pACYC184_hfq_fwd	CGCCGGAAGCGAGAAGAATC	
Kontroll_pACYC184_hfq_rev	CGCTCCTCCAAGCCAGTTAC	
adhE2_fwd_pfoI	TCCGGGAGGGCATATACCAACTTCCAG	*Pfo*I
adhE2_rev_pfoI	TCCGGGATGGATCAGAGCTGTAAGG	*Pfo*I
hfq_fwd	GTGCGAGAAAGAATAAGATAC	
hfq_rev	ATCGGTCTTAAAGGAGTTATG	
cyst_fwd	TATTTGCGGGATGCCTTATG	
cyst_rev	ACTCTTCCTTTCCTGCTATG	
miaA_fwd	TCTTCAAGCTATTGCTAAGG	
miaA_rev	CAGCTTCTTCCAAAGTAATG	
mutL_fwd	GTGGTGGAAGTGTTGATTAC	
mutl_rev	ATTGACCTATGACCCTAAGC	
mutS_fwd	CATGGAAAGCAGTGGATAGC	
mutS_rev	CTTGGCGCATATAGGTTGAC	
pre_fwd	TATGGGAACTCACAATACTC	
pre_rev	GTAAATGCTGAATCGTACTC	
EBS_universal	CGAAATTAGAAACTTGCGTTCAGTAAAC	
M1	AAGCAGTGGTATCAACGCAGAGT	
pMTL007-e2_nachweis_fwd	CCAACACATCAAGCCGTTAG	
pMTL007-e2_nachweis_rev	AGTCCCACCGACACATAATC	

RNA primers used for Northern blot analysis are listed in Table 2.4.

Table 2.4: RNA primers for Northern blot analysis

Primer	Sequence (5'→3')
SolB_sonde	UUUAUGUUUACCAUGAUAAGUUCUAGUAUAUAUAACCCUA
SolB_RNA_antisense	UAGGGUUAUAUAUACUAGAACUUAUCAUGGUAAACAUAAA

Primers for qRT-PCR are presented in Table 2.5.

Table 2.5: Primers used for qRT-PCR

Primer	Sequence (5'→3')
gryA_qRT_R1	TCTTGCCTTGTTTACCTGATATGG
gyrA_qRT_F1	GGCAAGTCTGGAATAAGAGCTG
spo0A_qRT_fwd	CAATACTACAGCTAGCAGAG
spo0A_qRT_rev	GTCTTAGCTTGTCAGCAATC
sol_qRT_fwd	GGTATGGGCTTAGTTGAAGAC
sol_qRT_rev	GTTACAGGGATTATAGCAGC
LC_hfq_fwd_1	GGATTTCAGATGAGAGGTAGTG
LC_hfq_rev_1	GTCTTAAAGGAGTTATGGTGG
LC_bdhB_fwd_2	CCTGCTGCTGTTTGATTGGTAG
LC_bdhB_rev_2	GCTGCAACAGGATCAGAAATGG
LC_bdhA_fwd_1	GCTCTAGCCTCGTAATCATC
LC_bdhA_rev_1	AATCAAACAGCAGCGGGAAC
Lc_adc_fwd_1	CAAACCTGACTAAGGGCTCATC
LC_adc_rev_1	TCGCCTGCATTTCCTAGAGGAC
LC_thiA_fwd_1	CTGTCTTGCTGGATTCTGTC
LC_thiA_rev_1	GCAGTAAGAACAGCGATTGG
LC_thiB_fwd_1	GTTCCCTGACCTCCACCAATAC
LC_thiB_rev_1	GGACATCCAATAGGTGCATCTG
LC_aor_fwd_2	ATGATCTCCGCCTCGAGTAG
LC_aor_rev_2	CTTGCCGAAGGTGCATACAG
LC_adcS_fwd_2	CCGCGGAAGATTGGTAACCAGC
LC_adcS_rev_2	GTGCCTTACAGCTCTGATCC

The DNA fragments of pKon, ec_hfq, cac_hfq, as_hfq, and as_hfq_solB were purchased by Thermo Fisher Scientific (Waltham, MA, USA). The detailed sequence information can be found in the supplement (Figure 8.1/Figure 8.2).

2.2 Cultivation and media

2.2.1 Media composition

E. coli cells were cultivated in LB (Luria Bertani) or for overproduction of proteins in TB (terrific broth) medium. For preparation of chemical competent cells SOB (super optimal broth) medium was used. *C. acetobutylicum* strains grow only under anaerobic conditions. For anaerobic clostridia growth medium (CGM), the compounds were weighted in and dissolved in anaerobic water in an anaerobic chamber. To prepare anaerobic water, the water was cooked for 20 min and afterwards cooled down on ice under N_2 sparging. For MES (2-(N-morpholino)ethanesulfonic acid) -buffered minimal

medium and starch medium (2x XYTGA), ingredients were dissolved aerobically and the pH was adjusted. Afterwards, oxygen was removed in the same way as anaerobic water was prepared. Complete medium was portioned in airtight Hungate tubes (Bellco Glass Inc., Vineland, USA) or flasks in an anaerobic chamber. All media were autoclaved for 15 to 20 min at 121 °C and 1.2 bar of positive pressure. Heat sensitive compounds were filter-sterilized and added after autoclaving. Solid medium was prepared by addition of 1.5 % agar to medium. After autoclaving, solid medium was poured into sterile petri dishes and allowed to solidify overnight at room temperature.

Media for *E. coli*

Luria Bertani (LB) (Green and Sambrook, 2012)

Tryptone	10.0	g	1.0	% (w/v)
NaCl	10.0	g	171.0	mM
Yeast extract	5.0	g	0.5	% (w/v)
ddH_2O	ad 1,000	mL		

Terrific broth (TB) (Green and Sambrook, 2012)

Glucose · H_2O	50.0	g	253.2	mM
Tryptone	12.0	g	1.2	% (w/v)
Yeast extract	24.0	g	2.4	% (w/v)
Glycerol	8.0	mL	109.4	mM
$Na_2HPO_4 \cdot 2\ H_2O$	11.8	g	66.3	mM
NaH_2PO_4	2.2	g	18.3	mM
ddH_2O	ad 1,000	mL		

Super optimal broth (SOB) (Green and Sambrook, 2012)

Tryptone	20.0	g	2.0	% (w/v)
Yeast extract	5.0	g	0.5	% (w/v)
$MgSO_4 \cdot 7\ H_2O$	2.4	g	9.9	mM
$MgCl \cdot 6\ H_2O$	2.0	g	10.0	mM
KCl	1.9	g	25.5	mM
NaCl	560.0	mg	10	mM
ddH_2O	ad 1,000	mL		

Media for *C. acetobutylicum*

Clostridia growth medium (CGM) (Wiesenborn et al., 1988)

Glucose · H_2O	50.0	g	201.9	mM
Yeast extract	5.0	g	0.5	% (w/v)
$(NH_4)_2SO_4$	2.0	g	15.1	mM
Asparagine · H_2O	2.0	g	13.3	mM
NaCl	1.0	g	17.1	mM
KH_2PO_4	750.0	mg	5.5	mM
K_2HPO_4	750.0	mg	4.3	mM
$MgSO_4$ · 7 H_2O	710.0	mg	2.9	mM
$MnSO_4$ · H_2O	10.0	mg	60.0	µM
$FeSO_4$ · 7 H_2O	10.0	mg	40.0	µM
Resazurin	1.0	mg	4.0	µM
ddH_2O (anaerobic)	ad 1,000	mL		

MES-buffered medium (Bertram et al., 1990)

Glucose · H_2O	40.0	g	201.9	mM
MES	21.3	g	100.0	mM
$(NH_4)_2SO_4$	2.0	g	15.1	mM
KH_2PO_4	0.1	g	0.7	mM
$MgSO_4$ · 7 H_2O	0.1	g	0.4	mM
$CaCl_2$ · 7 H_2O	0.1	g	68.0	µM
$MnSO_4$ · H_2O	15.0	mg	88.0	µM
$FeSO_4$ · 7 H_2O	15.0	mg	54.0	µM
NaCl	10.0	mg	171.0	µM
Na_2MoO_4 · 2 H_2O	10.0	mg	41.0	µM
Thiamin-HCl	2.0	mg	5.9	µM
4-Aminobenzoic acid	2.0	mg	14.6	µM
Biotin	0.1	mg	0.4	µM
Resazurin	1.0	mg	4.0	µM
ddH_2O	ad 1,000	mL		
pH(NaOH)	7.3			

2x XYTGA starch medium (Harris et al., 2002)

Trypton	16.0	g	1.6	% (w/v)
Yeast extract	10.0	g	1.0	% (w/v)
NaCl	2.0	g	34.2	mM
Glucose · H_2O	4.0	g	20.2	mM
Soluble starch	5.0	g	14.6	mM
MOPS	41.9	g	0.2	M
Agar	15.0	g	1.5	% (w/v)
ddH_2O	ad 1,000	mL		
pH(NaOH)	6.5			

Sporulation medium (Monot et al., 1982)

The compounds were dissolved in water and cooked for 20 min. After cooling down under N_2 sparging, medium was aliquoted into 4.4 ml in Hungate tubes in an anaerobic chamber and autoclaved. Prior to inoculation of the desired strain, 0.6 mL of a mixture, containing 10 mL glucose (20 % (w/v)), 1 mL butyric acid (1 M), and 1 mL of the trace element solution, was added to each Hungate tube.

Basic medium

$CaCO_3$	1.0	g	10.0	mM
KH_2PO_4	1.0	g	7.4	mM
K_2HPO_4	1.0	g	5.7	mM
$MgSO_4 \cdot 7\ H_2O$	0.1	g	0.4	mM
$(NH_4)_2SO_4$	2.0	g	15.1	mM
Resazurin	1.0	mg	4.0	µM
ddH_2O	ad 880	mL		

Trace element solution

NaCl	10.0	mg	171.1	µM
$Na_2MoO_4 \cdot 2\ H_2O$	10.0	mg	41.3	µM
$CaCl_2 \cdot 2\ H_2O$	10.0	mg	68.0	µM
$FeSO_4 \cdot 7\ H_2O$	15.0	mg	54.0	µM
$MnSO_4 \cdot H_2O$	15.0	mg	88.8	µM
p-Aminobenzoic acid	2.0	mg	14.6	µM
Thiamine	2.0	mg	5.9	µM
Biotin	0.1	mg	0.4	µM
ddH_2O (anaerobic)	ad 1,000	mL		

2.2.2 Media supplements

In Table 2.6 and Table 2.7 additional medium components and used antibiotics are shown. Medium compounds and antibiotics dissolved in water were filter-sterilized. Due to the heat sensitivity of antibiotics, the addition took place after the medium was autoclaved and cooled down to 50 °C. Methyl α-D-glucopyranoside was weighted in with the compounds of LB medium (2.2.1). Hydrogen peroxide was added to the medium directly prior to use.

Table 2.6: Additional medium compounds

Component	Solvent	Stock solution [mg mL^{-1}]	Working solution [µg mL^{-1}]
IPTG	ddH_2O	20	20
X-Gal[a]	DMF	20	32
Methyl α-D-glucopyranoside	-	-	10
H_2O_2	-	336	224

[a] photo sensitive

Table 2.7: Antibiotics used in this work

Component	Solvent	Stock solution [mg mL^{-1}]	Working solution [µg mL^{-1}]
Ampicillin	ddH_2O	100	100
Chloramphenicol	Ethanol, 96 % (v/v)	30	30
Clarithromycin[a]	ddH_2O	5	3
Erythromycin	Ethanol, 96 % (v/v)	100	250
Kanamycin	ddH_2O	30	30
Spectinomycin	ddH_2O	50	50
Tetracycline[b]	Ethanol, 96 % (v/v)	12	3

[a] for clarithromycin preparation the antibiotic was mixed with 20 mL of ultrapure water and acidulated with 2 M HCl until the clarithromycin is in solution (pH approximately 2.6). The solution was neutralized by the addition of 2 M NaOH until pH was adjusted to 6.5. [b] photo sensitive

2.2.3 Growth conditions

E. coli strains were cultivated aerobically at 37 °C in solid or liquid LB media. Test tubes were used for cultures less than 5 mL and buffled flasks for volumes greater than 5 mL. For continuous oxygenation of liquid culture, a rotary shaker at 120 to 180 rpm was necessary. For growth experiments with *E. coli,* 50 mL LB media were inoculated with 5 mL overnight culture to an optical density (OD_{600}) of 0.1.

C. acetobutylicum was grown anaerobically at 37 °C in Hungate tubes (Bellco Glass Inc., Vineland, USA), capped airtight with synthetic rubber stoppers (Ochs GmbH, Bovenden, Germany) and plastic screw caps for 5 mL cultures. Larger volumes were cultivated in Müller-Krempel bottles (Müller & Krempel AG, Bülach, Switzerland), closed with natural rubber stoppers (Maag Technic GmbH, Göppingen, Germany) and stainless steel screw caps. For growth experiments with *C. acetobutylicum*, 50 mL

MES-buffered medium (2.2.1) was inoculated with 5 mL overnight culture to an optical density (OD_{600}) of 0.1.

2.2.4 Determination of growth and production parameters

2.2.4.1 Determination of the optical density

The optical density during growth experiments was measured at 600 nm (OD_{600}) using an Ultrospec® 3100 pro (Amersham Bioscience Europe GmbH, Freiburg, Germany) and 1 mL cuvettes (VWR International GmbH, Darmstadt, Germany) with a thickness of 1 cm. As a blank, the medium of the corresponding growth experiment was measured. If samples reached values above 0.3, the cultures were diluted as well as the blank.

2.2.4.2 Analysis of products by gas chromatography (GC)

Products of growth experiments were determined by GC (McNair and Miller, 2009) using Clarus 600 GC (PerkinElmer Corp., Waltham, MA, USA). One mL cell culture was taken at different time points and stored until analysis at -20 °C. After thawing, samples were centrifuged (13,000 x g, 30 min, 4 °C) and supernatant was transferred to 2 mL crimp vials and mixed with 0.1 mL internal standard (110 mM isobutanol, 2 M HCl). Vials were sealed with aluminium crimp caps (CS Chromatographie Service GmbH, Langerwehe, Germany). Samples exceeding product amounts of 5 mM had to be diluted respectively. The device was calibrated with a solution of each substance (5 mM) and was adjusted to the following parameters:

Column: metal, packed (2 x 2,000 mm)
Packing material: Porapak P (80/100 mesh)
Carrier gas: N_2 (27.9 mL min^{-1})
Injection temperature: 200 °C (autosampler)
Detector temperature: 300 °C (FID)
Detector gases: H_2 (45 mL min^{-1}), synthetic air (450 mL min^{-1})
Program: 1. 130 °C, 1 min
2. 130-140 °C (5 °C min^{-1})
3. 140 °C, 20 min

Data were processed using the software TotalChrom Version 6.3.1 (PerkinElmer Corp., Waltham, MA, USA).

2.2.4.3 Analysis of substrate and products by high performance liquid chromatography (HPLC)

Beside analysis of fermentation products with the GC, substrates and metabolic products were determined by HPLC (Snyder et al., 2013). Therefore, the Infinity 1260 device (Agilent Technologies, Santa Clara, CA, USA) was applied, equipped with a diode array detector UV (DAD) for the detection of carboxyl groups and a refraction index detector (RID) for the detection of hydroxyl groups. Samples were prepared as described in section 2.2.4.2 without an internal standard. The device was calibrated with aqueous solutions of each analyzed substance in concentrations of 1 to 200 mM. For analysis, the following parameters were adjusted:

Column: CS-Organic acid (8 x 15 mm)
(CS Chromatographie Service GmbH, Langerwehe, Germany)
Packing material: Poly(styrene-divinylbenzene)
Mobile phase: 5 mM H_2SO_4 (0.7 mL min^{-1})
Injection temperature: 15 °C (autosampler)
Column temperature: 60 °C
Column pressure: 60 bar
Detector temperature: 40 °C (RID)
Detection wavelength: 210 nm
Running time: 11 min

Data were processed using the software Agilent OPEN-Lab CDS Version A.01.03 (Agilent Technologies, Santa Clara, CA, USA). For analysis of granulose production in *C. acetobutylicum*, 2 mL cell suspension was washed with 1x phosphate-buffered saline (PBS) and suspended in 0.3 mL H_2SO_4 (1 M) and boiled for 3 h at 95 °C. Afterwards, the pH was adjusted to 7 with 2 M KOH (Robson et al., 1974). Solutions were sterile-filtered and directly used for HPLC analysis.

10x PBS (Green and Sambrook, 2012)

NaCl	80.0	g	1.37	M
KCl	2.0	g	27.0	mM
Na_2HPO_4	14.4	g	0.1	mM
KH_2PO_4	2.4	g	18.0	M
ddH_2O	ad 1,000	mL		
pH(HCl)	7.4			

2.2.5 Strain conservation

E. coli strains were grown over night in 5 mL LB medium (2.2.1) with respective antibiotics. 500 µL of cell culture were mixed with 500 µL of 100 % glycerol and stored at -80 °C (Gherna, 2013). Ability of sporulation was used for long-term storage of *C. acetobutylicum* strains. Therefore, *C. acetobutylicum* strains were grown in sporulation medium (2.2.1) supplemented with antibiotics, if required, for at least one week. Afterwards, the successful sporulation was controlled via light microscopy (2.3.1). If at least 25 spores were present, suspensions were centrifuged (2,400 x g, 10 min, 4 °C) and supernatant was removed. Spores were suspended in 1 mL of CG medium and stored at -80 °C. For inoculation of spores, 200 µL were transferred into a new Hungate tube with 5 mL CG medium (2.2.1) and incubated for 20 min at 80 °C to kill still viable cells. After cooling down, antibiotics were supplemented and incubation took place overnight at 37 °C. *C. acetobutylicum* mutants, which lost the ability to sporulate, were grown in 5 mL CG medium and centrifuged (2400 x g, 10 min, 4 °C). The supernatant was removed and cells were suspended in 500 µL anaerobic glycerol (50 % (v/v)) and 500 µL CG medium. Cells were stored immediately at -80 °C.

2.3 Microscopy

2.3.1 Light microscopy

Spore formation or cell length were determined by light microscopy (Axioscope, Carl Zeiss AG, Oberkochen, Germany). 7 µL culture volume were pipetted on an object slide and covered with a cover glass. Depending on the optical density of the culture different dilutions were prepared. Cell length was calculated with the AxioVision LE (Carl Zeiss AG, Oberkochen, Germany) software.

2.3.2 Scanning and transmission electron microscopy

Electron microscopic images were taken from overnight grown cultures or later, if necessary. Therefore, 1 mL of culture was pelleted (10,000 x g, 5 min, RT) and washed with saline (0.9 % NaCl (w/v)). Cells were fixed with glutaraldehyde followed by postfixation with osmium tetraoxide. Samples were prepared for microscopy at the Central Facility for Electron Microscopy (Ulm University, Germany). Scanning electron and transmission electron micrographs were conducted with the S-5200 UltraHigh Resolution FE SEM (Hitachi Ltd. Corp., Chiyoda, Japan) and with the JEM1400 (Jeol, Akishima, Japan), respectively.

2.4 Nucleic acid methods

2.4.1 Preparation of solutions and devices

For work with nucleic acids, all used solutions and vessels were autoclaved and heat sensitive objectives were cleaned with 70 % ethanol. If experiments with RNA were performed, all solutions and vessels were autoclaved twice. Instead of ddH_2O, DEPC-treated water was used for dissolving precipitated RNA. Furthermore, the bench was cleaned with a decontamination reagent (RNase-ExitusPlus™, AppliChem GmbH, Darmstadt, Germany) and filter tips as well as gloves were used to prevent contamination with RNases.

2.4.2 DNA isolation from bacteria

2.4.2.1 Genomic DNA isolation from clostridia

Genomic DNA of *C. acetobutylicum* was isolated by MasterPure™ Gram Positive DNA Purification Kit (Epicentre, Madison, WI, USA). Therefore, 2 mL of cell culture were centrifuged (5,000 x g, 5 min, 4 °C) and treated according to manufactory practice. The obtained DNA was suspended in 50 µL ddH_2O.

2.4.2.2 Plasmid DNA isolation from E. coli

Plasmids were isolated from *E. coli* using the Zyppy™ Plasmid Miniprep Kit (Zymo Research Corp., Irvine CA, USA). Therefore, 2 mL of cell culture were centrifuged and cells were suspended in 500 µL water. The following procedure was performed according to manufactory practice. Plasmid DNA was eluted with 30 µL ddH_2O from the column.

2.4.3 RNA isolation from bacteria

2.4.3.1 Preparation with hot phenol

Preparation of RNA was performed with hot phenol (Aiba et al., 1981) for transcriptome analysis. 5 mL cell culture broth was centrifuged (3,900 x g, 5 min, 4 °C). The collected cells were suspended in 600 µL ice-cold ASE-buffer (20 mM sodium acetate, 17.3 mM SDS, 1.3 mM EDTA, pH 5.5) and afterwards mixed with 60 °C hot Roti®-AquaPhenol (pH 4.5-5, Carl Roth GmbH & Co. KG, Karlsruhe, Germany). Samples were incubated for 10 min at 60 °C. To separate phases, samples were centrifuged at 15,500 x g for 10 min at 4 °C. The upper aqueous layer was transferred into a new tube with 600 µL Rothi®-Phenol/Chloroform/Isoamylalkohol (25:24:1 (v/v/v), Carl Roth GmbH & Co. KG, Karlsruhe, Germany). After inverting the tube several times, phases were separated by centrifugation again. The aqueous phase was transferred into a new tube with

600 µL Rothi®-Chloroform/Isoamylalkohol (24:1 (v/v), Carl Roth GmbH & Co. KG, Karlsruhe, Germany). After inverting the tube several times, phases were separated by centrifugation. The aqueous phase was transferred into a new tube and an ethanol precipitation was conducted. Two volumes of 100 % ethanol were supplemented and stored for at least 12 h at -20 °C. RNA was collected by centrifugation at 15,500 x g for 60 min at 4 °C. Afterwards, the RNA pellet was washed once with 70 % ethanol (v/v) and afterwards dried until the ethanol completely evaporated. RNA was dissolved in 50 µL DEPC-treated water (Thermo Fisher Scientific, Waltham, MA, USA).

2.4.3.2 Preparation with TRIzol® Reagent

C. acetobutylicum cells were cultivated until stationary growth phase, followed by preparation of total RNA using TRIzol® Reagent (Invitrogen, Darmstadt, Germany). After centrifugation of 50 mL culture broth (15,500 x g, 10 min, 4 °C), cell pellet was suspended in 600 µL SET buffer (730 mM sucrose, 50 mM Tris–HCl, 50 mM EDTA, pH 7.6, 20 mg mL^{-1} lysozyme (Sigma-Aldrich Chemie GmbH, Steinheim, Germany)) and incubated for 5 min at 37 °C. 1 mL TRIzol® Reagent was added and mixed with the cell suspension. Next, 0.3 mL Rothi®-Chloroform/Isoamylalkohol (24:1 (v/v), Carl Roth GmbH & Co. KG, Karlsruhe, Germany) was added, and the suspension was inverted several times before centrifugation (15,500 x g, 15 min, 4 °C). The upper phase was transferred into a new reaction tube and mixed with 500 µL ice-cold isopropanol. After centrifugation (15,500 x g, 10 min, 4 °C), the supernatant was discarded, 1 mL ice-cold ethanol (70 %, v/v) was added, and centrifuged again (5,850 x g, 4 min, 4 °C). Ethanol was removed by a pipette, and the remaining ethanol was evaporated by drying at room temperature. The isolated RNA was suspended in 50 µL DEPC-treated water (Thermo Fisher Scientific, Waltham, MA, USA) and stored at -80 °C.

2.4.3.3 DNA digestion

DNA contamination of RNA was removed by desoxyribonucleases (Kunitz, 1950; Vanecko and Laskowski, 1961). DNA was digested with Ambion Turbo DNase (Thermo Fisher Scientific, Waltham, MA, USA). The reaction was performed using maximal 10 µg of nucleic acids in a 100 µL set-up with 1 µL Turbo DNase. After an incubation of 30 min at 37 °C, additionally 1 µL of Turbo DNase was pipetted into the solution. The mixture was incubated for 30 min and purification of RNA was performed with the Inactivation reagent (Thermo Fisher Scientific, Waltham, MA, USA) according

to the manufacturer's instructions. DNA-free RNA was verified by performing PCR (2.4.8.1) with RNA as template.

2.4.3.4 rRNA removal

For pulldown assays with RNA and Hfq (2.6.1), it was mandatory to remove rRNA from total RNA (Sonnleitner et al., 2008). Therefore, the Ribominus™ Transcriptome Isolation Kit (Invitrogen, Carlsbad, CA, USA) was used according to manual instructions.

2.4.4 Purification and concentration of nucleic acids

2.4.4.1 Phenol-chloroform-extraction (Green and Sambrook, 2012)

Nucleic acids, which are dissolved in aqueous solutions with salts or proteins, were mixed with ½ volume of Roti®-Phenol/Chloroform/Isoamyl alcohol (25:24:1 (v/v/v)), Carl Roth GmbH & Co. KG, Karlsruhe, Germany). After centrifugation (15,500 x g, 15 min, 4 °C) the upper aqueous phase was transferred to a new tube. This procedure was repeated until no protein interphase could be recognized. Afterwards, one volume of Roti®-Chloroform/Isoamyl alcohol (24:1 (v/v), Carl Roth GmbH & Co. KG, Karlsruhe, Germany) was mixed with the nucleic acid-containing phase and centrifuged (15,500 x g, 15 min, 4 °C). Again, the upper phase was transferred into a new tube and an ethanol precipitation (2.4.4.2) was performed. For extraction of DNA, Roti®-Phenol/Chloroform/Isoamyl alcohol (25:24:1 (v/v/v), pH 7.5-8, Carl Roth GmbH & Co. KG, Karlsruhe, Germany) and for RNA Roti®-Phenol/Chloroform/Isoamyl alcohol (25:24:1 (v/v/v), pH 4.5-5, Carl Roth GmbH & Co. KG, Karlsruhe, Germany) was used.

2.4.4.2 Ethanol precipitation

For ethanol precipitation of RNA or DNA (Wallace, 1987), one-tenth of sodium acetate was added and the cup was inverted several times. Two volumes of ethanol (96 %) were mixed with the aqueous solution. For precipitation, it was necessary to incubate DNA for at least 20 min at -20 °C and RNA overnight at -20 °C. Then, samples were centrifuged (15,500 x g, 60 min, 4 °C). Nucleic acids were washed once with 70 % ethanol (v/v) and centrifuged (15,500 x g, 10 min, 4 °C). Ethanol was removed with a pipette and pellets were dried until ethanol evaporated. Nucleic acids were dissolved in 30 µL ddH_2O.

2.4.4.3 Isolation and purification of nucleic acids

If it was necessary to purify or concentrate DNA/RNA after modification procedures, different kits were used. For direct or gel-purification of DNA, the NucleoSpin® Gel and PCR Clean-Up Kit (MACHEREY-NAGEL GmbH & Co. KG, Düren, Germany) was chosen. For RNA the RNA Clean & Concentrator™-5 (Zymo Research Corp., Irvine CA, USA) was used for direct purification. If RNA was to be gel purified, this was accomplished with NucleoSpin® Gel and PCR Clean-Up Kit (MACHEREY-NAGEL GmbH & Co. KG, Düren, Germany). If nucleic acid fragments had to be isolated from gels, the respective fragment was sliced out of an agarose gel (2.4.5.1) under UV-transillumination.

2.4.4.4 Quantification of nucleic acids

Nucleic acid concentration was determined photometrically with a NanoDrop 2000 spectrophotometer (Thermo Fisher Scientific, Waltham, MA, USA). Therefore, 1 µL of nucleic acid in aqueous phase was analyzed at 260 and 280 nm. An extinction of 1 at 260 nm represents a concentration of 50 µg mL^{-1} DNA or 40 µg mL^{-1} RNA (Green and Sambrook, 2012). The quotient of the extinction at 260 and 280 nm defines the purity of the nucleic acid. Values between 1.8 and 2.0 represent nucleic acid without protein contamination. Samples with values below 1.8 contain protein.

2.4.5 Gel electrophoresis

2.4.5.1 Non-denaturating agarose gel electrophoresis

Restriction digestions or PCR fragments were examined by non-denaturating agarose gel electrophoresis. For this purpose, agarose-gels with 0.8-2 % (w/v) were manufactured by dissolving agarose by heating in 1x TAE. The liquid agarose gel was poured in a horizontal chamber and a comb was positioned to form “pockets”. After cooling down, the gels were covered with 1x TAE. Samples were mixed with 6x Loading Dye (Thermo Fisher Scientific, Waltham, MA, USA) in the ratio 5:1 and pipetted into the pockets of the gels. Additionally, either 3 µL of GeneRuler™ DNA ladder Mix or GeneRuler™ 50 bp DNA ladder (Thermo Fisher Scientific, Waltham MA, USA) were used as marker. DNA or RNA was separated with 12-15 V cm^{-1} for 45 min. The gels were stained in an ethidium bromide (EtBr) bath (2.5 µM EtBr, 1x TAE (2.4.5.1)) and nucleic acids were visualized via a transilluminator at 312 nm (2.4.5.4).

50x TAE

Tris	242.3	g	2.0	M
EDTA	14.6	g	50	mM
Glacial acetic acid	57.1	mL	1	M
ddH_2O	ad 1,000	mL		
pH(HCl)	8.0			

2.4.5.2 Non-denaturating polyacrylamide gel electrophoresis

For binding assays of RNA and protein, it was necessary to perform non-denaturating polyacrylamide gel electrophoresis. Gels were composed of 6 % polyacrylamide in 1x Tris-Borate-EDTA (TBE) buffer (Table 2.8). The electrophoresis unit was filled with 0.5x TBE to cover wells completely with buffer. Wells were flushed and pre-electrophoresis was run for 1 h at 15 V cm^{-1}. Samples were loaded with a native RNA loading buffer (50 % glycerol (v/v), 0.1 % bromophenol blue sodium salt (w/v), 0.1 % xylene cyanol FF (w/v), 0.5x TBE) with a ratio of 3:1 onto the gels. Samples were separated for 2.5 h at an electric strength of 15 V cm^{-1}.

Table 2.8: Composition of a non-denaturating polyacrylamide gel

Component	Amount	
Rotiphorese® NF-Acrylamid/Bis-solution 40 % (29:1)[a]	15	mL
10x TBE (890 mM Tris-HCl, 890 mM boric acid, 20 mM EDTA)	10	mL
APS (10 % (w/v))	500	µL
TEMED	50	µL
ddH_2O	ad 100	mL

[a] Carl Roth GmbH & Co. KG, Karlsruhe, Germany

2.4.5.3 Denaturating polyacrylamide electrophoresis

For Northern blot analysis of small RNAs, denaturating polyacrylamide gels were used to reach a better resolution. 20 µg RNA samples were heated for 2 min at 95 °C and mixed with 2x RNA Loading Dye (Thermo Fisher Scientific, Waltham, MA, USA) in a ratio of 1:2. RNA samples and RiboRuler Low Range RNA Ladder ready-to-use (Thermo Fisher Scientific, Waltham MA, USA) were separated on Tris-borate-EDTA-urea polyacrylamide gel (6 % polyacrylamide gel, Table 2.9) using a Multigel-Long Gel Electrophoresis Apparatus (Biometra, Göttingen, Germany) with a power supply adjusted to 130 V for 3 hours. Separation of RNA was controlled by staining the gel with EtBr (2.4.5.4).

Table 2.9: Composition of a denaturating polyacrylamide gel

Component		Amount
Rotiphorese® NF-Acrylamid/Bis-solution 40 % (29:1)[a]	15	mL
Urea	424	g
10x TBE (890 mM Tris-HCl, 890 mM boric acid, 20 mM EDTA)	10	mL
APS (10 % (w/v))	500	µL
TEMED	50	µL
ddH_2O	ad 100	mL

[a] Carl Roth GmbH & Co. KG, Karlsruhe, Germany

2.4.5.4 Staining of nucleic acids

After separation of DNA or RNA in agarose or polyacrylamide gels, the nucleic acids were stained in an EtBr bath (2.5 µM EtBr, 1x TAE (2.4.5.1)). After an incubation of 10-15 min nucleic acids were visualized by transillumination at 312 nm using the E-Box VX2 2.0 MP Gel Documentation System (VWR International GmbH, Erlangen, Germany).

2.4.6 In vitro transcription of *solB*

For in vitro transcription (Beckert and Masquida, 2011), the plasmid [pGH_solB_runoff] was cleaved with the restriction enzyme FastDigest *Eco*RV (Thermo Fisher Scientific, Waltham, MA, USA) to linearize the vector (2.4.7.1). Afterwards, the plasmid was used as template for in vitro transcription with a set-up as follows. Components were delivered by Thermo Fisher Scientific (Waltham, MA, USA). The reaction was incubated at 37 °C for 4 h. Subsequently, a DNA digestion (2.4.3.3) was performed to get rid of template DNA. The production of RNA SolB was controlled by a 2 % agarose gel (2.4.5.1) and sliced out of the gel. Gel purification was accomplished as described in 2.4.4.3. In vitro transcribed SolB was stored at -80 °C.

Composition of in vitro transcription

T7 transcription buffer (5x)	10.0	µL		
Linearized pGH_solB	15.0	µL	3.0	µg
NTPs (10 mM each)	10.0	µL	2.0	mM
T7-polymerase	1.5	µL	30.0	U
Ribolock	1.2	µL	48.0	U
ddH_2O	ad 50	µL		

2.4.7 Enzymatic modification of nucleic acids

2.4.7.1 Restriction digestion of DNA

For conventional cloning, restriction cleavage is essential (Green and Sambrook, 2012). The enzymes were purchased by the company Thermo Fisher Scientific (Waltham, Ma, USA) and digestions were performed according to the manufacturer's instructions. For non-directional cloning, only one restriction enzyme was used. In contrast, for directional cloning two different restriction enzymes, producing sticky ends, were essential. The cleavage was controlled by non-denaturating agarose gel electrophoresis (2.4.5.1) and EtBr staining (2.4.5.4).

2.4.7.2 Blunting of DNA ends

To ligate sticky ends with non compatible ends, it was indispensable to blunt ends of the respective DNA fragment. Therefore, the blunting enzyme was used purchased by QIAGEN GmbH (Hilden, Germany). The blunting reaction was performed according to the manufacturer's instructions.

2.4.7.3 Dephosphorylation of DNA fragments

Dephosphorylation was necessary for cleaved plasmid backbones, which should be used in a ligation (2.4.7.4) to prevent self-ligation (Green and Sambrook, 2012). Therefore, the FastAP™ Thermosensitive Alkaline Phosphatase (Thermo Fisher Scientific, Waltham, MA, USA) was used according to the instructions of the manufacturer. To control dephosphorylation, dephosphorylated plasmid was applied in a ligation (2.4.7.4) without an insert and transformed into *E. coli* (2.4.10.1). Afterwards, the number of grown colonies was compared with the corresponding ligation set-ups.

2.4.7.4 Ligation of DNA fragments

Ligation of two DNA fragments was achieved by the ATP-dependent T4 DNA Ligase (Thermo Fisher Scientific, Waltham, MA, USA) through linkage of free 3' hydroxy groups and free 5' phosphate groups (Weiss et al., 1968). Ligation was set up according to the manufacturer's instructions and incubated either for 1 h at 22 °C or in a gradient mode. In this case, incubation of the ligation set-up started at 22 °C and the temperature was decreased every 10 min for 1 degree for 60 min. At the end, an inactivation step for 15 min at 65 °C was performed. Afterwards, the ligations were transformed into *E. coli* (2.4.10.1).

Ligation of PCR products with A-overlaps were ligated into the vector pDrive, purchased by QIAGEN PCR Cloning Kit (QIAGEN GmbH, Hilden, Germany). Additionally, 1 µl T4 DNA Ligase was supplemented to the recommended ligation set-up.

Synthesized DNA sequences (Supplement Figure 8.1/Figure 8.2/Figure 8.6) were ligated into the blunt-end vector pJET (Thermo Fisher Scientific, Waltham, MA, USA) according to the instructions of the manufacturer. Successful ligation was verified via PCR (2.4.8) with primers PJet_fwd and PJet_rev (Table 2.3).

2.4.7.5 Radioactive labelling of RNA

For Northern analysis (2.4.11), probe solB_sonde had to be radioactively labelled with [γ-^{32}P]-ATP (25 pmol, 7000Ci mmol^{-1}, 150mCi mL^{-1}) using T4 Polynucleotide Kinase (Thermo Fisher Scientific, Waltham, MA, USA) (Srivastava and Schonfeld, 1991). The T4 Polynucleotide Kinase catalyzes the transfer of the γ-phosphate from ATP to the 5' hydroxy group of oligonucleotides. The reaction was performed as described in the manual. The probe was purified by NucAway™ Spin Columns (Ambion, Thermo Fisher Scientific, Waltham, MA, USA).

2.4.7.6 Biotin labelling of RNA

For interaction studies (2.6), it was essential to label the in vitro transcribed small RNA SolB. Therefore, the Pierce™ RNA 3' End Biotinylation Kit (Thermo Fisher Scientific, Waltham, MA, USA) was used for labeling the 3' end of SolB with biotin (England et al., 1980). The reaction was set up as described in the manual and incubated at 16 °C for 4 h. Afterwards, a phenol/chloroform extraction (2.4.4.1) and an ethanol precipitation (2.4.4.2) were performed.

2.4.7.7 Poly(A) tailing of RNA

To perform RT-PCR with unknown sequences, it was necessary to polyadenylate the RNA (Bernstein and Ross, 1989; Lingner and Keller, 1993). Therefore, the RNA was poly(A) tailed via the Poly(A) Polymerase Tailing Kit (Epicentre, Madison, WI, USA). Afterwards, the RNA was purified as described in 2.4.4.3.

2.4.8 Polymerase chain reaction (PCR)

2.4.8.1 Standard PCR

Amplification of DNA fragments for cloning procedures or strain verification was achieved by polymerase chain reaction (PCR) (Mullis et al., 1986). Necessary primers

were ordered at biomers.net GmbH (Ulm, Germany) and are listed in Table 2.3. For any DNA amplification, a standardized reaction mixture was prepared.

Composition

Buffer S with $MgCl_2$ (10x)	2.0	µL		
Forward primer (100 µM)	0.5	µL	2.5	µMol
Reverse primer (100 µM)	0.5	µL	2.5	µMol
dNTPs (10 mM each)	0.5	µL	25.0	µMol
Template DNA	1.0	µL	2-0.1	ng/µL
Taq Polymerase	0.1	µL	2.5	U
ddH_2O	ad 20	µL		

Program

Step 1:	initial denaturation:	95 °C, 5 min
Step 2:	denaturation:	95 °C, 45 s
Step 3:	annealing:	52 °C, 45 s
Step 4:	elongation:	72 °C, *
Step 5:	final elongation:	72 °C, 10 min

32 cycles of step 2 to 4 were performed. Time of elongation (*) was calculated according to the amplified product assuming an amplification role of 1,000 bps min^{-1}. If the PCR was not successful, a gradient PCR with different annealing temperatures between 45 and 65 °C was performed to find the best suited annealing temperature.

2.4.8.2 Colony PCR

Screening of colonies with colony PCR was an useful tool for control of successful ligation (2.4.7.4) and transformation (2.4.10.1). Therefore, colonies were picked from the plate, streaked out on a masterplate as back up and transferred into 50 µL of water. This was boiled for 10 min at 95 °C and 1 µL was used for the standard PCR (2.4.8.1) procedure as template.

2.4.8.3 Reverse transcriptase PCR (RT-PCR)

2.4.8.3.1 Standard RT-PCR

To analyze transcription of distinct genes via RT-PCR, RNA had to be converted into cDNA (Green and Sambrook, 2012). After RNA isolation (2.4.3) and DNA digestion (2.4.3.3), cDNA was synthesized by Superscript III® Reverse Transcriptase (Thermo Fisher Scientific, Waltham, MA, USA). Random hexamer primers (Thermo Fisher Scientific, Waltham, MA, USA) were used to analyze several genes with the same

cDNA (Haymerle et al., 1986), and for investigating the operon structure of *hfq* gene the gene specific primer cys_rev (Table 2.3) was used.

Program and composition

RNA	1-11	ng		
Primer (100 µM)	1	µL	2.5	µM
dNTPs (10 mM each)	1	µL	25.0	µM
ddH_2O	ad 13	µL		

Compounds were incubated for 10 min at 65 °C and afterwards placed on ice for 5 min. The following compounds were supplemented:

5x buffer	4	µL		
DTT	1	µL	5	mM
Ribolock	1	µL	40	U
Reverse Transcriptase	1	µL	200	U

Incubation was performed for 5 min at room temperature and 60 min at 55 °C. Inactivation was performed at 65 °C for 10 min.

The synthesized cDNA was utilized in a standard PCR (2.4.8.1) to investigate transcription. For every sample, a second RT-PCR approach was performed without Reverse Transcriptase to control the purity of RNA with regard to DNA contamination.

2.4.8.3.2 cDNA synthesis for unknown sequences

To identify unknown RNA sequences, the RNA was first polyadenylated (2.4.7.7) and then converted into cDNA with the Mint-2 cDNA synthesis Kit (evrogen, Moscow, Russia). An overview over the mechanism of converting RNA in dcDNA is presented in Figure 2.1. Synthesis of first strand cDNA is initiated by a 3'-end adapter containing an poly(T) sequence that anneals to poly(A) stretches of RNA and Mint Reverse Transcriptase. At the 5'-end of the mRNA, Mint Reverse Transcriptase adds several deoxycytidines to the 3'-end of the newly synthesized cDNA (Schmidt and Mueller, 1999). The PlugOligo, which contains a poly(G) stretch at the 3'-end and a deoxyribooligonucleotide, can basepair with the complementary poly(C) stretch of the synthesized cDNA. Reverse Transcriptase identifies the PlugOligo as a further part of the RNA template and continues cDNA synthesis. At the end of the PlugOligo a terminator nucleotide blocks extension of cDNA by incorporation of further PlugOligos. For increasing the efficiency of this incorporation process, the IP-solution (solution for incorporation of PlugOligo) is necessary. When the process of first cDNA synthesis is finished, two known adapter sequences are provided for synthesis of dcDNA by PCR

(2.4.8.1). The PCR product is cloned into the cloning vector pDrive (2.4.7.4) and transformed in *E. coli*. For identification, colony PCRs were performed (2.4.8.2) with primers M13_fwd and M13_rev (2.1.3). The inserted fragments were sequenced (2.4.9.1).

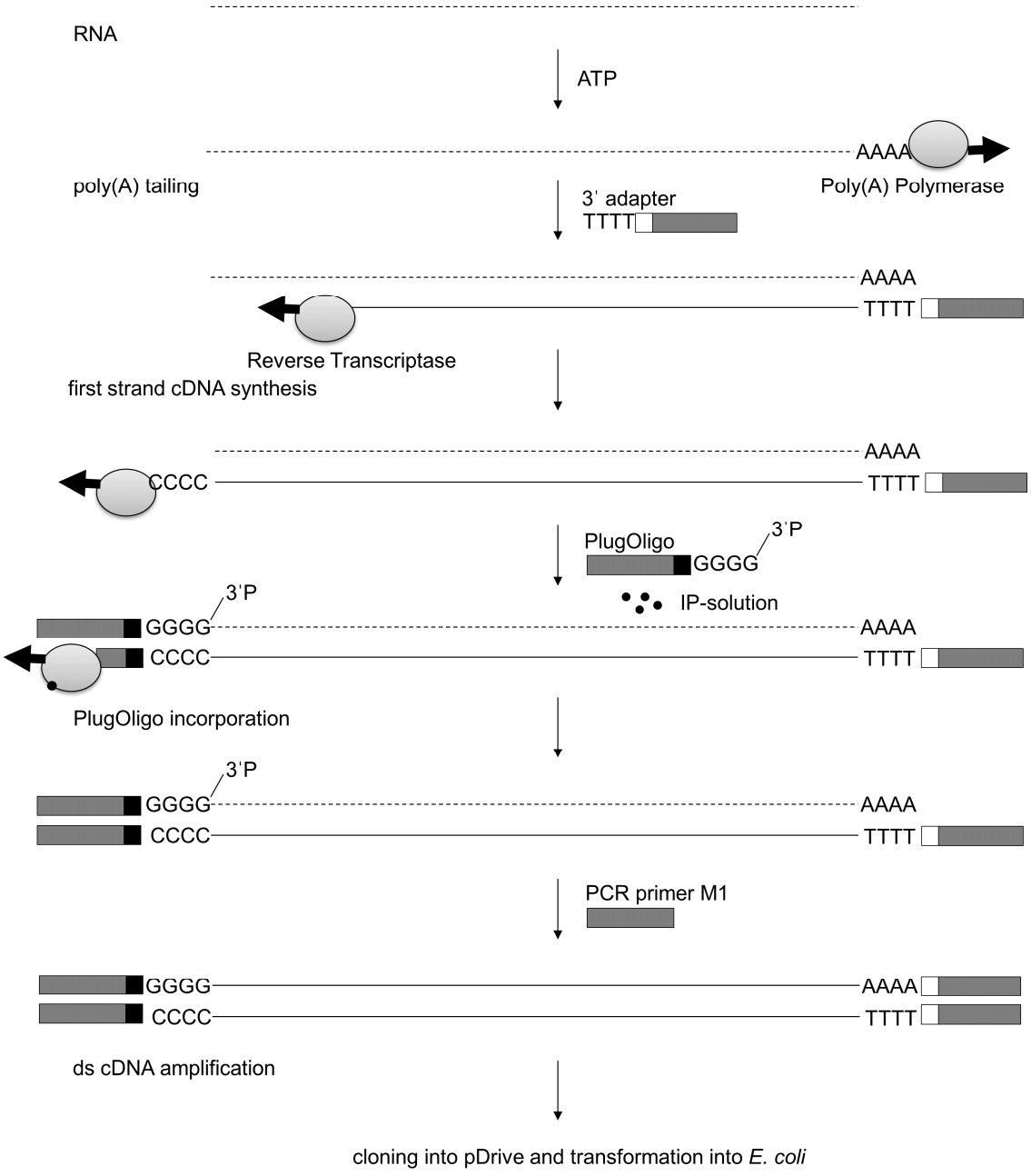

Figure 2.1: Schematic outline of reverse transcription of unknown RNA templates using the Mint-2 cDNA synthesis Kit. The rectangles represent the adapter and primer sequences and their complements. Within the rectangles, grey indicates the common external parts of the adapters, while black and white correspond to the internal parts that differ between the 3' end and 5' end adapters. The IP-solution (solution for incorporation of PlugOligo sequence) increases the efficiency of incorporation.

2.4.8.4 Quantitative real-time PCR (qRT-PCR)

Quantitative real-time PCR (qRT-PCR) is a DNA amplification method with live-quantification of produced DNA (Higuchi et al., 1993). gDNA of *C. acetobutylicum* was prepared as described previously (2.4.2.1) and diluted 1:1,000. PCR targets for genes encoded on the megaplasmid pSOL1 of *C. acetobutylicum* were *adhE2* (CA_P0035, primers: LC_adhE2_fwd, LC_adhE2_rev, Table 2.5) and *adc* (CA_P0165, primers: LC_adc_fwd, LC_Adc_rev, Table 2.5). PCR targets for genes encoded on the chromosome of *C. acetobutylicum* were *gyr* (CA_C007, primers: LC_gyr_fwd, LC_gry_rev, Table 2.5) and *spo0A* (CA_C2071, primers: LC_spo0A_fwd, LC_spo0A_rev, Table 2.5). Strains harbouring plasmids, which encode additional *adhE2* or *spo0A*, were only analyzed with the primers amplifying the genes *gyr* and *adc*. Quantification of *gyr*, *adc*, *adhE2*, and *spo0A* gene fragments was performed using CFX96 Touch™ Real-Time PCR Detection System (Bio-Rad Laboratories GmbH, München, Germany) and DyNAmo ColorFlash SYBR Green qPCR Kit (Thermo Fisher Scientific, Waltham, MA, USA) with 1 cycle of 95 °C for 3 min, 40 cycles of 95 °C for 10 s, 60 °C for 20 s and 72 °C for 10 s. Standard curves derived from applying different dilutions of total DNA. All data were evaluated with Bio-Rad CF-X Manager (Bio-Rad Laboratories GmbH, München, Germany).

Afterwards, relative quantification was achieved using the ΔΔct method (Livak and Schmittgen, 2001). For each strain, the Δct value (ct is threshold cycle) was calculated by the difference of ct values of megaplasmid fragments and chromosomal fragments. All Δct values were normalized to the wildtype strain by calculating the ΔΔct value as difference of the Δct value of wildtype and the Δct value of the recombinant strain. The ΔΔct value was raised to the power of 2 with the assumption that one cycle doubles all products. Therefore, all used primers displayed efficacies between 2.0 and 1.9. The copy number of the megaplasmid pSOL1 in the wildtype strain was set to 1.

For qRT-PCR quantifying the expression of different genes, DNA-free RNA was converted into cDNA and diluted 1:10 as template. Same devices and solutions for qRT-PCR were used as for qRT-PCR with DNA template. Primers are listed in Table 2.5. As housekeeping gene, the *gyr* gene (CA_C007) was selected. For the wild type strain of *C. acetobutylicum* and *C. acetobutylicum* [pIMP1_solB] the *gyr* and the examined genes (*sol* operon, *adc*, *adhE2*, *thlA*, *thlB*, *bdhA*, *bdhB*, *aor*, *hfq*, *spo0A*, *adcR/adcS* operon) were quantified and the Δct value was calculated by the difference

of ct values of the respective gene and the housekeeping gene *gyr* for normalization. For comparison of the wild type and mutant strains, the ΔΔct was generated as difference of the Δct value of wild type and the Δct value of the recombinant strain. The ΔΔct value was raised to the power of 2 with the assumption that one cycle doubles all products. Therefore, all used primers displayed efficacies between 2.0 and 1.9. This calculated value shows the difference in fold expression of the genes in different strains.

2.4.9 Sequencing of nucleic acids

2.4.9.1 Sequencing of PCR fragments and plasmid DNA

Plasmid DNA or PCR products were purified as previously described (2.4.2.2 and 2.4.4.3) and diluted to a final concentration of 20-50 ng μl^{-1}. Samples and respective primer pairs were send to GATC Biotech AG (Konstanz, Germany). Sanger sequencing was performed with the Sanger ABI 3730xl DNA Analyzer (Applied Biosystems, Foster City, CA, USA). Interpretation of results were accomplished either with Clone Manager Suite 7 (Version 7.11, Scientifical Educational Software; Cary, USA) and CLC Main Workbench software v7.6.1 (CLC bio, Aarhus, Denmark) or by alignment of the sequence with the NCBI database (nucleotide blast).

2.4.9.2 Sequencing of DNA

Chromosomal DNA of *C. acetobutylicum* strains was isolated using the MasterPure complete DNA purification Kit (Epicentre, Madison, WI, USA). Illumina shotgun libraries were generated from the extracted DNA according to the protocol of the manufacturer. Sequencing was performed using a MiSeq instrument and the MiSeq reagent Kit version 3, as recommended by the manufacturer (Illumina, San Diego, CA) resulting in between 1,709,028 and 4,887,078 paired end reads (301 bps). For details see Table 3.1. Trimmomatic version 0.32 (Bolger et al., 2014) was used for quality filtering and the remaining 2,036,834 paired end reads. The de novo assembly was performed with the SPAdes genome assembler software 3.5.0 (Bankevich et al., 2012). To determine the coverage of the single contigs generated by SPAdes, the gc_cov_annotate.pl script implemented in the Blobology pipeline (https://github.com/blaxterlab/blobology) was used. This is based on mapping the raw reads on the assembled genome using Bowtie2 (Langmead and Salzberg, 2012) and counting the average mapped number of reads per base for each single contig in the assembly.

2.4.9.3 Sequencing of RNA

RNA was isolated from *C. acetobutylicum* strains as previously described (2.4.3). Remaining genomic DNA was removed by digesting with DNase (2.4.3.3). The Ribo-Zero magnetic Kit (Epicentre Biotechnologies, Madison, WI, USA) was used to reduce the amount of rRNA derived sequences. For sequencing, the strand-specific cDNA libraries were constructed with a NEBNext Ultra directional RNA library preparation Kit for Illumina (New England BioLabs, Frankfurt am Main, Germany) and sequenced by using a MiSeq instrument (Illumina Inc., San Diego, CA, USA) in the paired-end mode and running 2 x 75 cycles. Between 10,499,048 and 21,194,826 raw reads were generated for the samples (Table 8.2). For quality filtering and removing of remaining adaptor sequences, Trimmomatic (Bolger et al., 2014) and a cutoff phred-33 score of 15 were used. The mapping of the remaining sequences was performed with the Bowtie2 program (Langmead and Salzberg, 2012) using the implemented end-to-end mode, which requires that the entire read align from one end to the other. Differential expression analysis were performed with the baySeq program (Mortazavi et al., 2008). Genes with a fold change in expression of ≥1.4, a likelihood value of ≥0.9, and an adjusted P value of ≤0.05 (the P value was corrected by the false discovery rate [FDR] on the basis of the Benjamini-Hochberg procedure) were considered differentially expressed.

2.4.10 DNA transfer in bacteria

2.4.10.1 DNA transfer in E. coli

Preparation of chemically competent cells and transformation

For preparation of chemically competent *E. coli* cells (Inoue et al., 1990) the respective *E. coli* strain was grown in 5 mL LB medium (2.2.1) overnight. 250 mL SOB (2.2.1) in a 2 L erlenmayer flask was inoculated with the overnight culture to an OD_{600} value of 0.1. Incubation was performed aerobically at 18 °C with shaking (100 rpm) to an OD_{600} of 0.6-0.8. After 10 min cooling on ice, the cells were centrifuged (3,900 x g, 10 min, 4 °C). After removing the supernatant, the cells were washed with 30 mL TB buffer (10 mM Pipes, 10 mM $KaCl_2$, pH 6.7) and further incubated for 10 min on ice. After centrifugation (3,900 x g, 10 min, 4 °C), TB buffer was removed and the pellet was dissolved in 10 mL TB Puffer and 1.5 mL dimethyl sulfoxide (DMSO). The chemically competent cells were aliquoted in 200 µL portions. For storage, cells were shocked in liquid nitrogen and stored at -80 °C.

For each transformation 1 µL of plasmid preparation (50-400 ng) or 20 µL ligation mixture (2.4.7.4) was added to 200 µL of chemical competent cells and incubated for 10 min on ice. Cells were heat-shocked by 42 °C for 1 min and afterwards cooled down on ice for 10 min. For regeneration, 800 µL of sterile LB medium were transferred to the cells. Afterwards, cells were grown for 45-60 min at 37 °C with shaking and aliquots of 100-200 µL were plated on agar plates (2.2.1) with respective antibiotics. After one day colonies were visible on the plates.

Preparation of electrocompetent cells and electroporation

For the preparation of electrocompetent *E. coli* cells (Dower et al., 1988) the respective *E. coli* strain was grown in 5 mL LB medium (2.2.1) overnight. 250 mL LB in a 2-L erlenmayer flask was inoculated with the overnight culture to an OD_{600} value of 0.1. Incubation was performed aerobically at 37 °C with shaking (150 rpm) to an OD_{600} of 0.5-0.8. After cooling on ice for 30 min, cells were sedimented by centrifugation (4,000 x g, 10 min, 4 °C). The supernatant was removed and cells were washed twice with 250 mL sterile water and twice with 25 mL of glycerol (10 % (v/v)) (5,000 x g, 10 min, 4 °C). Cells were suspended in 1 mL glycerol (10 % (v/v)) and aliquoted in 50 µL portions. For storage at -80 °C cells were shocked in liquid nitrogen.

For each transformation, 50 µL of electrocompetent cells were added to 1 µL of plasmid preparation (50-400 ng) in a cooled electroporation cuvette (gap width 2 mm) (Biozym Scientific GmbH, Hessisch Oldendorf, Germany). The cells were pulsed with the settings 2.5 kV, 25 µF, and 200 Ω (delay time 4.6 to 5.5 ms) of Gene Pulser Xcell™ pulse generator (Bio-Rad Laboratories GmbH, Munich, Germany). For regeneration 800 µL of sterile LB medium were transferred to the cells. Afterwards, cells were grown for 45-60 min at 37 °C with shaking and aliquots of 100-200 µL were plated on agar plates (2.2.1) with respective antibiotics. After one day colonies were visible on the plates.

2.4.10.2 *DNA transfer in* C. acetobutylicum

Methylation of plasmid DNA

C. acetobutylicum possesses like most bacteria a defense mechanism to differentiate between own DNA and foreign DNA. Therefore, the bacterium methylates its own DNA and unmethylated DNA is cleaved by restriction endonucleases (Adams and Burdon, 1985). To prevent restriction cleavage of transformed plasmids into *C. acetobutylicum*, *E. coli* strains without their natural restriction systems McrA, McrBC or Mrr, but with an

plasmid [pANS1] harbouring the restriction endonuclease of the *B. subitlis* phage Φ3T I (Noyer-Weidner et al., 1983, 1985; Tran-Betcke et al., 1986) were used to methylate the plasmids bevor they were transformed into *C. acetobutylicum.* This restriction endonuclease methylates sequences at the internal cytosine of 5'-GGCC-3' and 5'-GCNGC-3' (Balganesh et al., 1987). This methylation prevents cleavage by restriction endonuclease Cac824I (Mermelstein and Papoutsakis, 1993). After transformation (2.4.10.1) of the shuttle plasmid into *E. coli* XL-1 Blue MRF' [pANS1] for methylation, both plasmids were purified by plasmid preparation (2.4.2.2). Methylation was controlled by digestion (2.4.3.3) with *Sat*I (recognition site 5'-CG*NGC-3'). As the pANS1 plasmid did not contain a Gram-positive origin of replication (ori), it was not necessary to remove the plasmid prior to transformation.

Preparation of electrocompetent cells and electroporation

As described for *C. ljungdahlii* (Leang et al., 2013) the electrocompetent cells of *C. acetobutylicum* were prepared with slight modifications. 50 mL CG medium (2.2.1) were inoculated with OD_{600} 0.1 of a overnight culture of the respective *C. acetobutylicum* strain. Cells were grown anaerobically at 37 °C to an OD_{600} of 0.3-0.5. All further steps were performed in an anaerobic chamber (gas atmosphere: 95 % N_2 and 5 % H_2). The clostridial cells were harvested by centrifugation (3,500 x g, 10 min, 4 °C). The supernatant was removed and cells were washed twice with ice-cold SMP buffer (3,500 x g, 10 min, 4 °C). Afterwards, the pellet was suspended in 600 µL SMP buffer. Subsequently, 120 µL of anti-freezing buffer were added to the cells and mixed. The electrocompetent cells were stored at -80 °C.

SMP buffer

Sucrose	92.4	g	270.0	mM
$MgCl_2 \cdot 6\ H_2O$	0.2	g	1.0	mM
NaH_2PO_4	0.8	g	6.7	mM
ddH_2O	ad 1,000	mL		
pH	7.0			

Anti-freezing buffer contains six parts of DMSO and four parts of SMP buffer.

Preliminary to transformation of *C. acetobutylicum*, plasmids were methylated to protect them from restriction. The electroporation was performed under strictly anaerobic conditions. 25 µL of electrocompetent *C. acetobutylicum* were transferred into pre-cooled 1 mm electroporation cuvettes (Biozym Scientific GmbH, Hessisch Oldendorf, Germany), containing at least 2 µg of plasmid DNA. After an electric pulse

(0.625 kV, 600 Ω, and 25 mF; Gene Pulser Xcell™, Bio-Rad Laboratories GmbH, Munich, Germany), the cells were transferred immediately into 2 mL CG medium. Cell regeneration took place for at least 4 h at 37 °C. Afterwards, 200 µL of the culture were plated on CGM agar plates with appropriate antibiotics. The plates were incubated for 24-48 h at 37 °C. In order to verify the obtained transformants, genomic DNA was isolated (2.4.2.1) followed by PCR targeting respective plasmid DNA (primers: Tobi_primer_fwd_1 and Tobi_primer_rev) and 16S rDNA (primer: fD1 and rP1) (2.4.8.1).

2.4.10.3 Blue-white screening of recombinant E. coli *strains*

Blue-white screening is a useful tool to find transformants with succesfully ligated plasmids (Messing et al., 1977). Therefore, the use of an *E. coli* strain with a deleted lacI^{q}ZΔM15 gene is necessary. The strain is unable to produce the functional β-Galactosidase protein. Plasmids, which possess the *lacPOZ'*, can compensate this deletion. Plasmids such as pDrive habours this *lacPOZ'* gene located at the multiple cloning site. If a ligation is successfully transformed into the vector, the *lacPOZ'* gene is disrupted by integration of the new DNA fragment. After regeneration the transformed cells were streaked out on LB agar plates (2.2.1), which additionally contain 20 µL IPTG (30 mg mL^{-1}) as inducer for the *lacPOZ'* and X-Gal (20 mg mL^{-1}), which is converted by β-Galactosidase into galactose and 5-bromo-4-chloro-3-hydroxyindole. Subsequently, religands show a blue colour compared to successfully ligated transformants, which still exhibit a witish colour. Sequence of the inserted fragments were controlled by PCR (2.4.8) with primers M13 fwd and M13 rev (Table 2.3).

2.4.11 Northern blot analysis for small RNAs (Brown et al., 2001)

For Northern blot experiments DNA-free RNA were separated on denaturating polyacrylamide gels (2.4.5.3). Marker bands were indicated on the gel with a syringe after EtBr staining (2.4.5.4). Afterwards, separated RNA was blotted semi-dry on to an Amersham Hybond^{TM}-N^{+} membrane (GE Healthcare Europe GmbH, Freiburg, Germany) using a FastBlot B33 (Biometra, Göttingen, Germany) with a power supply adjusted to 2 mA cm^{-2}. The blot was constructed as follows starting at the anode side of the blotter: 3 layers of whatman paper, then the membrane and the gel, finally 3 layers of whatman paper again. Implied traces of the marker bands of the gels were transferred to the membrane. After drying the membrane for one hour, the unlabelled

probe SolB_RNA_antisense (Table 2.4), which is complementary to the labelled probe solB_sonde (Table 2.4), was pippeted on the indicated marker positions on the membrane. RNA was crosslinked by an Ultraviolet Crosslinker (Amersham Biosciences, Freiburg, Germany) adjusted to 254 nm, 90 s and 1200 µJ cm^{-2}. For hybridization of solB_sonde with the membrane, primer has to be radioactively labelled (2.4.7.5). Pre-hybridization of the membrane was achieved by incubation at 65 °C for one hour with hybridisation buffer (50 mM Tris, 0.1 % sodium pyrophosphate, 0.2 % albumin fraction V, 0.2 % polyvinylpyrrolidone, 0.2 % ficoll 400, 1 % SDS, 1 M NaCl, 0.1 mg mL^{-1} herring sperm) in a hybridisation oven (Biometra GmbH, Göttingen, Germany). Afterwards, the radioactively labelled primer was added to the hybridisation buffer and hybridisation took place over night at 65 °C. Labelled membrane was washed with washing solution 1 (2x SSC (0.3 M NaCl, 0.03 trisodium citrate), 1 % SDS) for 15 min at 65 °C, next with washing solution 2 (1x SSC, 1 % SDS) for 15 min at 65 °C, and with washing solution 3 (1x SSC, 1 % SDS) for 15 min at 65 °C.
The membrane was incubated over night with BAS-MP plates (Fujifilm, Tokyo, Japan), and the radioactively labelled results were visualized with a Bio-Imaging Analyzer BAS-100 (Fujifilm, Tokyo, Japan). RiboRuler Low Range RNA Ladder (Thermo Fisher Scientific, Waltham, MA, USA) ranging from 100 to 1,000 nt was used as RNA marker.

2.4.12 Engineering *C. acetobutylicum hfq* integration mutants

The ClosTron™ Gene Knockout System was used for gene inactivation in *C. acetobutylicum* by targeted integration in the *hfq* gene (Heap et al., 2007, 2010). The ClosTron™ system allows the construction of stable mutants in *Clostridium* species using a bacterial group II intron. Group II introns are catalytic active RNAs and are mobile elements as they contain an intron-encoded protein (IEP). The IEP can be programmed to integrate the group II intron at nearly every region of the genome. Additionally, the LtrA protein is essential for the process as it binds to the group II intron. This free protein-RNA-complex localises with the help of IEP at the desired gene and LtrA cleaves the DNA resulting in a double strand brake. Intron RNA is now integrated through the reverse transcription activity of LtrA and the repair system of the cell. To enforce this stable integration a resistance gene is essential. Therefore, the group II intron encodes for a clarithromycin resistance. This resistance gene is encoded in divergent direction to the other genes encoded in the group II intron and contains a group I intron. This leads to a strand specific cleavage. If the clarithromycin gene is transcribed in the right orientation for translation, the group I intron inhibits the

formation of the protein. In contrast, if the opposite strand is transcribed as for the group II intron, the intron group I is spliced out and after integration of the group II intron into the genome the clarithromycin gene can be transcribed without group I intron. This confers only clarithromycin resistance if the integration event took place.

The target sites of *hfq* (CA_C1834) integration were identified and the 353 bps intron-targeting fragment were designed using a computer algorithm (Perutka et al., 2004) available on the website http://www.clostron.com. For the *hfq* gene, two integration sites of group-II-intron were used, one at position 79 on the non-coding strand and the other at position 168 on the coding strand. The 353 bps intron-targeting fragments were synthesized and integrated into the shuttle vector [pMTL007C-E2] by DNA2.0 (Menlo Park, Ca, USA). The delivered plasmids were named [pMTL007C-E2_79shfq] for integration at position 79 and [pMTL007C-E2_168ahfq] for integration at position 168. The methylated plasmids (2.4.10.2) were electroporated into *C. acetobutylicum* and selected on CGM agar plates containing 15 µg mL^{-1} thiamphenicol (2.4.10.2). The correct transformants were transferred on CGM plates containing 2.5 µg mL^{-1} clarithromycin. Verification of correct integration was carried out by preparation of genomic DNA (2.4.2.1) and PCR (2.4.8.1) using the primers hfq_fwd and hfq_rev. After proved integration via PCR with primers hfq_fwd and hfq_rev (Table 2.5) the colonies were streaked out for further 3 times on agar plates containing 2.5 µg mL^{-1} clarithromycin. To check if the strains lost the integration plasmids and contain only the integration, strains were cultivated in CG medium containing 15 µg mL^{-1} thiamphenicol and 2.5 µg mL^{-1} clarithromycin. Furthermore, genomic DNA was prepared (2.4.2.1) and a PCR (2.4.8.1) conducted with primer pMTL007-e2_nachweis_fwd and pMTL007-e2_nachweis_rev targeting the plasmid [pMTL007C-E2].

2.5 Protein methods

2.5.1 Overproduction of proteins in *E. coli*

The heterologous expression of *hfq* (CA_C1834) was achieved by transformation of the plasmids pQE_hfq in *E. coli* M15 [pREP4]. The plasmid pQE_hfq is based on the vector system of pQE_30 purchased by the company QIAGEN GmbH (Hilden, Germany). This plasmid provides an N-terminal polyhistidin-tag (his-tag) for purification of the expressed gene and a T5 promoter which can be recognized by the RNA polymerase II. For each overexpression, plasmid pQE_hfq was again transformed into electrocompetent *E. coli* M15 [pREP4] cells (2.4.10.1). The preculture

was grown aerobically overnight at 37 °C in 5 mL LB medium (2.2.1) with 100 µg mL^{-1} ampicillin and 30 µg mL^{-1} kanamycin. 250 mL TB medium (2.2.1) was inoculated to an OD_{600} 0.1 with the preculture and respective antibiotics. Cells were grown to an OD_{600} of 1-2 and induced with 1 mM IPTG. This is necessary as the [pREP4] plasmid encodes the *lacI* repressor, which binds to the operator sites encoded upstream of the *hfq* gene in [pQE_hfq]. This mechanism prevents cell death of toxic protein products. After induction cells were harvested after 4 h and centrifuged (4,000 x g, 10 min, 4 °C). The supernatant was removed and pelleted cells were stored until disruption at -20 °C.

2.5.2 Cell disruption

2.5.2.1 Cell disruption via French Press

For purification of Hfq (CA_C1834) after heterologous production with *E. coli* M15 [pREP4][pQE_hfq], cells were disrupted via French Press (Milner et al., 1950). The cells were dissolved in 3 volumes of their wet weight with the appropriate buffer for further applications. Suspension was transferred into a precooled French® Pressure Cell (FRENCH® Pressure Cell/Press, G.HEINEMANN Ultraschall- und Labortechnik; Schwäbisch Gmünd, Germany). With this device cells were disrupted with a pressure of 10 MPa. To improve the results, disruption was repeated three times. Afterwards, cell fragments and membrane proteins were eliminated through ultracentrifugation (140,400 x g, 90 min, 7 °C). Further experiments were performed immediately with the supernatant.

2.5.2.2 Cell disruption via Ribolyser

For generating cell-free extract, 5 mL of *C. acetobutylicum* wild type were harvested and after centrifugation suspended in 0.8 mL 1x PBS (2.2.4.3). Cells were transferred in cryo tubes containing glass beads. Mechanical cracking of the cells was achieved by using a homogenisator (3 cycles, 45 s, 6,500 m s^{-1}, RiboLyser, Hybaid Ltd., Middlesex, UK), followed by centrifugation (11,000 x g, 20 min, 4 °C) to obtain cell-free extract for the stabilization assay (2.6.4).

2.5.3 Purification of proteins with magnetic beads

For the purification of the 6x his-tagged Hfq the Dynabeads® His-Tag Isolation and Pulldown (Thermo Fisher Scientific, Waltham, MA, USA) were used. These beads bind with high selectivity to his-tagged proteins. Prior to cell disruption (2.5.2.1) cells were suspended in 1x PBS (2.2.4.3). 700 µL of crude extract were added to the beads and incubated for 10 min at room temperature. After 5 washing steps with 1x binding buffer,

Hfq was either eluted in 75 µL 1x elution buffer or for pulldowns (2.6.1, 2.6.2) mixed with possible targets prepared in 700 µL 1x pulldown buffer. Pulldowns were incubated for a period of 30 min at room temperature and subsequently washed 5 times with 1x binding buffer. Hfq and targets were eluted identical to single Hfq elution. After elution, purification of Hfq was controlled by a SDS-polyacrylamide gelelectrophoresis (2.5.5).

2x Binding buffer				
$Na_2PO_4 \cdot 12\ H_2O$	19.0	g	100.0	mM
NaCl	17.5	g	600.0	mM
Tween®-20	100	mg	20.0	‰
ddH_2O	ad 500	mL		
pH	8.0			

2x Pulldown buffer				
$Na_3PO_4 \cdot 12\ H_2O$	2.5	g	6.5	mM
NaCl	4.1	g	140.0	mM
Tween®-20	100	mg	20.0	‰
ddH_2O	ad 500	mL		
pH	7.4			

Elution buffer				
Imidazole	10.2	g	300.0	mM
$Na_3PO_4 \cdot 12\ H_2O$	9.5	g	50.0	mM
NaCl	8.8	g	300.0	mM
Tween®-20	50.0	mg	10.0	‰
ddH_2O	ad 500	mL		
pH	8.0			

2.5.4 Determination of protein concentration

Protein concentration of cell-free extracts was determined by using BCA™ protein assay Kit (Thermo Fisher Scientific, Waltham MA, USA) following the manufacturer's instructions. BSA standard curves were accomplished with defined concentrations of BSA, ranging from 0 to 2 mg mL^{-1}. The colorimetric detection was measured at 562 nm in 96-well microtiter plates.

2.5.5 SDS-Polyacrylamide gelectrophorese (SDS-PAGE)

In order to verify protein purification, SDS-PAGE was performed. Here, proteins were separated according to their molecular mass as SDS denaturates the proteins and

adds a negative charge (Laemmli, 1970). Either ready-to-use gels (Novex® 16 % Tris-glycine gels, Thermo Fisher Scientific, Waltham, MA, USA) were used or individual gels with 15 % were prepared as described in Table 2.10 and Table 2.11. The prepared mixture of a resolving gel was poured into a vertical chamber. After polymerisation, the stacking gel was poured on top of the resolving gel and a comb was positioned. After polymerisation, the chamber was filled with 1x SDS running buffer and samples, mixed with 4x SDS loading buffer, were boiled for 10 min at 95 °C. After probes were pipetted onto the gel, gel electrophoresis was performed for 90 min at 120 V. Additionally, 3 µL of PageRuler™ Prestained Protein Ladder (Thermo Fisher Scientific, Waltham, MA, USA) as marker were used.

10x SDS running buffer

Glycine	150.1	g	2.0	M
Tris base	30.3	g	250.0	mM
SDS	10.0	g	34.7	mM
ddH_2O	ad 1,000	mL		

4x SDS loading buffer

Tris-HCl (1.25 M, pH 6.8)	10.0	mL	250.0	mM
β-Mercaptoethanol	10.0	mL	20.0	% (v/v)
Glycerol	20.0	mL	40.0	% (v/v)
SDS	2.0	g	138.7	mM
Bromphenol Blue	20.0	mg	1.2	mM
ddH_2O	ad 50	mL		

Table 2.10: Composition of the 15 % resolving gel

Component	Amount	
Rotiphorese® NF-Acrylamide/Bis-solution 40 % (29:1)[a]	7.5	mL
Resolving gel buffer (1.5 M Tris-HCl, 13.9 mM SDS, pH 8.8)	5.0	mL
APS (10 % (w/v))	0.20	mL
TEMED	0.02	mL
ddH_2O	ad 20	mL

[a] Carl Roth GmbH & Co. KG, Karlsruhe, Germany

Table 2.11: Composition of the 4 % stacking gel

Component	Amount	
Rotiphorese® NF-Acrylamide/Bis-solution 40 % (29:1)[a]	1.25	mL
Stacking gel buffer (500 mM Tris-HCl, 13.9 mM SDS, pH 6.8)	1.25	mL
APS (10 % (w/v))	0.10	mL
TEMED	0.01	mL
ddH_2O	ad 10	mL

[a] Carl Roth GmbH & Co. KG, Karlsruhe, Germany

2.5.6 Silver staining

To control SDS-PAGE, gels were stained with silver (Chevallet et al., 2006). Proteins on gels were fixed with fixative solution and afterwards washed twice with ethanol (50 % (v/v)) for 5 min. Gels were incubated for 1 min in thiosulfate solution and washed three times with H_2O for 5 s. Then, gels were covered with freshly prepared staining solution and incubated for 15 min. After three washing steps with H_2O for 5 s proteins were visualized in the gel with developer solution. Finally, the reaction was stopped by addition of an aqueous solution of EDTA (50 mM).

Fixative solution

Methanol	500.0	mL	50.0	% (v/v)
Formaldehyde (37 %)	0.5	µL	18.5	‰ (v/v)
Glacial acetic acid	120.0	mL	12.0	% (v/v)
ddH_2O	ad 1,000	mL		

Thiosulfate solution

$Na_2S_2O_3 \cdot (H_2O)_5$	25.0	mg	0.2	mM
ddH_2O	ad 500	mL		

Staining solution

Formaldehyde (37 %)	50.0	µL	18.5	‰ (v/v)
$AgNO_3$	0.2	mg	11.7	mM
ddH_2O	ad 100	mL		

Developer solution

Na_2CO_3	6.0	g	56.6	mM
Formaldehyde (37 %)	50.0	µL	1.9	‰ (v/v)
$Na_2S_2O_3 \cdot (H_2O)_5$	0.4	mg	12.6	mM
ddH_2O	ad 1,000	mL		

2.5.7 Western blot

Western blot analysis was used to transfer proteins from SDS-PAGE to nitrocellulose membranes (Towbin et al., 1979). The negative charge of the proteins results im migration to the anode. In this study, the method of semi dry Western blot was applied. Blotting paper and the Porablot NCP (MACHEREY-NAGEL GmbH & Co. KG, Düren) were sliced to the size of the membrane and soaked with transfer buffer. The blot was constructed as follows: 3 layers of blotting paper on top of the anode side (Fastblot B3,

Biometra GmbH, Göttingen, Germany), then the nitrocellulose membrane and the gel were applied. Finally, three layers of blotting paper completed the set-up. Proteins were transferred onto the membrane with 0.8 mA cm^{-2} for 45 min.

Transfer buffer

Tris	5.8	g	47.9	mM
SDS	0.4	g	1.3	mM
Glycine	2.8	g	37.3	mM
Methanol	200.0	mL	20.0	% (v/v)
ddH_2O	ad 1,000	mL		

2.5.8 Dot blot

The advantage of a dot blot is an easy verification for presence of antigens without need for gel electrophoresis. The membrane was first covered with TE buffer for 10 min. After drying the membrane, 10 µL of the antigen containing solution was pipetted directly on the membrane. The membrane was crosslinked by an Ultraviolet Crosslinker (Amersham Biosciences, Freiburg, Germany) adjusted to 254 nm, 90 s and 1200 µJ cm^{-2}. It is possible to store the membrane at 4 °C.

2.5.9 Immunostaining

Immunostaining was performed for detection of heterologously produced Hfq from *C. acetobutylicum* in *E. coli* with a his-tag. After blotting (2.5.7) the membrane was blocked with blocking buffer overnight at 4 °C. Next, an incubation for 1 h with mouse monoclonal antibody Anti-His_6 (Roche Diagnostics Deutschland GmbH, Mannheim; Germany) was applied (1:200 in blocking buffer). After three washing steps with 1x PBS (2.2.4.3) for 15 min, the second antibody Polyclonal Rabbit Anti-Mouse Immunoglobulins/HRP (Dako Deutschland GmbH, Hamburg, Germany) was diluted in 1x PBS (1:1,000) and incubated for 1 h. To remove unbound antibodies, three additional washing steps with 1x PBS were conducted. For detection, the horseradish peroxidase is coupled to the second antibody, which can oxidise luminol. This reaction leads to emission of light. Therefore, substrate and an enhancer, which were provided by the Pierce ECL Western Blotting Substrate (Thermo Fisher Scientific, Waltham, MA, USA), have to be added to the membrane. Reaction was performed as described in the provided protocol and for detection of light emission Kodak Biomax XAR film (Sigma-Aldrich Chemie GmbH, Steinheim, Germany) were used and developed after respective length of exposure.

Blocking buffer

BSA	1.0	g	2.0	% (w/v)
Tween®-20	250.0	µL	0.5	% (v/v)
1x PBS (2.2.4.3)	ad 50	mL		

2.5.10 Amylase activity test

Amylase activity test was performed with *C. acetobutylicum* strains for verification of presence of the megaplasmid pSOL1 (Harris et al., 2002; Sabathé et al., 2002). 100 colonies of each strain were streaked out on 2x XYTGA (2.2.1) and incubated for 1-2 days. Grown colonies were sprayed with Lugol's Solution (1 g iodine, 2 g potassium iodide, 300 mL H_2O). Reaction of iodine with starch shows a brownish colour on the plates. If starch is degraded in the plates, no brownish colour is developed around the bacteria.

2.6 Interaction assays

2.6.1 Pulldown assay with Hfq and RNA

In order to identify targets of Hfq, pulldown assays with isolated DNA-free and rRNA-free RNA from *C. acetobutylicum* wild type (2.4.3.1, 2.4.3.3, 2.4.3.4) and heterologously produced as well as purified Hfq (2.5.1, 2.5.2.1, 2.5.3) from *E. coli* M15 [pREP4][pQE_hfq] were performed. After binding of Hfq to the magnetic beads and 5 washing steps, RNA of *C. acetobutylicum* (20 µg) was added in 1x pulldown buffer. After incubation of 30 min at room temperature, beads with Hfq and target RNA were washed and eluted (2.5.3). Next, phenol/chloroform extraction (2.4.4.1) was accomplished to get rid of Hfq and RNA was purified by ethanol precipitation (2.4.4.2). Hfq purification was controlled after elution with an SDS-PAGE and silver staining (2.5.5, 2.5.6). RNA was poly(A) tailed for reverse transcription into dcDNA (2.4.8.3.2) and cloned into the pDrive vector (2.4.7.4). After transformation (2.4.10.1) of the constructed plasmids, clones were analyzed via colony PCR (2.4.8.2) and agarose gel electrophorese (2.4.5.1) for inserts. PCR, which showed an integrated fragment, were sent for sequencing (2.4.9.1).

2.6.2 Pulldown assay with Hfq and labelled SolB

Hfq from *C. acetobutylicum* was heterologously produced in *E. coli* M15 [pREP4][pQE_hfq] and purified with magnetic beads. Before elution of Hfq, biotin-labelled SolB was added to the Hfq-bead complex and incubated for 30 min at room

temperature. After 5 washing steps, elution was accomplished. Hfq purification was controlled with an SDS-PAGE and silver staining (2.5.5, 2.5.6). Co-purification of SolB was proved by performing a dot blot (2.5.8) by detection of SolB via biotin with Chemiluminescent Nucleic Acid Detection Module (Thermo Fisher Scientific, Waltham, MA, USA) and X-ray films. As a control, labelled SolB was incubated together with magnetic beads, but without Hfq.

2.6.3 Electrophoretic mobility shift assay (EMSA)

Interaction between SolB and Hfq was tested with electrophoretic mobility shift assays. SolB was labelled as mentioned in section 2.4.7.6. Hfq from *C. acetobutylicum* was heterologously produced in *E. coli* M15 [pREP4][pQE_hfq] and purified with magnetic beads (2.5.1, 2.5.2.1, 2.5.3.). EMSA was performed as described in the manual instructions of LightShift™ Chemiluminescent RNA EMSA Kit (Thermo Fisher Scientific, Waltham, MA, USA). Deviations were made regarding the amount of the unlabelled RNA SolB, which was just used in threefold molar excess to the labelled SolB. Reactions were incubated for 30 min at room temperature containing different concentrations of Hfq. Binding reactions were mixed with native RNA loading buffer and run on a non-denaturating polyacrylamide gel (0). Afterwards, protein and RNA were transferred onto a membrane (2.5.7) and biotin was visualized with Chemiluminescent Nucleic Acid Detection Module (Thermo Fisher Scientific, Waltham, MA, USA) and X-ray films.

2.6.4 Stabilization assay

Hfq from *C. acetobutylicum* was heterologously produced in *E. coli* M15 [pREP4][pQE_hfq] and purified with magnetic beads (2.5.1, 2.5.2.1, 2.5.3.). SolB was produced via in vitro transcription. For the experiment, RNases of *C. acetobutylicum* were necessary and were generated by using cell-free extract of *C. acetobutylicum* (2.5.2.2). Composition of reactions was set up as described below and samples were incubated at 37 °C for different period of times ranging from 0 to 18 min. Subsequently, a non-denaturating gel electrophoresis was performed (2.4.5.1) following staining with EtBr (2.4.5.4). As a control, two approaches were incubated without crude extract either 0 min and 18 min. Furthermore, a control was used with 1x elution buffer instead of Hfq.

Composition	1	2
RNA SolB	1.0 µL	1.0 µL
Hfq	2.0 µL	
1x Elution buffer (2.5.3)		2.0 µL
1x PBS (2.2.4.3)	2.0 µL	2.0 µL
Cell free extract	5.0 µL	5.0 µL

2.7 Bioinformatics

Databases used for e.g. blast analysis are listed in Table 2.12.

Table 2.12: Databases used in this study (as of October 2016)

Database	Source
Integrated Microbial Genomes Expert Review database (IMG/ER)	http://img.jgi.doe.gov/er
Kyoto Encyclopedia of Genes and Genomes (KEGG)	http://www.genome.jp/kegg
National Center for Biotechnology Information (NCBI)	http://www.ncbi.nlm.nih.gov

Used software during this work are displayed in Table 2.13.

Table 2.13: Software used in this study

Software	Version	Source
CLC Main Workbench	7.6.1	CLC bio, Aahrus, Denmark
Clone Manager	7.11	Scientific & Educational Software, Cary, USA
Enhance Map Draw	4.10	Scientific & Educational Software, Cary, USA
MacBAS	2.3	Fuji Photo Film Co, Ltd., Tokyo, Japan
TotalChrom	6.3.1	PerkinElmer Inc., Waltham, MA, USA
OPEN-Lab CDS	A.01.03.	Agilent Technologies, Santa Clara, CA, USA
The mfold Web Server (Zuker, 2003)	3.6	http://mfold.rna.albany.edu/?q=mfold/RNAFolding-Form
IntaRNA (Smith et al., 2010)	1.2.5	http://rna.informatik.unifreiburg.de:8080/index.jsp
Clustal Omega (Sievers et al., 2014)	1.2.2	http://www.ebi.ac.uk/Tools/msa/clustalo/
TargetRNA2 (Kery et al., 2014)		http://tempest.wellesley.edu/~btjaden/TargetRNA2/contact.html

3 Results

3.1 Characterizing the regulatory RNA SolB of *C. acetobutylicum*

3.1.1 Transcription of *solB* and genes involved in solventogenesis

The small regulatory RNA SolB represses the production of acetone and butanol in a *Clostridium acetobutylicum solB* overexpression mutant (Schiel et al., 2010). The transcription of *solB* was proven for *C. acetobutylicum* [pIMP1_solB] by Northern blot, however, in the *C. acetobutylicum* wild type strain the transcription of *solB* was not detected by Northern blot (Zimmermann, 2013). In this study, Northern blot was again performed, but this time adapted to small RNAs, in contrast to the previously performed experiments. Therefore, a denaturating polyacrylamide gel instead of an agarose gel was used and blotting procedure was performed with a semi-dry method. RNA was prepared with TriZol of strains *C. acetobutylicum* wild type and *C. acetobutylicum* [pIMP1_solB] out of 50 mL culture medium (MES). 20 µg DNA-free RNA was separated on a polyacrylamide gel and blotted onto the membrane. After hybridization of the membrane with radioactively labelled probe solB_sonde, the blot was visualized via Bio-Imaging Analyzer BAS-100 (Fujifilm, Tokyo, Japan). The experimental procedure was performed for at least 6 times with an identical result. One result is displayed exemplary in Figure 3.1. The RNA of *C. acetobutylicum* [pIMP1_solB] (lane 2) showed a transcript just below 200 nt. No signal was detected for the RNA of *C. acetobutylicum* wild type (lane 1).

The following step was to elucidate which genes of solvent production are affected by the overexpression of *solB* in *C. acetobutylicum*. For this purpose, qRT-PCR was performed. Triplicates of strains *C. acetobutylicum* wild type and *C. acetobutylicum*

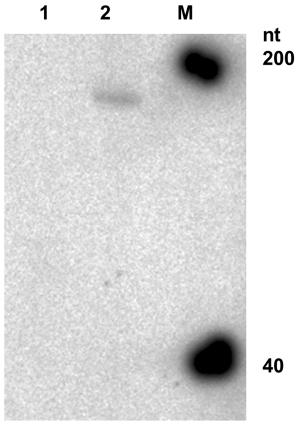

Figure 3.1: Northern blot analysis of SolB detected with a specific γ-[ATP]-labelled RNA probe in total RNA derived from *C. acetobutylicum* wild type (1) and *C. acetobutylicum* [pIMP1_solB] (2). M, RiboRuler Low Range (Thermo Fisher Scientific, Waltham, MA, USA) and probe solB_sonde**.**

[pIMP1_solB] were grown in 50 mL MES medium and harvested after reaching the stationary growth phase. At this time point, production of solvents started in the wild type strain. DNA-free RNA was isolated and cDNA was synthesized using random primers. Transcript levels were determined for the following genes: *sol* operon (comprising *ctfA* (CA_P162), *ctfB* (CA_P163), and *adhE* (CA_P164)), *adc* (CA_P165), *adhE2* (CA_P0035), *thlA* (CA_C2873), *thlB* (CA_P0078), *bdhA* (CA_C3299), *bdhB* (CA_C3298), *aor* (CA_C2018), *hfq* (CA_C1834), *spo0A* (CA_C2071), and the *adcS/R* operon (comprising *adcS* (CA_P0036), and *adcR* (CA_P0037)). None of the tested genes showed an up-regulation in expression in the *C. acetobutylicum solB* overexpression strain compared to the wild type strain (Figure 3.2). Genes *thlA, bdhA, bdhB, aor, hfq,* and *spo0A* were not differentially expressed in the *C. acetobutylicum* overexpression mutant. A significant down-regulated expression was determined for the genes *adc*, *adhE2*, and *thlB* in the *C. acetobutylicum solB* overexpression strain. Furthermore, the genes of *sol* and *adcS/R* operon showed a reduced expression in the *C. acetobutylicum solB* overexpression strain (Figure 3.2).

To sum up, expression of *solB* could only be proven in the strain *C. acetobutylicum* [pIMP1_solB]. Overexpression of *solB* in the strain *C. acetobutylicum* decreased transcription of several genes involved in solventogenesis, which are encoded on the megaplasmid pSOL1.

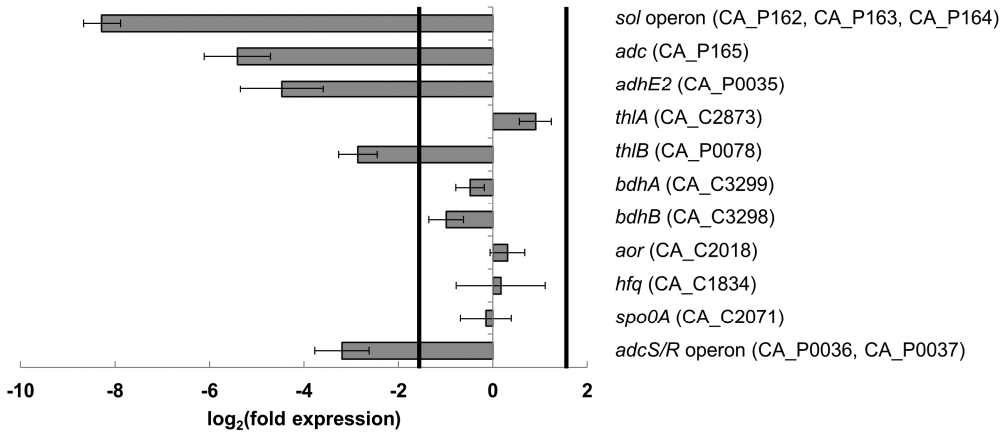

Figure 3.2: Fold expression of different genes of strain *C. acetobutylicum* [pIMP1_solB] compared to *C. acetobutylicum* wild type. Negative values represent down-regulation and positive values represent up regulation compared to the *C. acetobutylicum* wild type strain. Black lines indicate threshold of differentially expressed genes. *sol* operon, acetoacetyl-CoA:acetate/butyrate-CoA-transferase (*ctfA/B*) and alcohol/aldehyde dehydrogenase (*adhE*); *adc*, acetoacetate decarboxylase; *adhE2*, alcohol/aldehyde dehydrogenase ; *thlA*, acetyl-CoA acetyltransferase; *thlB*; acetyl-CoA acetyltransferase; *bdhA*, NADH dependent butanol dehydrogenase; *bdhB*, NADH dependent butanol dehydrogenase; *aor*, aldehyde:ferredoxin-oxidoreductase; *hfq*, host factor I protein Hfq; *spo0A*, transcription factor Spo0A; *adcS/R* operon comprising AdcS and AdcR.

3.1.2 Binding partners of SolB

The transcripts of s*po0A* and *adhE2* were predicted as possible binding partners of SolB (Zimmermann, 2013). The transcription factor Spo0A plays a crucial role for solventogensis and sporulation (Harris et al., 2002) and AdhE2 is important for butanol production (Fontaine et al., 2002; Yoo et al., 2016). Both mRNAs offer a putative binding site for SolB at their ribosomal binding site (RBS), which could lead to a blocked translation and in turn a decreased solvent production. Phenotypic effects of *solB* overexpression in *C. acetobutylicum* can be suppressed by overexpression of *spo0A* in the *C. acetobutylicum solB* overexpression mutant (Zimmermann, 2013). In order to elucidate if overexpression of *adhE2* is also able to reverse impacts of overexpressed *solB,* strain *C. acetobutylicum* [pIMP1_solB_adhE2] was analyzed. For the construction of plasmid pIMP1_solB_adhE2 (Figure 3.3A), the *adhE2* gene was amplified via PCR with primers adhE2_fwd_pfoI and adhE2_rev_pfoI (Table 2.5) from gDNA of *C. acetobutylicum* wild type. The PCR product was ligated into the restriction site *Pfo*I of the pIMP1_solB plasmid. Afterwards, the respective plasmid pIMP1_solB_adhE2 was transformed into *C. acetobutylicum* and successful transformation was proven by preparation of gDNA and PCR with primers Tobi_primer_fwd_1 and Tobi_primer_rev (Table 2.5).

To analyze growth behaviour and product formation of *C. acetobutylicum* [pIMP1_solB_adhE2] growth experiments were performed with strains *C. acetobutylicum* [pIMP1], *C. acetobutylicum* [pIMP1_solB], *C. acetobutylicum* [pIMP1_solB_spo0A], and *C. acetobutylicum* [pIMP1_solB_adhE2] in 50 mL MES-buffered medium. Mean values of at least three independent experiments are displayed in Figure 3.3 monitoring optical density (B) and product formation of butanol (C), butyrate (D), ethanol (E), and acetone (F). All strains showed similar growth rates and reached comparable maximal optical density. The empty vector control strain *C. acetobutylicum* [pIMP1] as well as the double overexpression strains *C. acetobutylicum* [pIMP1_solB_spo0A] and *C. acetobutylicum* [pIMP1_solB_adhE2] produced approximately 65 mM butanol and 30 mM butyrate. The production of acetone differs between the respective strains from 10 mM to 30 mM. In contrast, strain *C. acetobutylicum* [pIMP1_solB] showed an increased butyrate concentration of 100 mM. The production of butanol and acetone was significantly reduced and only marginal amounts of 10 mM and 2 mM, respectively, were detected. The highest level

of ethanol was measured for strain *C. acetobutylicum* [pIMP1_solB_adhE2] with 30 mM. All other strains reached only a maximum of 10 mM ethanol.

The putative binding motif for SolB is located in the 5' untranslated region of the *spo0A* and *adhE2* mRNA. The question arose whether the putative binding site in the transcripts of the genes *spo0A* and *adhE2* is sufficient to generate double overexpression mutants, which are still able to produce high amounts of solvents. Therefore, plasmids were constructed containing the sequence encoding SolB and the putative binding sequence of the genes *spo0A* or *adhE2* for SolB, but without the complete protein coding sequence of *spo0A* or *adhE2*. To achieve this, the

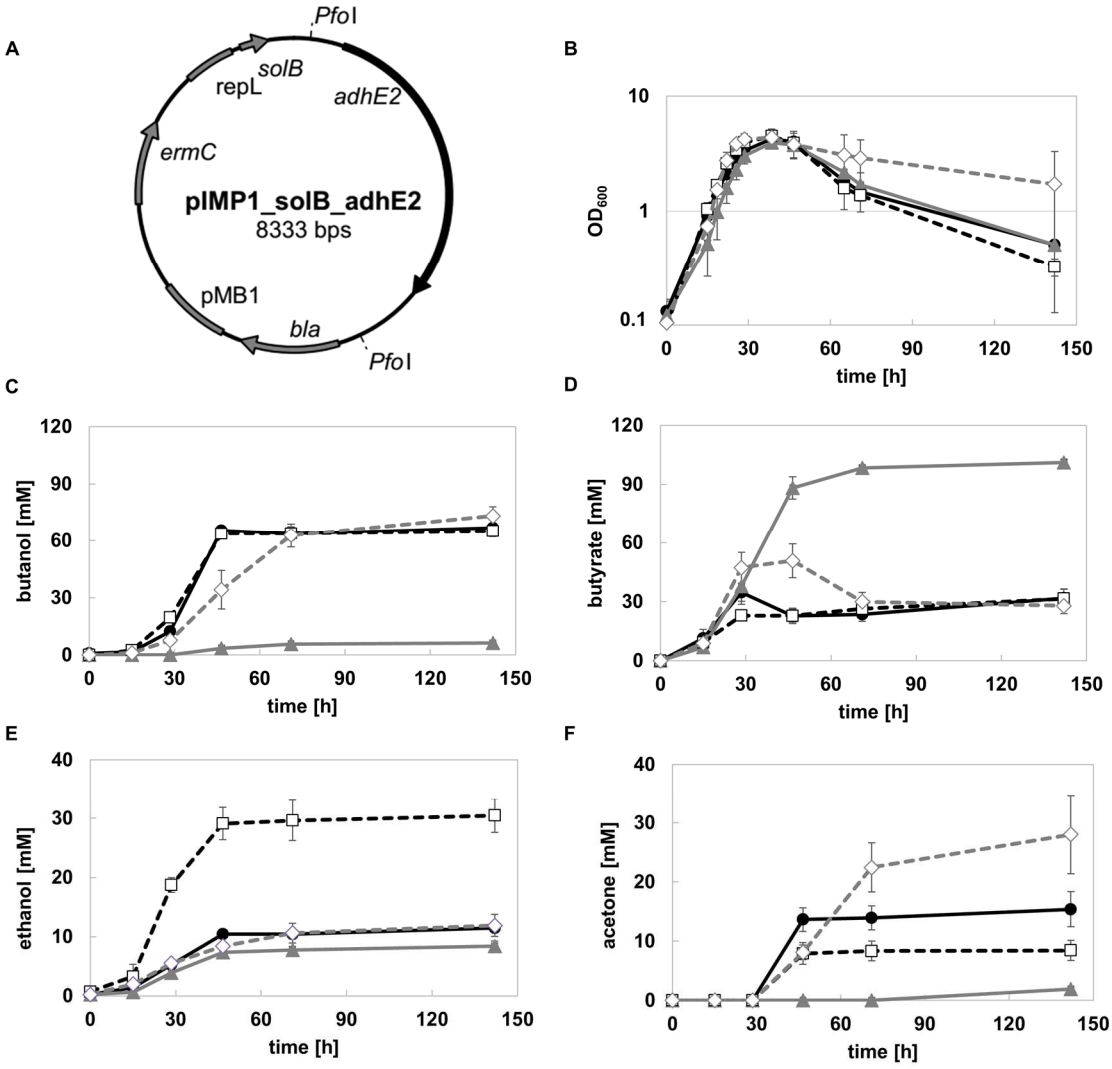

Figure 3.3: (A) Overexpression plasmid pIMP1_solB_adhE2 containing *solB* and *adhE2*. (B-F) Growth behaviour and product formation of *C. acetobutylicum* [pIMP1] (●), *C. acetobutylicum* [pIMP1_solB] (▲), *C. acetobutylicum* [pIMP1_solB_adhE2] (□), and *C. acetobutylicum* [pIMP1_solB_spo0A] (◇) were measured during growth in batch fermentation with 50 mL MES-buffered medium (n = 3); (B) growth behaviour, (C) butanol, (D) butyrate, (E) ethanol, and (F) acetone. *bla*, ampicillin resistance gene; pMB1, ori for Gram-negative bacteria; *ermC*, erythromycin resistance gene; repL, ori for Gram-positive bacteria; *solB*, regulatory RNA SolB; *adhE2*, alcohol/aldehyde dehydrogenase 2 gene.

plasmid pIMP1_solB_spo0A was digested with *Sfo*I and *Mun*I and plasmid pIMP1_solB_adhe2 was digested with *Eco*O109I. The digested plasmids were blunted and ligated containing now shortened selected sequences of the genes *spo0A* and *adhE2*. Constructed plasmids were named pIMP1_solB_spo0A_begin (Figure 3.5A) and pIMP1_solB_adhE2_begin (Figure 3.4A) and transformed into *C. acetobutylicum*. Successful transformation was proven by preparation of gDNA and PCR with primers Tobi_primer_fwd_1 and Tobi_primer_rev (Table 2.5).

Growth experiments were conducted in 50 mL MES-buffered medium with strain *C. acetobutylicum* [pIMP1], the *solB* overexpression strain *C. acetobutylicum* [pIMP1_solB], the double overexpression strain *C. acetobutylicum* [pIMP1_solB_spo0A], and the double overexpression strain with the shortened

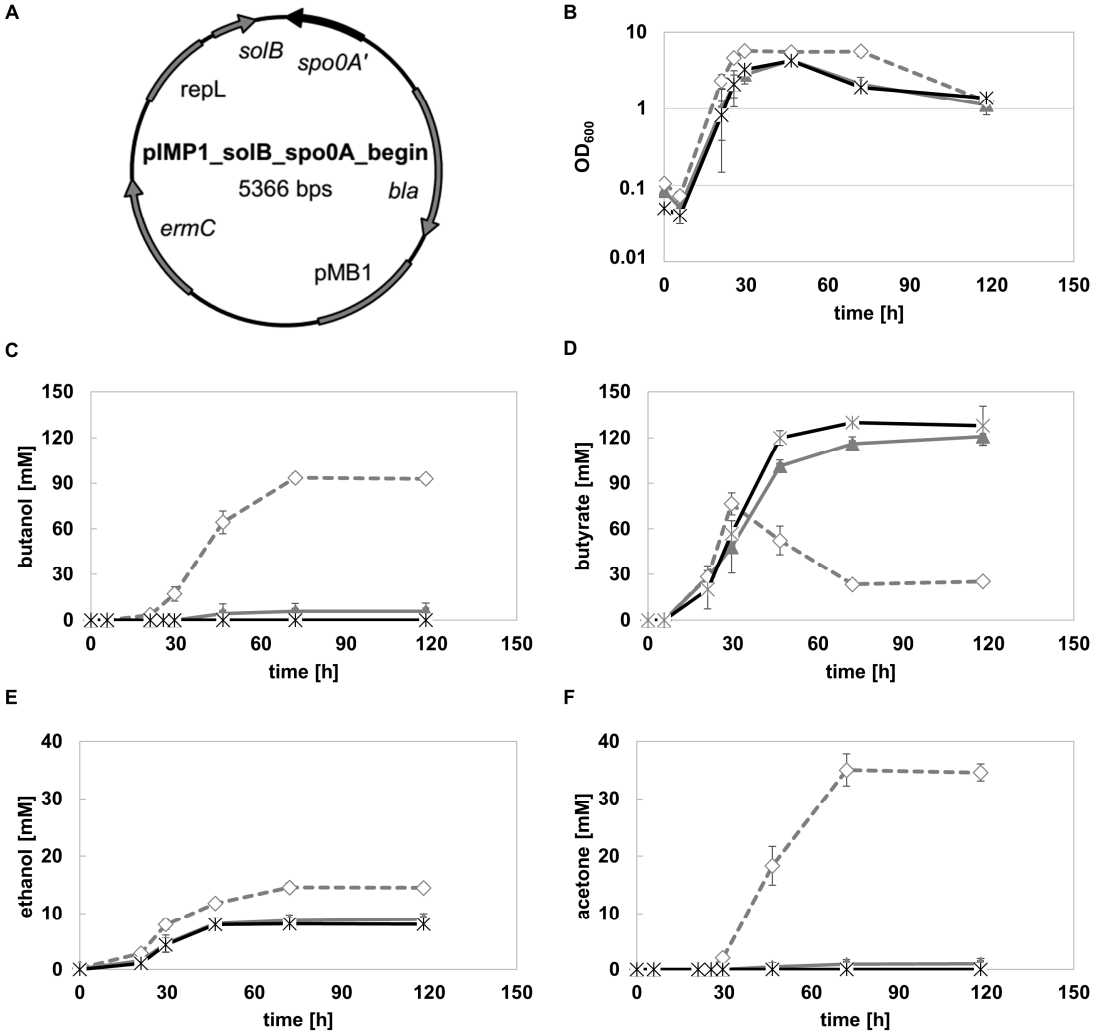

Figure 3.4: (A) Overexpression plasmid pIMP1_solB_spo0A_begin containing *solB* and part of *spo0A* comprising the 5' untranslated region and the start of the coding sequence of *spo0A*. (B-F) Growth behaviour and product spectrum of *C. acetobutylicum* [pIMP1_solB] (▲), *C. acetobutylicum* [pIMP1_solB_spo0A] (◇), and *C. acetobutylicum* [pIMP1_solB_*spo0A*_begin] (∗) was measured during growth in batch fermentation with 50 ml MES-buffered medium (n = 3); (B) growth behaviour, (C) butanol, (D) butyrate, (E) ethanol, and (F) acetone. *bla*, ampicillin resistance gene; pMB1, ori for Gram-negative bacteria; *ermC*, erythromycin resistance gene*;* repL, ori for Gram-positive bacteria; *solB*, regulatory RNA SolB; spo0A', truncated gene of transcription factor Spo0A..

fragment of *spo0A C. acetobutylicum* [pIMP1_solB_spo0A_begin]. Growth behaviour and product formation was analyzed via OD_{600} and GC analysis. Mean values of at least three independent experiments are displayed for OD_{600} in Figure 3.4A as well as butanol, butyrate, ethanol, and acetone production in Figure 3.4C-F. All strains showed similar growth curves. The product formation differed between the *C. acetobutylicum* strains. Strain *C. acetobutylicum* [pIMP1_solB_spo0A] produced nearly 100 mM butanol, 35 mM butyrate, 15 mM ethanol, and 35 mM acetone, whereas strains *C. acetobutylicum* [pIMP1_solB] and *C. acetobutylicum* [pIMP1_solB_spo0A_begin]

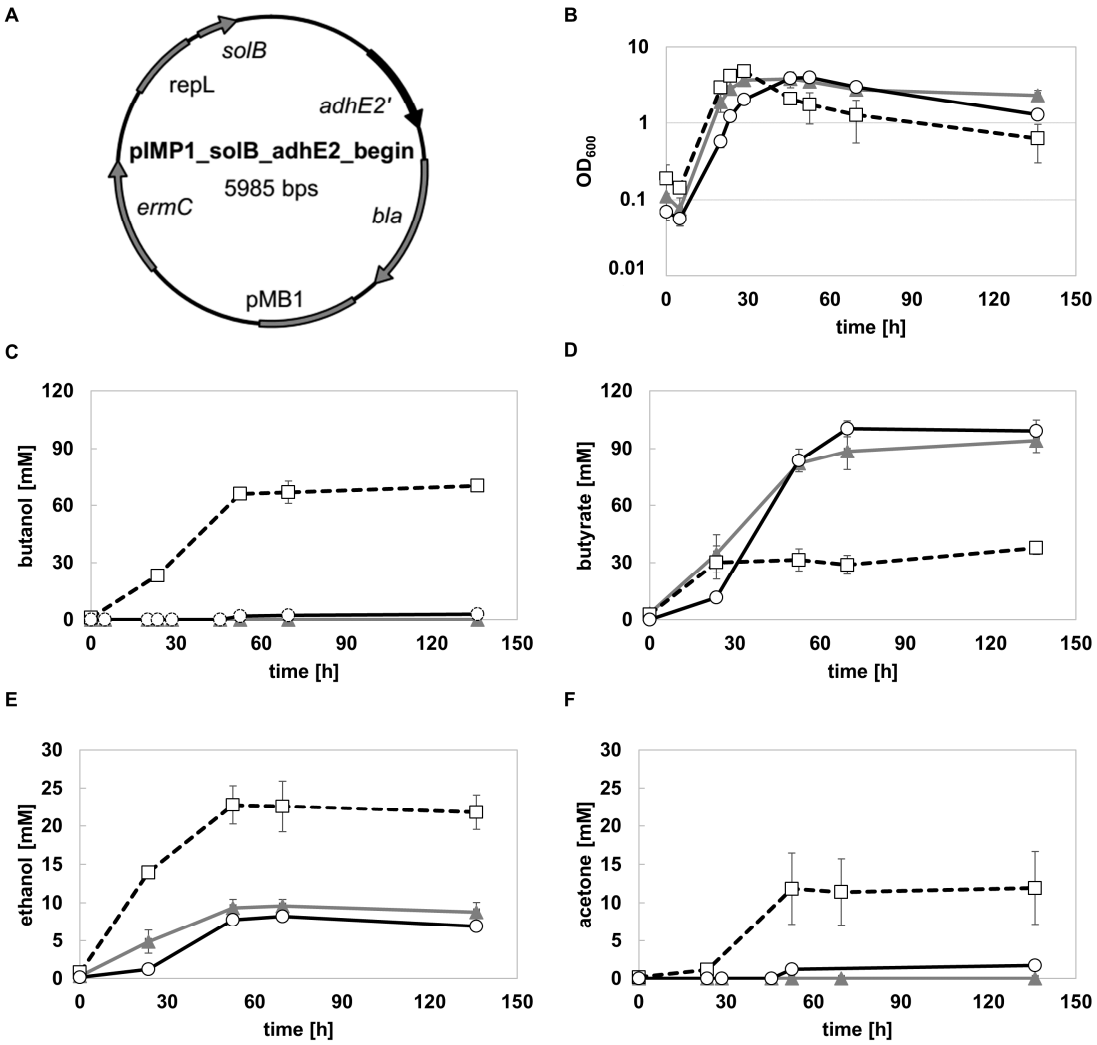

Figure 3.5: (A) Overexpression plasmid pIMP1_solB_adhE2_begin of *solB* and part of *adhE2* comprising the 5' untranslated region and the start of the coding sequence of *adhE2*. (B-F) Growth behaviour and product formation of *C. acetobutylicum* [pIMP1_solB] (▲), *C. acetobutylicum* [pIMP1_solB_*adhE2*] (□), and *C. acetobutylicum* [pIMP1_solB_adhE2_begin] (○) was measured during growth in batch fermentation with 50 mL MES-buffered medium (n = 3); (B) growth behaviour, (C) butanol, (D) butyrate, (E) ethanol, and (F) acetone. *bla*, ampicillin resistance gene; pMB1, ori for Gram-negative bacteria; *ermC*, erythromycin resistance gene*;* repL, ori for Gram-positive bacteria; *solB*, regulatory RNA SolB; a*dhE2*', shortened gene of aldehyde/alcohol dehydrogenase 2.

produced approximately 120 mM butyrate and 8 mM ethanol, and only marginal concentrations of acetone and butanol were detected.

Analogous growth experiments were performed with strains *C. acetobutylicum* [pIMP1_solB], *C. acetobutylicum* [pIMP1_solB_adhE2], and *C. acetobutylicum* [pIMP1_solB_adhE2_begin]. Mean values of at least three independent experiments are shown for OD_{600} in Figure 3.5B as well as butanol, butyrate, ethanol, and acetone production in Figure 3.5C-F. All strains exhibited similar growth curves. However, strain *C. acetobutylicum* [pIMP1_solB_adhE2_begin] showed a prolonged lag phase and reached the stationary growth phase later. Strain *C. acetobutylicum* [pIMP1_solB_adhE2] produced approximately 70 mM butanol and 37 mM butyrate, acetone and ethanol were produced in a maximum concentration of 24 mM and 12 mM, respectively. In contrast, strain *C. acetobutylicum* [pIMP1_solB] did neither produce butanol nor acetone, but more than 100 mM butyrate and 9 mM ethanol were produced. These results concerning product formation were similar to those obtained for strain *C. acetobutylicum* [pIMP1_solB_adhE2_begin]. Strain *C. acetobutylicum* [pIMP1_solB_adhE2_begin] produced also high levels of butyrate and only marginal concentrations of butanol and acetone.

Thus, overexpression of *adhE2* or *spo0A* together with *solB* increased solvent production in *C. acetobutylicum* compared to strain *C. acetobutylicum* [pIMP1_solB]. However, overexpression of a truncated sequence of the genes *adhE2* or *spo0A* containing the 5' untranslated region and the first part of the coding sequence together with *solB* resulted in a minimal production of solvents.

3.1.3 Transcriptome analysis of *C. acetobutylicum* [pIMP1_solB]

To better understand the function and mechanism of SolB, transcriptome analysis were performed with strains *C. acetobutylicum* wild type, *C. acetobutylicum* [pIMP1_solB], and *C. acetobutylicum Δspo0A.* As the deletion strain of *spo0A*, *C. acetobutylicum Δspo0A,* exhibited a similar phenotype as the *solB* overexpression strain *C. acetobutylicum* [pIMP1_solB], the transcriptome analysis was performed to clarify if SolB and Spo0A interact with the same targets. All strains were grown in biological triplicates in 50 mL MES-buffered medium. Cells from 5 mL grown medium suspension were harvested after reaching exponential growth (OD_{600} of 1) and 2 mL cells were collected after strains stayed for at least 4 h in the stationary growth phase. RNA was prepared with hot-phenol and DNA-free RNA was used for the transcriptome analysis. All differentially expressed genes in stationary growth phase between strains

C. acetobutylicum [pIMP1_solB] and *C. acetobutylicum Δspo0A* compared to strain *C. acetobutylicum* wild type were categorized into one Cluster of Orthologous group (COG) (Tatusov et al., 1997). In Figure 3.6, the percentage of differentially expressed genes in each group is compared between strain *C. acetobutylicum* [pIMP1_solB] and *C. acetobutylicum Δspo0A*. Both mutants show significant changes in nearly all COG categories and most of the differentially expressed genes are down-regulated compared to the *C. acetobutylicum* wild type. The effect of s*po0A* deletion leads to an enlarged down-regulation in most of the COGS. The same is true for the

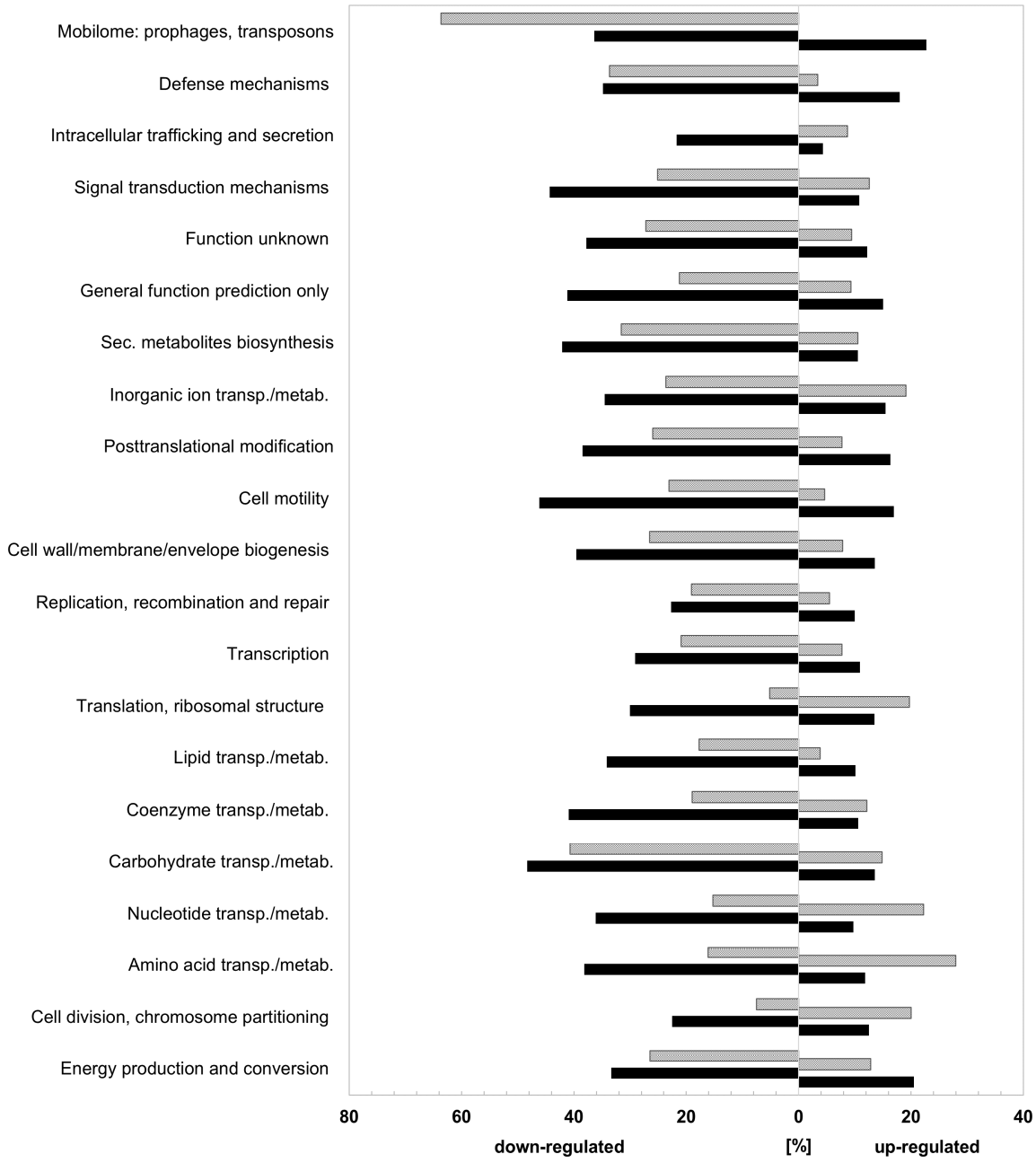

Figure 3.6: Assembly of differentially expressed genes in solventogenic phase of *C. acetobutylicum* [pIMP1_solB] (grey) and *C. acetobutylicum* Δspo0A (black) compared to the *C. acetobutylicum* wild type into Clusters of Orthologous Groups (COG). The figure displays the percentage of differentially expressed genes according to the respective COG cetagory.

overexpression of *solB* in *C. acetobutylicum.* COGs, which were affected most by deletion of *spo0A,* are coding for genes involved in signal transduction mechanism, cell motility, coenzyme transport/metabolism, and carbohydrate transport/metabolism. These categories showed a down-regulation of at least 40 %. The *solB* overexpression strain displayed the highest influences in COGs of mobilome, defense mechanism, secondary metabolites biosynthesis, and carbohydrate transport and metabolism. The percentage of down-regulated genes was over 35 % in these groups. In contrast, *C. acetobutylicum* [pIMP1_solB] revealed an up-regulation of at least 20 % in the COGs of nucleic acid transport/metabolism, amino acid transport/metabolism, and cell division.

Comparing differentially expressed genes of exponential and stationary growth phase of *C. acetobutylicum* [pIMP1_solB] and *C. acetobutylicum Δspo0A*, it is striking that the portion of down-regulated genes is increasing with the change of the growth phase and the shift from acidogenic to solventogenic phase (Figure 3.7A). The number of down-regulated genes was higher for strain *C. acetobutylicum Δspo0A* than for

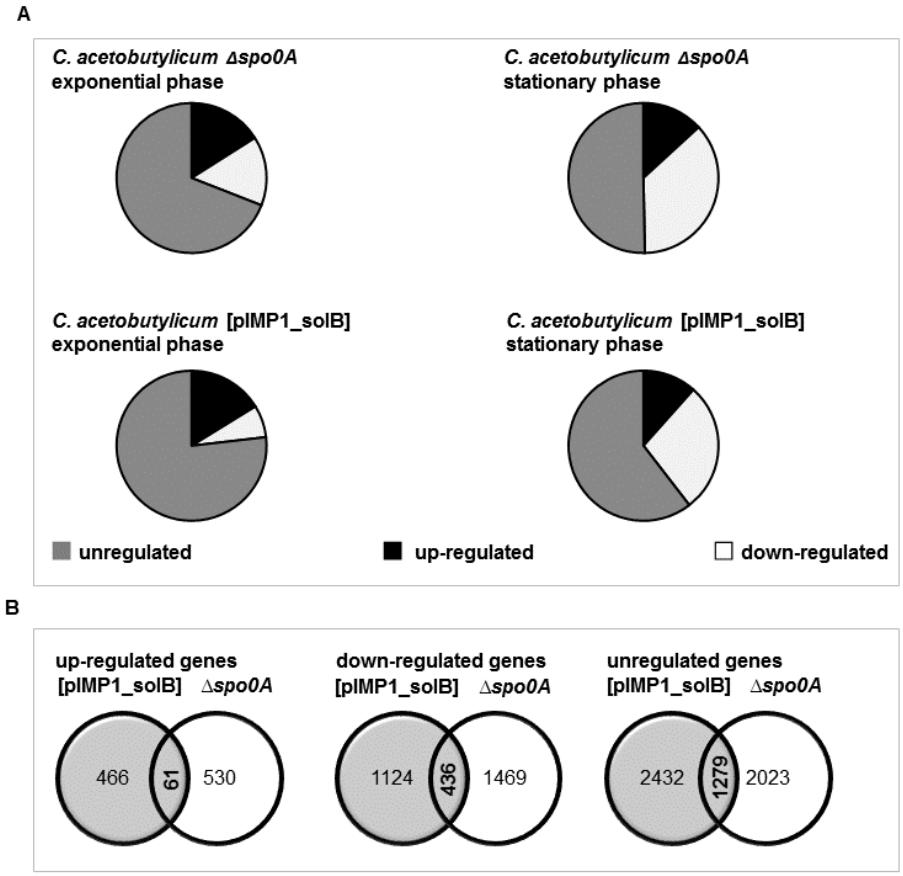

Figure 3.7: (A) Pie chart showing the rates of up-, down-, and unregulated genes from *C. acetobutylicum* [pIMP1_solB] and *C. acetobutylicum* Δ*spo0A* compared to *C. acetobutylicum* wild type in exponential and stationary growth phase. (B) Venn diagram showing the numbers of differentially expressed genes of *C. acetobutylicum* [pIMP1_solB] (grey) and *C. acetobutylicum* Δ*spo0A* (white) compared to *C. acetobutylicum* wild type in solventogenic phase.

C. acetobutylicum [pIMP1_solB]. In contrast, the number of up-regulated genes did not differ significantly between the two phases in both mutants. Furthermore, the percentage of up-regulated genes is comparable for both strains (Figure 3.7A). The overlap of identically up-regulated genes was quite low, as only 13 % of up-regulated genes of strain *C. acetobutylicum* [pIMP1_solB] were also up-regulated in *C. acetobutylicum Δspo0A* compared to the *C. acetobutylicum* wild type (Figure 3.7B). However, the overlap of down-regulated genes for strains *C. acetobutylicum* [pIMP1_solB] and *C. acetobutylicum Δspo0A* was apparently higher. In this case, 39 % of down-regulated genes of strain *C. acetobutylicum* [pIMP1_solB] were also down-regulated in strain *C. acetobutylicum Δspo0A* (Figure 3.7B).

To get a more detailed view of down- and up-regulated genes of strain *C. acetobutylicum* [pIMP1_solB] in solventogenic phase compared to strain *C. acetobutylicum* wild type, the logarithm of the basis two was calculated for the fold change of each gene of strain *C. acetobutylicum* [pIMP1_solB] and displayed in a diagram according to the position in the genome (Figure 3.8). In the section below, the calculated values will be abbreviated as fold changes. The fold change describes the change between the initial expression of the *C. acetobutylicum* wild type strain and the expression in the *C. acetobutylicum solB* overexpression strain. At the start of the x-axis, all genes located on the megaplasmid pSOL1 are displayed, followed by the genes encoded in the chromosome. Fold changes of all genes mentioned in the text below are reported in Table 8.1 and genes were annotated according to the NCBI data base. The following genes revealed a significant higher expression in the

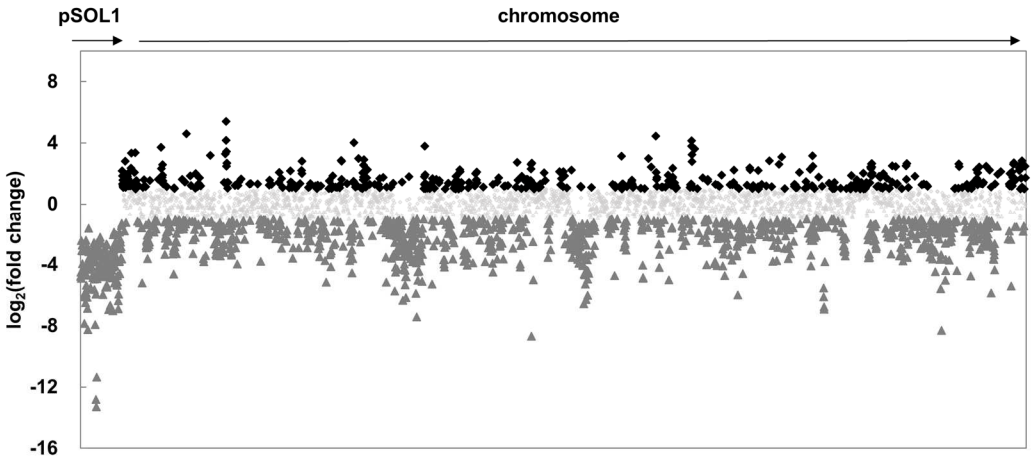

Figure 3.8: Effects of *C. acetobutylicum solB* overexpression on RNA transcriptome level. Distribution of up- (◆) and down-regulated (▲) genes across the megaplasmid pSOL1 and the genome of *C. acetobutylicum* [pIMP1_solB] compared to the *C. acetobutylicum* wild type in solventogenic phase. Faint dots are not regarded as differentially expressed.

C. acetobutylicum solB overexpression strain compared to the *C. acetobutylicum* wild type: *CA_C0218* and *CA_C0384*, encoding a protein containing a lysM motif repeat and a phosphotransferase system (PTS) for cellobiose, respectively. Also, the *sigE* (CA_C1965) gene reached higher transcript levels in the *C. acetobutylicum solB* overexpression strain than in the *C. acetobutylicum* wild type strain. Transcription of the genes encoded on the megaplasmid pSOL1 was dramatically decreased in strain *C. acetobutylicum* [pIMP1_solB] compared to the transcription in *C. acetobutylicum* wild type during solventogenic growth phase. This significant decrease was already recognized in the exponential growth phase as shown in Figure 8.3 (Supplement). Also, the genes *CA_C2964-2966* displayed a down-regulation in the *C. acetobutylicum* [pIMP1_solB] strain. The genes *CA_C2964*, *CA_C2965*, and *CA_C2967* are annotated as PTS for lactose including a gene encoding a repressor for the PTS. One predicted permease (*CA_C3482*) showed also severe down-regulation of expression in strain *C. acetobutylicum* [pIMP1_solB]. Furthermore, in strain *C. acetobutylicum* [pIMP1_solB] a cluster of genes (*CA_C1915-1944*), which are not yet characterized, was also down-regulated. *CA_C1201*, which also revealed a strong inhibition of expression, was not yet identified. Furthermore, the *sigG* (CA_C1696) transcription level was decreased 8.7-fold in *C. acetobutylicum* [pIMP1_solB] compared to *C. acetobutylicum* wild type. Strain *C. acetobutylicum int::sigG* was described to produce a higher level of granulose (Tracy et al., 2011). Thus, it is possible that the overexpression of *solB* also leads to higher granulose levels in the cell. For quantitative determination of granulose production via HPLC, *C. acetobutylicum* [pIMP1] and *C. acetobutylicum* [pIMP1_solB] were grown in CG medium. By boiling cell samples in sulfuric acid cells were lysed and granulose was split to the monomeric compound glucose. The results of glucose determination are displayed in Figure 3.9. At all measured time points, the concentration of glucose was higher in *C. acetobutylicum* [pIMP1_solB] as in the empty vector strain *C. acetobutylicum* [pIMP1] shown in Figure 3.9A. Mean values of two independent experiments were displayed. The highest glucose concentration was measured after 24 h in *C. acetobutylicum* [pIMP1_solB] with 5.5 mM. Over time, the concentration of glucose decreased to 1.7 mM after 72 h. Also, a decrease was measured for strain *C. acetobutylicum* [pIMP1]. After 24 h, 3.9 mM glucose were measured and after 72 h the concentration dropped to 1.2 mM.

For qualitative analyses of granulose production, TEM images of *C. acetobutylicum* [pIMP1] and *C. acetobutylicum* [pIMP1_solB] were taken. Cells were grown in CG

medium and harvested after 18 h, 25 h, 42 h, and 66 h. After 66 h, cells of both strains were already largely lysed or the cell surface was disrupted. Therefore, only the earlier time points were reported in Figure 3.9B-D. After 18 h of growth, cells of *C. acetobutylicum* [pIMP1] displayed a rod-shape structure and consistent distribution of electrons as no granula or other bigger structures could be observed (Figure 3.9B). Several cells were in process of cell division. In contrast, *C. acetobutylicum* [pIMP1_solB] showed cells with a couple of black granula, which were either distributed over the whole cell or just in one part of the cell body. Furthermore, these cells exhibited the clostridial cell shape, which is characterised by swelling of the middle part of the bacterial cell. Besides, some cells appeared in the same

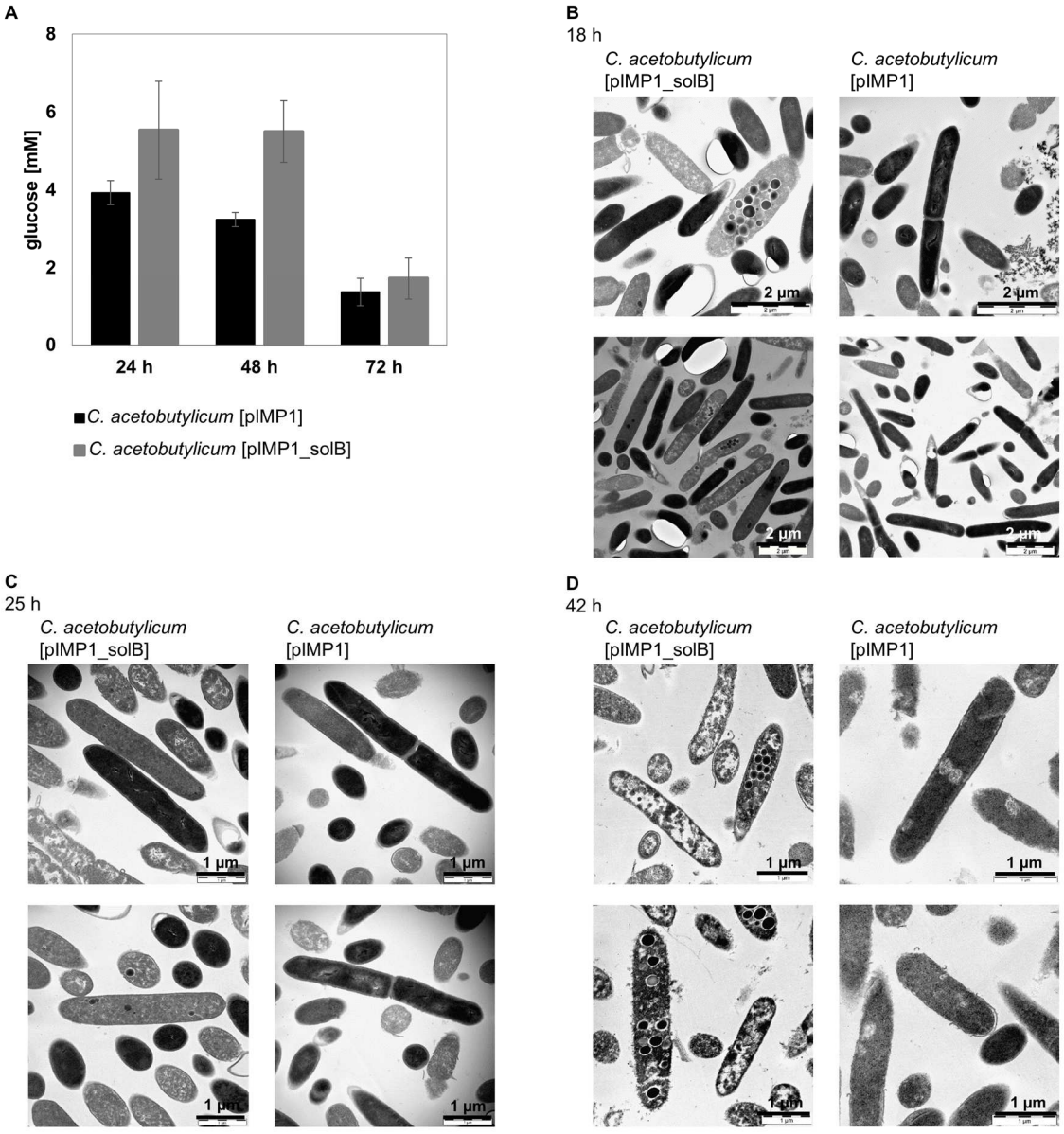

Figure 3.9: (A) Granulose determination via glucose measurement of *C. acetobutylicum* [pIMP1] and *C. acetobutylicum* [pIMP1_solB] cells at different time points of growth. (B-D) TEM images of *C. acetobutylicum* [pIMP1] and *C. acetobutylicum* [pIMP1_solB] after 25 h (B, scale bar representing 2 µm), 48 h (C, scale bar representing 1 µm) and 64 h (D, scale bar representing 1 µm).

manner as the empty vector strain *C. acetobutylicum* [pIMP1] with a consistent structure. This subgroup of cells also showed dividing cells. After 25 h (Figure 3.9C) the situation was quite similar to 18 h. *C. acetobutylicum* [pIMP1] appeared in rod-shaped structure and a lot of cells were imaged during cell division. In the cytoplasm of the cells, a thin structure like a strand or filament was visible. The *C. acetobutylicum solB* overexpression strain revealed two types of cells. One exhibited similarities with the cells of *C. acetobutylicum* [pIMP1] and the other was clearly brighter and contained black granula. However, the granula were decreased in size compared to 18 h growth. After 42 h, cells of *C. acetobutylicum* [pIMP1_solB] contained several black granula in different sizes. Some of the cells seemed to be already lysed as they did not exhibit inner structures, but white fields in the cell (Figure 3.9D). Some of the cells were swollen and differed from the typical rod-shaped structure. Also, *C. acetobutylicum* [pIMP1] cells manifested incomplete cell membranes and some cells had white vacuoles. It was still not possible to find the black granula at this time point, which were observed in the cells of *C. acetobutylicum* [pIMP1_solB]. Furthermore, nearly none of the cells showed such white areas as recognized for *C. acetobutylicum* [pIMP1_solB]. To sum up HPLC analysis displayed higher granulose concentrations in *C. acetobutylicum* [pIMP1_solB] cells and TEM images revealed the production of black granula in *C. acetobutylicum* [pIMP1_solB] cells. SEM images of *C. acetobutylicum* wild type and *C. acetobutylicum* [pIMP1_solB] did not display differences in cell shape (Supplement Figure 8.5).

C. acetobutylicum [pIMP1_solB] shared similarities in the expression profile with *C. acetobutylicum Δspo0A.* However, only *C. acetobutylicum* [pIMP1_solB] showed a minimized transcription of all genes encoded on the megaplasmid pSOL1. Furthermore, *C. acetobutylicum* [pIMP1_solB] showed an increased granulose production.

3.1.4 Copy number determination of pSOL1

The results of the transcriptome analysis pointed out that the expression of all genes encoded on the megaplasmid pSOL1 was dramatically reduced in *C. acetobutylicum* [pIMP1_solB] compared to the wild type. This finding raised the question, whether the megaplasmid was still present in *C. acetobutylicum* [pIMP1_solB] strain. To elucidate the presence of the megaplamid pSOL1, *C. acetobutylicum* [pIMP1_solB] and the empty vector strain *C. acetobutylicum* [pIMP1] were streaked onto starch agar plates (2x XYTGA). After incubation at 37 °C for at least two days, the starch was stained

with Lugol's solution in the agar plates. As the starch-degrading enzyme α-amylase (CA_P0098) is encoded on the megaplasmid pSOL1, *C. acetobutylicum* strains without pSOL1 are no longer able to degrade starch (Harris et al., 2002). One stained agar plate with both strains is displayed exemplary in Figure 8.4 (Supplement). A clear and bright halo was visible around the bacterial colonies. In contrast, at the outer surrounding of the plate the colour of the agar was brown. To exclude that *C. acetobutylicum* [pIMP1_solB] was a mixed culture of *C. acetobutylicum* [pIMP1_solB] containing pSOL1 and *C. acetobutylicum* [pIMP1_solB] without pSOL1, plasmid [pIMP1_solB] was transformed again in *C. acetobutylicum.* After successful transformation, single colonies were transferred on to agar plates containing starch. After incubation of three days, the colonies were visible and agar plates were stained with Lugol's solution. All grown clones showed clear halo surrounding the colonies (Supplement Figure 8.4B).

As the megaplasmid was still present in the genome of *C. acetobutylicum* [pIMP1_solB], it was necessary to determine the copy number of the megaplasmid pSOL1. Therefore, gDNA was prepared of 4 independent clones of *C. acetobutylicum* [pIMP1_solB] as well as of *C. acetobutylicum* [pIMP1]. Strains were grown in CG medium and 2 mL cells were collected in exponential and stationary growth phase. For normalization, genomic DNA of *C. acetobutylicum* wild type was additionally prepared. Afterwards, qRT-PCR was performed with two primer pairs amplifying parts of the chromosome (LC_gyr_fwd and LC_gyr_rev, LC_spo0A_fwd and LC_spo0A_rev, Table 2.5) and two primer pairs amplifying parts of the megaplasmid pSOL1 (LC_adhE2_fwd and LC_adhE2_rev, LC_adc_fwd and LC_adc_rev, Table 2.5). Each qRT-PCR was performed in technical duplicates. After normalization of the values to *C. acetobutylicum* wild type, the plasmid copy number of *C. acetobutylicum* [pIMP1] and *C. acetobutylicum* [pIMP1_solB] were compared in Figure 3.10A. *C. acetobutylicum* [pIMP1] displayed an increased copy number of 1-fold compared to the wild type strain in both growth phases. In contrast, the pSOL1 copy number of *C. acetobutylicum* [pIMP1_solB] was decreased dramatically compared to the *C. acetobutylicum* wild type strain in both growth phases. The *C. acetobutylicum* wild type strain harbours about 50 times more copies of pSOL1 as *C. acetobutylicum* [pIMP1_solB]. The difference was even greater between strains *C. acetobutylicum*

Table 3.1: Results of mapped sequences on chromosome and megaplasmid pSOL1 of sequenced gDNA from *C. acetobutylicum* [pIMP1_solB], *C. acetobutylicum* [pIMP1], and *C. acetobutylicum* wild type.

C. acetobutylicum	Pre reads after Trimmomatic	Total	Coverage chromosome	Coverage pSOL1	Coverage pSOL1/ chromosome
[pIMP1_solB]	4,641,668	4,887,078	150.96	27.46	0.18
[pIMP1_solB]	2,322,902	2,429,278	105.97	9.14	0.09
[pIMP1_solB]	2,727,710	2,845,298	107.78	9.81	0.09
[pIMP1]	2,231,180	2,384,150	67.82	189.28	2.79
[pIMP1]	2,505,338	2,621,194	70.73	212.11	3.00
[pIMP1]	2,537,014	2,656,516	68.63	176.66	2.57
wild type	3,621,716	7,691,944	166.98	467.78	2.80
wild type	1,635,744	1,709,028	83.30	156.94	1.88
wild type	1,969,676	2,047,532	104.31	155.04	1.49

[pIMP1_solB] and the empty vector strain *C. acetobutylicum* [pIMP1]. These results were supported by genome sequencing of *C. acetobutylicum* wild type, *C. acetobutylicum* [pIMP1], and *C. acetobutylicum* [pIMP1_solB]. Strains were grown in triplicates in MES-buffered medium until stationary growth phase. 2 mL of cells were used for preparation of gDNA and sequencing analysis. In Table 3.1, results of the genome sequencing are summarized. The coverage of the megaplasmid pSOL1 was more than 5 times lower as the coverage of the chromosome in *C. acetobutylicum* [pIMP1_solB]. In contrast, the coverage of pSOL1 and the chromosome of the *C. acetobutylicum* wild type strain showed approximately same amounts. The empty vector strain *C. acetobutylicum* [pIMP1] behaved similarly as the wild type. For calculating the relative plasmid copy number of pSOL1 normalized to the chromosome the coverage of pSOL1 was divided by the coverage of the chromosome for all strains. In comparison to the *C. acetobutylicum* wild type, the *C. acetobutylicum* [pIMP1_solB] showed a relative plasmid copy number, which was approximately 17.1 times lower, while *C. acetobutylicum* [pIMP1] showed a 1.4 times higher value. These results were similar to the calculated relative plasmid copy number of pSOL1 in the qRT-PCR experiments (Figure 3.10A).

Another interesting point was to examine the plasmid copy number of pSOL1 in the double overexpression strains *C. acetobutylicum* [pIMP1_solB_spo0A] and *C. acetobutylicum* [pIMP1_solB_adhE2]. As the growth phases did not influence the copy number, only the solventogenic phase was investigated for these strains. Strains were grown in triplicates on 50 mL MES-buffered medium and 2 mL were used for preparation of gDNA. Afterwards, qRT-PCR was performed in technical duplicates. Mean values of relative copy number of pSOL1 are presented for the empty vector

strain *C. acetobutylicum* [pIMP1], the *solB* overexpression strain *C. acetobutylicum* [pIMP1_solB], and the double overexpression strains *C. acetobutylicum* [pIMP1_solB_adhE2], and *C. acetobutylicum* [pIMP1_solB_spo0A] in Figure 3.10B. The reference strains *C. acetobutylicum* [pIMP1] and *C. acetobutylicum* [pIMP1_solB] showed similar results compared to prior experiments. Overexpression of *solB* decreased the copy number of pSOL1 to one-tenth compared to the wild type strain and the copy number of the empty vector strain was doubled compared to the wild type strain. *C. acetobutylicum* [pIMP1_solB_adhE2] and *C. acetobutylicum* [pIMP1_solB_spo0A] exhibited an increased copy number compared to the *solB* overexpression strain. Both strains displayed nearly similar amounts of pSOL1 as the *C. acetobutylicum* wild type.

Also, the double overexpression strains with the truncated fragments of *adhE2* and *spo0A* were tested to determine the copy number of pSOL1. *C. acetobutylicum* [pIMP1_solB], *C. acetobutylicum* [pIMP1_solB_adhE2], *C. acetobutylicum* [pIMP1_solB_spo0A], and *C. acetobutylicum* [pIMP1_solB_adhE2_begin], and *C. acetobutylicum* [pIMP1_solB_spo0A_begin] were grown in triplicates in 50 mL MES-buffered medium until stationary growth phase. Afterwards, gDNA of all strains was prepared and qRT-PCR was performed. Mean values of relative copy number were shown in Figure 3.11. The lowest level of pSOL1 was observed for

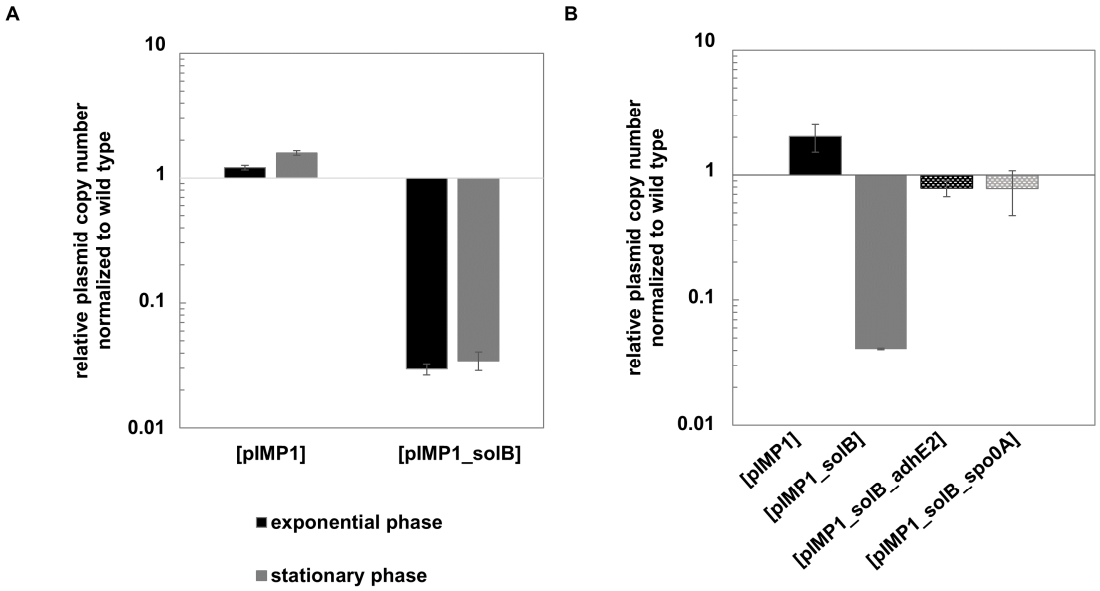

Figure 3.10: (A) Relative plasmid copy number of pSOL1 in *C. acetobutylicum* [pIMP1] and *C. acetobutylicum* [pIMP1_solB] in exponential (black) and stationary growth phase (broken grey). (B) Relative plasmid number of pSOL1 in *C. acetobutylicum* [pIMP1] (black), *C. acetobutylicum* [pIMP1_solB] (grey), *C. acetobutylicum* [pIMP1_solB_adhE2] (broken black) and *C. acetobutylicum* [pIMP_solB_spo0A] (broken grey). The copy number of pSOL1 in *C. acetobutylicum* wild type was set to 1.

C. acetobutylicum [pIMP1_solB] with 30 times less compared to the *C. acetobutylicum* wild type strain. *C. acetobutylicum* [pIMP1_solB_adhE2] and *C. acetobutylicum* [pIMP1_solB_spo0A] displayed similar levels of pSOL1 compared to *C. acetobutylicum* wild type strain. For strains *C. acetobutylicum* [pIMP1_solB_adhE2_begin] and *C. acetobutylicum* [pIMP1_solB_spo0A_begin], the copy numbers of pSOL1 were similar to the *solB* overexpression mutant. This implied a reduction of 90 % compared to the *C. acetobutylicum* wild type level.

Summarizing, overexpression of *solB* in *C. acetobutylicum* led to a decrease of at least 30 times of the copy number of pSOL1 compared to the *C. acetobutylicum* wild type strain. However, the level of megaplasmid pSOL1 can be restored in *C. acetobutylicum* [pIMP1_solB] by overexpression of the entire *adhE2* or *spo0A* genes. However, overexpression of the truncated sequences of *adhE2* or *spo0A*, which cannot be translated into a functional protein, was unable to inhibit effects of *solB* overexpression.

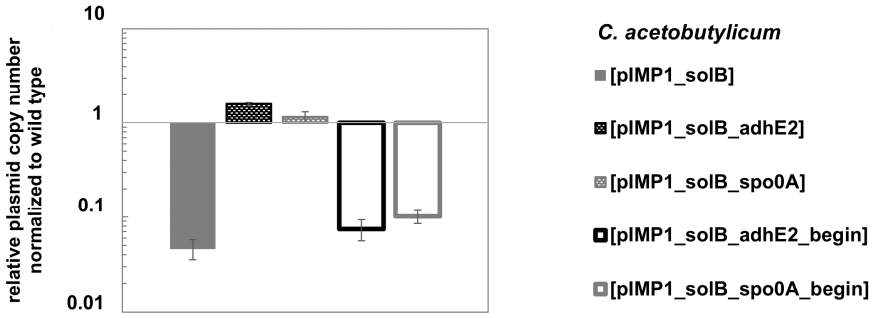

Figure 3.11: Relative plasmid copy number of pSOL1 in *C. acetobutylicum* [pIMP1_solB] (grey), *C. acetobutylicum* [pIMP1_solB_adhE2] (broken black), *C. acetobutylicum* [pIMP1_solB_spo0A] (broken grey). *C. acetobutylicum* [pIMP1_solB_adhE2_begin] (solid black lines), and *C. acetobutylicum* [pIMP1_solB_spo0A_begin] (solid grey lines) in stationary growth phase. The copy number of pSOL1 in *C. acetobutylicum* wild type was set to 1.

3.2 Characterizing the RNA-binding protein Hfq

3.2.1 Organisation of *hfq* in the genome

The RNA-binding protein Hfq (CA_C1834) is encoded on the chromosome in *C. acetobutylicum* (Figure 3.12A). Upstream of *hfq,* the genes *miaA*, *mutL*, and *mutS* are annotated. *miaA* encodes an tRNA modification enzyme (Connolly and Winkler, 1989, 1991), whereas *mutL* and *mutS* are involved in the DNA mismatch repair system (Acharya et al., 2003; Fukui, 2010). Further upstream, CA_C1833 is predicted to be a tRNA-2-methylthio-N(6)-dimethylallyladenosine synthase. Downstream of *hfq, CA_C1838* is annotated as cystathionine beta-lyase family protein and in divergent direction *lexA* is predicted as transcriptional repressor for SOS response (Nuyts et al., 2001). To analyze the organisation of the gene cluster including *hfq*, DNA-free RNA of *C. acetobutylicum* wild type was used for RT-PCR. cDNA synthesis was accomplished with primer cyst_rev (Table 2.3) annealing to the mRNA transcript of *CA_C1833*. Afterwards, PCRs were conducted with primers amplifying the following genes *CA_C1833* (cyst_fwd, cyst_rev), *hfq* (hfq_fwd, hfq_rev), *miaA* (miaA_fwd. miaA_rev), *mutL* (mutL_fwd, mutL_rev), *mutS* (mutS_fwd, mutS_rev), and *CA_C1838* (pre_fwd, pre_rev) using respective cDNA as template. Primer sequences can be found in Table 2.3. Results of the performed RT-PCR are shown in Figure 3.12B. All samples

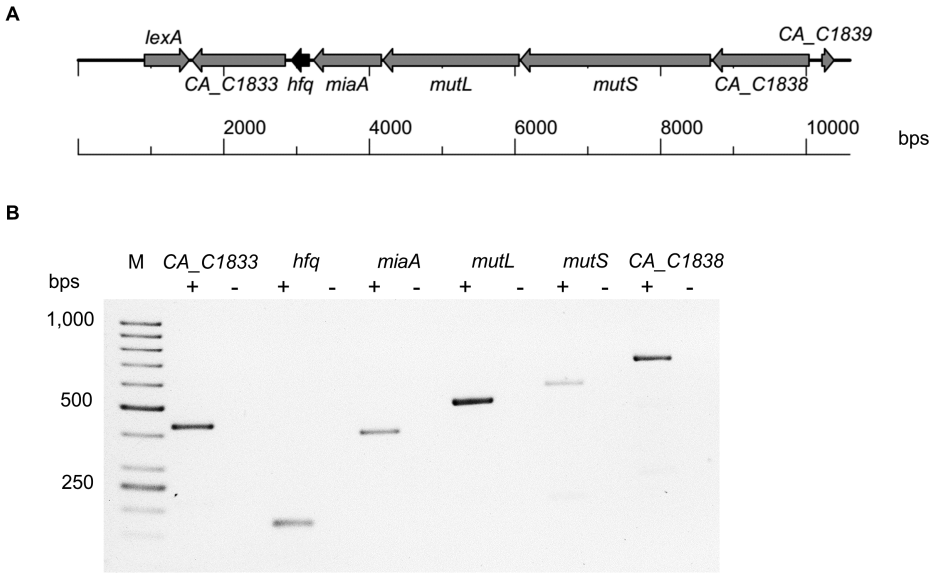

Figure 3.12: (A) Schematic representation of the genomic localization of *C. acetobutylicum hfq.* (B) RT-PCR analysis of the *C. acetobutylicum* CA_C1833-CA_C1838 region on a 2 % agarose gel. Starting point for cDNA synthesis was accomplished at the *CA_C1833* gene. PCRs were performed with primers (named in brackets) amplifying the following genes *CA_C1833* (cyst_fwd, cyst_rev), *hfq* (hfq_fwd, hfq_rev), *miaA* (miaA_fwd. miaA_rev), *mutL* (mutL_fwd, mutL_rev), *mutS* (mutS_fwd, mutS_rev), and *CA_C1838* (pre_fwd, pre_rev) using respective cDNA as template. +, RT-PCR approach with Reverse Transcriptase; -, RT-PCR approach without Reverse Transcriptase; M, 50 Bp Ladder Mix (Thermo Fisher Scientific, Waltham, Ma, USA). *lexA* (CA_C1832), transcriptional repressor; *hfq* (CA_C1834), host factor I protein Hfq; *miaA* (CA_C1835), tRNA dimethyltransferase; *mutL* (CA_C1836), DNA mismatch repair protein; *mutS* (CA_C1837), DNA mismatch repair protein.

without Reverse Transcriptase (-) did not exhibit a signal. RT-PCRs, which contained Reverse Transcriptase (+), revealed a signal at 430 bps, targeting *CA_C1833*; 160 bps, targeting *hfq*; 500 bps targeting *mutL*; 600 bps targeting *mutS*; and 700 bps targeting CA_C1838. Thus, all genes from *CA_C1833* to *CA_C1838* were transcribed in one mRNA.

3.2.2 Complementation experiments with Hfq from *C. acetobutylicum* in *E. coli* cells

For characterizing *hfq,* one commonly used method is the complementation of *E. coli Δhfq* with *hfq* from a different organism. For complementation of *E. coli Δhfq* JW4130 with *hfq* from *C. acetobutylicum*, the coding sequence of *hfq*, starting at the ATG, had to be fused with the promoter of *hfq* from *E. coli*. As *hfq* in *E. coli* contains actually three promoters (Tsui et al., 1994), a shorter promoter sequence was used, which was already successfully tested in an *hfq* complementation experiment (Chambers and Bender, 2011). The construct was named hfq_cac. In the same manner, the construct hfq_ec was accomplished, which harbours the coding sequence of *E. coli hfq* and was used as positive control for complementation. The sequence pKon contained only the mentioned promoter sequence of *E. coli hfq* and was used as negative control. The detailed sequence information of pKon, hfq_ec, and hfq_cac is displayed in Figure 8.2 (Supplement). For plasmid construction, the backbone of plasmid pACYC184 was used with the p15a origin of replication (ori). The ori p15A is described as low copy plasmid and thereby, the plasmid creates a similar situation regarding the level of DNA as in the chromosome. The plasmid pACYC184 was digested with *Eag*I and *Hin*dIII. Afterwards, the sequences pKon, hfq_ec, and hfq_cac were cloned into the respective restriction sites.

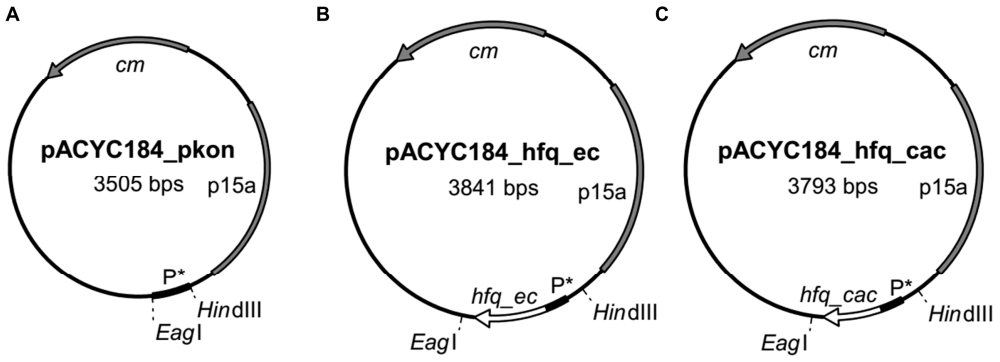

Figure 3.13: Plasmid maps of (A) pACYC184_pkon, (B) pACYC184_hfq_ec, and (C) pACYC184_hfq_cac for complementation experiments in *E. coli* Δ*hfq*. *cm*, chloramphenicol resistance gene; p15A, Gram-negative ori; P*, promoter sequence of *hfq* from *E. coli; hfq_cac,* sequence of *hfq* from *C. acetobutylicum; hfq_ec,* sequence of *hfq* from *E. coli*.

The resulting plasmids were named pACYC184_pkon, pACYC184_hfq_ec, and pACYC184_hfq_cac. Plasmid maps of pACYC184_pkon, pACYC184_hfq_ec, and pACYC184_hfq_cac are shown in Figure 3.13 A-C. Successful ligation was verified by PCR with primers Kontroll_pACYC184_hfq_fwd and Kontroll_pACYC184_hfq_fwd. Afterwards, plasmids were transformed into the *E. coli* Δ*hfq* strain. With strains *E. coli Δhfq*, *E. coli Δhfq* [pACYC184_pkon], *E. coli Δhfq* [pACYC184_hfq_ec], and *E. coli Δhfq* [pACYC184_hfq_cac] growth experiments were accomplished in LB medium. Mean values of at least three independent growth experiments are displayed in Figure 3.14A monitoring the optical density. All strains reached the stationary growth phase at the same time point. *E. coli Δhfq* and *E. coli Δhfq* [pACYC184_pkon] showed similar growth characteristics. Both strains, *E. coli Δhfq* and *E. coli Δhfq* [pACYC184_pkon], possessed the lowest growth rate (0.83 h^{-1} and 0.80 h^{-1}, respectively) and the lowest maximal optical density with 3.2 compared to the strains *E. coli Δhfq* [pACYC184_hfq_ec], *E. coli Δhfq* [pACYC184_hfq_cac]. The positive control *E. coli Δhfq* [pACYC184_hfq_ec] grew most rapidly with a growth rate of 1.12 h^{-1} and reached a maximal optical density of 7.2. The complementation strain *E. coli Δhfq* [pACYC184_hfq_cac] reached values between the positive and the negative control. The growth rate of 0.87 h^{-1} was smaller compared to the growth rate of *E. coli Δhfq*

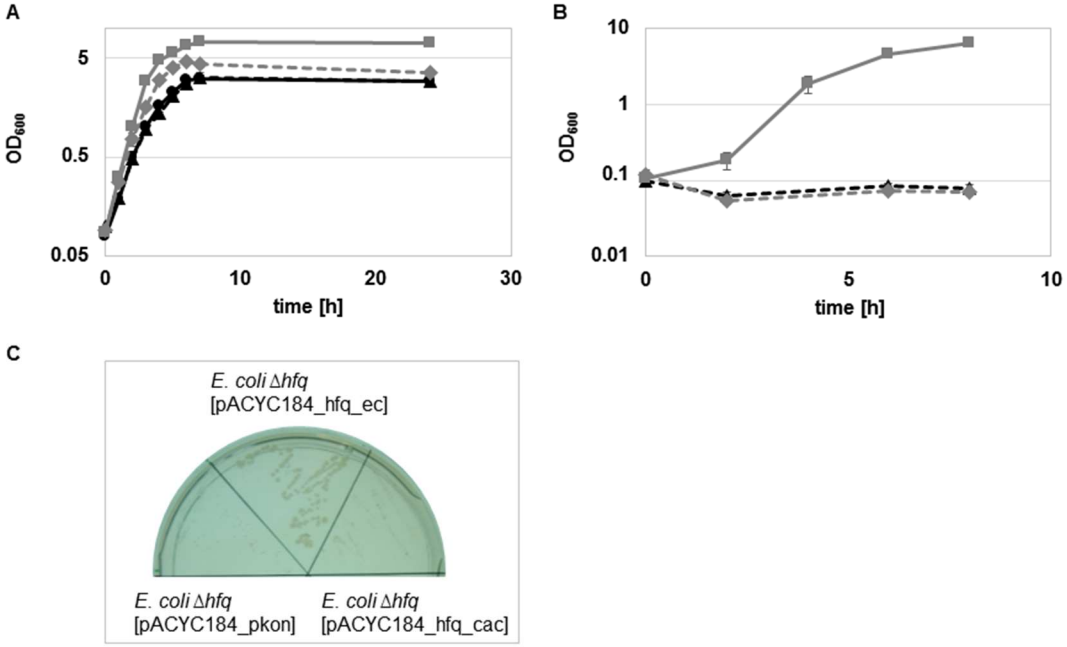

Figure 3.14: Growth behaviour of different *E. coli* strains with different supplements. (A) Growth curves of *E. coli* Δ*hfq* (●), *E. coli* Δ*hfq* [pACYC184_pkon] (▲), *E. coli* Δ*hfq* [pACYC184_hfq_ec,] (■), and *E. coli* Δ*hfq* [pACYC184_hfq_cac] (◆) under standard conditions. (B) Growth curves of *E. coli* Δ*hfq* [pACYC184_pkon] (▲), *E. coli* Δ*hfq* [pACYC184_hfq_ec,] (■), and *E. coli* Δ*hfq* [pACYC184_hfq_cac] (◆) under oxygen stress (0.02 %). (C) *E. coli* Δ*hfq* [pACYC184_pkon], *E. coli* Δ*hfq* [pACYC184_hfq_ec,], and *E. coli* Δ*hfq* [pACYC184_hfq_cac] under sugar stress on LB agar plates with 1 mM methyl α-D-glucopyranoside.

[pACYC184_hfq_ec], but the strain grew faster as *E. coli Δhfq* [pACYC184_pkon] and *E. coli Δhfq.* Same can be observed for the maximal optical density of *E. coli Δhfq* [pACYC184_hfq_cac] with 4.7. Further growth experiments were conducted with different stress stimuli. One stress growth experiment was conducted with hydrogen peroxide to activate the oxygen stress response in *E. coli*. Therefore, LB medium containing 0.02 % hydrogen peroxide was used. Mean values of at least three independent growth experiments were shown in Figure 3.14B. After a lag phase of nearly two hours, *E. coli Δhfq* [pACYC184_hfq_ec] entered the exponential growth phase. The maximal optical density was reached after 8 h with a value of 6.4. Compared to growth at standard conditions (Figure 3.14A), *E. coli Δhfq* [pACYC184_hfq_ec] showed significantly slower growth behaviour. In contrast, *E. coli Δhfq* [pACYC184_hfq_pkon] and *E. coli Δhfq* [pACYC184_hfq_cac] did not grow at all. Furthermore, growth was tested under sugar stress. Therefore, LB agar plates were prepared with 1 mM methyl α-D-glucopyranoside. *E. coli Δhfq* [pACYC184_hfq_pkon], *E. coli Δhfq* [pACYC184_hfq_ec], and *E. coli Δhfq* [pACYC184_hfq_cac] were streaked on to agar plates with and without methyl α-D-glucopyranoside. Afterwards, all plates were incubated for 1 day at 37 °C. The experiment was conducted independently three times. All strains were clearly visible and showed strong growth on the control agar plates without methyl α-D-glucopyranoside (data not shown). A representative LB plate containing methyl α-D-glucopyranoside is displayed in Figure 3.14C. For *E. coli Δhfq* [pACYC184_pkon], no growth could be detected. In contrast, *E. coli Δhfq* [pACYC184_hfq_ec] grew well. *E.coli Δhfq* [pACYC184_hfq_cac] growth was distinctly reduced compared to *E. coli Δhfq* [pACYC184_hfq_ec]. However, growth could be detected under sugar stress.

Also, the cell shape and morphology of the complementation strains were analyzed by different microscopy methods. To determine the cell length, light microscopy images were taken from overnight cultures. Exemplary one image of each *E. coli Δhfq* [pACYC184_hfq_cac], *E. coli Δhfq* [pACYC184_hfq_ec], and *E. coli Δhfq* [pACYC184] are displayed in Figure 3.15A. All bacteria showed a rod-shaped structure. Interestingly, some *E. coli Δhfq* [pACYC184] displayed a different colour scheme at the cell poles compared to the other strains. Furthermore, cell length of *E. coli Δhfq* [pACYC184] was increased compared to *E. coli Δhfq* [pACYC184_hfq_cac] and *E. coli Δhfq* [pACYC184_hfq_ec]. Cells of *E. coli Δhfq* [pACYC184_hfq_cac] also displayed

an increased cell length compared to *E. coli Δhfq* [pACYC184_hfq_ec]. To verify the results of the cell length, a minimum of 29 cells were measured of each strain. Mean values with standard deviation of *E. coli Δhfq* [pACYC184_hfq_cac], *E. coli Δhfq* [pACYC184_hfq_ec], and *E. coli Δhfq* [pACYC184] are shown in Figure 3.15B. The average length of *E. coli Δhfq* [pACYC184_hfq_ec] and *E. coli Δhfq* [pACYC184] was determined with 3.4 µm and 6.3 µm, respectively. The difference is highly significant between these strains as the p-value is below 0.001. The cell length of *E. coli Δhfq* [pACYC184_hfq_cac] was determined to be 5.6 µm. Thus, the strain *E. coli Δhfq* [pACYC184_hfq_cac], complemented with *hfq* from *C. acetobutylicum,* exhibited an increased cell length compared to *E. coli Δhfq* [pACYC184_hfq_ec], but a decreased length compared to *E. coli Δhfq* [pACYC184]. Also, in this case a significant difference between *E. coli Δhfq* [pACYC184_hfq_cac] and *E. coli Δhfq* [pACYC184] was assessed ($p < 0.05$). To take a closer look at the cells, SEM and TEM images of *E. coli Δhfq*, *E. coli Δhfq* [pACYC184], *E. coli Δhfq* [pACYC184_hfq_ec], and *E. coli Δhfq* [pACYC184_hfq_cac] were taken. Therefore, cells were grown over night in LB medium and afterwards prepared for imaging. In Figure 3.16, exemplary images of the SEM microscopy were shown. All strains displayed a rod-shaped structure. The surface of *E. coli Δhfq* [pACYC184_hfq_ec] seemed to be smoother compared to the other strains. Also, *E. coli Δhfq* [pACYC184_hfq_ec] exhibited the shortest cell length with about 1 µm. Notably, the *E. coli Δhfq* strain exhibited poles, which look as if they were squeezed together. *E. coli Δhfq* and *E. coli Δhfq* [pACYC184_pkon] exhibited the

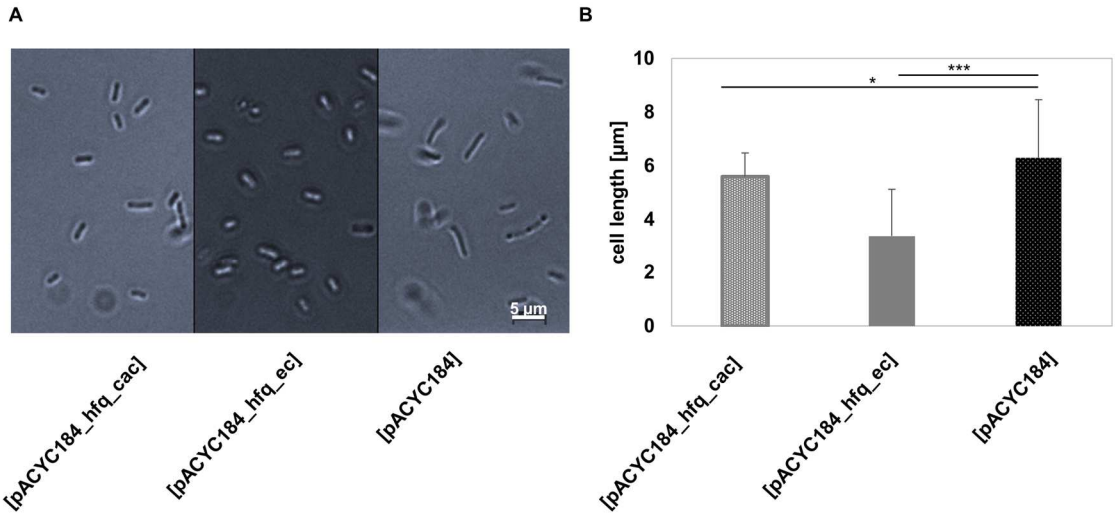

Figure 3.15: (A) Light microscopy images of *E. coli* Δ*hfq* [pACYC184_hfq_cac], *E. coli* Δ*hfq* [pACYC184_hfq_ec], and *E. coli* Δ*hfq* [pACYC184] (scale bar representing 5 µm). (B) Cell length of *E. coli* Δ*hfq* [pACYC184_hfq_cac] (n = 64), *E. coli* Δ*hfq* [pACYC184_hfq_ec] (n = 59), and *E. coli* Δ*hfq* [pACYC184] (n = 29) (*: p < 0.05, ***: p < 0.001).

largest cell length with approximately 2 µm. Cells of *E. coli Δhfq* [pACYC184_hfq_cac] displayed a cell length ranging between the positive and negative control. To analyse differences of the cell structure, TEM images were taken. Representative images of strains *E. coli Δhfq*, *E. coli Δhfq* [pACYC184_pkon], *E. coli Δhfq* [pACYC184_hfq_ec], and *E. coli Δhfq* [pACYC184_hfq_cac] are shown in Figure 3.16B. Again, the differences regarding cell length were apperent. Cell length increased in the following order: *E. coli Δhfq* [pACYC184_hfq_ec], *E. coli Δhfq* [pACYC184_hfq_cac] *E. coli Δhfq*, and *E. coli Δhfq* [pACYC184_pkon]. The negative control strains *E. coli Δhfq* and *E. coli Δhfq* [pACYC184_pkon] exposed a big gap in between the cytoplasm membrane and the outer membrane. This gap was represented in a bright area containing a few black granula. The content of the cytoplasm was darker in comparison to the poles. In contrast, the positive control *E. coli Δhfq* [pACYC184_hfq_ec] did not show the bright gap between the cytoplasm and the outer membrane. Cells of *E. coli Δhfq* [pACYC184_hfq_ec] were completely dark coloured. However, the poles seemed to have a different structure compared to the cells of the other strains. Strain *E. coli Δhfq* [pACYC184_hfq_cac] displayed similarities to the positive and the negative control. The bright gap between the cytoplasm and the outer membrane was visible in *E. coli Δhfq* [pACYC184_hfq_cac] as well. Indeed, the gap was apparently smaller in the case of *E. coli Δhfq* [pACYC184_hfq_cac] compared to the strains *E. coli Δhfq* or in *E. coli*

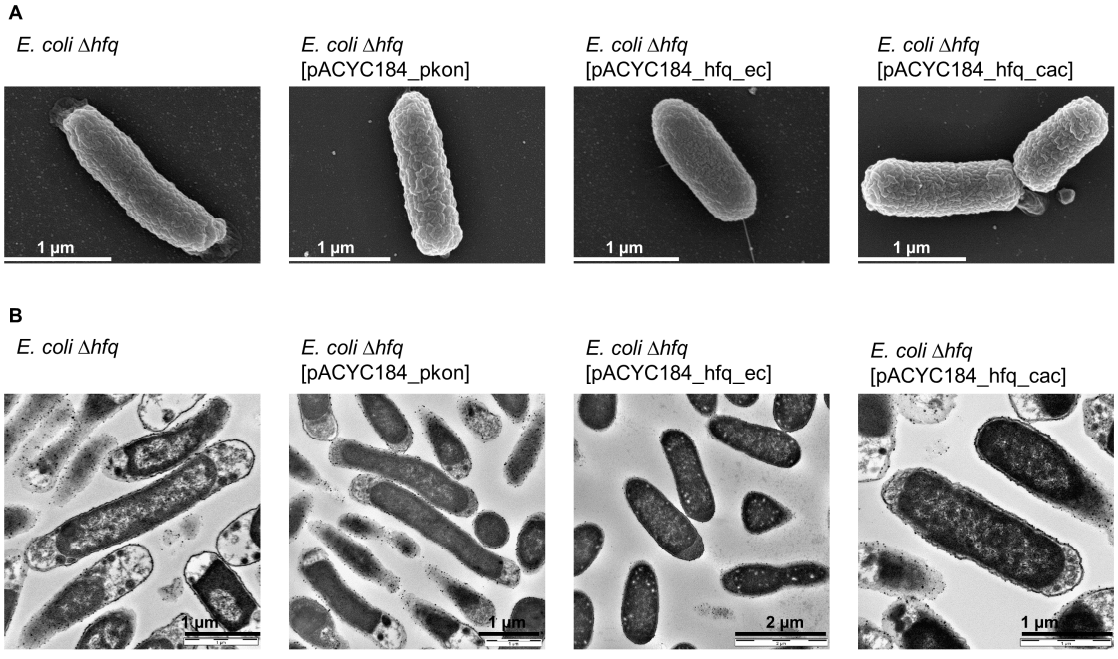

Figure 3.16: (A) SEM and (B) TEM images of *E. coli* Δ*hfq* , *E. coli* Δ*hfq* [pACYC184_pkon], *E. coli* Δ*hfq* [pACYC184_hfq_ec], and *E. coli* Δ*hfq* [pACYC184_hfq_cac]. Scale bar representing 1 µm, except *E. coli* Δ*hfq* [pACYC184_hfq_ec] (B), here, scale bar representing 2 µm.

Δhfq [pACYC184_pkon] and no black granula were observed. The content of the cytoplasm of *E. coli Δhfq* [pACYC184_hfq_cac] exhibited the same colour as the other investigated strains.

The Hfq protein of *C. acetobutylicum* was able to partly compensate effects of the *E. coli hfq* deletion such as growth deficiency, sugar stress sensitivity, increased cell length, and altered morphology. However, under oxygen stress the Hfq protein from *C. acetobutylicum* failed to replace functions of the *E. coli* Hfq.

3.2.3 Overexpression of *hfq* in *C. acetobutylicum*

To elucidate the functions of Hfq from *C. acetobutylicum*, *hfq* was overexpressed in *C. acetobutylicum*. Therefore, *hfq* was amplified from gDNA of *C. acetobutylicum* wild type. Primers used, hfq_fwd_bamHI and hfq_rev_ecoRI (Table 2.3), flanked the region 300 bps upstream of the start codon and the predicted terminator structure of *hfq*.Digested PCR product was ligated into the restriction sites *Bam*HI and *Eco*RI of pIMP1. The resulting plasmid pIMP1_hfq (Figure 3.17A) was transformed into competent *C. acetobutylicum* cells. Afterwards, growth experiments with the following strains were performed: *C. acetobutylicum* wild type, *C. acetobutylicum* [pIMP1], and *C. acetobutylicum* [pIMP1_hfq]. Strains were grown in triplicates in 50 mL MES-buffered medium. Mean values are displayed in Figure 3.17 monitoring optical density (B) and product formation of butanol (C), butyrate (D), ethanol (E), and acetone (F). The *C. acetobutylicum* wild type entered stationary growth phase first after 30 h. *C. acetobutylicum* [pIMP1] and *C. acetobutylicum* [pIMP1_hfq] displayed a significant lower starting OD_{600} and reached the stationary growth phase after 60 h. Comparison of the growth rates revealed an increased rate for *C. acetobutylicum* wild type (0.28 h^{-1}) in contrast to *C. acetobutylicum* [pIMP1] (0.12 h^{-1}) and *C. acetobutylicum* [pIMP1_hfq] (0.11 h^{-1}). All strains reached similar maxima OD_{600} vales of around 4. *C. acetobutylicum* wild type and *C. acetobutylicum* [pIMP1] produced approximately 73 mM butanol, 50 mM butyrate, 12 mM ethanol, and 50 mM acetone. Although similar amounts were produced, the production of butanol, butyrate, ethanol, and acetone started about 10 h later in *C. acetobutylicum* [pIMP1] compared to the *C. acetobutylicum* wild type. Strain *C. acetobutylicum* [pIMP1_hfq] also produced similar amounts of butyrate, ethanol, and acetone. The production of acetone and butanol formation started 10 h later compared to *C. acetobutylicum* [pIMP1]. However, in this case, the production not only began later, the produced amount of butanol and acetone was also lower, too. *C. acetobutylicum* [pIMP1] produced 60 mM butanol and

38 mM acetone after 60 h. In contrast, *C. acetobutylicum* [pIMP1_hfq] reached only an amount of 45 mM butanol and 31 mM acetone after 110 h. Moreover, the maximal production of butanol was decreased by 20.8 % in comparison to strains *C. acetobutylicum* wild type and *C. acetobutylicum* [pIMP1]. Summarizing, strain *C. acetobutylicum* [pIMP1_hfq] revealed a delayed and reduced solvent production.

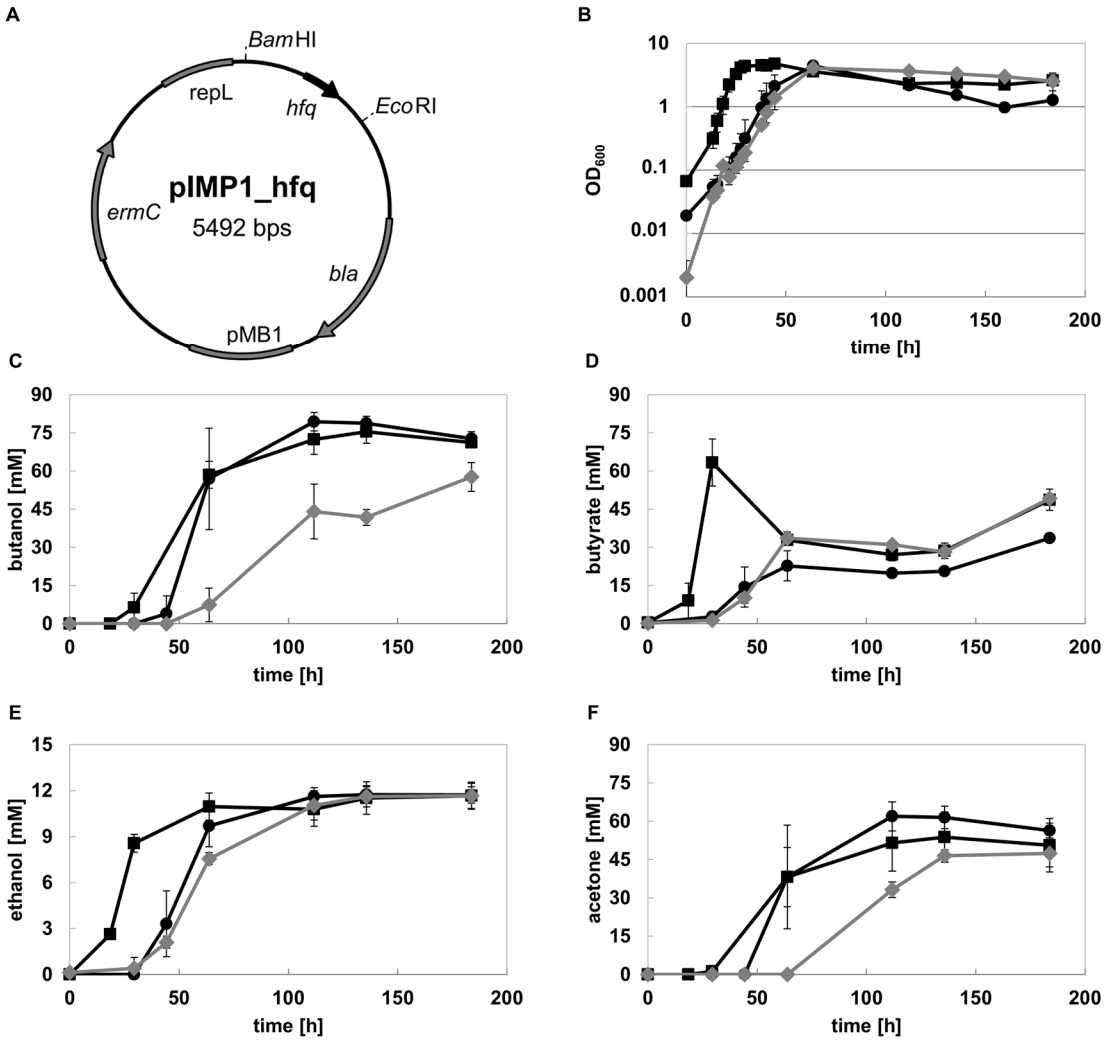

Figure 3.17: (A) Overexpression plasmid pIMP1_hfq. (B-F) Growth behaviour and product formation of *C. acetobutylicum* wild type (■), *C. acetobutylicum* [pIMP1] (●), and *C. acetobutylicum* [pIMP1_hfq] (◆) during growth in batch fermentation with 50 ml MES-buffered medium (n = 3); (B) growth behaviour, (C) butanol, (D) butyrate, (E) ethanol, and (F) acetone. *bla*, ampicillin resistance gene; pMB1, ori for Gram-negative bacteria; *ermC*, erythromycin resistance gene, repL, ori for Gram-positive bacteria; *hfq*, host factor I protein Hfq.

3.2.4 Identification of possible Hfq targets

To identify targets of Hfq in *C. acetobutylicum,* it was mandatory to purify Hfq. Therefore, *hfq* of *C. acetobutylicum* was expressed in *E. coli* [prep4][pQE_hfq] growing in TB medium. After reaching an OD_{600} value of 1, cells were induced with IPTG and incubated for 3 further hours. Cells were disrupted via French Press and purification of Hfq was achieved with magnetic beads by binding to the linked his-tag of the Hfq

protein. Purification was controlled by SDS-PAGE with silver staining (Figure 3.18A) and Western blot with immunostaining targeting the his-tag (Figure 3.18B). Cell-free extracts of the overexpression strain *E. coli* [prep4][pQE_hfq] and the control strain *E. coli* [prep4] showed a multitude of signals, especially in the higher molecular weight range. However, extract of *E. coli* [prep4][pQE_hfq] displayed one clear and intense signal between the 10 and 15 kDa marker bands. The elution fraction of *E. coli* [prep4] exhibited signals with more than 20 kDa. In contrast, the elution fraction of *E. coli* [prep4][pQE_hfq] contained one intense signal at about 12 kDa. The Western blot exposed only signals for cell-fee extract and elution fraction of *E. coli* [prep4][pQE_hfq]. Both samples showed two signals in close proximity in the lower molecular range.

As overexpression and purification worked successfully, Hfq pulldown assays were performed with DNA- and rRNA-free RNA of *C. acetobutylicum*. After phenol/chloroform extraction and ethanol precipitation, eluted RNA was transcribed into dcDNA. After ligation of the produced dcDNA into the pDrive vector, constructed plasmids were transformed into *E. coli* to generate a gen library of Hfq target RNAs. Afterwards, 432 colony PCRs were performed to determine clones with integrated dcDNA (Figure 3.19). 221 clones showed an integration into the pDrive vector. The PCR fragments of these clones were sequenced and blasted with the help of the NCBI database. 34 sequences mapped against the genome of *C. acetobutylicum* without hits mapping on rDNA of *C. acetobutylicum*. Remaining sequences originated from the

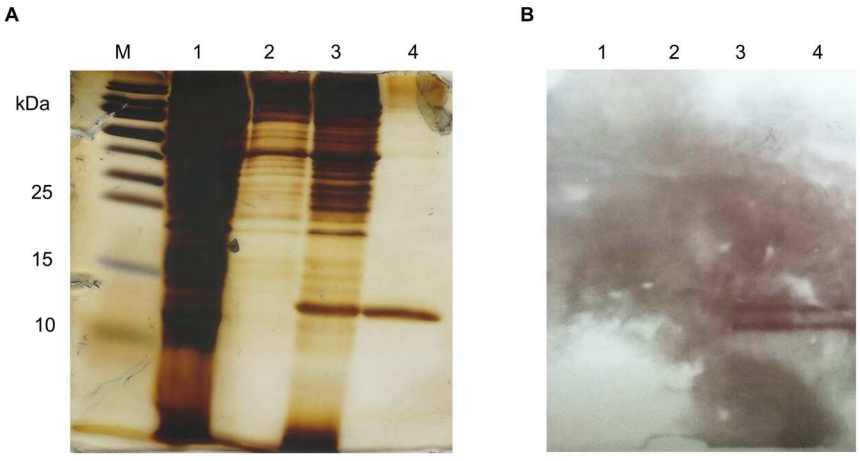

Figure 3.18: Purification control of Hfq via SDS-PAGE and Western blot. (A) SDS-PAGE of Hfq purified from *E. coli* M15 [pREP4] [pQE_hfq]; M, Prestained Protein Ladder (Thermo Fisher Scientific, Waltham, Ma, USA); 1, cell-free extract of *E. coli* M15 [pREP4]; 2, elution of magnetic beads after incubation with cell-free extract of *E. coli* M15 [pREP4]; 3, cell-free extract of *E. coli* M15 [pREP4] [pQE_hfq]; 4, elution of magnetic beads after incubation with cell-free extract of *E. coli* M15 [pREP4] [pQE_hfq]. (B) Western blot of Hfq purified from *E. coli* M15 [pREP4] [pQE_hfq); 1, cell-free extract of *E. coli* M15 [pREP4]; 2, elution of magnetic beads after incubation with cell-free extract of *E. coli* M15 [pREP4]; 3, cell-free extract of *E. coli* M15 [pREP4] [pQE_hfq]; 4, elution of magnetic beads after incubation with cell-free extract of *E. coli* M15 [pREP4] [pQE_hfq].

E. coli chromosome or did not reveal a positive sequencing result. In Table 3.2 locus tags, annotation, and COG category are listed of each identified sequence. Noteworthy, some transcripts were found twice in the analyzed samples and were attributed to the following genes: *CA_C1707*, permease of ATP-dependent phosphate uptake system; *CA_C2703*, molecular chaperone GroEL; *CA_C2866*, ATP synthase F0F1 subunit gamma; *CA_C3136*, elongation factor Tu; and *CA_C3648*, acetyltransferase. Furthermore, the sequences of *hfq* (CA_C1834) and the transcription antitermination protein *nusG* (CA_C3149) could be identified. The target genes were distributed to different COG categories. No preference for Hfq targets of distinct categories could be determined.

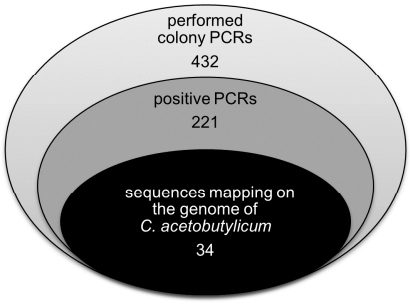

Figure 3.19: Number of results after the cloning process for the identification of RNAs which interact with Hfq. Colony PCRs (light grey) were performed to identify clones with plasmids containing an additional DNA fragment. PCRs showing products, which display an integration of a fragment into the cloned plasmid (dark grey), were sequenced and blasted. The number of sequences, which showed similarities with *C. acetobutylicum* genome, can be found in the black circle without results mapping on rDNA genes of *C. acetobutylicum*.

Table 3.2: Identified sequences via nucleotide blast of fished *C. acetobutylicum* RNAs with Hfq. Genes were assigned according to categories of Clusters of orthologous groups (COG): J, translation, ribosomal structure and biogenesis; K, transcription; L, replication, recombination and repair; V, defence mechanism; T, signal transduction mechanisms; M, cell wall/membrane/envelope biogenesis, U, intracellular trafficking, secretion, and vesicular transport; O, posttranslational modification, protein turnover, chaperones; C, energy production and conversion; G, carbohydrate transport and metabolism; E, amino acid transport and metabolism; F, nucleotide transport and metabolism; H, coenzyme transport and metabolism; P, inorganic ion transport and metabolism; R, general function prediction only; S, function unknown.

Locus tag	Gene product description[a]	COG category
CA_C0001	chromosome replication initiator DnaA	R
CA_C0147	ABC transporter ATP-binding protein	S
CA_C0285	DNA-damage repair protein	L
CA_C0595	glutamine amidotransferase subunit PdxT	H
CA_C1589	malate dehydrogenase	C
CA_C1707	permease of ATP-dependent phosphate uptake system	P
CA_C1707	permease of ATP-dependent phosphate uptake system	P
CA_C1804	exopolyphosphatase	F
CA_C1834	host factor I protein Hfq	T
CA_C2240	cyclomaltodextrin glucanotransferase	
CA_C2325	N-acetylglucosaminidase domain- and ChW repeat-containing cell wall hydrolase	G
CA_C2333	dTDP-glucose pyrophosphorylase	M
CA_C2535	hypothetical protein	R
CA_C2565	NifU-like domain-containing protein	O
CA_C2647	arginase	
CA_C2655	hypothetical protein	S
CA_C2703	molecular chaperone GroEL	O
CA_C2703	molecular chaperone GroEL	O
CA_C2808	beta-lactamase class C domain-containing protein	V
CA_C2846	preprotein translocase subunit SecA	U
CA_C2866	ATP synthase F0F1 subunit gamma	C
CA_C2866	ATP synthase F0F1 subunit gamma	C
CA_C2880	ribose-5-phosphate isomerase B	G
CA_C2894	hypothetical protein	S
CA_C3076	phosphotransbutyrylase	C
CA_C3136	elongation factor Tu	J
CA_C3136	elongation factor Tu	J
CA_C3149	transcription antitermination protein NusG	K
CA_C3150	preprotein translocase subunit SecE	U
CA_C3373	pectin methylesterase	G
CA_C3618	polar amino acid ABC transporter ATPase	E
CA_C3648	acetyltransferase	
CA_C3648	acetyltransferase	
CA_C3682	potassium-transporting ATPase subunit A	P

[a] description based on NCBI database

3.3 Interaction analysis of Hfq with SolB

To test whether Hfq interacts with SolB, in vitro transcription of *solB* was necessary. Therefore, pGH_solB_runoff was linearized and incubated with T7 polymerase and NTPs. Different incubation times and temperatures were tested to optimize production. For in vitro transcription of SolB the best results were observed after 4 h at 37 °C. Production of SolB was controlled by agarose gel electrophoresis (Figure 3.20). The in vitro transcription of SolB showed two intense signals. One signal was visible in the range of 3,000 bps to 10,000 bps, and the other one below 300 bps. Furthermore, one weak signal could be observed at about 200 bps. The linearized plasmid pGH_SolB_runoff displayed only one band between 3,000 bps and 10,000 bps.

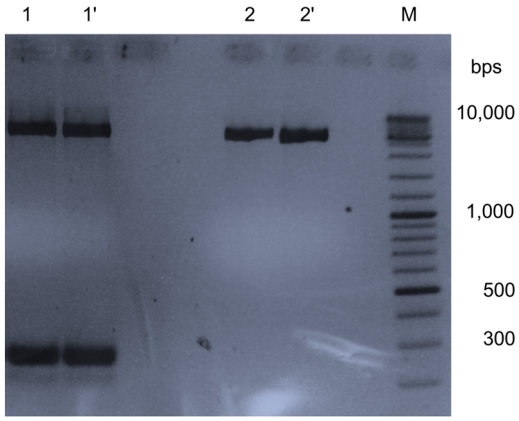

Figure 3.20: In vitro transcription of *solB* from linearized pGH_solB_runoff on a 2 % agarose gel. M, Gene Ruler Mix (Thermo Fisher Scientific, Waltham, Ma, USA); 1/1', in vitro transcription of *solB* from linearized [pGH_solB_runoff]; 2/2', linearized plasmid pGH_solB_runoff.

3.3.1 Pull down experiment with Hfq and SolB

In order to elucidate if Hfq is able to bind SolB, a pull down assay was performed. Therefore, SolB was transcribed by in vitro transcription using pGH_solB as template. Afterwards, SolB was labelled with biotin. The *hfq* gene was expressed in *E. coli* [pREP4][pQE_hfq]. The Hfq protein was linked with the help of the included his-tag to magnetic beads. Biotinylated SolB was added to the beads linked with Hfq. After incubation, Hfq was eluted off the beads. A schematic overview of the experimental approach is displayed in Figure 3.21A. The second attempt was performed using only biotinylated SolB and beads without linkage of Hfq. After elution, Hfq purification was controlled by silver stained SDS-PAGE (Figure 3.21B). Sample containing Hfq showed a clear signal below 15 kDa. In contrast, the approach without Hfq, did not reveal a signal. To determine whether SolB was present in the elution fractions, dot blots were performed by chemiluminescence detection of the biotin-labelled SolB (Figure 3.21C).

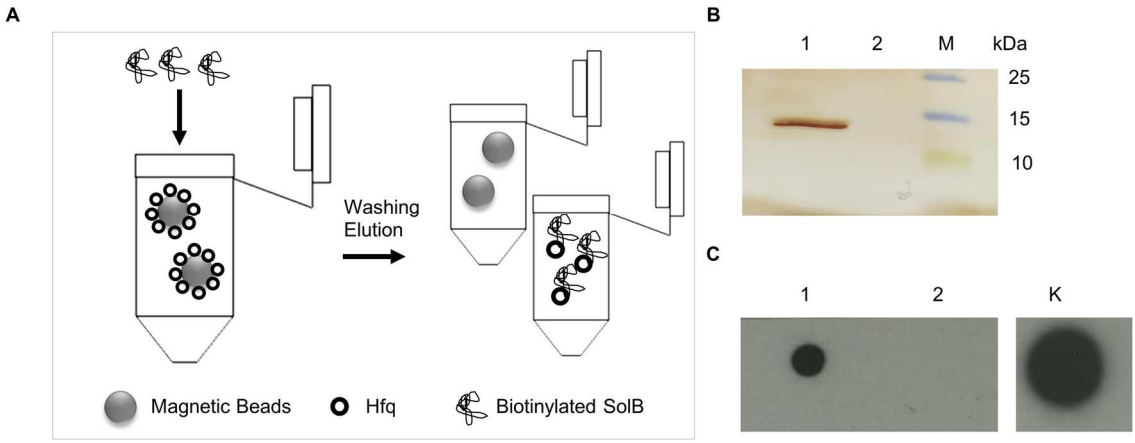

Figure 3.21: (A) Simplified model of the pull down assay between his-tagged Hfq and biotinylated SolB. (B) Purification control of Hfq after pull down assay via SDS-PAGE with silver staining. (C) Dot blot of elution fraction from pull down assay to detect biotinylated SolB. 1, elution fraction of pull down assay between his-tagged Hfq and biotinylated SolB; 2, elution fraction of pulldown assay between magnetic beads and biotinylated SolB; M, Prestained Protein Ladder (Thermo Fisher Scientific, Waltham, Ma, USA); K, biotinylated SolB.

A signal was obtained for the sample with Hfq and biotinylated SolB. Also, the positive control, which was performed by direct pipetting of biotinylated SolB onto the membrane, showed an intense signal. For the approach without Hfq, no signal was determined. Summarizing, Hfq was able to bind SolB in a pull down experiment.

3.3.2 Electrophoretic mobility shift assay of Hfq and SolB

Furthermore, interaction of Hfq and SolB was investigated by electrophoretic mobility shift assay (EMSA). For EMSA, in vitro transcribed SolB was biotinylated and Hfq of *C. acetobutylicum* was purified after recombinant overexpression in *E. coli* [pREP4][pQE_hfq]. Afterwards, SolB was incubated with increasing amounts of Hfq. Samples were analyzed by non-denaturating polyacrylamide gelelectrophorese and Western blot with chemiluminescence detection (Figure 3.22). The approaches containing SolB with concentrations of 0 nM and 0.37 nM Hfq displayed a signal in the lower part of the blot. The sample containing 3.7 nM Hfq and biotinylated SolB already showed an extended signal into the upper part of the blot. For samples including 37 nM and 141 nM Hfq, a clear shift of the signal could be determined into the upper part of the blot. Biotinylated SolB, unlabelled SolB, and Hfq also exhibited a signal in the upper part of the blot. However, intensity was decreased compared to samples with biotinylated SolB and Hfq. Signal of biotinylated SolB in presence of 1x elution buffer was similar to signals of biotinylated SolB in presence of 0-0.37 nm Hfq. A clear shift of SolB was recognized in presence of minimum 37 nM Hfq indicating the binding of Hfq and SolB.

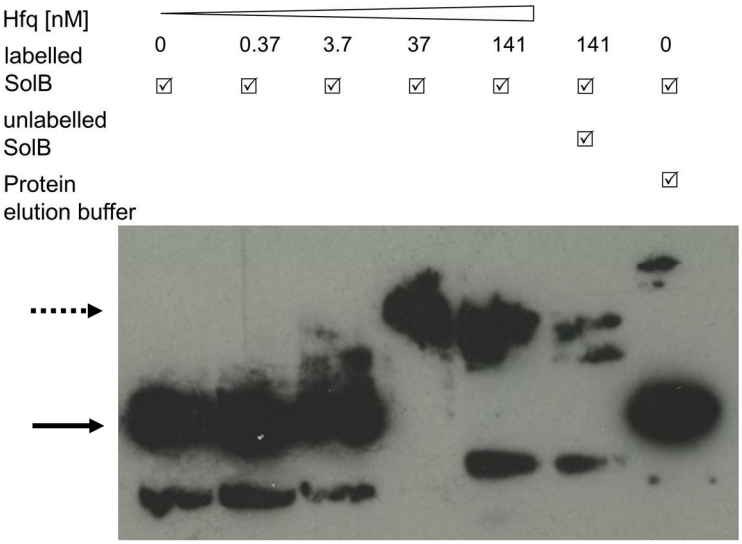

Figure 3.22: Direct binding of Hfq to the SolB sRNA assessed by EMSA. Biotin-labelled SolB was incubated with increasing amounts (0 to 141 nM) of Hfq protein. For competition reactions, unlabelled SolB was included in the binding reaction mixture in molar excess as indicated in lane 6. Negative control was performed by using the elution buffer instead of the elution fraction containing Hfq in lane 7. Hfq-SolB complexes are indicated by a dotted arrow. Free SolB is indicated by a black arrow.

3.3.3 Stabilization assay of Hfq and SolB

To determine effects regarding stability of SolB in interaction with Hfq, a stabilization assay was conducted. Therefore, *solB* was in vitro transcribed from the plasmid pGH_solB. *hfq* was recombinantly expressed in *E. coli* [prep4][pQE_hfq] and the Hfq protein was purified by the included his-tag. For the assay, RNases of *C. acetobutylicum* were mandatory to boost RNA decay. Hence, strain *C. acetobutylicum* wild type was grown in CG medium for two days. To generate a cell-free extract, cells were ribolyzed and cell debris were removed by centrifugation. SolB was incubated with cell-free extract at 37 °C. The reaction was set up 7 times and analyzed after

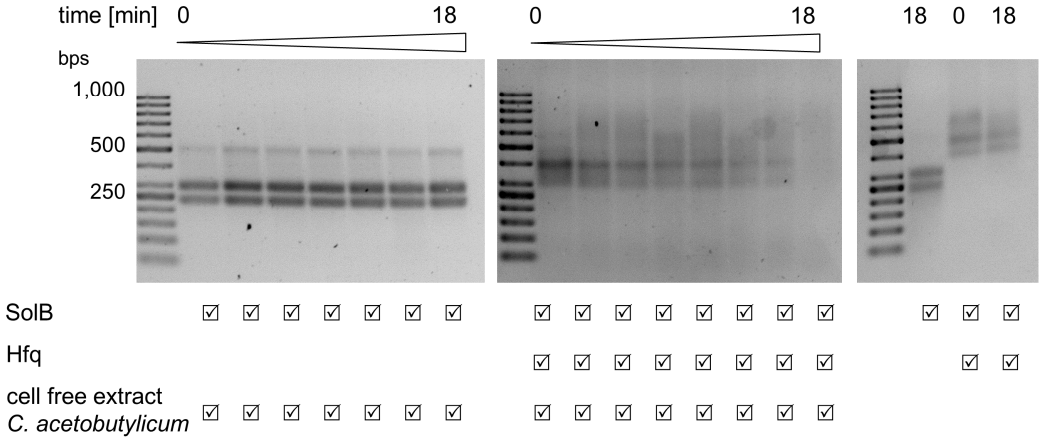

Figure 3.23: Stabilization assay of regulatory RNA SolB with Hfq and cell-free extract of *C. acetobutylicum* on a 2 % agarose gel. Samples were incubated for 0, 2.5, 5.0, 7.5, 10.0, 12.5, 15.0, and 18.0 min. GeneRuler™ 50 bp DNA ladder (Thermo Fisher Scientific, Waltham MA, USA) was used as marker.

different incubation times (0-18 min) on a 2 % agarose gel (Figure 3.23, left part). Each sample showed the same signal pattern regarding separation and intensity. In each lane it was possible to recognize signals at approximately 230 bps, 250 bps, and 300 bps. Moreover, SolB was incubated with Hfq and cell-free extract of *C. acetobutylicum* at 37 °C. The reaction was analyzed after different incubation times (0-18 min) on a 2 % agarose gel (Figure 3.23, right part). The signals of SolB decreased with increasing incubation time. At the last analzyed time point (18 min), no signal was detectable for SolB in the agarose gel. In contrast, SolB showed an intense signal at approximately 400 bps at the beginning of the experiment (0 min). The control sample, which contained only SolB, displayed the same signal as the reaction with SolB and cell-free extract after 18 min of incubation. Samples with SolB and Hfq showed similar patterns as the starting reactions (0 min) of SolB, Hfq, and cell-free extract of *C. acetobutylicum.* The approaches with Hfq and SolB were either incubated 0 or 18 min and displayed a signal at about 500 bps. Summarizing, the signal shifted to a higher bps range if Hfq was present and the signal intensitiy of labelled SolB decreased if Hfq was incubated over time with SolB and cell-free extract.

3.3.4 Characterizing genetically modified *C. acetobutylicum* strains

As binding of SolB by Hfq was possible, the next step was to find out if SolB's mode of action is dependent on Hfq. Therefore, plasmids were constructed to knockdown the *hfq* expression by antisense RNA. Shuttle vector pBS77 was used as backbone, which additionally contains the *ptb-buk* promoter compared to the pIMP1 shuttle vector. The promoter was necessary as the antisense sequences had to be expressed by a strong promoter. Thus, the antisense construct of the *hfq* sequence (as_hfq) was

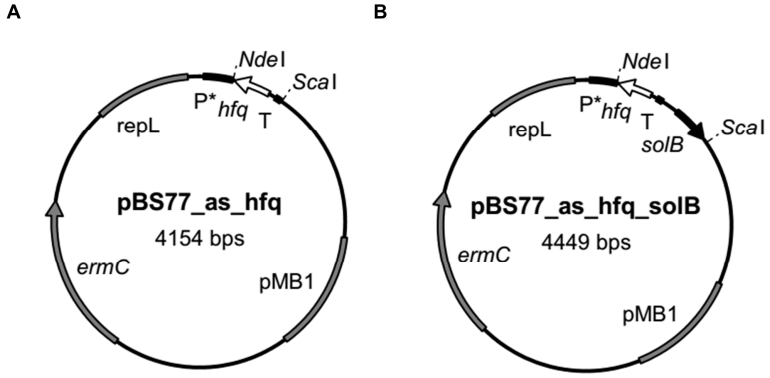

Figure 3.24: Plasmid maps of (A) [pBS77_as_hfq] and (B) [pBS77_as_hfq_solB]. Both plasmids contain an antisense construct of *hfq* from *C. acetobutylicum.* [pBS77_as_hfq_solB] encodes the regulatory RNA SolB. pMB1, ori for Gram-negative bacteria; *ermC,* erythromycin resistance gene*;* repL, ori for Gram-positive bacteria; P*, sequence of *ptb-buk* promoter; *hfq*, sequence of host factor I protein Hfq; T, predicted terminator of the *hfq* gene*; solB,* regulatory RNA SolB.

cloned into the restriction sites of *Nde*I and *Sca*I downstream of the *ptb-buk* promoter. The resulting plasmid was named pBS77_as_hfq (Figure 3.24A). Detailed sequence information of as_hfq can be found in Figure 8.1A (Supplement). In same manner, the sequence of as_hfq_solB (Supplement Figure 8.1B) was cloned into pBS77 and the constructed plasmid was named pBS77_as_hfq_solB, which harbours the antisense sequence of *hfq* and the complete *solB* gene. Plasmid map of pBS77_as_hfq_solB is displayed in Figure 3.24B.

Constructed plasmids were transformed into *C. acetobutylicum*. Successfully transformed clones were used with strains *C. acetobutylicum* [pIMP1] and *C. acetobutylicum* [pIMP1_solB] for growth experiments in 50 mL MES-buffered medium. Mean values of three independent growth experiments are shown in Figure 3.25 monitoring optical density (A) and product formation of butanol (B), butyrate (C), and acetone (F). All strains displayed similar growth behaviour, whereas, the start point of exponential growth phase was delayed for strains *C. acetobutylicum* [pIMP1], *C. acetobutylicum* [pBS77_as_hfq], and *C. acetobutylicum* [pBS77_as_hfq_solB] in comparison to *C. acetobutylicum* [pIMP1_solB] (Figure 3.25A). The maximal optical density was determined for all strains to be approximately 3.6. Similar yields of butanol, acetone, and butyrate were measured over time of the growth experiment for strains

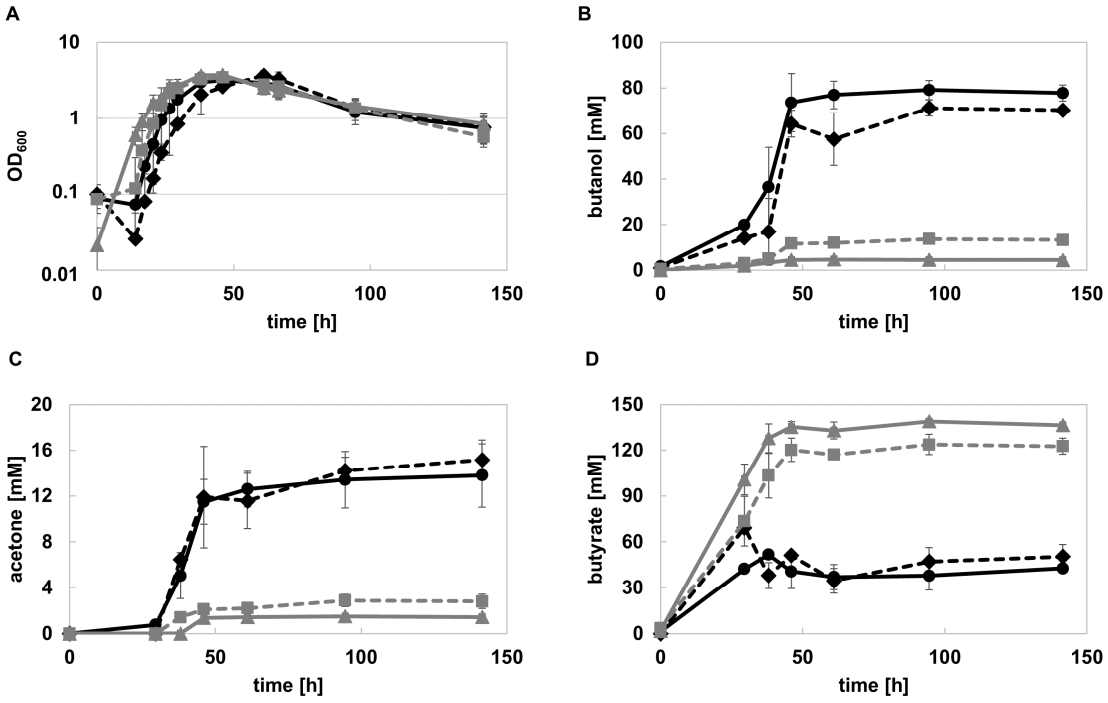

Figure 3.25: Growth behaviour and product formation of *C. acetobutylicum* [pIMP1] (●), *C. acetobutylicum* [pIMP1_solB] (▲), *C. acetobutylicum* [pBS77_as_hfq] (◆), and *C. acetobutylicum* [pBS77_as_hfq_solB] (■) during growth in batch fermentation with 50 ml MES-buffered medium (n = 3); (A) growth behaviour, (B) butanol, (C) acetone, and (D) butyrate.

C. acetobutylicum [pIMP1] and *C. acetobutylicum* [pBS77_as_hfq]. Approximately 80 mM butanol, 15 mM acetone, and 50 mM butyrate were produced by the respective strains. The amount of acetone and butanol was significantly lower in strains *C. acetobutylicum* [pIMP1_solB] and *C. acetobutylicum* [pBS77_as_hfq_solB] than in strains *C. acetobutylicum* [pIMP1] and *C. acetobutylicum* [pBS77_as_hfq]. The production of butyrate was increased in strains *C. acetobutylicum* [pIMP1_solB] and *C. acetobutylicum* [pBS77_as_hfq_solB] compared to *C. acetobutylicum* [pIMP1] and *C. acetobutylicum* [pBS77_as_hfq]. However, the amounts of acids and solvents differed between the strains *C. acetobutylicum* [pIMP1_solB] and *C. acetobutylicum* [pBS77_as_hfq_solB]. The *solB* overexpression strain *C. acetobutylicum* [pIMP1_solB] produced only 4.4 mM butanol and 1.4 mM acetone. In contrast, strain *C. acetobutylicum* [pBS77_as_hfq_solB] exhibited three times more butanol and two times more acetone compared to *C. acetobutylicum* [pIMP1_solB]. Butyrate concentration was 136 mM for *C. acetobutylicum* [pIMP1_solB] and 123 mM for *C. acetobutylicum* [pBS77_as_hfq_solB]. Concluding, the strain *C. acetobutylicum* [pBS77_as_hfq_solB], which overexpresses the *solB* gene and an antisense sequence to the *hfq* gene, showed an increased solvent production compared to strain *C. acetobutylicum* [pIMP1_solB]. *C. acetobutylicum* [pBS77_as_hfq] displayed no differences in growth and product formation compared to the strain without the antisense sequence of *hfq, C. acetobutylicum* [pIMP1].

Beside product formation, the copy number of pSOL1 was determined of the respective strains at the end of exponential growth phase. Therefore, gDNA of strains *C. acetobutylicum* [pIMP1], *C. acetobutylicum* [pIMP1_solB], *C. acetobutylicum* [pBS77_as_hfq], and *C. acetobutylicum* [pBS77_as_hfq_solB] was prepared and qRT-PCR was performed amplifying the chromosome encoded genes: gyr (CA_C007, primers: LC_gyr_fwd, LC_gyr_rev, Table 2.5) and *spo0A* (CA_C2071, primers: LC_spo0A_fwd, LC_spo0A_rev, Table 2.5), as well as the megaplasmid encoded genes: *adhE2* (CA_P0035, primers: LC_adhE2_fwd, LC_adhE2_rev, Table 2.5) and *adc* (CA_P0165, primers: LC_adc_fwd, LC_adc_rev, Table 2.5). Afterwards, the relative copy number of pSOL1 was calculated for each strain by normalizing to the wild type of *C. acetobutylicum.* Strains *C. acetobutylicum* [pIMP1] and *C. acetobutylicum* [pIMP1_solB] showed the same results as in previous experiments. The pSOL1 level in *C. acetobutylicum* [pIMP1] was approximately two times higher as in the *C. acetobutylicum* wild type strain. *C. acetobutylicum* [pIMP1_solB] offered a

30 times lower amount of pSOL1 compared with the *C. acetobutylicum* wild type. Strain *C. acetobutylicum* [pBS77_as_hfq] displayed a value in between the amount of the wild type and the empty vector strain *C. acetobutylicum* [pIMP1]. The level of pSOL1 in *C. acetobutylicum* [pBS77_as_hfq_solB] was sigficantly decreased compared to *C. acetobutylicum* [pIMP1] and *C. acetobutylicum* [pBS77_as_hfq]. In contrast to *C. acetobutylicum* [pIMP1_solB], which revealed a decreased copy number of 30 times in comparison with the *C. acetobutylicum* wild type strain, the amount of pSOL1 in *C. acetobutylicum* [pBS77_as_hfq_solB] was reduced 12 times compared to the *C. acetobutylicum* wild type. One further approach to elucidate SolB's dependency on Hfq was performed by construction of an *hfq* integration mutant in *C. acetobutylicum*. For generating integration mutants, the ClosTron™ Gene Knockout system was used. Two integration sites were chosen: one integration site was located 79 bps downstream of the *hfq* start codon on the codon strand and the other integration site was located 168 bps downstream of the *hfq* start codon on the template strand (Figure 3.27A). For integration at position 79, the plasmid pMTL007C-E2_79shfq was used and for integration at position 168 the plasmid pMTL007C-E2_168ahfq, respectively. Both plasmids were methylated and transformed into *C. acetobutylicum.* After two rounds of selection on thiamphenicol and three rounds of selection on clarithromycin, gDNA of transformants was prepared. PCRs were performed with primers miaA_fwd and cyst_rev (Table 2.3) to identify integrations in the *hfq* genes. Orientation of the integration was determined via PCR either with primers hfq_fwd and EBS_universal for integration in sense orientation (Figure 3.27B) or with primers hfq_rev and EBS_universal for integration in antisense orientation to the *hfq* gene (Figure 3.27C).

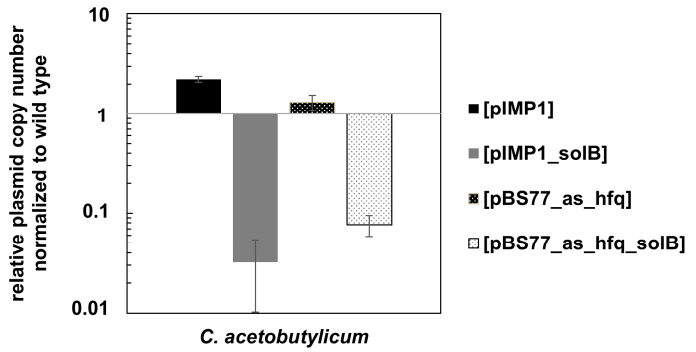

Figure 3.26: Relative plasmid copy number of pSOL1 in *C. acetobutylicum* [pIMP1] (black), *C. acetobutylicum* [pIMP1_solB] (grey), *C. acetobutylicum* [pBS77_as_hfq] (broken black) and *C. acetobutylicum* [pBS77_as_hfq_solB] (broken grey). The copy number of pSOL1 in the wild type strain was set to 1.

PCR products were analyzed on non-denaturating agarose gel. PCRs with template DNA of *C. acetobutylicum int::hfq* and primer miaA_fwd and cyst_rev displayed one signal just below the 4,000 bps mark of the ladder. Same PCR set-up showed with template DNA of *C. acetobutylicum* wild type a fragment with approximately 1,800 bps (Figure 3.27D). PCR products targeting part of the integration and the *hfq* gene exhibited a signal at 250 bps, except the approaches with water, which did not show a signal (Figure 3.27E).

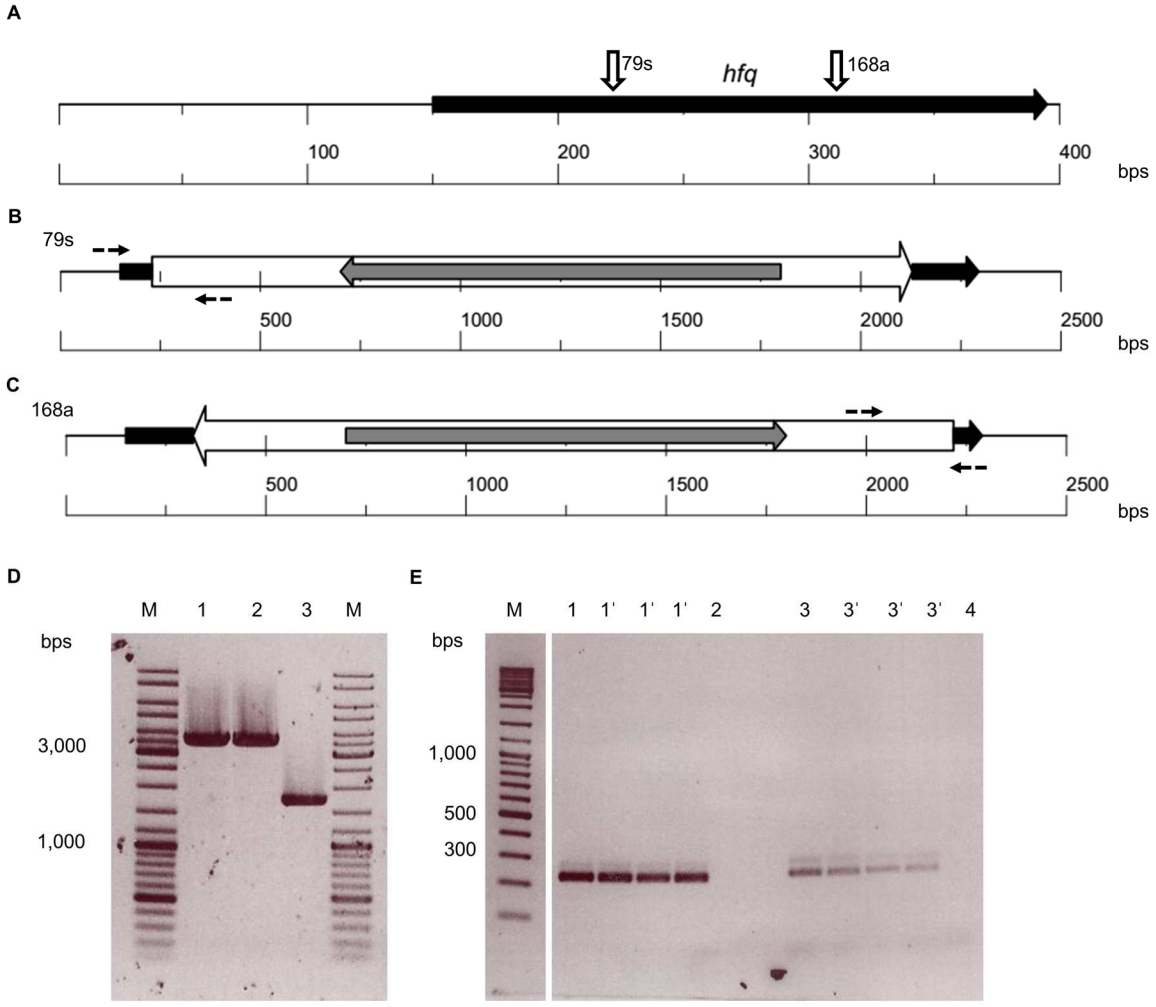

Figure 3.27: (A) Integration sites of introns of the ClosTron™ plasmids: pMTL007C-E2_79shfq (79s), integration should be positioned 79 bps downstream of the *hfq* start codon; pMTL007C-E2_168ahfq (168a) integration should be positioned 168 bps after *hfq* start codon. a, integration in antisense orientation to *hfq* gene*;* s, integration in sense orientation to *hfq* gene. **(B) Genetic organisation of *int::hfq* conducted with [pMTL007C-E2_79shfq]. White arrow, ClosTron™ intron;** grey arrow, erythromycin resistance gene; black arrow, host factor Q gene; dotted arrows, primer EBS_universal and hfq_fwd. **(C) Genetic organisation of *int::hfq* conducted with [pMTL007C-E2_168hfq].** White arrow, ClosTron™ intron; grey arrow, erythromycin resistance gene; black arrow, host factor Q gene; dotted arrows, primer EBS_universal and hfq_rev. **(D) Verification of integration in *C. acetobutylicum* by PCR analysis and non-denaturating electrophoresis in a 0.8 % agarose gel.** Primer miaA_fwd and cyst_rev were used for amplification of genomic DNA. 1, *C. acetobutylicum int::hfq* 79s; 2, *C. acetobutylicum int::hfq* 168a; 3, *C. acetobutylicum* wild type; M, Gene Ruler Mix (Thermo Fisher Scientific, Waltham, Ma, USA). **(E) Verification of integration in *C. acetobutylicum* by PCR analysis and non-denaturating electrophoresis on a 2 % agarose gel**. Primer hfq_fwd and EBS_universial were used for amplification of gDNA of *C. acetobutylicum int::hfq* 79s (1/1') and water (2/2'). Primers hfq_rev and EBS_universal were used for amplification of gDNA of *C. acetobutylicum int::hfq* 168a (3) and water (4). M, Gene Ruler Mix (Thermo Fisher Scientific, Waltham, Ma, USA).

Next step was to transform the plasmids pIMP1_catp and pIMP1_catp_solB into strains *C. acetobutylicum int::hfq* 79s and *C. acetobutylicum int::hfq* 168a. Furthermore, complementation of *C. acetobutylicum int::hfq* was achieved by construction of the following plasmids pIMP1_catp_ptb_hfq and pIMP1_catp_solB_ptb (Figure 3.28). For this purpose, the coding sequence of *hfq* was fused with the constitutive *ptb-buk* promoter of *C. acetobutylicum* (Supplement Figure 8.6). The sequence was cloned into the *Sfo*I restriction sites of pIMP1_catp and pIMP1_catp_solB. Afterwards, the plasmids pIMP1_catp, pIMP1_catp_solB, pIMP1_catp_ptb_hfq, and pIMP1_catp_solB_ptb_hfq were transformed in *C. acetobutylicum int::hfq* 79s as well as in *C. acetobutylicum int::hfq* 168s. After selection on clarithromycin and thiamphenicol, grown clones were verified via preparation of gDNA and PCR with primers Tobi_primer_fwd1 and Tobi_primer_rev (Table 2.3). Furthermore, the integration was verified by PCR with primer miaA_fwd and cys_rev (Table 2.3).

Growth experiments were conducted with *C. acetobutylicum int::hfq* 79s [pIMP1_catp], *C. acetobutylicum int::hfq* 79s [pIMP1_catp_solB], *C. acetobutylicum int::hfq* 79s [pIMP1_catp_ptb_hfq], and *C. acetobutylicum int::hfq* 79s [pIMP1_catp_solB_ptb_hfq] in 50 mL MES-buffered medium to investigate the role of Hfq for the functionality of SolB. Mean values of at least three independent experiments are displayed in Figure 3.29 reporting optical density (A) and product formation of butanol (B), acetone (C), and butyrate (D). Except for *C. acetobutylicum int::hfq* 79s [pIMP1_catp_solB], strains showed similar growth behaviour with a maximal optical density of approximately 5.3. *C. acetobutylicum int::hfq* 79s [pIMP1_catp_solB] stayed 15 h longer in the lag phase compared to the other strains. However, *C. acetobutylicum int::hfq* 79s [pIMP1_catp_solB] reached a similar growth rate and maximal optical density.

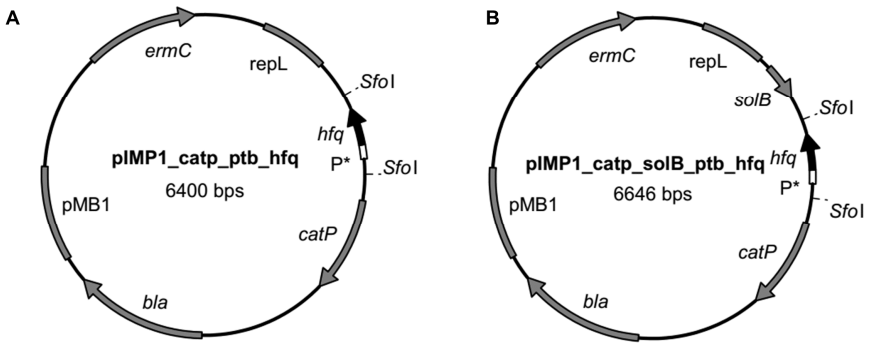

Figure 3.28: Plasmid maps of (A) pIMP1_catp_ptb_hfq and (B) pIMP1_catp_solB_ptb_hfq for complementation of *C. acetobutylicum int::hfq*. pMB1, ori for Gram-negative bacteria; *ermC,* erythromycin resistance gene; repL, ori for Gram-negative bacteria; *solB*, regulatory RNA gene; P*, sequence of *ptb-buk* promoter; *hfq*, host factor I protein Hfq; *catP*, thiamphenicol resistance gene; *bla*, ampicillin resistance gene.

C. acetobutylicum int::hfq 79s [pIMP1_catp], *C. acetobutylicum int::hfq* 79s [pIMP1_catp_ptb_hfq], and *C. acetobutylicum int::hfq* 79s [pIMP1_catp_solB_ptb_hfq] produced approximately 58 mM butanol, 12 mM acetone, and 40 mM butyrate. Solvent production of *C. acetobutylicum int::hfq* 79s [pIMP1_catp_solB] was decreased compared to the other strains. Levels of only 3 mM acetone and 25 mM butanol were reached by strain *C. acetobutylicum int::hfq* 79s [pIMP1_catp_solB]. In contrast, production of butyrate was increased with an end concentration of 64 mM compared to strains *C. acetobutylicum int::hfq* 79s [pIMP1_catp] (37 mM), *C. acetobutylicum int::hfq* 79s [pIMP1_catp_ptb_hfq] (47 mM), and *C. acetobutylicum int::hfq* 79s [pIMP1_catp_solB_ptb_hfq] (37 mM). All strains produced approximately 10 mM ethanol.

Also, growth experiments were performed with strains *C. acetobutylicum int::hfq* 168a [pIMP1_catp], *C. acetobutylicum int::hfq* 168a [pIMP1_catp_solB], *C. acetobutylicum int::hfq* 168a [pIMP1_catp_ptb_hfq], and *C. acetobutylicum int::hfq* 79s [pIMP1_catp_solB_ptb_hfq] in 50 mL MES-buffered medium to investigate the role of Hfq for the functionality of SolB. Mean values of growth behaviour and product formation are displayed in Figure 3.30A-D. All strains displayed similar growth curves. However, the lag phase of *C. acetobutylicum int::hfq* 168a [pIMP1_catp_ptb_hfq] was

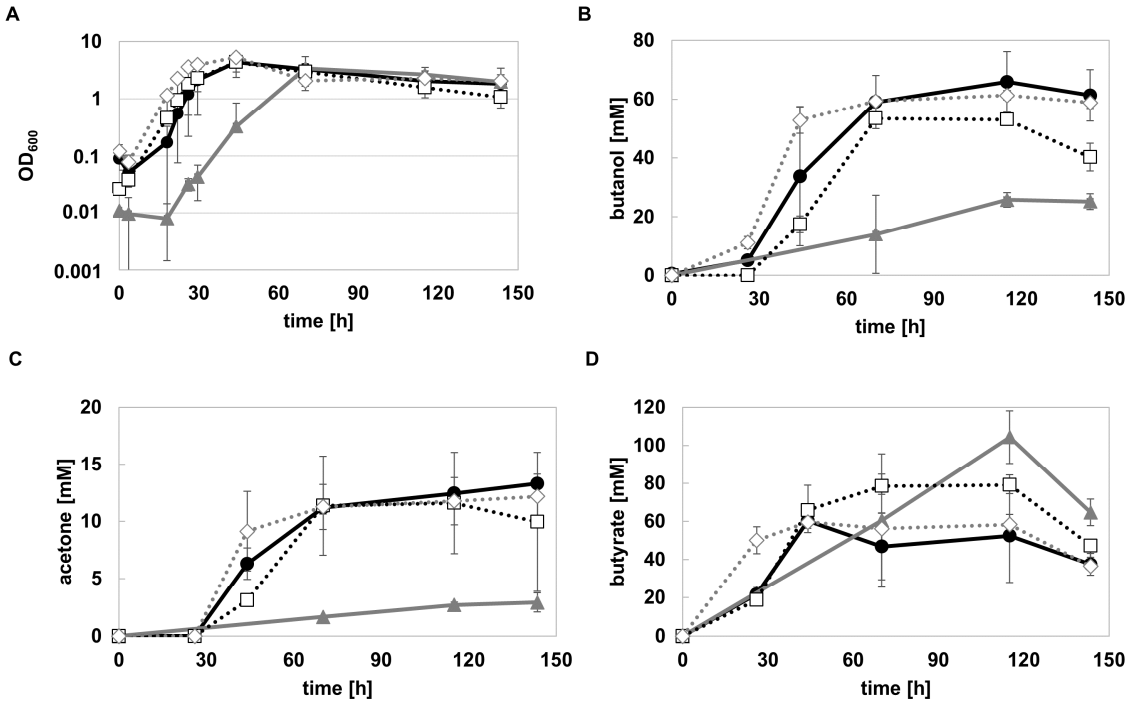

Figure 3.29: Growth behaviour and product formation of *C. acetobutylicum int::hfq* 79s [pIMP1_catp] (●), *C. acetobutylicum int::hfq* 79s [pIMP1_catp_solB] (▲), *C. acetobutylicum int::hfq* 79s [pIMP1_catp_ptb_hfq] (□), and *C. acetobutylicum int::hfq* 79s [pIMP1_catp_solB_ptb_hfq] (◇) during growth in batch fermentation with 50 ml MES-buffered medium (n = 3); (A) growth behaviour, (B) butanol, (C) acetone, and (D) butyrate.

increased compared to the other strains and as a consequence the stationary growth phase was reached later. The maximal optical density was roughly the same for all strains with approximately 5. The highest level of solvents was produced by *C. acetobutylicum int::hfq* 168a [pIMP1_catp] yielding 67 mM butanol and 12 mM acetone. *C. acetobutylicum int::hfq* 168a [pIMP1_catp_solB] produced 60 mM butanol and 6 mM acetone. However, production of acetone started after reaching the stationary growth phase. The other strains already began production in the exponential growth phase. The complementation strains *C. acetobutylicum int::hfq*168a [pIMP1_catp_ptb_hfq] and *C. acetobutylicum int::hfq* 168s [pIMP1_catp_solB_ptb_hfq] reached concentrations of 37 mM and 47 mM butanol. End concentration of acetone was determined with 10 mM and 8 mM. Production of butyrate was increased in strains *C. acetobutylicum int::hfq* 168a [pIMP1_catp_solB] (60 mM) and *C. acetobutylicum int::hfq* 168a [pIMP1_catp_ptb_hfq] (56 mM) compared to *C. acetobutylicum int::hfq* 168a [pIMP1_catp] (30 mM) and *C. acetobutylicum int::hfq* 168a [pIMP1_catp_solB_ptb_hfq] (41 mM).

Results of the growth experiments with strains *C. acetobutylicum int::hfq* 79s and strains of *C. acetobutylicum int::hfq* 168a revealed similar end product concentration

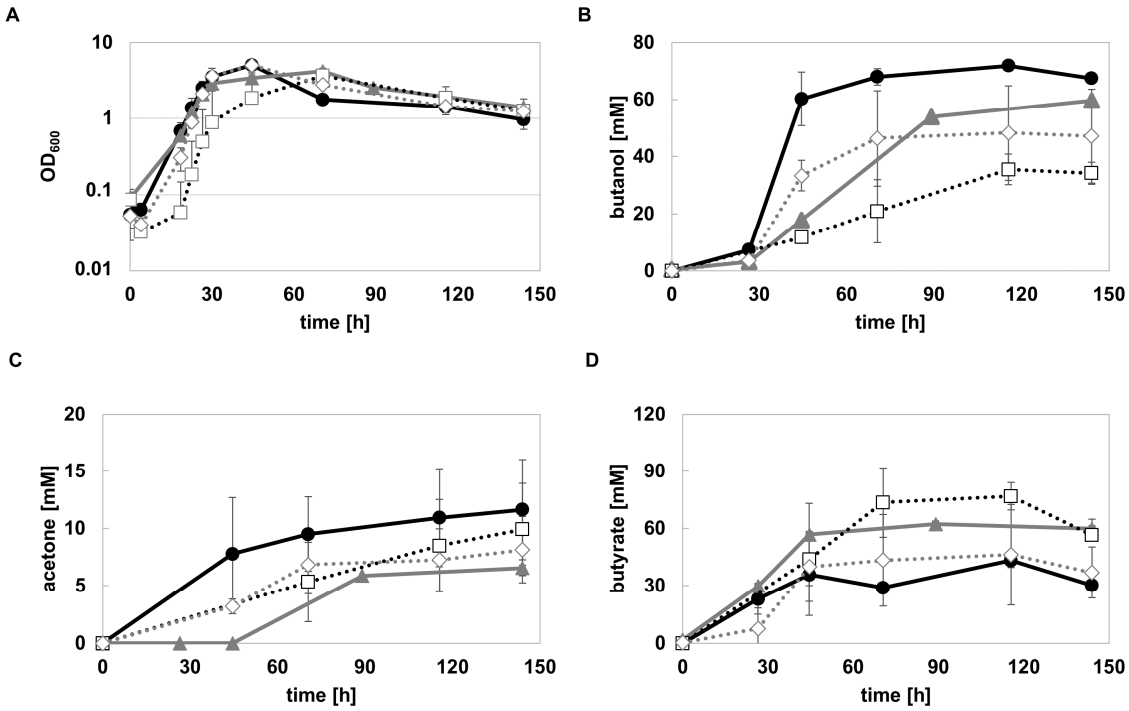

Figure 3.30: Growth behaviour and product formation of *C. acetobutylicum int::hfq* 168s [pIMP1_catp] (●), *C. acetobutylicum int::hfq* 168s [pIMP1_catp_solB] (▲), *C. acetobutylicum int::hfq* 168s [pIMP1_catp_ptb_hfq] (□), and *C. acetobutylicum int::hfq* 168s [pIMP1_catp_solB_ptb_hfq] (◇) during growth in batch fermentation with 50 ml MES-buffered medium (n = 3); (A) growth behaviour, (B) butanol, (C) acetone, and (D) butyrate.

for the same strains independent of the integration sites (Figure 3.31). Only strains *C. acetobutylicum int::hfq* 79s [pIMP1_catp_solB] and *C. acetobutylicum int::hfq* 168a [pIMP1_catp_solB] displayed major differences in the butanol concentrations. *C. acetobutylicum int::hfq* 168a [pIMP1_catp_solB] produced two times more butanol in comparison to *C. acetobutylicum int::hfq* 79s [pIMP1_catp_solB].

Furthermore, all strains used in the growth experiments were analyzed regarding their copy number of the megasplasmid pSOL1. gDNA was prepared at the beginning of the stationary growth phase. qRT-PCR was performed amplifying the chromosome encoded genes: *gyr* (CA_C007, primers: LC_gyr_fwd, LC_gyr_rev, Table 2.5) and *spo0A* (CA_C2071, primers: LC_spo0A_fwd, LC_spo0A_rev, Table 2.5), as well as the megaplasmid encoded genes: *adhE2* (CA_P0035, primers: LC_adhE2_fwd, LC_adhE2_rev, Table 2.5) and *adc* (CA_P0165, primers: LC_adc_fwd, LC_adc_rev, Table 2.5). Afterwards, the relative copy number of pSOL1 was calculated for each strain normalized to the wild type of *C. acetobutylicum.* Results of strains *C. acetobutylicum int::hfq* 79s are displayed in Figure 3.32A. *C. acetobutylicum int::hfq* 79s [pIMP1_catp] showed similar results as the complementation strains *C. acetobutylicum int::hfq* 79s [pIMP1_catp_ptb_hfq] and *C. acetobutylicum int::hfq* 79s [pIMP1_catp_solB_ptb_hfq]. All three exhibited an increased copy number of pSOL1 compared to the *C. acetobutylicum* wild type. In contrast, the level of pSOL1 in *C. acetobutylicum int::hfq* 79s [pIMP1_catp_solB] was minimized by 50 % compared to the *C. acetobutylicum* wild type. Results of copy number determination in

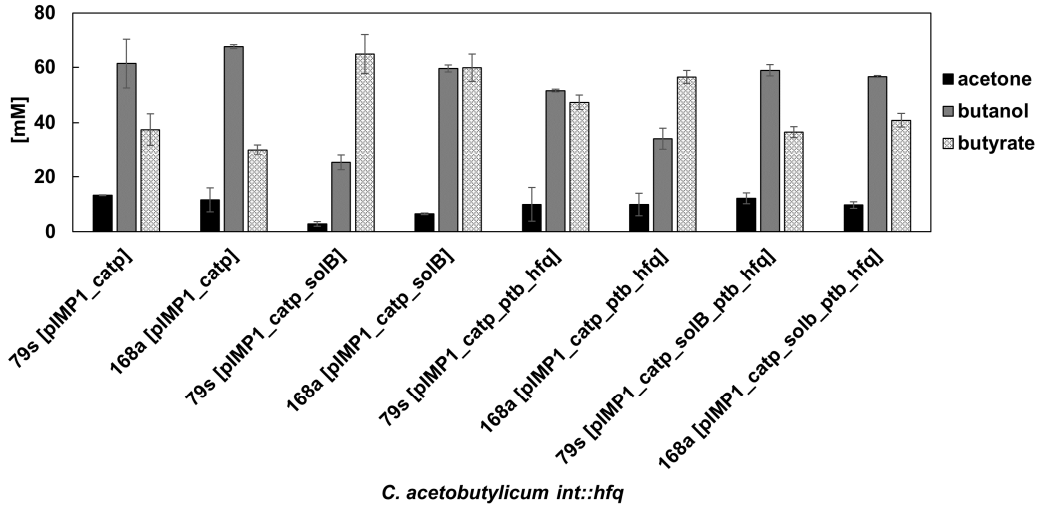

Figure 3.31: End product formation of different *C. acetobutylicum* strains after growth in batch fermentation with 50 ml MES-buffered medium (n = 3).

C. acetobutylicum int::hfq 168a strains are shown in Figure 3.32B. *C. acetobutylicum int::hfq* 168a [pIMP1_catp] and *C. acetobutylicum int::hfq* 168a [pIMP1_catp_solB_ptb_hfq] had a value of 1.4, which represented a slight increase of pSOL1 compared to the *C. acetobutylicum* wild type strain. In contrast, copy number of *C. acetobutylicum int::hfq* 168a [pIMP1_catp_solB] was reduced by 70 % compared to the wild type strain. *C. acetobutylicum int::hfq* 168a [pIMP1_catp_ptb_hfq] exhibited also a decreased copy number. However, the copy number was just 20 % lower as in the *C. acetobutylicum* wild type strain. In direct comparison, strains *C. acetobutylicum int::hfq* 79s and *C. acetobutylicum int::hfq* 168a revealed roughly the same results for the copy number if the strains were transformed with the same plasmids. For example, *C. acetobutylicum int::hfq* [pIMP1_catp_solB] revealed the lowest copy number of pSOL1 compared to strains *C. acetobutylicum int::hfq* [pIMP1_catp_ptb_hfq], *C. acetobutylicum int::hfq* [pIMP1_catp_solB], and *C. acetobutylicum int::hfq* [pIMP1_catp_solB_ptb_hfq] regardless whether the integration was at position 79 or 168 of the *hfq* gene. *C. acetobutylicum int::hfq* [pIMP1_catp] showed the highest copy number of pSOL1 in comparision to the other strains used in the experiment. Moreover, the differences between the strains *C. acetobutylicum int::hfq* 79s [pIMP1_catp], *C. acetobutylicum int::hfq* 79s [pIMP1_catp_solB], *C. acetobutylicum int::hfq* 79s [pIMP1_catp_ptb_hfq], and *C. acetobutylicum int::hfq* 79s [pIMP1_catp_solB_ptb_hfq] were proportional to the results of the strains *C. acetobutylicum int::hfq* 168a [pIMP1_catp], *C. acetobutylicum int::hfq* 168a [pIMP1_catp_solB], *C. acetobutylicum*

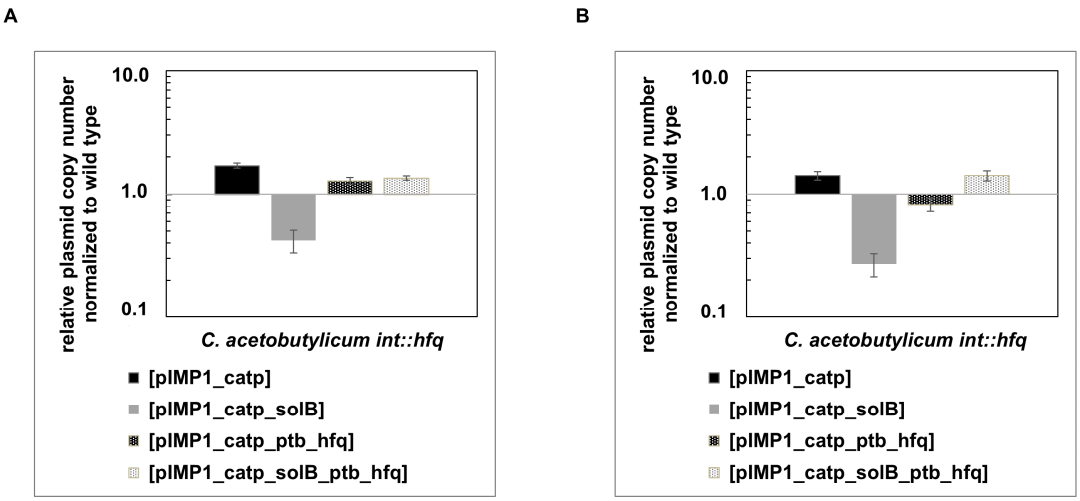

Figure 3.32: (A) Relative plasmid copy number of pSOL1 in *C. acetobutylicum int::hfq* 79s [pIMP1_catp] (black), *C. acetobutylicum int::hfq* 79s [pIMP1_catp_solB] (grey), *C. acetobutylicum int::hfq* 79s [pIMP1_catp_ptb_hfq] (broken black), and *C. acetobutylicum int::hfq* 79s [pIMP1_catp_solB_ptb_hfq] (broken grey). (B) Relative plasmid number of pSOL1 in *C. acetobutylicum int::hfq* 168a [pIMP1_catp] (black), *C. acetobutylicum int::hfq* 168a [pIMP1_catp_solB] (grey), *C. acetobutylicum int::hfq* 168a [pIMP1_catp_ptb_hfq] (broken black), and *C. acetobutylicum int::hfq* 168a [pIMP1_catp_solB_ptb_hfq] (broken grey). The copy number of pSOL1 in the wild type strain was set to 1.

int::hfq 168a [pIMP1_catp_ptb_hfq], and *C. acetobutylicum int::hfq* 168a [pIMP1_catp_solB_ptb_hfq].

In conclusion, overexpression of *solB* in an *hfq* integration mutant of *C. acetobutylicum* led to a decreased solvent production and reduced copy number of the megaplasmid pSOL1. It was irrelevant at what position the integration was performed as results were similar for strains *C. acetobutylicum int::hfq* 79s and *C. acetobutylicum int::hfq* 168a. However, the effects of *solB* overexpression were minimized in *C. acetobutylicum int::hfq* compared to *C. acetobutylicum* [pIMP1_solB] (Figure 3.3/Figure 3.10). Complementation of *hfq* in strains *C. acetobutylicum int::hfq* 79s [pIMP1_solB_ptb_hfq] and *C. acetobutylicum int::hfq* 168a [pIMP1_solB_ptb_hfq] did not reveal the suppressed solvent production and decreased copy number as strain *C. acetobutylicum* [pIMP1_solB].

4 Discussion

4.1 Characterizing the regulatory RNA SolB

4.1.1 Effects of *solB* overexpression on the transcriptome of *C. acetobutylicum*

The sRNA SolB of *Clostridium acetobutylicum* is located upstream of the *sol* (CA_P0162-CA_P164) and the *adc* operon (CA_P0165), which are encoded on the megaplasmid pSOL1 of *C. acetobutylicum* (Figure 1.3). Overexpression of *solB* blocked butanol and acetone production in *C. acetobutylicum*. Indeed, ethanol production was not affected (Schiel et al., 2010). Further investigations determined the transcription start point of *solB* and the length of SolB with 197 nt (Zimmermann, 2013). The expression of *solB* could be proven by RT-PCR, but not by Northern blot analysis in the *C. acetobutylicum* wild type strain (Zimmermann, 2013; Jones, 2015). As RNA sequencing data revealed that the expression of *solB* was quite low under standard growth conditions in the *C. acetobutylicum* wild type strain (Grimmler et al. 2011, Venkataramanan et al., 2013), a new protocol for the verification of SolB using Northern blot analysis was established. Therefore, a denaturating polyacrylamide gel was used increasing the resolution of the blot (Brown et al., 2001; López-Gomollón, 2011), and RNA probes were applied for improvement of sensitivity (Srivastava and Schonfeld, 1991). However, no signal was detected for *C. acetobutylicum* wild type (Figure 3.1, lane 1). In contrast, RNA of the *solB* overexpression strain, *C. acetobutylicum* [pIMP1_solB], revealed a signal just below the 200 nt marker range matching with the expected length of SolB. From the experiment, the functionality of the Northern blot can be concluded, the improvements did not allow detection of the *solB* transcript in the *C. acetobutylicum* wild type strain. The difference in the expression levels between the *C. acetobutylicum* wild type and *C. acetobutylicum* [pIMP1_solB] can be explained by the Gram-positive origin of replication (ori) repL. This *B. subtilis* based ori leads to a plasmid copy number of approximately eight in *C. acetobutylicum* (Lee et al., 1993). Zimmermann (2013) assumed that the increased number of *solB* sequences in *C. acetobutylicum* [pIMP1_solB] raised the expression level eight times as well resulting in the detection of SolB in the strain *C. acetobutylicum* [pIMP1_solB] in contrast to the *C. acetobutylicum* wild type. In this study, the questioned was raised whether solely an increase of eight times in the transcript level of SolB is responsible for the detection of SolB in strain *C. acetobutylicum* [pIMP1_solB] in opposite to the *C. acetobutylicum* wild type. Assuming that the SolB signal of the *C. acetobutylicum solB* overexpression strain resulted in a 100 %

intensity, the decrease of eight times in the *solB* transcription in the *C. acetobutylicum* wild type strain leads to a signal with approximately 12.5 % intensity. In comparison with the 100 % signal of the *C. acetobutylicum* [pIMP1_solB] strain, the signal intensity of 12.5 % should be enough to visualize the *solB* transcript of the *C. acetobutylicum* wild type in the Northern blot. This is contradictory to the experimental data gathered during this thesis. Therefore, it is proposed that SolB has a mechanism of autoregulation leading to an induction of its own promoter after reaching a distinct concentration. In the case of *C. acetobutylicum* [pIMP1_solB], the strain reached the mandatory SolB concentration for autoinduction due to the overexpression of *solB* on the pIMP1_solB plasmid. This effect increased the level of SolB in *C. acetobutylicum* [pIMP1_solB] more than eight times compared to the *C. acetobutylicum* wild type and thus, SolB is detectable in the Northern blot of *C. acetobutylicum* [pIMP1_solB]. Another reason could be that the determined copy number of pIMP1 suggested by Lee et al. (1993) is actually higher than the authors assumed. In the study of Lee et al. (1993), a 100 % yield in plasmid preparation was supposed. Maybe, the preparation method did not reach a yield of 100 %, then the calculated copy number is lower than the real plasmid number. Moreover, the DNA sequencing data revealed a much higher copy number for pIMP1 and pIMP1_solB (Table 8.3). However, this absolute quantification method is not approved for plasmid copy number determination as the used preparation method of genomic DNA was not shown to isolate chromosomal DNA and plasmids in the same ratio as occurring naturally in the cell. Further experiments are necessary for determine the exact copy number of pIMP1 in *C. acetobutylicum*.

To characterize the sRNA SolB in more detail, influenced genes were identified via qRT-PCR (Figure 3.2). The experiment performed with RNA of the strains *C. acetobutylicum* [pIMP1_solB] and *C. acetobutylicum* wild type showed severe down-regulation for the transcripts of the *sol* operon (CA_P0162-0164), and the genes *adhE2* (CA_P0035), *adc* (CA_P0165), *adcS/R* (CA_P0036-0037), as well as *thiB* (CA_P0078) in *C. acetobutylicum* [pIMP1_solB]. The *sol* operon comprises the *adhE* gene together with the genes *ctfA* and *ctfB*. AdhE is an aldehyde/alcohol dehydrogenase and catalyzes the reduction of butyryl-CoA to butanol (Fischer et al., 1993). It has been shown that AdhE is the most important contributor for butanol production among the predicted aldehyde/alcohol dehydrogenases in *C. acetobutylicum* wild type (Dai et al., 2016). However, it could be demonstrated that only the aldehyde dehydrogenase activity of AdhE2 is functional (Yoo et al., 2016).

However, inactivation of *adhE* led to a significant reduction of butanol production (Cooksley et al., 2012; Dai et al., 2016). Therefore, downregulation of *adhE* might be one reason for the loss of butanol production in the *C. acetobutylicum solB* overexpression mutant.

The blocked acetone production in strain *C. acetobutylicum* [pIMP1_solB] could be explained by the qRT-PCR revealed that the *adc* and *ctfA/ctfB* genes were down-regulated compared to the *C. acetobutylicum* wild type strain. *ctfA* and *ctfB* code for the acetoacetyl-CoA:acetate/butyrate-CoA-transferase, which start the solventogenesis by converting acetate and butyrate to butyryl-CoA and acetyl-CoA as well as acetoacetyl-CoA conversion to acetoacetate, which is the precursor of acetone (Fischer et al., 1993). The *adc* gene is important for acetone production coding for an acetoacetate decarboxylase. Adc catalyzes the last reaction from acetoacetate to acetone (Gerischer and Dürre, 1990; Petersen et al., 1993). Deletion of the genes *adc* and *ctfA/B* resulted in a lack of acetone production (Cooksley et al., 2012), also shown in *C. acetobutylicum* [pIMP1_solB].

The reduced expression of the *adhE2* gene in the strain *C. acetobutylicum* [pIMP1_solB] revealed a further reason for the inhibited solvent formation in the *solB* overexpression strain. AdhE2 operates as an aldehyde/alcohol dehydrogenase and catalyzes the reduction of butyryl-CoA to butanol (Fontaine et al., 2002; Yoo et al., 2016). In contrast to AdhE, AdhE2 is mainly responsible for alcohol production under alcohologenic conditions (Fontaine et al., 2002; Yoo et al., 2016). Alcohologenic conditions are characterized by a neutral pH and a high NAD(P)H availability. Growth experiments with *C. acetobutylicum* [pIMP1_solB] under alcohologenic conditions showed an inhibited solvent formation as well (Zimmermann, 2013), supporting the influence of SolB on the transcript of *adhE2*.

Furthermore, the transcription of the genes encoding the proteins AdcR and AdcS was down-regulated in *C. acetobutylicum* [pIMP1_solB], compared to the *C. acetobutylicum* wild type strain. Respective genes are transcribed in one operon and at least AdcR acts as transcription factor by DNA binding (Nguyen et al., 2016). Binding sites for AdcR are found in the promoter region of the *sol* operon and *adc* gene (Nguyen et al., 2016). Moreover, overexpression experiments of *adcS* and *adcR* revealed an involvement in acetone and butanol production. However, the effects described in literature were inconclusive regarding the role in solvent formation (Flitsch, 2015; Nguyen et al., 2016). Thus, further characterization of the proteins AdcS and AdcR has

to be performed to explain the transcript decrease in context with *solB* overexpression in *C. acetobutylicum*.

Since the IntaRNA tool (Sievers et al., 2014) and RNAtarget2 (Kery et al., 2014) predicted the *thlB* transcript as a highly potential binding partner for SolB (Supplement Figure 8.7), the two homologous genes *thlB* and *thlA* were an interesting target for determining the expression via qRT-PCR. ThlA and ThlB catalyze the conversion of two molecules of acetyl-CoA into acetoacetyl-CoA. The *thlA* gene is highly and constitutively expressed in the *C. acetobutylicum* wild type strain (Sillers et al., 2009). However, in contrast to *thlB*, the expression of the *thlA* gene did not display changes between the strains *C. acetobutylicum* [pIMP1_solB] and *C. acetobutylicum* wild type. The *thlB* gene is only highly expressed during the shift from acidogenic to solventogenic growth phase in the *C. acetobutylicum* wild type strain (Winzer et al., 2000). However, as the production of acetoacetyl-CoA is necessary for butyrate production and ThlA seems to be the more active enzyme for this reaction, the function of ThlB has to be further elucidated to understand the reasons for the determined down-regulation in strain *C. acetobutylicum* [pIMP1_solB] in the qRT-PCR experiment. Moreover, the qRT-PCR revealed no changes in transcript concentration for the genes *bdhA, bdhB, aor, hfq,* and *spo0A* between the strains *C. acetobutylicum* [pIMP1_solB] and *C. acetobutylicum* wild type (Figure 3.2). In the section below, the reasons for the qRT-PCR analysis of these genes are discussed as well as the consequences of the unchanged expression of these genes in *C. acetobutylicum* [pIMP1_solB].

The genes *bdhA* and *bdhB* encode for butanol dehydrogenases (Petersen et al., 1991; Walter et al., 1992). As butanol formation is inhibited by *solB* overexpression in *C. acetobutylicum*, it was assumed that SolB down-regulates the expression of the genes *bdhA* and *bdhB*. The transcript of *bdhB* even exhibits a potential binding site for SolB in the 5' untranslated region (Schiel et al., 2010), supporting an interaction of SolB with the transcript of *bdhB*. Unexpectedly, neither *bdhA* nor *bdhB* showed a change in the expression. However, deletion of these genes also did not lead to changes in solvent production (Cooksley et al., 2012), demonstrating that the butanol dehydrogenase activity of BdhA and BdhB can be replaced by other dehydrogenases as AdhE and/or AdhE2, which are possibly influenced by SolB.

The *aor* gene encodes an aldehyde:ferredoxin-oxidoreductase catalyzing the reaction of D-glyceraldehyde to glycerate in the pentose-phosphate-pathway (Ren et al., 2012). A *C. acetobutylicum aor* deletion strain is characterized by inhibited acetone and

butanol production (Flitsch, 2015), which is similar to the observed phenotype of *C. acetobutylicum* [pIMP1_solB]. If SolB down-regulates the expression of the *aor* gene, the mentioned phenotype would occur. However, the expression of the *aor* gene was not influenced in the *solB* overexpression mutant. Thus, the *aor* gene is not involved in the regulatory network of SolB.

The RNA-binding protein Hfq is an important factor for the majority of trans-encoded sRNAs, and it was published that MtvS, a sRNA of *Burkholderia cenocepacia*, down-regulates the transcription of *hfq* (Ramos et al., 2014). Furthermore, also a sRNA was found regulating *hfq* expression in *Legionella pneumophila* (Oliva et al., 2017). However, in the qRT-PCR results, the transcription of *hfq* was unchanged in *C. acetobutylicum* [pIMP1_solB] compared to the *C. acetobutylicum* wild type. Thus, it can be concluded that SolB has no influence on the expression of the *hfq* gene.

The gene of the master regulator for sporulation and solventogenesis Spo0A was another tested target in the qRT-PCR experiment. The transcription factor Spo0A binds to so called 0A boxes with the sequence TGNCGAA (Strauch et al., 1990), encoded in several promoter regions (e.g. *adc* (Ravagnani et al., 2000)*, adcS/R* operon (Schiel, 2006), *sol* operon (Nguyen et al., 2016)) and it activates transcription of genes involved in sporulation and solvent production (Ravagnani et al., 2000; Harris et al., 2002). As sporulation and solvent production were inhibited in *C. acetobutylicum* [pIMP1_solB] and a possible binding sequence for SolB was found in the 5' untranslated region of the *spo0A* transcript (Zimmermann, 2013), the transcript of *spo0A* was a promising target for SolB. The interaction was expected to down-regulate the transcript amount of *spo0A* in *C. acetobutylicum* [pIMP1_solB] resulting in the inhibited solvent formation for *C. acetobutylicum* [pIMP1_solB]. In contrast to the expectations, the expression of the *spo0A* gene was similar for strains *C. acetobutylicum* [pIMP1_solB] and *C. acetobutylicum* wild type. However, it was shown that simultaneous overexpression of *solB* and *spo0A* was able to restore solvent production (Zimmermann, 2013). This supports the hypothesis that an interaction takes place between the transcript of *spo0A* and SolB. The predicted binding site for SolB is located at the RBS of the *spo0A* transcript (Zimmermann, 2013). This could lead to a blocked translation without RNA decay, meaning that the transcript concentration remains constant resulting in the detected unchanged expression level of *spo0A*. However, the active protein level of Spo0A could be decreased and sporulation and solvent production could not be

activated in the *C. acetobutylicum* [pIMP1_solB] strain. Thus, the qRT-PCR could not clarify whether the transcript of Spo0A is influenced by SolB.

The results of the qRT-PCR experiments were confirmed by the data of the transcriptome analysis of strains *C. acetobutylicum* wild type and *C. acetobutylicum* [pIMP1_solB]. The analyzed genes in the qRT-PCR experiment showed the same expression pattern in the transcriptome analysis. Moreover, the transcriptome data exhibited further transcripts with severe changes in the expression pattern in *C. acetobutylicum* [pIMP1_solB] compared to the *C. acetobutylicum* wild type strain, supporting further targets of SolB. Several genes (e.g. CA_C1201, CA_C1915-1944) displayed distinct down- or up-regulation of expression in strain *C. acetobutylicum* [pIMP1_solB] compared to the *C. acetobutylicum* wild type strain. Unfortunately, these genes are not yet characterized. Thus, it is not yet feasible to include them into the model of SolB.

Furthermore, two phosphotransferase systems (PTS) were differentially expressed in the strain *C. acetobutylicum* [pIMP1_solB] compared to the *C. acetobutylicum* wild type. Interestingly, the first PTS (CA_C2964-64) annotated for lactose transport displayed a decreased expression and the second PTS (CA_C0382-3) annotated for cellobiose showed an increased expression compared to the *C. acetobutylicum* wild type strain. Both metabolites were not used in the growth experiments as the MES-buffered medium contained only glucose as carbon source. As the genes are only predicted to encode lactose or cellobiose phosphotransferase systems, it is likely that these systems can transport other sugars as glucose. *C. acetobutylicum* [pIMP1_solB] revealed no altered glucose consumption in comparison to *C. acetobutylicum* [pIMP1] supporting that the changes in the expression of these PTS systems only play a minor role for the observed phenotypic effects of *C. acetobutylicum* [pIMP1_solB].

Another interesting point is the down-regulation of the sporulation sigma factor σ^G (CA_C1696). Activation of sporulation in *C. acetobutylicum* wild type is achieved by histidine kinases phosphorylating Spo0A (Steiner et al., 2011). Afterwards, phosphorylated Spo0A promotes transcription of several genes including the first prespore specific sigma factor *sigF* (σ^F). σ^F activates the mother cell-specific sigma factor σ^E and the second prespore-specific sigma factor σ^G (Al-Hinai et al., 2015). The *C. acetobutylicum sigG* integration mutant revealed a blocked sporulation at the engulfment stage (Tracy et al., 2011). The decreased expression of *sigG* explains the reduced sporulation of *C. acetobutylicum* [pIMP1_solB] reported by Zimmermann

(2013). Moreover, the increased *sigE* and *sigF* expression observed in the *C. acetobutylicum sigG* integration mutant was also recognized in the *C. acetobutylicum* [pIMP1_solB] strain. As mentioned in the study of Tracy et al. (2011), this is possibly caused by stagnation of *sigG* activation. Besides, in *C. acetobutylicum* strains with inactivated *sigE,* it was impossible to detect granulose production (Jones et al., 2011). Granulose is a storage component containing only (1→4) linked d-glucopyranose units and is produced during the sporulation process in *C. acetobutylicum* (Jones et al., 1982; Reysenbach et al., 1986). Due to the higher expression of *sigE* in *C. acetobutylicum* [pIMP1_solB], the granulose production was increased compared to the *C. acetobutylicum* wild type strain (Figure 3.9A). Furthermore, the TEM images exhibited an increased number of black granula, which can be assumed to be granulose as the granula show the same shape as detected granulose in previous publications (Jones et al., 2008; Tracy et al., 2011). Furthermore, the genes *CA_C2237* and *CA_C2240* were predicted to be responsible for granulose biosynthesis (Alsaker and Papoutsakis, 2005; Jones et al., 2008; Tracy et al., 2011). Both revealed an increased expression level in *C. acetobutylicum* [pIMP1_solB] compared to the *C. acetobutylicum* wild type supporting the higher granulose production (Table 8.1). However, *sigG* inactivation did not cause changes in solvent production (Tracy et al., 2011). Thus, the absence of solvent production was independent of the decrease in *sigG* expression in the *C. acetobutylicum* [pIMP1_solB] strain. Also, a direct interaction between SolB and the transcript of *sigG* is unlikely, as no potent binding site could be predicted by the IntaRNA tool. However, the complex mechanism of sporulation in *C. acetobutylicum* is not completely elucidated in *C. acetobutylicum* and maybe an additional regulator is involved in σ^G regulation, which is influenced by SolB.

The gene *CA_C0213* showed in the transcriptome data an increased expression in the *C. acetobutylicum* [pIMP1_solB] strain compared to *C. acetobutylicum* wild type strain. The gene is annotated as LysM domain-containing protein (IPR018392). The LysM motif is a small globular domain with approximately 40 amino acids containing lysine. First, it was found in enzymes involved in bacterial cell wall degradation (Joris et al., 1992). Meanwhile, the LysM domain was found in over 4000 proteins including bacterial lysins and bacteriophage proteins as well as in certain proteins of eukaryotes. Proteins with LysM domains bind to peptidoglycan, an important component of the bacterial cell wall (Buist et al., 2008). As several LsyM containing proteins were

responsible for autolysis or cell wall degradation (Buist et al., 1997; Heilmann et al., 2005; Mesnage et al., 2014), it is very likely that the highly expressed gene *CA_C0213* in *C. acetobutylicum* [pIMP1_solB] is responsible for the mentioned functions in *C. acetobutylicum*. As the TEM images of *C. acetobutylicum* [pIMP1_solB] showed a significant earlier disruption of the cell wall compared to the *C. acetobutylicum* wild type strain (Figure 3.9B-D), the increased expression of *CA_C0213* in *C. acetobutylicum* [pIMP1_solB] could be the reason for this finding. The hypothesis that CA_C0213 acts as an autolysin or cell wall degradation protein should be proven by recombinant overexpression in *E. coli* and determination of its enzyme activity. Besides, one autolysin of *C. acetobutylicum* has already been characterized and the authors predict the existence of at least one further autolysin (Liu et al., 2015). Possibly, the origin of the bright colour of *C. acetobutylicum* [pIMP1_solB] cells in TEM images is due to the degradation of cell walls. The high amounts of acids produced by the *C. acetobutylicum* [pIMP1_solB] strain can lower the pH value within the cells, because the membrane of the respective cells is not intact. The low pH value within the cells can disrupt cell structures, which were responsible for the dark colour in the control strain *C. acetobutylicum* [pIMP1] (Figure 3.9B-D). However, it is questionable whether the effects of cell wall disruption are associated with SolB or whether the high acid concentration in the medium of *C. acetobutylicum* [pIMP1_solB] are exclusively responsible for the cell wall disruption. For example cell wall disruption driven by low pH values was reported in *Lactococcus lactis* (Ramírez-Nuñez et al., 2011).

The most significant effect revealed by the transcriptome data is the down-regulation of all genes encoded on the megaplasmid pSOL1 in *C. acetobutylicum* [pIMP1_solB] (Figure 3.8). The down-regulated expression of all genes encoded on pSOL1 was found in both growth phases, exponential growth (Supplement Figure 8.3) and stationary growth (Figure 3.8). But the effect was significantly higher in the stationary growth phase. Nearly all important genes for solvent production are located on the megaplasmid pSOL1 in *C. acetobutylicum* (Cornillot et al., 1997). Respective genes show a common induction pattern as they increase their expression during the late exponential growth phase. Due to this expression pattern, the down-regulation by SolB seemed to be increased in the stationary growth phase, however, the result is attributed to the further induction of the genes in the *C. acetobutylicum* wild type strain. Moreover, *C. acetobutylicum* [pIMP1_solB] revealed a different expression pattern in all COG categories compared to the *C. acetobutylicum* wild type strain (Figure 3.6).

From these findings can be concluded that SolB acts as global regulator and does not interfere with only one target as it influences several pathways. Several trans-encoded sRNAs were already described as regulators of different regulons (Altuvia, 2004; Wang et al., 2015; Fröhlich et al., 2016). Indeed, the likelihood that SolB interferes with every single transcript of the megaplasmid pSOL1 is quite low as it codes for 178 open reading frames (Nölling et al., 2001). There is a high probability that SolB influences the copy number of the megaplasmid pSOL1. A further discussion regarding the influence of SolB on the DNA level of pSOL1 can be found in the section 4.1.2.

4.1.2 Effects of *solB* overexpression on the copy number of pSOL1

As the transcriptome data revealed a dramatically decreased expression of all genes encoded on the megaplasmid pSOL1, the question arose if the megaplasmid is lost in strain *C. acetobutylicum* [pIMP1_solB]. Many important genes involved in solventogenesis as well as sporulation are located on the megaplasmid pSOL1. pSOL1 is not essential for *C. acetobutylicum* (Tomas et al., 2003). *C. acetobutylicum* strains lacking pSOL1 were asporogenous and nonsolventogenic (Clark et al., 1989). This phenotype is quite similar to the observed phenotype of strain *C. acetobutylicum* [pIMP1_solB] (Schiel et al., 2010; Zimmermann, 2013). However, the experiment provided evidence for amylase activity in all grown clones of *C. acetobutylicum* [pIMP1_solB] (Supplement Figure 8.4A/B). The *amyP* (CA_P0168) gene is only encoded on the megaplasmid and not on the chromosome of *C. acetobutylicum.* The α-amylase (*amyP*) catalyzes the reaction of starch degradation. Strains lacking pSOL1 were not able to degrade starch as the necessary α-amylase is missing (Harris et al., 2002; Sabathé et al., 2002). Thus, the reason for the phenotype of *C. acetobutylicum* [pIMP1_solB] and the down-regulation of all pSOL1 genes in *C. acetobutylicum* [pIMP1_solB] is not due to the loss of pSOL1. As the loss of pSOL1 in *C. acetobutylicum* [pIMP1_solB] was excluded, it was assumed that possibly the copy number of pSOL1 was down-regulated to achieve the low expression of the pSOL1-encoded genes. The performed DNA-sequencing and qRT-PCR experiments, which analyzed genes being encoded on the chromosome and on the megaplasmid, exhibited the same result. *C. acetobutylicum* [pIMP1_solB] showed a significant lower ratio of pSOL1 DNA to chromosomal DNA compared to *C. acetobutylicum* wild type and *C. acetobutylicum* [pIMP1] (Figure 3.10/Table 3.1). To avoid misunderstanding, the copy number determination of pSOL1 by DNA sequencing and qRT-PCR was a relative quantification. Thus, the preparation method is similar for all samples and has

no influence on the relative numbers. In contrast, the discussed copy number of pIMP1 in section 4.1.1 was determined in absolute numbers, hence the preparation method has a major impact. In this study, the copy number experiments revealed that SolB is able to interact directly or indirectly with the origin of replication (ori) of pSOL1 and reduces the copy number of pSOL1. In literature, several sRNAs are described inhibiting plasmid replication (Persson et al., 1990; Eguchi et al., 1991; del Solar and Espinosa, 1992; Brantl and Wagner, 1996; Le Chatelier et al., 1996; Asano and Mizobuchi, 1998; Wagner et al., 2002). Different mode of actions are possible to control the copy number by sRNAs, for example transcription attenuation, inhibition of primer maturation, translation inhibition, and mRNA stability (Brantl, 2007). However, all of these described sRNAs are cis-acting sRNAs (Brantl, 2002), in contrast to SolB, which is described as trans-encoded sRNA (Zimmermann, 2013). The pSOL1 sequencing data revealed one single skew inflection indicating the ori of pSOL1 (Nölling et al., 2001). Furthermore, a homolog of the *repA* gene (CA_P0175) was annotated 2.2 kbps upstream of the ori. The RepA protein belongs to the group of replication initiation proteins (Chattoraj et al., 1985; del Solar et al., 1998). However, SolB is located approximately 13.0 kbps upstream from the postulated *repA* gene. As the described sRNAs involved in plasmid copy control are in close proximity to the ori, SolB seems to offer a new possibility of plasmid copy control. To confirm that SolB down-regulates the copy number of pSOL1 two additional strains have to be constructed. The first *C. acetobutylicum* strain should lack the megaplasmid pSOL1 and contain a plasmid encoding the predicted ori of pSOL1. The second strain has to be additionally transformed with the plasmid pIMP1_solB. Both plasmids can coexist in *C. acetobutylicum* as the oris of pSOL1 and pIMP1 were shown to be compatible, for example in *C. acetobutylicum* [pIMP1]. Afterwards, the plasmid copy number of the plasmid containing the ori of pSOL1 should be determined in the both strains. The theory that SolB decreases the copy number of pSOL1 would be supported in the mentioned experiment if the plasmid copy number in the second strain overexpressing *solB* is decreased in comparison to the first *C. acetobutylicum* strain, which contains only the plasmid with the ori of pSOL1.

4.1.3 Spo0A and AdhE2 possible opponents of SolB

In silico analysis revealed that the transcripts of the sporulation factor Spo0A (CA_C2071) and of the aldehyde/alcohol dehydrogenase AdhE2 (CA_P0035) act as possible binding partners of SolB (Zimmermann, 2013). As already mentioned above

(4.1.1), both play crucial roles in solvent production. Overexpression of *spo0A* in a *C. acetobutylicum solB* overexpression strain revealed wild type amounts of acetone and butanol (Zimmermann, 2013). Furthermore, the similar copy number of pSOL1 in strains *C. acetobutylicum* [pIMP1] and *C. acetobutylicum* [pIMP1_solB_spo0A] support the transcript of *spo0A* as potent binding partner for SolB. As the overexpression of *spo0A* results in an increased number of *spo0A* transcripts, SolB could just partly block translation of the *spo0A* mRNA or rather did not interfere with other binding partners (Figure 3.10B). Moreover, *spo0A* deletion in *C. acetobutylicum* exhibited an asporogenous and solventogenesis-deficient phenotype (Harris et al., 2002), which is similar to *C. acetobutylicum* [pIMP1_solB]. This supports the assumption that SolB interacts with the *spo0A* transcript or respectively interferes with the same targets. However, the influence on the targets is divergent as Spo0A promotes solventogenesis and sporulation and in opposite, SolB blocks the same pathways. This was confirmed by the transcriptome data of *C. acetobutylicum* [pIMP1_solB] and *C. acetobutylicum Δspo0A* compared to the *C. acetobutylicum* wild type strain. Both mutant strains showed a decreased expression of more than 25 % of all encoded genes compared to the *C. acetobutylicum* wild type strain (Figure 3.7). Thus, SolB acts as a repressor like most sRNAs (Gottesman, 2005; Aiba, 2007) as the *C. acetobutylicum solB* overexpression strain decreased the transcription of several genes. In contrast, Spo0A works expectably as an inducer of gene expression as the deletion of *spo0A* in *C. acetobutylicum* leads to a reduced transcription of several genes (Thormann et al., 2002; Tomas et al., 2003). Furthermore, more than 40 % of the down-regulated genes in *C. acetobutylicum* [pIMP1_solB] and *C. acetobutylicum Δspo0A* were identical, supporting that Spo0A and SolB interfere with the same targets (Figure 3.7C). However, it has to be mentioned that also differences were found between the two mutants. *C. acetobutylicum Δspo0A* did not exhibit down-regulation of all genes encoded on the megaplasmid pSOL1. Thus, it can be assumed that SolB has further interaction partners besides Spo0A or Spo0A targets.

One additional target seems to be the *adhE2* transcript. The growth experiments with strains *C. acetobutylicum* [pIMP1_solB_adhE2] showed that overexpression of *adhE2* along with *solB* is also able to restore the solvent production (Figure 3.3B/D). The increased amount of ethanol compared to the *C. acetobutylicum* wild type strain is due to the fact that AdhE2 acts as aldehyde/alcohol dehydrogenase (Figure 3.3C). As a consequence, AdhE2 catalyzes the reaction of acetyl-CoA to ethanol (Dai et al., 2016).

As the ethanol production is not impaired in *C. acetobutylicum* [pIMP1_solB] (Schiel et al., 2010), the presence of further AdhE2 protein led to an increased ethanol production in strain *C. acetobutylicum* [pIMP1_solB_adhE2]. The restored solvent production in *C. acetobutylicum* [pIMP1_solB_adhE2] is achieved by the increased transcription of *adhE2*. Hereby, SolB interferes preferentially with the mRNA of *adhE2* as it is present in high amounts compared to the other targets of SolB. This mechanism is termed titration effect. Thus in *C. acetobutylicum* [pIMP1_solB_adhE2], the other targets of SolB are not influenced and solvent production and copy number of pSOL1 is a comparable to the *C. acetobutylicum* wild type. To confirm the postulated interaction site of SolB within the transcript of *adhE2*, growth experiments were performed with strain *C. acetobutylicum* [pIMP1_solB_adhE2_begin]. The strain overexpressed only a truncated sequence of *adhE2* containing the promoter and the first part of the coding sequence, because the binding site of SolB was assumed to be in the 5' untranslated region of the *adhE2* transcript (Zimmermann, 2013). It was expected that SolB interacts in the same way with the truncated *adhE2* transcript as with the complete version of the *adhE2* transcript, because in both transcripts the binding motif for SolB is present. Thus, SolB should interact with the truncated *adhE2* transcript resulting in equivalent solvent amounts and copy numbers of pSOL1 as in the *C. acetobutylicum* [pIMP1_solB_adhE2] strain. However, in strain *C. acetobutylicum* [pIMP1_solB_adhE2_begin] no solvent production was measured and the copy number was decreased compared to strain *C. acetobutylicum* [pIMP1_solB_adhE2] (Figure 3.5/Figure 3.11). This indicates that the active AdhE2 protein is necessary to accomplish solvent production and an increased copy number of pSOL1. The assumption of a titration effect between SolB and the transcript of *adhE2* could not be proven by the performed experiment. Similar results were observed for the transcription regulator Spo0A. Growth experiments with a *C. acetobutylicum* strain containing a plasmid overexpressing a truncated transcript of *spo0A* along with SolB revealed a blocked solvent production and reduced copy number of pSOL1 as well (Figure 3.4/Figure 3.11). Also here, the predicted binding site of SolB is localized in the 5' untranslated region of the *spo0A* transcript (Zimmermann, 2013).Thus, it was expected that SolB preferentially interferes with the truncated transcript and will not interact with other targets of the *C. acetobutylicum* genome resulting in an increased amount of solvents and pSOL1 compared to strain *C. acetobutylicum* [pIMP1_solB].

Indeed, the experimental data did not confirm the suggested titration effect of SolB and the transcript of *spo0A*.

First, the above finding suggestes that the mentioned titration effect takes place between the active protein Spo0A and SolB in *C. acetobutylicum* [pIMP1_solB_spo0A]. However, Zimmermann (2013) performed an experiment supporting that the interaction takes place between SolB and the mRNA of *spo0A*. For the experiment, the gene sequences of *solB* and *spo0A* were overexpressed together in *C. acetobutylicum* resulting in strain *C. acetobutylicum* [pIMP1_solB_spo0A$_{mut}$]. The overexpressed *spo0A* sequence contained a base exchange of 9 bases directly upstream of the RBS. Thus, the *spo0A* transcript can be translated, but the potential binding site for SolB in the *spo0A* transcript was blocked for SolB. If SolB interacts with the protein of Spo0A, the titration effect will take place between SolB and Spo0A. SolB is bound to the Spo0A protein and cannot interfere with other targets. Thus, the strains *C. acetobutylicum* [pIMP1_solB_spo0A$_{mut}$] and *C. acetobutylicum* wild type should produce comparable amounts of acetone and butanol. However, solvents were not detected in the strain *C. acetobutylicum* [pIMP1_solB_spo0A$_{mut}$]. Taking this into account, SolB was not bound to the Spo0A protein and did instead interact with other targets of the genome in strain *C. acetobutylicum* [pIMP1_solB_spo0A$_{mut}$], which led to blocked solvent formation. Moreover, the results confirmes the assumption that SolB intereferes with the transcript of *spo0A* as in the case of *C. acetobutylicum* [pIMP1_solB_spo0A] solvents were produced and in strain *C. acetobutylicum* [pIMP1_solB_spo0A$_{mut}$] no solvents were produced. The difference between the two mentioned genes is based on the mutated binding site in the *spo0A* transcript for SolB leading to an inhibited interaction of SolB and the mutated *spo0A* transcript.

However, the question remains, why the *C. acetobutylicum* [pIMP1_solB_spo0A_begin] strain did not produce solvents as the transcript offers a binding site for SolB. One possible reason is that Spo0A enhances its transcription by binding to its own promotor. This mechanism is already described for Spo0A of *B. subtilis* (Strauch et al., 1992; Chibazakura et al., 1995; Chastanet and Losick, 2011). *B. subtilis* and *C. acetobutylicum* belong to the phylum *Firmicutes* and both share several similarities in the sporulation process. The induction of transcription of the truncated *spo0A* gene is the missing link for understanding the observed results as the functional Spo0A protein is not produced in strain *C. acetobutylicum* [pIMP1_solB_spo0A _begin]. Taking this into account, the amount of the truncated

spo0A transcript expressed from the transformed plasmid is too low to bind all present *solB* transcripts. Thus, SolB interferes with binding partners of the genome. This leads to the blocked solvent formation and decreased copy number of pSOL1 in *C. acetobutylicum* [pIMP1_solB_spo0A _begin].

In Figure 4.1 a model is postulated on the mode of action of SolB with the *spo0A* transcript in the different *C. acetobutylicum* strains. In strain *C. acetobutylicum* [pIMP1_solB], SolB binds to targets encoded on the chromosome and pSOL1. In *C. acetobutylicum* [pIMP1_solB_spo0A], SolB preferentially interacts with the *spo0A* transcript from the transformed plasmid. The observed phenomenon can be described as a titration effect of SolB with the mRNA of *spo0A*. Crucial for this point is that the expression is high from the plasmid. In this case, Spo0A needs to activate its own expression as it is described for Spo0A in *B. subtilis* (Chastanet and Losick, 2011; Chibazakura et al., 1995; Strauch et al., 1992). Targets of the chromosome and pSOL1 are not influenced by SolB in this strain. In contrast, the targets of the chromosome and pSOL1 are repressed by SolB in the strain *C. acetobutylicum* [pIMP1_solB_spo0A_begin]. Actually, SolB binds to the transcript of *spo0A* encoded on the plasmid. However, it is impossible to activate the transcription of the truncated sequence of *spo0A* as no functional Spo0A protein is translated. The amount of expressed *spo0A'* is too low to inhibit interactions of SolB with targets encoded on the chromosome and pSOL1. Moreover, the reason for the strain *C. acetobutylicum* [pIMP1_solB_spo0A$_{mut}$] to produce no acetone or butanol is based on in the overexpressed mutated *spo0A* gene as it contains the wrong binding motif for SolB. Thus, SolB will bind to the actual targets encoded on the chromosome and pSOL1. Furthermore, the experiment proved that SolB interacts with mRNA and does not interfere with the protein of Spo0A.

Same explanations are suggested for the results of the *C. acetobutylicum* strains overexpressing the *adhE2* gene. Actually, AdhE2 is characterized as aldehyde/alcohol dehydrogenase. No regulatory function is postulated or described for AdhE2 as for the transcription factor Spo0A. One possibility to describe the results is that the AdhE2 protein belongs to the group of moonlighting proteins. Moonlighting proteins have more than one biological function (Campbell and Scanes, 1995; Jeffery, 1999). The most common, primary function of moonlighting proteins is enzymatic catalysis. The second function of the moonlighting proteins vary from transcription or translation regulation to virulence (Sriram et al., 2005). For example, in *B. subtilis* the glutamate

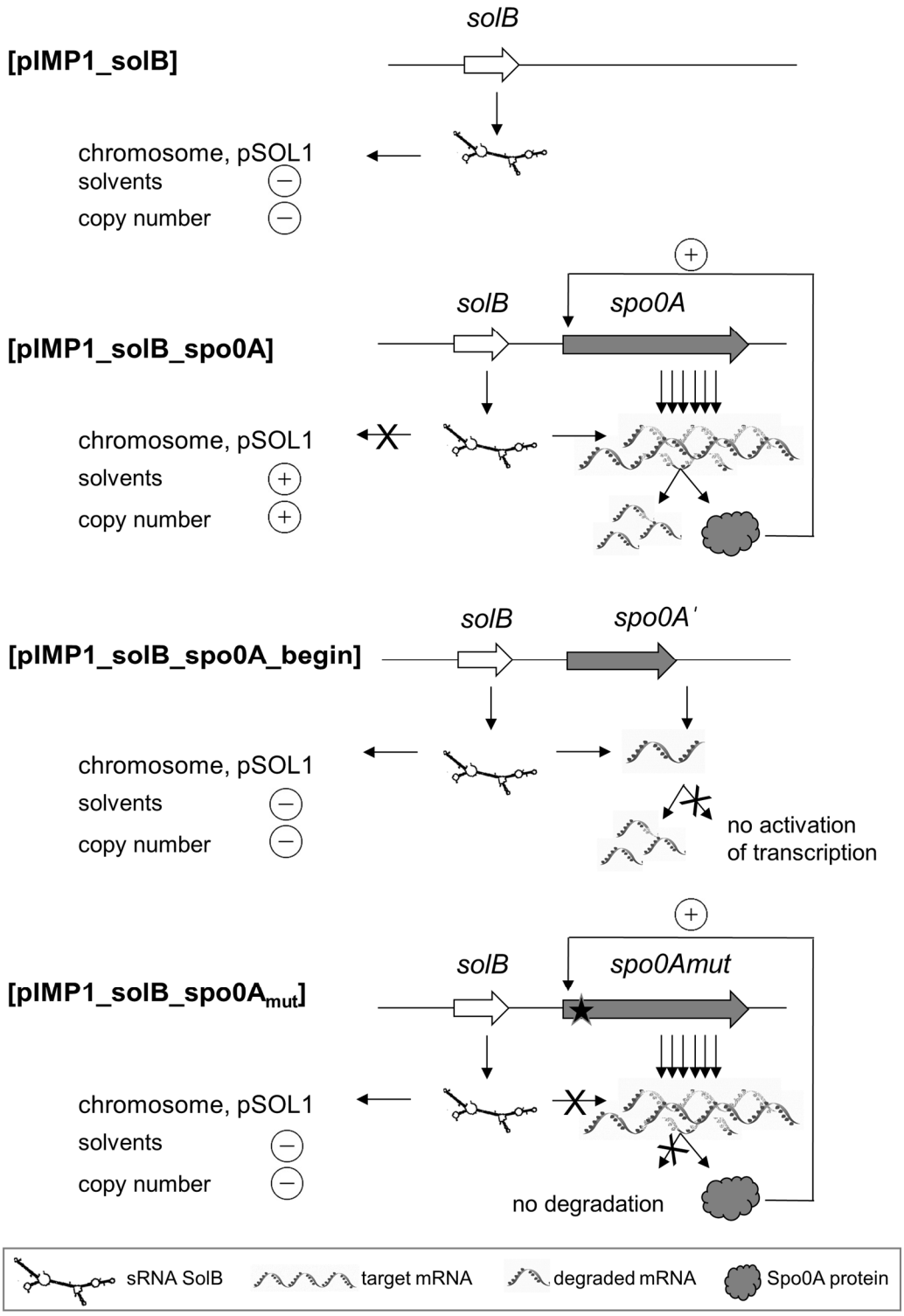

Figure 4.1: Schematic overview of SolB interaction with its targets. In *C. acetobutylicum* [pIMP1_solB] SolB interacts with transcripts encoded on the chromosome and pSOL1 resulting in an inhibited solvent production and decreased copy number of the megaplasmid pSOL1. In *C. acetobutylicum* [pIMP1_solB_spo0A] SolB interacts preferentially with transcripts of *spo0A* expressed from the transformed plasmid as the overexpression of *spo0A* leads to a titration effect of SolB. The *spo0A* gene encoded on the plasmid is highly expressed due to the activation by the active Spo0A protein. Transcripts of the chromosome and pSOL1 are not affected by SolB. The strain [pIMP1_solB_spo0A] produced comparable concentrations of solvents and pSOL1 to the *C. acetobutylicum* wild type strain. In *C. acetobutylicum* [pIMP1_solB_spo0A_begin] SolB interacts with transcripts encoded on the chromosome and pSOL1 and leads to repression of solvent production and a decrease of the pSOL1 copy number. The amount of *spo0A* transcripts expressed from the [pIMP1_solB_spo0A_begin] plasmid is too low as the positive activation by Spo0A is missing. In *C. acetobutylicum* [pIMP1_solB_spo0A$_{mut}$] SolB interacts with transcripts derived from genes encoded on the chromosome and pSOL1, leading to repression of solvent production and the copy number of pSOL1. SolB is not able to bind to the transcript of *spo0A* in strain *C. acetobutylicum* [pIMP1_solB_spo0A$_{mut}$] as the binding sequence is incorrect.

dehydrogenase and glutamate synthetase interact with different transcription regulators beside their catalytic activity (Commichau et al., 2007). Moonlighting proteins were not yet detected in *C. acetobutylicum* (Mani et al., 2015). However, a moonlighting function of AdhE2 is a suitable explanation for the results of the growth experiment with strain *C. acetobutylicum* [pIMP1_solB_adhE2] as AdhE2 could activate via its moonlighting function the transcription of the *adhE2* gene in contrast to the *C. acetobutylicum* [pIMP1_solB_adhE2_begin] strain.

Taking into account all the results, the function of SolB in *C. acetobutylicum* seems to be a prevention of solvent production in exponential growth phase. Actually, most genes for solvent production are not expressed during the exponential growth phase. However, a lot of promoters are leaky and to prevent this leaky expression SolB is used. Low concentrations of SolB are enough to block the low, leaky expression of the genes involved in solventogenesis. In contrast, in the stationary growth phase, the expression of genes involved in solventogenesis is activated and the low concentration of SolB does not compromise this gene expression. This model of SolB is supported by mathematical predictions, which suggest the “threshold linear response” for sRNAs (Jost et al., 2011; Levine et al., 2007). This means that effects of sRNA depends on its relative abundance to the possible target mRNA. The sRNA is ineffective as long the expression of the target is higher compared to the sRNA. This is the case for SolB in the *C. acetobutylicum* wild type strain during stationary growth phase. As the sRNA is abundant in an increased level in comparison of its target mRNA, it will silence rapidly the mRNA. In the overexpression mutant, *C. acetobutylicum* [pIMP1_solB], SolB exceeds the level of its target mRNA and diminishes translation leading to the decreased copy number of pSOL1 and blocked solvent formation. The threshold level represents the tolerance to a particular stress or transient environmental changes. This mechanism is mandatory as below the threshold the sRNA buffers translational noise (Levine and Hwa, 2008). Thereby, SolB is able to inhibit solvent formation and sporulation in the exponential growth phase in *C. acetobutylicum* as the expression of involved genes is under the threshold level.

4.2 Characterizing the RNA-binding protein Hfq of *C. acetobutylicum*

In the late 1960s, Hfq was first recognized in *Escherichia coli* as host factor required for initiation of plus-strand synthesis by the replicase of the RNA bacteriophage Q (Franze de Fernandez et al., 1968). More than 20 years later, it was localized in the genome of *E. coli* and the genetical disruption of the *hfq* gene revealed pleiotropic effects, like growth deficiency, elongated cell length, and increased stress sensitivity (Tsui et al., 1994), leading to further investigations of *hfq* (Sobrero and Valverde, 2012). Meanwhile, Hfq has emerged to one of the central players in gene regulation on the post-transcriptional level. By interacting with sRNAs, Hfq interferes with the stability of these sRNAs and/or promotes imperfect base-pairing of these sRNAs and their target mRNAs. In most cases, the sRNAs interacting with Hfq are encoded in trans to their target mRNAs resulting in sRNAs, which are just partly complementary to their target mRNAs (Vogel and Luisi, 2011; Wagner and Vogel, 2003). However, a few examples of antisense sRNAs binding to Hfq can be found (Opdyke et al., 2004; Ross et al., 2013; Ellis et al., 2015). For the majority of trans-encoded sRNAs an interaction without Hfq is impossible or the sRNA is able to bind to the target, but the regulatory function is lost without Hfq (Udekwu et al., 2005; Papenfort et al., 2009; Nielsen et al., 2010; Wilms et al., 2012). Extensive research revealed several Hfq-mediated regulation mechanisms. Hfq can boost translation by guiding the respective sRNA to the 5' region of the target mRNA. The interaction of the sRNA with the 5' region of the target mRNA induces a conformational change generating excess for the ribosome to the shine dalgarno sequence of the target mRNA (Fröhlich and Vogel, 2009; Soper et al., 2010). A more frequent mechanism, Hfq-sRNA complexes mask the ribosomal binding site (RBS) of the mRNA target and supress translation (Aiba, 2007; Bobrovskyy and Vanderpool, 2016). Furthermore, Hfq can increase the stability of sRNAs by binding to recognition partners of ribonucleases, such as RNase E (Moll et al., 2003; Viegas et al., 2007). In contrast, Hfq can also enhance the RNA decay of the sRNA-mRNA complexes by recruitment of ribonucleases (Massé et al., 2005; Morita et al., 2005; Ikeda et al., 2011). The mode of action performed by Hfq is reliant on the structural information encoded by the interacting RNA molecule (Vogel and Luisi, 2011).

Hfq is a member of the conserved RNA-binding Sm-like protein family. This group has been found in eukaryotes, bacteria, and archaea (Wilusz and Wilusz, 2005). In contrast to the Sm proteins, which form heteromultimeric rings (Khusial et al., 2005), bacterial

Hfqs were characterized as homomultimeric enzymes with a doughnut-like structure (Møller et al., 2002). This ring shape enables Hfq to bind different RNAs at different parts of the ring. Uridine-rich RNAs can bind to the proximal face and to the outer rim of the ring structure (Mikulecky et al., 2004; Sauer and Weichenrieder, 2011; Sauer et al., 2012). RNAs containing a A-R-N motif were identified to interact with the distal face of Hfq (Link et al., 2009).

Homologs of Hfq have been found in more than 50% of sequenced bacteria (Sun et al., 2002). Some organism even have multiple copies of *hfq* annotated in their genomes (Sun et al., 2002; Ramos et al., 2014; Vrentas et al., 2015). The physiological role of Hfq is quite well elucidated in Gram-negative bacteria, in contrast, the role of Hfq has been incompletely characterized in Gram-positive bacteria. In the Gram-positive *Staphylococcus aureus,* deletion of *hfq* did not cause phenotypic effects (Bohn et al., 2007) and several trans-encoded sRNAs were identified, which act independently of Hfq (Heidrich et al., 2006; Jousselin et al., 2009). However, in the Gram-positive bacteria *Listeria monocyotgenes* and *Bacillus subtilis* several sRNAs were identified, which depend on Hfq (Dambach et al., 2013; Nielsen et al., 2010). The role and the function of Hfq in *C. acetobutylicum* is not yet identified nor investigated. In contrast, the function of Hfq from *Escherichia coli* and C*lostridium difficile* (proposal reclassified as *Peptoclostridium difficile* (Yutin and Galperin, 2013) or *Clostridioides difficile* (Lawson et al., 2016)) was described in more detail (Tsui et al., 1994; Boudry et al., 2014; Caillet et al., 2014). Therefore, the protein sequences of Hfq from *E. coli* K12, *C. difficile* 630, and *C. acetobutylicum* were compared regarding similarities by the Clustal Omega program (Sievers et al., 2011) (Figure 4.2). Hfq from *C. acetobutylicum*

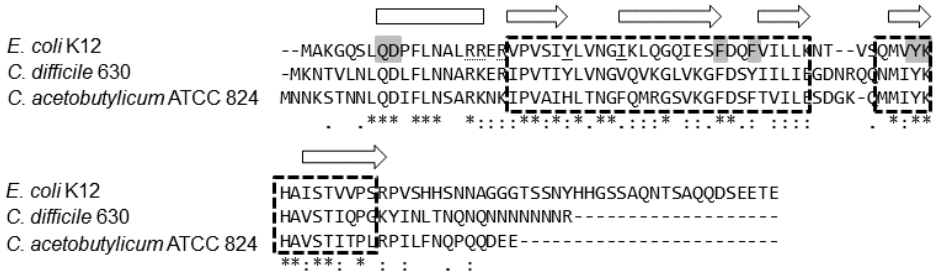

Figure 4.2: Alignment of the Hfq proteins from *E. coli* K12, C*. difficile* 630, and *C. acetobutylicum* ATCC 824 using the Clustal Omega program (Sievers et al., 2011). Periods designate semi-conserved substitutions, colons designate conserved substitutions, and asterisks designate residues found in all strains. The location of *E. coli* Sm1 and Sm2 sequence motifs are boxed with dotted lines. Proximal face residues important for the interaction with RNA are highlighted in gray. Residues important for distal face interaction are underlined and crucial residues at the rim are underlined with dots in the Hfq from *E. coli* (Mikulecky et al. 2004; Zhang et al. 2013). The secondary structure is indicated by boxes (α-helix) and arrows (β sheets).

exhibits 40 % identity with Hfq of *E. coli* and 61 % identity with Hfq of *C. difficile* respectively, excluding the C-terminal ends. In all three Hfq amino acid sequences the two Sm motifs can be recognized and the typical secondary structure of one α-helix followed by 5 β-strands is obvious. The residues Q8, D9, F39, F42, Y55, and K56 were identified as necessary for the proximal binding surface in *E. coli* (Mikulecky et al. 2004; Zhang et al. 2013). All these amino acids were also present in Hfq of *C. acetobutylicum*. In contrast, the amino acids responsible for binding at the distal site (Y25 and I30) and at the rim (R17 and R19) are missing in Hfq of *C. acetobutylicum*. Only R16, which is also necessary for binding of RNAs at the rim, can be found in the Hfq amino acid sequence of *C. acetobutylicum*. However, R17 and R19 are replaced by K, whereby the positive charge remains. As the existence of further binding sites or additional binding motifs was already reported in Hfqs of Gram-positive bacteria (Kovach et al., 2014; Robinson et al., 2014), the differences were not surprising. The C-terminus of all Hfq protein sequences differs between the three. Hfq of *C. difficile* contains an unusual stretch of 7 asparagine and is significantly shorter than the *E. coli* C-terminus. Hfq of *C. acetobutylicum* harbours an even shorter C-terminus compared to *E. coli* and *C. difficile*. The mentioned variations in the C-terminus of the Hfqs were negligible as the deletion of the C-terminal part of *E. coli* Hfq did not cause phenotypic changes (Tsui et al., 1994). Furthermore, several sRNAs can also fulfil the regulatory function with a truncated version of Hfq without the C-terminus (Sonnleitner et al., 2004; Olsen et al., 2010). In conclusion, Hfq of *C. acetobutylicum* revealed significant similarities to the core amino acid sequence of *E. coli* and *C. difficile.* The analogies between the three Hfqs support that Hfq of *C. acetobutylicum* accomplishes functions of sRNA regulation and stress response as the Hfq of *E. coli* and *C. difficile* are involved in these pathways.

Moreover, the *hfq* complementation experiments in *E. coli* promote that Hfq of *C. acetobutylicum* also plays a crucial role in sRNA regulation as Hfq of *C. acetobutylicum* can partly replace the functions of Hfq from *E. coli.* Several Hfqs of different organisms, e.g. *Pseudomonas aeruginosa*, *Moraxella catarrhalis,* and C*. difficile,* were able to replace functions of the *E. coli* Hfq (Sonnleitner et al., 2002; Attia et al., 2008; Caillet et al., 2014). Hfq of *C. acetobutylicum* increased the growth rate (Figure 3.14A), reduced the cell length (Figure 3.15/Figure 3.16), and achieved sugar stress insensitivity (Figure 3.14C) of *E. coli Δhfq* compared to the negative control without any encoded *hfq*. However, the positive control expressing the *E. coli*

hfq performed even better in the experimental set-up. One reason for these findings could be the differences in the Hfq protein sequence between *E. coli* and *C. acetobutylicum.* Furthermore, the increased GC-content of *E. coli* (50.8 % (Blattner et al., 1997)) in comparison to *C. acetobutylicum* (30.9 % (Nölling et al., 2001)) results in differences in the sequence of the target RNAs of Hfq in *C. acetobutylicum* and *E. coli*. Both facts could lead to decreasing binding affinities of *C. acetobutylicum* Hfq to RNAs of *E. coli*. For example, growth on LB medium containing methyl α-D-glucopyranoside induces rapidly sugar stress in *E. coli* cells. The expression of the sRNA *sgrS* is activated and SgrS destabilizes the *ptsG* mRNA to prevent glucose uptake. For degradation of the *ptsG* transcript, SgrS is dependent on Hfq and RNase E (Morita et al., 2003, 2004). Without Hfq*, E. coli* is unable to grow on the methyl α-D-glucopyranoside medium as SgrS cannot degrade the *ptsG* mRNA (Vanderpool, 2007). The slower growth of *E. coli ΔhfqI* [pACYC184_hfq_cac] expressing the *hfq* of *C. acetobutylicum* suggests that an interaction takes place, but the interaction is ineffective compared to interaction of the natural partners of *E. coli*. This is conclusively shown by experiments performed by Cho and Lee (2017). They used for gene knockdown in *C. acetobutylicum* a synthetic sRNA based on the scaffold of the *E. coli* sRNA MicC, which requires Hfq for interaction (Chen et al., 2004). The gene knockdown using the synthetic RNA and the chromosomally encoded Hfq of *C. acetobutylicum* resulted in a remaining protein activity of 8 %. Similar to the improved results by usage of *E. coli* Hfq in the *hfq* complementation experiments in this study, Cho and Lee (2017) increased the efficiency of the knockdown by usage of the *E. coli* Hfq as well. The author concluded that Hfq of *C. acetobutylicum* would not interact with the MicC scaffold as co-immunoprecipitation of Hfq did not show results for MicC. However, the knockdown worked properly with Hfq from *C. acetobutylicum*. Possibly, the binding capacity of Hfq from *C. acetobutylicum* was lower for the *E. coli* MicC scaffold and thus, MicC was under the detection limit of the co-immunoprecipitation as only standard PCR-techniques were used.

The observed stagnation of growth for strain *E. coli* [pACYC184_hfq_cac] under oxygen stress concludes that Hfq of *C. acetobutylicum* is not able to replace the functions of Hfq in *E. coli* under these conditions. As *C. acetobutylicum* is an obligate anaerobic organism and in contrast to *C. acetobutylicum*, *E. coli* can grow in presence as well as in absence of oxygen, the response to oxygen will propably work differently

in these organisms. Therefore, in this case Hfq of *C. acetobutylicum* cannot fulfil the functions of *E. coli* Hfq.

Interestingly, the recorded TEM images of the *hfq* complementation strains revealed a new phenotype of the *E. coli Δhfq* strain (Figure 3.16B). The phenotype of strain *E. coli Δhfq* was quite well described (Tsui et al., 1994), however, nothing is reported regarding the observed translucent areas in the periplasm at the poles of the *E. coli Δhfq* cells. As Hfq was described to play an important role in envelope stress response (Guisbert et al., 2007; Vogt and Raivio, 2014; Chao and Vogel, 2016) and is localized near the membrane (Diestra et al., 2009; Fortas et al., 2015), the results of this study emphasize the function of Hfq in cell wall structure. As the strain *E. coli Δhfq* [pACYC184_hfq_cac] exhibited reduced translucent areas in comparison to the negative control strains *E. coli Δhfq* and *E. coli Δhfq* [pACYC184_pkon], Hfq of *C. acetobutylicum* seems to be involved in the regulation of cell wall structure as well.

Not only the sequence of the *hfq* gene is conserved among several bacteria, but also, the genetic organization of the *hfq* gene displays similarities between the bacteria. Hfq is located in an operon in several bacteria, e.g. *E. coli* (Tsui and Winkler, 1994), *Francisella novicida* (Chambers and Bender, 2011), and *Acinetobacter baylyi* (Schilling and Gerischer, 2009). The results of the RT-PCR (Figure 3.12B) proved an operon structure for the genes CA_C1833-CA_C1838 surrounding *hfq* in *C. acetobutylicum* as well. In general, the *hfq* operons include the *miaA* gene and the *mutL* gene. This is also the case in *C. acetobutylicum*. *mutL* codes for a DNA mismatch repair protein (Acharya et al., 2003; Fukui, 2010) and as Hfq is involved in stress-response of UV radiation (Tsui et al., 1994), which can lead to DNA damage, a joined transcription would be useful. The second mentioned gene encodes MiaA, a tRNA modification enzyme. The linkage between the *hfq* and *miaA* gene remains unclear, however, Hfq was described to bind tRNAs, which could be a first hint for their joined transcription (Lee and Feig, 2008). The conservation of *hfq* in the genetic organization indicates a conservation of the function of Hfq supporting that Hfq in *C. acetobutylicum* fulfils the same functions as the Hfqs with identical genetic organization.

For further characterization of the *hfq* gene in *C. acetobutylicum*, a *C. acetobutylicum hfq* overexpression strain was constructed. As the *hfq* gene is organized in an operon structure, the question was raised how to achieve just the overexpression of *hfq* excluding the transcription of all genes encoded in the operon. In *E. coli* further promoters direct upstream of the *hfq* gene can activate the transcription of *hfq*

separately (Tsui and Winkler, 1994). As the gene region of *hfq* seems to be conserved, the probability is high that further promoters exist upstream of the *hfq* gene in *C. acetobutylicum* as well. Therefore, just a sequence of 150 bps upstream of the *hfq* gene was used as promoter for the *hfq* overexpression. The overexpression strain *C. acetobutylicum* [pIMP1_hfq] revealed a delayed and reduced solvent production of acetone and butanol in the growth experiment. The shift of the acidogenic phase to the solventogenic phase of *C. acetobutylicum* is induced by the pH value (Gottwald and Gottschalk, 1985). As during the production of acids the pH drops, *C. acetobutylicum* counteracts by taking up the acids to produce solvents (Jones and Woods, 1986). This mechanism is mandatory as it prevents the breakdown of the transmembrane proton gradient needed for energy conservation. The low pH during the shift is a stressful environment for the cell and in most bacteria the low pH values activate the stress response mechanisms. Moreover, Hfq is known to be active in acid stress response. For example, *Zymomonas mobilis* wild type showed an increased acid tolerance compared to the *hfq* deletion strain. The overproduction of Lsm ("like Sm", Hfq homologue) proteins in *Saccharomyces cerevisae* revealed also higher tolerance against acid stress (Yang et al., 2010). In *F. novicida* and *Shigella flexneri*, the *hfq* expression was increased under growth at low pH values (Chambers and Bender, 2011; Yang et al., 2015). Furthermore, Hfq activates expression of acid resistance genes in *S. flexneri* (Yang et al., 2015). Taking this into account, it would be possible that overexpression of *hfq* in *C. acetobutylicum* leads to an improved acid response and *C. acetobutylicum* is able to cope longer with these conditions before it starts to take up the acids. This explanation is supported by another study focusing on butyrate stress in *C. acetobutylicum*. Here, 19 sRNAs were upregulated (Venkataramanan et al., 2013), which were possibly dependent on Hfq. However, Venkataramanan et al. (2013) could not detect an increased expression level of Hfq under butyrate stress. In contrast to the physiological internal produced acid stress, this study used an external stimulus. The stress response regulation often differs between external stimuli, as performed in Venkataramanan et al. (2013) and internal stimuli. Thus, it is quite likely that Hfq plays a central role in acid stress response in *C. acetobutylicum*.

To identify further functions of *C. acetobutylicum* Hfq, a *C. acetobutylicum hfq* knockdown or knockout strain should be constructed. As the construction of a *C. acetobutylicum hfq* integration strain with the ClosTron™ system (Standfest, personal communication) failed before and also in *C. difficile* difficulties occurred to

inactivate *hfq* by the ClosTron™ system (Boudry et al., 2014), the strain *C. acetobutylicum* [pBS_as_hfq] was constructed. The strain *C. acetobutylicum* [pBS_as_hfq] expressed an antisense sequence to the transcript of the *hfq* gene, which in theory should knockdown the *hfq* expression by formation of double-stranded RNA followed by degradation of the *hfq* transcript. Growth experiments with *C. acetobutylicum* [pBS_as_hfq] did not display changes in growth behaviour or solvent production in comparison to the control strain *C. acetobutylicum* [pIMP1] (Figure 3.25). However, the success of the knockdown could not be proven or quantified as an antibody against the Hfq protein of *C. acetobutylicum* was not available. Furthermore, an interaction of the antisense RNA with other targets cannot be excluded, which enhance the ClosTron™ method as better choice. Here, problems can only occur if the integration site of the resistance cassette is located in the last part of the gene. Then, it would be possible to generate a truncated version of the disrupted gene, which can be be active. Therefore, the integration sites at position 79 and 168 were used. As *hfq* is encoded by 247 bps, both integration sites can be found in the middle of the *hfq* sequence coding for the core part of the Hfq protein. Therefore, disruption of *hfq* can be assumed to be successful at the positions 79 and 168. Unexpectedly, the integration mutants, *C. acetobutylicum int::hfq* 79/168 [pIMP1_catp] did not exhibit growth deficiencies or changes in the solvent formation under standard growth conditions (Figure 3.29/Figure 3.30), as the knockout of *hfq* was found to decrease the growth rate and leads to further changes in most bacteria (Tsui et al., 1994; Sobrero and Valverde, 2012; Bibova et al., 2013), Possibly, growth under different stress stimuli could uncover growth defects in the *C. acetobutylicum hfq* knockdown strains as several *hfq* deletion strains showed increased stress sensitivity (Chao and Vogel, 2010; Sobrero and Valverde, 2012). For example, growth defects of *F. novicida int::hfq* were not detected under standard growth conditions, but growth with different stress stimuli revealed decreased growth rates of *F. novicida int::hfq* (Chambers and Bender, 2011).

As the main function of Hfq is to bind RNA, an Hfq immunoprecipitation (Hfq-IP) was performed to identify target RNAs of the *C. acetobutylicum* Hfq. 29 transcripts were identified out of the RNA pool of *C. acetobutylicum* in the Hfq-IP. The identified targets (Table 3.2) displayed a wide range of Hfq interaction partners as the targets were categorized to completely different COGs supporting that Hfq plays a global regulatory role in *C. acetobutylicum* like in other bacteria (Gao et al., 2010; Liu et al., 2010; Boudry

et al., 2014; Mégroz et al., 2016). Comparison of the identified transcripts with the RNA-sequencing data of the *C. acetobutylicum* wild type strain demonstrate that the identified transcripts show different expression patterns in *C. acetobutylicum*. As the experimental set-up did not only precipitate targets, which were present in high concentrations in the cell, the Hfq-IP experiment characterized specific interactions between Hfq and the identified transcript. It is striking that the identified targets were annotated genes with open reading frames and transcription start sites. These targets will not interact with Hfq as sRNAs, because most sRNAs can be found in intergenic regions. Either the identified transcripts operate as antisense RNAs or they were bound to a sRNA, which is linked with Hfq. Antisense RNAs were not famous for interacting with Hfq, however, in *Salmonella enterica* the Hfq-IP showed 3 % of Hfq-bound RNA mapped antisense to protein coding regions (Sittka et al., 2008) and in *Mycobacterium smegmatis* about 25 % (Li et al., 2013). Although these results are quite interesting, it is more likely that the identified targets are mRNAs. In general, mRNAs are longer and more stable as the short sRNAs. As the used method for Hfq-IP included several amplification and purification steps, the fact of stability is not negligible. Unfortunately, this is not the only disadvantage of the method. Due to the low GC-content of *C. acetobutylicum* it was often impossible to identify the source of the RNA regarding transcription of the plus or minus DNA strand as polyA-stretches occurred more frequently than only at the 3' termini, which was added to start the dcDNA synthesis (Figure 2.1). Moreover, the percentage of successfully transformed and sequenced transcripts was quite low as nearly 50 % of the screened clones showed no insertion in the transformed plasmid and only 10 % of the PCR verified positives could be successfully sequenced and mapped to the genome of *C. acetobutylicum*. A high number of sequencing results were found to map to the genome of *E. coli*. As Hfq of *C. acetobutylicum* was shown to be able to replace functions of the *E. coli* Hfq (Figure 3.14), the recombinantly expressed Hfq of *C. acetobutylicum* will also interact with transcripts of *E. coli* present in the cells during the production of Hfq. In the future, this could be avoided by performing a further RNA digestion of the purified Hfq elution fraction to remove all linked RNAs of *E. coli*. However, an additional purification step would be necessary to get rid of the RNases. The low efficacy of the performed time-consuming method suggest to perform the faster Hfq-IP with additional RNA-sequencing (Sharma and Vogel, 2009). Advantages would be that the results also can be statistically proven as all linked RNAs are captured. In the performed study,

some transcripts were found twice. The probability is high that the reason is not based on a higher concentration of the transcript, but rather in an ideal insert backbone ratio for transformation. Furthermore, RNA-sequencing data provides a more detailed view on all interacting RNAs with Hfq. Although the used methods revealed disadvantages, it was possible to support the assumption that Hfq of *C. acetobutylicum* acts like most characterized RNA-binding proteins. For example, the *nusG* gene, which was identified in the Hfq-IP experiment, is an important factor of transcription antitermination and Hfq was shown to be involved in this process in *E. coli* (Rabhi et al., 2011). Moreover, the identification of the *hfq* transcript suggests an autoregulation of the *hfq* expression in *C. acetobutylicum*. In *E. coli*, two binding sites of Hfq were found in the 5' region of the *hfq* transcript and Hfq of *E. coli* as well as of *Sinorhizobium meliloti* were able to suppress translation of the *hfq* transcript (Vecerek et al., 2005; Sobrero and Valverde, 2011). The transcript of the chaperone GroEL emphasizes that Hfq of *C. acetobutylicum* plays a crucial role in stress response in *C. acetobutylicum*. GroEL is involved in cytoplasmic stress response and was found to be downregulated in *E. coli* cells lacking *hfq* (Guisbert et al., 2007).

In conclusion, Hfq of *C. acetobutylicum* seems to play crucial role in sRNA regulation as it can replace partly functions of the *E. coli* Hfq, which is characterized as mandatory unit of sRNA regulation. Furthermore, the genetic organisation of *hfq* revealed similarities between *E. coli* and *C. acetobutylicum* supporting also a conservation in functionality. Moreover, the Hfq-IP suggest a global role for Hfq in *C. acetobutylicum*. Some RNA targets identified by Hfq-IP were already found in other organisms to be influenced by Hfq. However, the phenomenon of growth deficiency by *hfq* disruption was not detected in *C. acetobutylicum*. Overexpression of *hfq* in *C. acetobutylicum* decreased and delayed the production of solvents since the overexpression possibly improved the acid stress response. All in all, the results indicate that Hfq in *C. acetobutylicum* is involved in sRNA and stress response regulation, but the importance of Hfq in regulation of *C. acetobutylicum* seems to be minor compared to Hfq of *E. coli* as knockdown of *hfq* in *C. acetobutylicum* revealed no growth deficiency.

4.3 SolB – a further dependent sRNA of Hfq?

In this study, experiments displayed that Hfq seems to be involved in the regulatory network of *C. acetobutylicum* (4.2). As SolB is characterized as a trans-encoded sRNA (Zimmermann, 2013) and a common denominator of trans-encoded sRNAs is in general a dependency on Hfq (Vogel and Luisi, 2011), it was necessary to elucidate the role of Hfq in the regulatory mechanism of SolB. In general, Hfq-dependent sRNAs interact directly with Hfq. However, the Hfq 2 of *B. anthrax* was unable to bind sRNAs at all (Panda et al., 2015). Therefore, the binding capacity of Hfq from *C. acetobutylicum* for the sRNA SolB was tested. The performed pull down assay of Hfq with labelled SolB (Figure 3.21) confirmed the binding ability of Hfq to the sRNA SolB. Moreover, the stabilization assay verfied the binding of SolB by Hfq as a clear shift of the SolB signal was detectable in comparison to the signal of SolB without Hfq (Figure 3.23). The EMSA showed a more detailed view of the binding properties between Hfq and SolB. The labelled SolB started to shift at Hfq concentrations of 3.7 nM and a clear shift was detected at 37 nM of Hfq (Figure 3.22). Compared to the results with other Hfq-sRNA EMSAs, the shift was detected in a typical concentration range. For example, the sRNA MicA of *E. coli* shifted at Hfq concentrations of 15 nM (Henderson et al., 2013) and the sRNA RydC of *E. coli* started to shift at Hfq concentrations of 5 nM (Dimastrogiovanni et al., 2014). To confirm the specifity of the binding between SolB and Hfq, the competitor approach was used. It was expected that the signal of labelled SolB would be comparable with the signal of the set-up without Hfq, because Hfq would interact with the unlabelled SolB as it is used in molar excess to the labelled SolB. Indeed, the signal did not shift back, but it was weaker compared to the other set-ups. Still, the shift here was not attributable to unspecific binding of labelled SolB to Hfq as the molar excess was just three times between labelled und unlabelled SolB. The manual of the LightShift™ Chemiluminescent RNA EMSA Kit suggested a 1,000-fold excess. Unfortunately, it was not possible to produce SolB by in vitro transcription in these amounts. Thus, the shift of labelled SolB is dedicated to the low amount of unlabelled SolB used. The binding potential of SolB by Hfq supports that Hfq plays a significant role for SolB. However, in *S. aureus* the RNAIII was also bound by Hfq (Huntzinger et al., 2005), but Hfq was neither necessary for the function nor for the stability (Geisinger et al., 2006; Boisset et al., 2007). The same phenomenon was discovered for sRNA SR1 of *B. subtilis* (Heidrich et al., 2006, 2007). In contrast to the mentioned sRNA-Hfq interactions, Hfq showed a significant influence

on the stability of SolB (Figure 3.23). In presence of the crude extract of *C. acetobutylicum* and the Hfq protein, SolB was faster degraded than in presence of the crude extract of *C. acetobutylicum* alone. Generally, Hfq was reported to protect sRNAs from RNA cleavage, particularly RNase E cleavage (Massé et al., 2003; Moll et al., 2003; Vogel and Luisi, 2011). Both proteins, RNase E and Hfq, tend to bind to AU rich sequences in *E. coli* (McDowall et al., 1994; Brescia et al., 2003; Massé et al., 2003). A homologue of RNase E is also present in *C. acetobutylicum*, the RNase E/G (Durand et al., 2015). Nevertheless, a stabilization experiment revealed an increase of RNA decay for SolB in presence of Hfq. Thus, Hfq of *C. acetobutylicum* does not stabilize SolB. Hfq can also boost degradation of sRNA-mRNA complexes. Hereby, the mRNA is degraded as well as the sRNA (Massé et al., 2003; Morita et al., 2005; De Lay and Gottesman, 2012). It is proven that Hfq can directly interact with RNase E, which can interfere with the degradosome of the bacterial cells (Viegas et al., 2007; Ikeda et al., 2011; De Lay et al., 2013). This recruitment of RNase E by Hfq leads to rapid degradation of mRNA and sRNA complexes. In the case of the sRNA SolB, degradation of SolB was significantly faster in presence of Hfq supporting the theory that in *C. acetobutylicum* Hfq can boost degradation of sRNA-mRNA complexes. Beside RNases, the applied crude extract of *C. acetobutylicum* contained the target mRNAs of SolB. By binding of SolB to the target mRNAs, Hfq activated the degradation of SolB and the mRNA. This assumption is supported by the stability of SolB in presence of Hfq without crude extract (Figure 3.23). Thus, RNases of *E. coli* were not co-isolated by heterologous expression and purification of Hfq from *C. acetobutylicum* in *E. coli*. No degradation process was observed without Hfq, although the target mRNAs in the set-up originating from the crude extract of *C. acetobutylicum* were present. Without Hfq, it was either impossible to recruit the degradation machinery of *C. acetobutylicum* for the SolB-mRNA complex or SolB was unable to bind the mRNA targets without Hfq as degradation of sRNA-mRNA complexes can be also performed without Hfq (Saramago et al., 2014).Summarizing, Hfq plays a significant role in the degradation process of SolB.

In order to analyze if SolB is completely dependent on the RNA-binding protein Hfq, different approaches to knockdown or knockout the *hfq* gene were performed. The basic idea here was that an Hfq-dependent SolB would be unable to suppress solvent formation or diminish the copy number of pSOL1 in a *C. acetobutylicum hfq*-deficient, but *solB*-overexpressing strain. First, an antisense approach to knockdown the *hfq*

expression was tested. The experiments revealed a two-fold increase in solvent production and also an increase in the copy number of pSOL1 for *C. acetobutylicum* [pBS_as_hfq_solB] compared to strain *C. acetobutylicum* [pIMP1_solB] (Figure 3.25/Figure 3.26). However, effects of *solB* overexpression in *C. acetobutylicum* [pBS_as_hfq_solB] were still tremendous in comparison to strain *C. acetobutylicum* [pIMP1]. Concluding, the knockdown of *hfq* is either inefficient as discussed in section 4.2 or Hfq plays only a minor role in the functionality of SolB. As no Western blot for the Hfq protein of *C. acetobutylicum* was available to exclude the inefficiency of the knockdown, the ClosTron™ system was revisited to generate an integration mutant and to obtain more convincing results. Two integration sites were chosen to increase the likelihood of a successful integration. The growth experiments with the *C. acetobutylicum int::hfq* strains overexpressing *solB* displayed an increased solvent production as well as increased copy number of pSOL1 in comparison to the strain *C. acetobutylicum* [pIMP1_solB] (Figure 3.31/Figure 3.32/Figure 3.10). The results were similar to the *hfq* knockdown approach by antisense RNA as the strain *C. acetobutylicum* [pBS_as_hfq_solB] reached also higher levels of solvents and pSOL1. However, the values of pSOL1, acetone and butanol of strains *C. acetobutylicum int::hfq* 79s [pIMP1_catp_solB] and *C. acetobutylicum int::hfq* 168a [pIMP1_catp_solB] were significantly higher in comparison to strain *C. acetobutylicum* [pBS_as_hfq_solB]. Especially, the butanol production was enhanced with values of at least 25 mM for *C. acetobutylicum int::hfq* 79s [pIMP1_catp_solB] and 59 mM for *C. acetobutylicum int::hfq* 168a [pIMP1_catp_solB]. As expected, the *hfq* knockdown by RNA antisense mechanism was not as efficient as the disruption by integration of the *hfq* gene resulting in severe effects in *C. acetobutylicum int::hfq* 79s/168a [pIMP1_catp_solB] compared to *C. acetobutylicum* [pBS_as_hfq_solB]. Moreover, both integration sites revealed similar effects in the *C. acetobutylicum int::hfq* strains. Thus, the disruption of *hfq* was achieved successfully at position 79 as well as at position 168. The growth experiments clearly revealed that effects of *solB* overexpression in *C. acetobutylicum int::hfq* were significantly diminished in comparison to *C. acetobutylicum* [pIMP1_solB]. However, the strains *C. acetobutylicum int::hfq* 79s/168a [pIMP1_catp_solB] were not able to produce the same amount of solvents and were not able to reach the same copy number of pSOL1 as the control strain *C. acetobutylicum int::hfq* 79s/168a [pIMP1_catp]. Recapitulating, SolB is able to fulfill its function on its own, nevertheless, the presence of Hfq increases

the activity of SolB. Thus, Hfq is not essential for the mode of action of SolB, but Hfq increases the effectiveness of SolB. To completely prove this assumption, the complementation strains *C. acetobutylicum int::hfq* 79s/168a [pIMP1_catp_solB_ptb_hfq] should display the same phenotype as the strain *C. acetobutylicum* [pIMP1_solB] with suppressed solvent production and decreased copy number of pSOL1. In contrast to the expectations, the complementation strains *C. acetobutylicum int::hfq* 79s/168a [pIMP1_catp_solB_ptb_hfq] exhibited the same phenotype as the strain *C. acetobutylicum int::hfq* 79s/168a [pIMP1_catp]. This raised the question, why the overexpressed *solB* in presence of Hfq is not able to block solvent formation in *C. acetobutylicum* as in the strain *C. acetobutylicum* [pIMP1_solB]. The strains *C. acetobutylicum int::hfq* 79s/168a [pIMP1_catp_solB_ptb_hfq] and *C. acetobutylicum* [pIMP1_solB] differ in the number of encoded *hfq* genes. *C. acetobutylicum int::hfq* 79s/168a [pIMP1_catp_solB_ptb_hfq] encoded the *hfq* gene on the plasmid. The plasmid pIMP1 seems to be a high copy number plasmid in *C. acetobutylicum* as discussed in section 4.1.1. In contrast, the strain *C. acetobutylicum* [pIMP1_solB] encodes the *hfq* gene once in the genome. Furthermore, the strain *C. acetobutylicum int::hfq* 79s/168a [pIMP1_catp_solB_ptb_hfq] expressed the *hfq* gene by the strong and constitutive *ptb-buk* promoter (Feustel et al., 2004), which led to a further increase in Hfq proteins compared to *C. acetobutylicum* [pIMP1_solB]. The use of a different promoter was chosen as the precise location was not characterized yet. As the Hfq protein in *E. coli* was found to supress its own expression/translation (Vecerek et al., 2005) and also Hfq of *C. acetobutylicum* is able to bind the mRNA of *hfq* (Table 3.2), the autoregulation was possibly blocked as the 5' untranslated region differed in the fusion transcript of *hfq* gene and the *ptb-buk* promoter. This should further increase the level of Hfq in the strains *C. acetobutylicum int::hfq* 79s/168a [pIMP1_catp_solB_ptb_hfq]. In *E. coli,* it was proven that for sRNA-Hfq interaction the Hfq set point is essential meaning that the Hfq concentration has an optimal level for maximal sRNA activity (Sagawa et al., 2015). If the concentration of Hfq was too high or low for optimal binding of the sRNA, the activity of the sRNA was diminished (Sagawa et al., 2015). This report is in line with the behaviour of SolB and Hfq in *C. acetobutylicum.* After disruption of the *hfq* gene the function of SolB in *C. acetobutylicum int::hfq* 79s/168a [pIMP1_catp_solB] was reduced as Hfq was missing. In the complementation strain *C. acetobutylicum*

int::hfq 79s/168a [pIMP1_catp_solB_ptb_hfq] the function of SolB was diminished as the concentration of Hfq was too high.

In conclusion, the following model is postulated for the SolB Hfq interaction: Free SolB binds to a target mRNA and blocks translation (Figure 4.3A). It has to be elucidated in further studies whether the complex of SolB and target mRNA without Hfq is degraded as the blocked translation of the mRNA target by SolB already can lead to the observed effects in *C. acetobutylicum int::hfq* 79s/168a [pIMP1_catp_solB] (Figure 3.31/Figure 3.32). It is also possible that Hfq interacts with SolB and afterwards, the complex of Hfq and SolB binds to the mRNA (Figure 4.3B). SolB and the mRNA are then degraded by RNases. This mode of action for SolB is more efficient as the mode of action without Hfq, as seen in the growth experiments with *C. acetobutylicum int::hfq* 79s/168a [pIMP1_catp_solB] (Figure 3.31/Figure 3.32) compared to *C. acetobutylicum* [pIMP1_solB] (Figure 3.3/Figure 3.10). However, due to *hfq* overexpression in *C. acetobutylicum* SolB is degraded, before it can interact with its target mRNAs (Figure 4.3C). As shown in strain *C. acetobutylicum int::hfq* 79s/168a [pIMP1_catp_solB_ptb_hfq], the overexpressed *solB* has no influence on solvent production and the copy number of pSOL1 (Figure 3.31/Figure 3.32). The degradation of SolB by RNases without mRNA target is supported by the following points: The

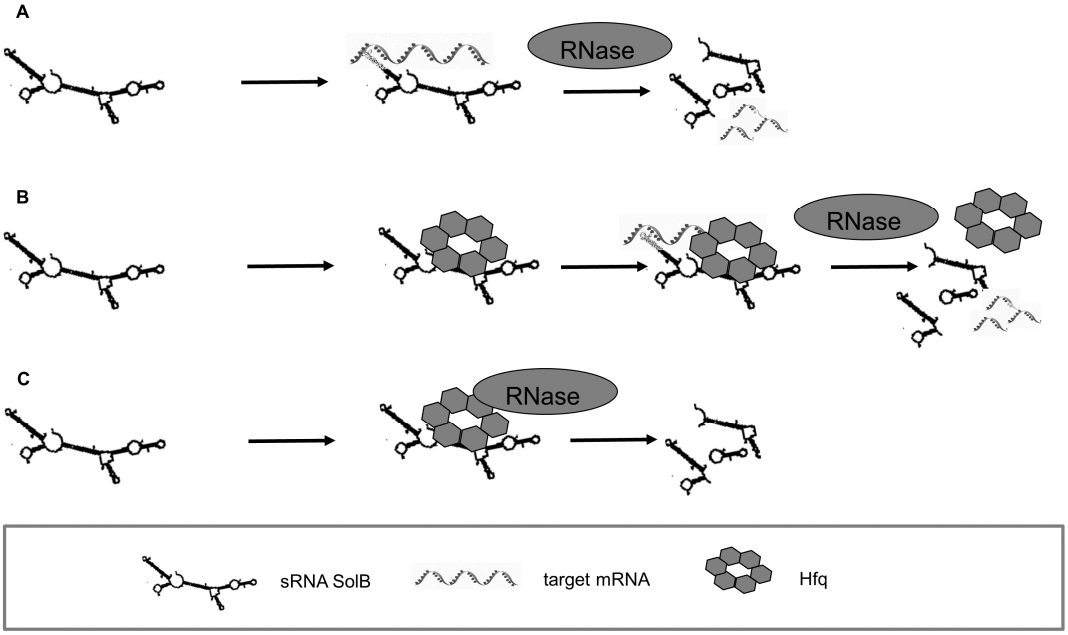

Figure 4.3: Simplified model of SolB interaction with Hfq and its target mRNAs. (A) SolB binds to its target and translation of the mRNA is blocked. Eventually, the complex is degraded by RNases. (B) SolB binds first to Hfq and afterwards the SolB-Hfq complex interferes with the mRNA target. SolB and the mRNA will be degraded by RNases. (C) In presence of an increased Hfq concentration, SolB binds first to Hfq, which is coupled with RNases, and SolB will be degraded without interaction of mRNA targets.

stabilization assay displayed an obvious degradation of SolB in presence of Hfq (Figure 3.23). Overexpression of *hfq* in *E. coli* repressed sRNA regulation (Sagawa et al., 2015) and Hfq was found to be coupled with RNases (Viegas et al., 2007). Taking these points into account, SolB seems to be degraded at a high concentration of Hfq.

5 Summary

The small regulatory RNA (sRNA) SolB is able to repress the production of acetone and butanol as well as the sporulation process in a *C. acetobutylicum solB* overexpression strain. The aim of this study was to identify targets and the role of SolB in solventogenesis. Moreover, the function of the RNA-binding protein Hfq should be elucidated in *C. acetobutylicum*.

1. The transcriptome analysis and quantitative real-time PCR revealed down-regulation of all genes encoded on the megaplasmid pSOL1 of *C. acetobutylicum* [pIMP1_solB] compared to the *C. acetobutylicum* wild type strain.

2. DNA sequencing data and quantitative real-time PCR demonstrated a 50 times decreased copy number of the megaplasmid pSOL1 in the *C. acetobutylicum solB* overexpression strain compared to the control strain, *C. acetobutylicum* [pIMP1]. Concluding, SolB can regulate the copy number of pSOL1 and the reduced level of pSOL1 in *C. acetobutylicum* [pIMP1_solB] seems to be the bottleneck for the low expression of the genes encoded on the megaplasmid pSOL1.

3. Simultaneous overexpression of *solB* and *adhE2* in strain *C. acetobutylicum* [pIMP1_solB_adhE2] restored solvent production and increased the copy number of pSOL1 supporting the interaction of SolB with the transcript of *adhE2.* Further growth experiments with genetically modified *C. acetobutylicum* strains indicated that the overexpression of *adhE2* as well as the overexpression of *spo0A* leads to a titration effect of SolB.

4. The sporulation process of strain *C. acetobutylicum* [pIMP1_solB] seems to be inhibited on the level of the sporulation factor σ^G as in the transcriptome analysis a decreased transcription of *sigG* was observed and increased amounts of granulose were determined via HPLC in *C. acetobutylicum* [pIMP1_solB] compared to the control strains.

5. Transmission electron microscopy images and transcriptome analysis (*C. acetobutylicum* [pIMP1_solB] vs. *C. acetobutylicum spo0A*) supported the assumption that SolB acts as global regulator due to severe changes in cell morphology and similarity in effects to the global regulator Spo0A.

6. Similarities between the RNA-binding protein Hfq of *C. acetobutylicum* and *E. coli* in the amino acid sequence as well as in the genetic organisation of the *hfq* gene indicated a related function of the *C. acetobutylicum* and *E. coli* Hfq. Complementation experiments supported this assumption as Hfq of *C. acetobutylicum* was able to compensate cell changes and growth deficiency under different conditions in an *E. coli Δhfq* strain.

7. The RNA-binding capacity of *C. acetobutylicum* Hfq was proven by Hfq-immunoprecipitation experiments. Several mRNA targets were identified, which were involved in Hfq interactions in different organisms.

8. Overexpression of *hfq* in *C. acetobutylicum* supported an increased acid stress response as the production of solvents was delayed and decreased. *C. acetobutylicum hfq* knockdown and knockout strains did not show phenotypic changes supporting a minor important role as displayed for Hfq in *E. coli*.

9. The analysis of the *C. acetobutylicum* Hfq protein suggests that *C. acetobutylicum* Hfq is involved in stress response and sRNA regulation.

10. Most trans-encoded sRNAs require the RNA-binding protein Hfq for stability or functionality. Pulldown and electrophoretic mobility shift assays proved that SolB is bound to Hfq. Faster degradation of SolB was observed in presence of Hfq. Furthermore, the effects of *solB* overexpression in an *hfq*-deficient *C. acetobutylicum* strain were diminished confirming the dependency of SolB on Hfq. Moreover, an increased Hfq concentration suppressed the effects of *solB* overexpression in *C. acetobutylicum* suggesting that the Hfq concentration plays a crucial role for the function of SolB.

6 Zusammenfassung

Die regulatorische RNA SolB unterdrückt sowohl die Bildung der Lösungsmittel von Aceton und Butanol als auch die Sporulation in einer *C. acetobutylicum solB* Überexpressionsmutante. Ziel dieser Studie war es, Bindepartner von SolB zu identifizieren und die Rolle von SolB bezüglich der Lösungsmittelbildung zu charakterisieren. Desweiteren sollte die Funktion des RNA-Bindeproteins Hfq in *C. acetobutylicum* untersucht werden.

1. Die *C. acetobutylicum solB* Überexpressionsmutante zeigte im Vergleich zum *C. acetobutylicum* Wildtyp in Transkriptomanalysen und quantitativen *real-time* PCR-Experimenten eine Abnahme der Transkriptmenge aller Gene, die auf dem Megaplasmid pSOL1 kodiert sind.

2. Durch DNA-Sequenzierungen und quantitative *real-time* PCR-Experimente konnte eine um 50-fach verringerte Menge an pSOL1 in der *C. acetobutylicum solB* Überexpressionsmutante im Vergleich zum Kontrollstramm, *C. acetobutylicum* [pIMP1], festgestellt werden. Folglich reguliert SolB die Plasmidkopienzahl des Megaplasmids pSOL1. Außerdem ist die verringerte Kopienzahl von pSOL1 in der *C. acetobutylicum* [pIMP1_solB] Mutante verantwortlich für die reduzierte Transkription dieser Gene.

3. Die gleichzeitige Überexpression der Gene *solB* und *adhE2* in *C. acetobutylicum* [pIMP1_solB_adhE2] führte zu einer wildtyp-ähnlichen Lösungsmittelproduktion und Plasmidkopienzahl von pSOL1. Dies ist eine Bestätigung für die Interaktion von SolB mit der mRNA des *adhE2*-Gens. Darüber hinaus deuten weitere Wachstumsversuche mit genetisch veränderten *C. acetobutylicum*-Stämmen darauf hin, dass die Überexpression der Gene *adhE2* und *spo0A* zu einem Titrationseffekt von SolB führt.

4. Der Sporulationsprozess der *C. acetobutylicum* [pIMP1_solB] Mutante scheint auf der Stufe des Sporulationsfaktors σ^G inhibiert zu sein, da in den Transkriptomanalysen eine Abnahme der Expression des *sigG*-Gens bestimmt und ein Anstieg der Granuloseproduktion im Vergleich zu den Kontrollstämmen mit Hilfe der HPLC aufgezeigt wurde.

5. Aufnahmen mit Transmissionselektronenmikroskopie und Transkriptomanalysen (*C. acetobutylicum* [pIMP1_solB] vs. *C. acetobutylicum spo0A*) bestätigten, dass

SolB als globaler Regulator fungiert, da deutliche Veränderungen in der Zellmorphologie festgestellt wurden und Ähnlichkeiten in den Wirkmechanismen zum globalen Regulator Spo0A bestehen.

6. Gemeinsamkeiten in der Aminosäuresequenz und der genetischen Organisation des RNA-Bindeproteins Hfq von *C. acetobutylicum* und *E. coli* weisen darauf hin, dass das Hfq-Protein in *C. acetobutylicum* ähnliche Funktionen übernimmt wie das Hfq-Protein in *E. coli*. Dies wurde durch Komplementationsexperimente bestätigt, in denen das Hfq-Protein von *C. acetobutylicum* Zellveränderungen und Wachstumsdefizite in dem Stamm *E. coli Δhfq* kompensieren konnte.

7. Mit Hfq-Immunpräzipitationen konnte nachgewiesen werden, dass das Hfq-Protein von *C. acetobutylicum* in der Lage ist, RNAs zu binden. Hierbei wurden einige mRNAs entdeckt, die auch in anderen Organismen an Hfq-Interaktionen beteiligt sind.

8. Da die Überexpression des *hfq*-Gens in *C. acetobutylicum* zu einer verspäteten und verringerten Lösungsmittelbildung führte, wird angenommen, dass das Hfq-Protein zu einer verbesserten Säure-Stress-Antwort führt. *C. acetobutylicum hfq knockdown*- und *knockout*-Mutanten wiesen keine phenotypischen Veränderungen auf und führen zu dem Schluss, dass das Hfq-Protein in *C. acetobutylicum* eine untergeordnetere Rolle als das Hfq-Protein in *E. coli* spielt.

9. Die Untersuchungen zum Hfq-Protein von *C. acetobutylicum* unterstützen die Vermutung, dass Hfq an der Stressantwort und der sRNA-Regulation in *C. acetobutylicum* beteiligt ist.

10. Die meisten trans-kodierten sRNAs benötigen das RNA-Bindeprotein Hfq für ihre Stabilität bzw. Funktion. Durch *pulldown* und *electrophoretic mobility shift assays* konnte bewiesen werden, dass das Hfq-Protein an SolB bindet. Außerdem wurde eine gesteigerte Degradation von SolB in Anwesenheit des Hfq-Proteins festgestellt. Die Hfq-Abhängigkeit von SolB wurde durch die verringerten Effekte der Überexpression von *solB* in verschiedenen *C. acetobutylicum hfq knockout*-und *knockdown*-Mutanten bestätigt. Desweiteren zeigte sich, dass die Überproduktion des Hfq-Proteins die Auswirkungen der *solB* Überexpression unterdrückt. Daher scheint die Hfq Konzentration für die Funktion von SolB eine entscheidende Rolle zu spielen.

7 References

Acharya, S., Foster, P.L., Brooks, P., Fishel, R., 2003. The coordinated functions of the *E. coli* MutS and MutL proteins in mismatch repair. Mol. Cell 12, 233–246.

Adams, R.L.P., Burdon, R.H., 1985. The methylation machinery: DNA methyltransferases, chapt. 5, p. 43-71, in: Molecular biology of DNA methylation. Springer, New York, USA.

Aiba, H., 2007. Mechanism of RNA silencing by Hfq-binding small RNAs. Curr. Opin. Microbiol. 10. doi:10.1016/j.mib.2007.03.010.

Aiba, H., Adhya, S., de Crombrugghe, B., 1981. Evidence for two functional *gal* promoters in intact *Escherichia coli* cells. J. Biol. Chem. 256, 11905–11910.

Al-Hinai, M.A., Jones, S.W., Papoutsakis, E.T., 2015. The *Clostridium* sporulation programs: diversity and preservation of endospore differentiation. Microbiol. Mol. Biol. Rev. 79, 19–37. doi:10.1128/MMBR.00025-14.

Alsaker, K.V., Papoutsakis, E.T., 2005. Transcriptional program of early sporulation and stationary-phase events in *Clostridium acetobutylicum*. J. Bacteriol. 187, 7103–7118. doi:10.1128/JB.187.20.7103-7118.2005.

Altuvia, S., 2004. Regulatory small RNAs: The key to coordinating global regulatory circuits. J. Bacteriol. 186, 6679–6680. doi:10.1128/JB.186.20.6679-6680.2004.

Altuvia, S., Wagner, E.G.H., 2000. Switching on and off with RNA. Proc. Natl. Acad. Sci. USA 97, 9824–9826. doi:10.1073/pnas.97.18.9824.

Altuvia, S., Zhang, A., Argaman, L., Tiwari, A., Storz, G., 1998. The *Escherichia coli* OxyS regulatory RNA represses *fhlA* translation by blocking ribosome binding. EMBO J. 17, 6069–6075. doi:10.1093/emboj/17.20.6069.

Asano, K., Mizobuchi, K., 1998. Copy number control of IncIα plasmid ColIb-P9 by competition between pseudoknot formation and antisense RNA binding at a specific RNA site. EMBO J. 17, 5201–5213. doi:10.1093/emboj/17.17.5201.

Attia, A.S., Sedillo, J.L., Wang, W., Liu, W., Brautigam, C.A., Winkler, W., Hansen, E.J., 2008. *Moraxella catarrhalis* expresses an unusual Hfq protein. Infect. Immun. 76, 2520–2530. doi:10.1128/IAI.01652-07.

Baba, T., Ara, T., Hasegawa, M., Takai, Y., Okumura, Y., Baba, M., Datsenko, K.A., Tomita, M., Wanner, B.L., Mori, H., 2006. Construction of *Escherichia coli* K-12 in-frame, single-gene knockout mutants: The Keio collection. Mol. Syst. Biol. 2, 2006.0008. doi:10.1038/msb4100050.

Babitzke, P., Romeo, T., 2007. CsrB sRNA family: Sequestration of RNA-binding regulatory proteins. Curr. Opin. Microbiol. 10, 156–163. doi:10.1016/j.mib.2007.03.007.

Balasubramanian, D., Ragunathan, P.T., Fei, J., Vanderpool, C.K., 2016. A prophage-encoded small RNA controls metabolism and cell division in *Escherichia coli*. mSystems 1, e00021-15. doi:10.1128/mSystems.00021-15.

Balganesh, T.S., Reiners, L., Lauster, R., Noyer-Weidner, M., Wilke, K., Trautner, T.A., 1987. Construction and use of chimeric SPR/Φ3T DNA methyltransferases in the definition of sequence recognizing enzyme regions. EMBO J. 6, 3543–3549.

Bankevich, A., Nurk, S., Antipov, D., Gurevich, A.A., Dvorkin, M., Kulikov, A.S., Lesin, V.M., Nikolenko, S.I., Pham, S., Prjibelski, A.D., Pyshkin, A.V., Sirotkin, A.V., Vyahhi, N., Tesler, G., Alekseyev, M.A., Pevzner, P.A., 2012. SPAdes: A new genome assembly algorithm and its applications to single-cell sequencing. J. Comput. Biol. 19, 455–477. doi:10.1089/cmb.2012.0021.

Bardill, J.P., Hammer, B.K., 2012. Non-coding sRNAs regulate virulence in the bacterial pathogen *Vibrio cholerae*. RNA Biol. 9, 392–401. doi:10.4161/rna.19975.

Beckert, B., Masquida, B., 2011. Synthesis of RNA by in vitro transcription, chap. 3, p. 29–41, in: Nielsen, H. (Eds.), RNA. Humana Press, Totowa, USA,. doi:10.1007/978-1-59745-248-9_3.

Beisel, C.L., Storz, G., 2010. Base pairing small RNAs and their roles in global regulatory networks. FEMS Microbiol. Rev. 34, 866–882. doi:10.1111/j.1574-6976.2010.00241.x.

Bernstein, P., Ross, J., 1989. Poly(A), poly(A) binding protein and the regulation of mRNA stability. Trends Biochem. Sci. 14, 373–377.

Bertram, J., Kuhn, A., Dürre, P., 1990. Tn*916*-induced mutants of *Clostridium acetobutylicum* defective in regulation of solvent formation. Arch. Microbiol. 153, 373–377. doi:10.1007/BF00249008.

Bibova, I., Skopova, K., Masin, J., Cerny, O., Hot, D., Sebo, P., Vecerek, B., 2013. The RNA chaperone Hfq is required for virulence of *Bordetella pertussis*. Infect. Immun. 81, 4081–4090. doi:10.1128/IAI.00345-13.

Blattner, F.R., Plunkett, G., Bloch, C.A., Perna, N.T., Burland, V., Riley, M., Collado-Vides, J., Glasner, J.D., Rode, C.K., Mayhew, G.F., Gregor, J., Davis, N.W., Kirkpatrick, H.A., Goeden, M.A., Rose, D.J., Mau, B., Shao, Y., 1997. The complete genome sequence of *Escherichia coli* K-12. Science 277, 1453–1462.

Bobrovskyy, M., Vanderpool, C.K., 2016. Diverse mechanisms of post-transcriptional repression by the small RNA regulator of glucose-phosphate stress. Mol. Microbiol. 99, 254–273. doi:10.1111/mmi.13230.

Bohn, C., Rigoulay, C., Bouloc, P., 2007. No detectable effect of RNA-binding protein Hfq absence in *Staphylococcus aureus*. BMC Microbiol. 7, 10. doi:10.1186/1471-2180-7-10.

Böhringer, M., 2002. Molekularbiologische und enzymatische Untersuchungen zur Regulation des Gens der Acetacetat-Decarboxylase von *Clostridium acetobutylicum.* Ph.D. thesis. Ulm University, Germany.

Boisset, S., Geissmann, T., Huntzinger, E., Fechter, P., Bendridi, N., Possedko, M., Chevalier, C., Helfer, A.C., Benito, Y., Jacquier, A., Gaspin, C., Vandenesch, F., Romby, P., 2007. *Staphylococcus aureus* RNAIII coordinately represses the synthesis of virulence factors and the transcription regulator Rot by an antisense mechanism. Genes Dev. 21, 1353–1366. doi:10.1101/gad.423507.

Bolger, A.M., Lohse, M., Usadel, B., 2014. Trimmomatic: A flexible trimmer for Illumina sequence data. Bioinformatics 30, 2114–2120. doi:10.1093/bioinformatics/btu170.

Bouché, F., Bouché, J.P., 1989. Genetic evidence that DicF, a second division inhibitor encoded by the *Escherichia coli dicB* operon, is probably RNA. Mol. Microbiol. 3, 991–994.

Boudry, P., Gracia, C., Monot, M., Caillet, J., Saujet, L., Hajnsdorf, E., Dupuy, B., Martin-Verstraete, I., Soutourina, O., 2014. Pleiotropic role of the RNA chaperone protein Hfq in the human pathogen *Clostridium difficile*. J. Bacteriol. 196, 3234–3248. doi:10.1128/JB.01923-14

Brantl, S., 2002. Antisense RNAs in plasmids: Control of replication and maintenance. Plasmid 48, 165–173.

Brantl, S., 2007. Regulatory mechanisms employed by cis-encoded antisense RNAs. Curr. Opin. Microbiol. 10, 102–109. doi:10.1016/j.mib.2007.03.012

Brantl, S., Brückner, R., 2014. Small regulatory RNAs from low-GC Gram-positive bacteria. RNA Biol. 11, 443–456. doi:10.4161/rna.28036

Brantl, S., Wagner, E.G., 1996. An unusually long-lived antisense RNA in plasmid copy number control: in vivo RNAs encoded by the streptococcal plasmid pIP501. J. Mol. Biol. 255, 275–288. doi:10.1006/jmbi.1996.0023

Brescia, C.C., Mikulecky, P.J., Feig, A.L., Sledjeski, D.D., 2003. Identification of the Hfq-binding site on DsrA RNA: Hfq binds without altering DsrA secondary structure. RNA 9, 33–43.

Brown, T., Mackey, K., Du, T., 2004. Analysis of RNA by Northern and Sot blot hybridization, chap. 4.9.1, suppl. 67, in: Ausubel, F.M., Brent, R., Kingston, R.E., Moore, D.D., Seidman, J.G., Smith, J.A., Struhl, K. (Eds.), Current protocols in molecular biology. John Wiley & Sons, Inc., Hoboken, USA.

Buist, G., Karsens, H., Nauta, A., van Sinderen, D., Venema, G., Kok, J., 1997. Autolysis of *Lactococcus lactis* caused by induced overproduction of its major autolysin, AcmA. Appl. Environ. Microbiol. 63, 2722–2728.

Buist, G., Steen, A., Kok, J., Kuipers, O.P., 2008. LysM, a widely distributed protein motif for binding to (peptido)glycans. Mol. Microbiol. 68, 838–847. doi:10.1111/j.1365-2958.2008.06211.x.

Caillet, J., Gracia, C., Fontaine, F., Hajnsdorf, E., 2014. *Clostridium difficile* Hfq can replace *Escherichia coli* Hfq for most of its function. RNA 20, 1567–1578. doi:10.1261/rna.043372.113.

Campbell, R.M., Scanes, C.G., 1995. Endocrine peptides “moonlighting” as immune modulators: Roles for somatostatin and GH-releasing factor. J. Endocrinol. 147, 383–396. doi:10.1677/joe.0.1470383.

Cao, Y., Förstner, K.U., Vogel, J., Smith, C.J., 2016. Cis-encoded sRNAs, a conserved mechanism for repression of polysaccharide utilization in the *Bacteroides*. J. Bacteriol. JB.00381-16. doi:10.1128/JB.00381-16.

Chai, Y., Winans, S.C., 2005. A small antisense RNA downregulates expression of an essential replicase protein of an *Agrobacterium tumefaciens* Ti plasmid. Mol. Microbiol. 56, 1574–1585. doi:10.1111/j.1365-2958.2005.04636.x.

Chambers, J.R., Bender, K.S., 2011. The RNA chaperone Hfq is important for growth and stress tolerance in *Francisella novicida*. PloS One 6, e19797. doi:10.1371/journal.pone.0019797.

Chao, Y., Vogel, J., 2010. The role of Hfq in bacterial pathogens. Curr. Opin. Microbiol. 13, 24–33. doi:10.1016/j.mib.2010.01.001.

Chao, Y., Vogel, J., 2016. A 3' UTR-derived small RNA provides the regulatory noncoding arm of the inner membrane stress response. Mol. Cell 61, 352–363. doi:10.1016/j.molcel.2015.12.023.

Chastanet, A., Losick, R., 2011. Just-in-time control of Spo0A synthesis in *Bacillus subtilis* by multiple regulatory mechanisms. J. Bacteriol. 193, 6366–6374. doi:10.1128/JB.06057-11.

Chattoraj, D.K., Snyder, K.M., Abeles, A.L., 1985. P1 plasmid replication: Multiple functions of RepA protein at the origin. Proc. Natl. Acad. Sci. USA 82, 2588–2592.

Chen, S., Zhang, A., Blyn, L.B., Storz, G., 2004. MicC, a second small-RNA regulator of Omp protein expression in *Escherichia coli*. J. Bacteriol. 186, 6689–6697. doi:10.1128/JB.186.20.6689-6697.2004.

Chen, Y., Indurthi, D.C., Jones, S.W., Papoutsakis, E.T., 2011. Small RNAs in the genus *Clostridium*. mBio 2, e00340-10. doi:10.1128/mBio.00340-10.

Chevallet, M., Luche, S., Rabilloud, T., 2006. Silver staining of proteins in polyacrylamide gels. Nat. Protoc. 1, 1852–1858. doi:10.1038/nprot.2006.288.

Chibazakura, T., Kawamura, F., Asai, K., Takahashi, H., 1995. Effects of *spo0* mutations on *spo0A* promoter switching at the initiation of sporulation in *Bacillus subtilis*. J. Bacteriol. 177, 4520–4523.

Cho, C., Lee, S.Y., 2017. Efficient gene knockdown in *Clostridium acetobutylicum* by synthetic small regulatory RNAs. Biotechnol. Bioeng. 114, 374–383. doi:10.1002/bit.26077.

Clark, S.W., Bennett, G.N., Rudolph, F.B., 1989. Isolation and characterization of mutants of *Clostridium acetobutylicum* ATCC 824 deficient in acetoacetyl-coenzyme A:acetate/butyrate:coenzyme A-transferase (EC 2.8.3.9) and in other solvent pathway enzymes. Appl. Environ. Microbiol. 55, 970–976.

Commichau, F.M., Herzberg, C., Tripal, P., Valerius, O., Stülke, J., 2007. A regulatory protein-protein interaction governs glutamate biosynthesis in *Bacillus subtilis*: The glutamate dehydrogenase RocG moonlights in controlling the transcription factor GltC. Mol. Microbiol. 65, 642–654. doi:10.1111/j.1365-2958.2007.05816.x.

Connolly, D.M., Winkler, M.E., 1991. Structure of *Escherichia coli* K-12 *miaA* and characterization of the mutator phenotype caused by *miaA* insertion mutations. J. Bacteriol. 173, 1711–1721.

Connolly, D.M., Winkler, M.E., 1989. Genetic and physiological relationships among the *miaA* gene, 2-methylthio-N6-(delta 2-isopentenyl)-adenosine tRNA modification, and spontaneous mutagenesis in *Escherichia coli* K-12. J. Bacteriol. 171, 3233–3246.

Cooksley, C.M., Zhang, Y., Wang, H., Redl, S., Winzer, K., Minton, N.P., 2012. Targeted mutagenesis of the *Clostridium acetobutylicum* acetone–butanol–ethanol fermentation pathway. Metab. Eng. 14, 630–641. doi:10.1016/j.ymben.2012.09.001.

Cornillot, E., Nair, R.V., Papoutsakis, E.T., Soucaille, P., 1997. The genes for butanol and acetone formation in *Clostridium acetobutylicum* ATCC 824 reside on a large plasmid whose loss leads to degeneration of the strain. J. Bacteriol. 179, 5442–5447.

Dai, Z., Dong, H., Zhang, Y., Li, Y., 2016. Elucidating the contributions of multiple aldehyde/alcohol dehydrogenases to butanol and ethanol production in *Clostridium acetobutylicum*. Sci. Rep. 6, 28189. doi:10.1038/srep28189.

Dambach, M., Irnov, I., Winkler, W.C., 2013. Association of RNAs with *Bacillus subtilis* Hfq. PLoS One 8, e55156. doi:10.1371/journal.pone.0055156.

De Lay, N., Schu, D.J., Gottesman, S., 2013. Bacterial small RNA-based negative regulation: Hfq and its accomplices. J. Biol. Chem. 288, 7996–8003. doi:10.1074/jbc.R112.441386.

del Solar, G., Espinosa, M., 1992. The copy number of plasmid pLS1 is regulated by two trans-acting plasmid products: The antisense RNA II and the repressor protein, RepA. Mol. Microbiol. 6, 83–94.

del Solar, G., Giraldo, R., Ruiz-Echevarría, M.J., Espinosa, M., Díaz-Orejas, R., 1998. Replication and control of circular bacterial plasmids. Microbiol. Mol. Biol. Rev. 62, 434–464.

De Lay, N., Gottesman, S., 2012. RNase E finds some sRNAs stimulating. Mol. Cell 47, 825–826. doi:10.1016/j.molcel.2012.09.007.

Delihas, N., 1995. Regulation of gene expression by trans-encoded antisense RNAs. Mol. Microbiol. 15, 411–414. doi:10.1111/j.1365-2958.1995.tb02254.x.

Desnoyers, G., Bouchard, M.-P., Massé, E., 2013. New insights into small RNA-dependent translational regulation in prokaryotes. Trends Genet. 29, 92–98. doi:10.1016/j.tig.2012.10.004.

Diestra, E., Cayrol, B., Arluison, V., Risco, C., 2009. Cellular electron microscopy imaging reveals the localization of the Hfq protein close to the bacterial membrane. PLoS One 4, e8301. doi:10.1371/journal.pone.0008301.

Dimastrogiovanni, D., Fröhlich, K.S., Bandyra, K.J., Bruce, H.A., Hohensee, S., Vogel, J., Luisi, B.F., 2014. Recognition of the small regulatory RNA RydC by the bacterial Hfq protein. eLife 3. doi:10.7554/eLife.05375.

Dower, W.J., Miller, J.F., Ragsdale, C.W., 1988. High efficiency transformation of *E. coli* by high voltage electroporation. Nucleic Acids Res. 16, 6127–6145.

Durand, S., Tomasini, A., Braun, F., Condon, C., Romby, P., 2015. sRNA and mRNA turnover in Gram-positive bacteria. FEMS Microbiol. Rev. 39, 316–330. doi:10.1093/femsre/fuv007.

Dürre, P., 2008. Fermentative butanol production: Bulk chemical and biofuel. Ann. N. Y. Acad. Sci. 1125, 353–362. doi:10.1196/annals.1419.009.

Dürre, P., 2007a. Clostridia. Encyclopedia of Life Sciences. doi:10.1002/9780470015902.a0020370.

Dürre, P., 2007b. Biobutanol: An attractive biofuel. Biotechnol. J. 2, 1525–1534. doi:10.1002/biot.200700168.

Dürre, P., 2005. Formation of solvents in clostridia, chapt. 30, p. 671-685, in: Dürre, P. (Eds.), Handbook on Clostridia. CRC Press-Taylor and Francis Group, Boca Raton, USA.

Dürre, P., Böhringer, M., Nakotte, S., Schaffer, S., Thormann, K., Zickner, B., 2002. Transcriptional regulation of solventogenesis in *Clostridium acetobutylicum*. J. Mol. Microbiol. Biotechnol. 4, 295–300.

Eguchi, Y., Itoh, T., Tomizawa, J., 1991. Antisense RNA. Annu. Rev. Biochem. 60, 631–652. doi:10.1146/annurev.bi.60.070191.003215.

Elfasakhany, A., Mahrous, A.F., 2016. Performance and emissions assessment of n-butanol-methanol-gasoline blends as a fuel in spark-ignition engines. Alex. Eng. J. 55, 3015–3024. doi:10.1016/j.aej.2016.05.016.

Ellis, M.J., Trussler, R.S., Haniford, D.B., 2015. A cis-encoded sRNA, Hfq and mRNA secondary structure act independently to suppress IS *200* transposition. Nucleic Acids Res. 43, 6511–6527. doi:10.1093/nar/gkv584.

England, T.E., Bruce, A.G., Uhlenbeck, O.C., 1980. Specific labeling of 3' termini of RNA with T4 RNA ligase. Methods Enzymol. 65, 65–74.

Feustel, L., Nakotte, S., Dürre, P., 2004. Characterization and development of two reporter gene systems for *Clostridium acetobutylicum*. Appl. Environ. Microbiol. 70, 798–803. doi:10.1128/AEM.70.2.798-803.2004.

Fierro-Monti, I.P., Reid, S.J., Woods, D.R., 1992. Differential expression of a *Clostridium acetobutylicum* antisense RNA: Implications for regulation of glutamine synthetase. J. Bacteriol. 174, 7642–7647.

Finne, G., Matches, J.R., 1974. Low-temperature-growing clostridia from marine sediments. Can. J. Microbiol. 20, 1639–1645. doi:10.1139/m74-255.

Fischer, R.J., Helms, J., Dürre, P., 1993. Cloning, sequencing, and molecular analysis of the *sol* operon of *Clostridium acetobutylicum*, a chromosomal locus involved in solventogenesis. J. Bacteriol. 175, 6959–6969.

Flitsch, S., 2015. Identifikation und Charakterisierung von Regulatoren der Lösungsmittelbildung in *Clostridium acetobutylicum*. Ph.D. thesis. Ulm University, Germany.

Fontaine, L., Meynial-Salles, I., Girbal, L., Yang, X., Croux, C., Soucaille, P., 2002. Molecular characterization and transcriptional analysis of *adhE2*, the gene encoding the NADH-dependent aldehyde/alcohol dehydrogenase responsible for butanol production in alcohologenic cultures of *Clostridium acetobutylicum* ATCC 824. J. Bacteriol. 184, 821–830.

Fortas, E., Piccirilli, F., Malabirade, A., Militello, V., Trépout, S., Marco, S., Taghbalout, A., Arluison, V., 2015. New insight into the structure and function of Hfq C-terminus. Biosci. Rep. 35, 1–9. doi:10.1042/BSR20140128.

Franze de Fernandez, M.T., Eoyang, L., August, J.T., 1968. Factor fraction required for the synthesis of bacteriophage Qβ-RNA. Nature 219, 588–590. doi:10.1038/219588a0.

Fröhlich, K.S., Haneke, K., Papenfort, K., Vogel, J., 2016. The target spectrum of SdsR small RNA in *Salmonella*. Nucleic Acids Res. 44. doi:10.1093/nar/gkw632.

Fröhlich, K.S., Vogel, J., 2009. Activation of gene expression by small RNA. Curr. Opin. Microbiol. 12, 674–682. doi:10.1016/j.mib.2009.09.009.

Fukui, K., 2010. DNA mismatch repair in eukaryotes and bacteria. J. Nucleic Acids 2010, 1–16. doi:10.4061/2010/260512.

Gabriel, C.L., 1928. Butanol fermentation process. Ind. Eng. Chem. 20, 1063–1067. doi:10.1021/ie50226a020.

Gao, M., Barnett, M.J., Long, S.R., Teplitski, M., 2010. Role of the *Sinorhizobium meliloti* global regulator Hfq in gene regulation and symbiosis. Mol. Plant. Microbe Interact. 23, 355–365. doi:10.1094/MPMI-23-4-0355.

Geisinger, E., Adhikari, R.P., Jin, R., Ross, H.F., Novick, R.P., 2006. Inhibition of *rot* translation by RNAIII, a key feature of *agr* function. Mol. Microbiol. 61, 1038–1048. doi:10.1111/j.1365-2958.2006.05292.x.

Gerischer, U., Dürre, P., 1990. Cloning, sequencing, and molecular analysis of the acetoacetate decarboxylase gene region from *Clostridium acetobutylicum*. J. Bacteriol. 172, 6907–6918.

Gherna, R.L., 2010. Culture Preservation, p. 153–162, in: Flickinger, M.C. (Eds.), Encyclopedia of industrial biotechnology, 2nd ed. John Wiley & Sons, Hoboken, USA.

Girbal, L., Soucaille, P., 1998. Regulation of solvent production in *Clostridium acetobutylicum.* Trends Biotechnol. 16, 11–16. doi:10.1016/S0167-7799(97)01141-4.

Gottesman, S., 2005. Micros for microbes: non-coding regulatory RNAs in bacteria. Trends Genet. 21, 399–404. doi:10.1016/j.tig.2005.05.008.

Gottesman, S., 2004. The small RNA regulators of *Escherichia coli*: roles and mechanisms. Annu. Rev. Microbiol. 58, 303–328. doi:10.1146/annurev.micro.58.030603.123841.

Gottesman, S., Storz, G., 2011. Bacterial small RNA regulators: versatile roles and rapidly evolving variations. Cold Spring Harb. Perspect. Biol. 3, a003798. doi:10.1101/cshperspect.a003798.

Gottwald, M., Gottschalk, G., 1985. The internal pH of *Clostridium acetobutylicum* and its effect on the shift from acid to solvent formation. Arch. Microbiol. 143, 42–46. doi:10.1007/BF00414766.

Green, M.R., Sambrook, J., 2012. Molecular cloning: A laboratory manual, 4th ed. Cold Spring Harbor Laboratory Press, Cold Spring Harbor, USA.

Grimmler, C., Janssen, H., Krauße, D., Fischer, R.-J., Bahl, H., Dürre, P., Liebl, W., Ehrenreich, A., 2011. Genome-wide gene expression analysis of the switch between acidogenesis and solventogenesis in continuous cultures of *Clostridium acetobutylicum*. J. Mol. Microbiol. Biotechnol. 20, 1–15. doi:10.1159/000320973.

Grupe, H., Gottschalk, G., 1992. Physiological events in *Clostridium acetobutylicum* during the shift from acidogenesis to solventogenesis in continuous culture and presentation of a model for shift induction. Appl. Environ. Microbiol. 58, 3896–3902.

Guillier, M., Gottesman, S., Storz, G., 2006. Modulating the outer membrane with small RNAs. Genes Dev. 20, 2338–2348. doi:10.1101/gad.1457506.

Guisbert, E., Rhodius, V.A., Ahuja, N., Witkin, E., Gross, C.A., 2007. Hfq modulates the σE-mediated envelope stress response and the σ^{32}-mediated cytoplasmic stress response in *Escherichia coli*. J. Bacteriol. 189, 1963–1973. doi:10.1128/JB.01243-06.

Hammer, B.K., Bassler, B.L., 2007. Regulatory small RNAs circumvent the conventional quorum sensing pathway in pandemic *Vibrio cholerae.* Proc. Natl. Acad. Sci. USA 104, 11145–11149. doi:10.1073/pnas.0703860104.

Hanahan, D., 1983. Studies on transformation of *Escherichia coli* with plasmids. J. Mol. Biol. 166, 557–580.

Harris, L.M., Welker, N.E., Papoutsakis, E.T., 2002. Northern, morphological, and fermentation analysis of *spo0A* inactivation and overexpression in *Clostridium acetobutylicum* ATCC 824. J. Bacteriol. 184, 3586–3597. doi:10.1128/JB.184.13.3586-3597.2002.

Heap, J.T., Kuehne, S.A., Ehsaan, M., Cartman, S.T., Cooksley, C.M., Scott, J.C., Minton, N.P., 2010. The ClosTron: mutagenesis in *Clostridium* refined and streamlined. J. Microbiol. Methods 80, 49–55. doi:10.1016/j.mimet.2009.10.018.

Heap, J.T., Ehsaan, M., Cooksley, C.M., Ng, Y.-K., Cartman, S.T., Winzer, K., Minton, N.P., 2012. Integration of DNA into bacterial chromosomes from plasmids without a counter-selection marker. Nucleic Acids Res. 40, e59–e59. doi:10.1093/nar/gkr1321.

Heap, J.T., Pennington, O.J., Cartman, S.T., Carter, G.P., Minton, N.P., 2007. The ClosTron: a universal gene knock-out system for the genus *Clostridium*. J. Microbiol. Methods 70, 452–464. doi:10.1016/j.mimet.2007.05.021.

Heap, J.T., Theys, J., Ehsaan, M., Kubiak, A.M., Dubois, L., Paesmans, K., Mellaert, L.V., Knox, R., Kuehne, S.A., Lambin, P., Minton, N.P., 2014. Spores of *Clostridium* engineered for clinical efficacy and safety cause regression and cure of tumors in vivo. Oncotarget 5, 1761–1769. doi:10.18632/oncotarget.1761.

Heidrich, N., Chinali, A., Gerth, U., Brantl, S., 2006. The small untranslated RNA SR1 from the *Bacillus subtilis* genome is involved in the regulation of arginine catabolism: small RNA SR1 from *B. subtilis* involved in arginine catabolism. Mol. Microbiol. 62, 520–536. doi:10.1111/j.1365-2958.2006.05384.x.

Heidrich, N., Moll, I., Brantl, S., 2007. In vitro analysis of the interaction between the small RNA SR1 and its primary target *ahrC* mRNA. Nucleic Acids Res. 35, 4331–4346. doi:10.1093/nar/gkm439.

Heilmann, C., Hartleib, J., Hussain, M.S., Peters, G., 2005. The multifunctional *Staphylococcus aureus* autolysin aaa mediates adherence to immobilized fibrinogen and fibronectin. Infect. Immun. 73, 4793–4802. doi:10.1128/IAI.73.8.4793-4802.2005.

Henderson, C.A., Vincent, H.A., Stone, C.M., Phillips, J.O., Cary, P.D., Gowers, D.M., Callaghan, A.J., 2013. Characterization of MicA interactions suggests a potential novel means of gene regulation by small non-coding RNAs. Nucleic Acids Res. 41, 3386–3397. doi:10.1093/nar/gkt008.

Higuchi, R., Fockler, C., Dollinger, G., Watson, R., 1993. Kinetic PCR analysis: real-time monitoring of DNA amplification reactions. Biotechnology 11, 1026–1030.

Huntzinger, E., Boisset, S., Saveanu, C., Benito, Y., Geissmann, T., Namane, A., Lina, G., Etienne, J., Ehresmann, B., Ehresmann, C., Jacquier, A., Vandenesch, F., Romby, P., 2005. *Staphylococcus aureus* RNAIII and the endoribonuclease III coordinately regulate *spa* gene expression. EMBO J. 24, 824–835. doi:10.1038/sj.emboj.7600572.

Ikeda, Y., Yagi, M., Morita, T., Aiba, H., 2011. Hfq binding at RhlB-recognition region of RNase E is crucial for the rapid degradation of target mRNAs mediated by sRNAs in *Escherichia coli.* Mol. Microbiol. 79, 419–432. doi:10.1111/j.1365-2958.2010.07454.x.

Inoue, H., Nojima, H., Okayama, H., 1990. High efficiency transformation of *Escherichia coli* with plasmids. Gene 96, 23–28.

International Energy Agency (IEA), 2016. CO_2 emissions from fuel combustions 2016. IEA Publications, Paris, France.

Jeffery, C.J., 1999. Moonlighting proteins. Trends Biochem. Sci. 24, 8–11.

Jones, A., 2015. An investigation of the roles of small RNA on solvent tolerance and production in *Clostridium acetobutylicum*. Master thesis. University of Delaware, USA.

Jones, D.T., van der Westhuizen, A., Long, S., Allcock, E.R., Reid, S.J., Woods, D.R., 1982. Solvent production and morphological changes in *Clostridium acetobutylicum*. Appl. Environ. Microbiol. 43, 1434–1439.

Jones, D.T., Woods, D.R., 1986. Acetone-butanol fermentation revisited. Microbiol. Rev. 50, 484–524.

Jones, S.W., Paredes, C.J., Tracy, B., Cheng, N., Sillers, R., Senger, R.S., Papoutsakis, E.T., 2008. The transcriptional program underlying the physiology of clostridial sporulation. Genome Biol. 9, R114. doi:10.1186/gb-2008-9-7-r114.

Jones, S.W., Tracy, B.P., Gaida, S.M., Papoutsakis, E.T., 2011. Inactivation of σ^F in *Clostridium acetobutylicum* ATCC 824 blocks sporulation prior to asymmetric division and abolishes σ^E and σ^G protein expression but does not block solvent formation. J. Bacteriol. 193, 2429–2440. doi:10.1128/JB.00088-11.

Joris, B., Englebert, S., Chu, C.P., Kariyama, R., Daneo-Moore, L., Shockman, G.D., Ghuysen, J.M., 1992. Modular design of the *Enterococcus hirae* muramidase-2 and *Streptococcus faecalis* autolysin. FEMS Microbiol. Lett. 70, 257–264.

Jost, D., Nowojewski, A., Levine, E., 2011. Small RNA biology is systems biology. BMB Rep. 44, 11–21. doi:10.5483/BMBRep.2011.44.1.11.

Jousselin, A., Metzinger, L., Felden, B., 2009. On the facultative requirement of the bacterial RNA chaperone, Hfq. Trends Microbiol. 17, 399–405. doi:10.1016/j.tim.2009.06.003.

Kawano, M., Aravind, L., Storz, G., 2007. An antisense RNA controls synthesis of an SOS-induced toxin evolved from an antitoxin. Mol. Microbiol. 64, 738–754. doi:10.1111/j.1365-2958.2007.05688.x.

Kazantsev, A.V., Pace, N.R., 2006. Bacterial RNase P: A new view of an ancient enzyme. Nat. Rev. Microbiol. 4, 729–740. doi:10.1038/nrmicro1491.

Keis, S., Bennett, C.F., Ward, V.K., Jones, D.T., 1995. Taxonomy and phylogeny of industrial solvent-producing clostridia. Int. J. Syst. Bacteriol. 45, 693–705. doi:10.1099/00207713-45-4-693.

Keis, S., Shaheen, R., Jones, D.T., 2001. Emended descriptions of *Clostridium acetobutylicum* and *Clostridium beijerinckii*, and descriptions of *Clostridium saccharoperbutylacetonicum* sp. nov. and *Clostridium saccharobutylicum* sp. nov. Int. J. Syst. Evol. Microbiol. 51, 2095–2103. doi:10.1099/00207713-51-6-2095.

Kery, M.B., Feldman, M., Livny, J., Tjaden, B., 2014. TargetRNA2: Identifying targets of small regulatory RNAs in bacteria. Nucleic Acids Res. 42, W124–W129. doi:10.1093/nar/gku317.

Khusial, P., Plaag, R., Zieve, G.W., 2005. Lsm proteins form heptameric rings that bind to RNA via repeating motifs. Trends Biochem. Sci. 30, 522–528. doi:10.1016/j.tibs.2005.07.006.

Killeffer, D.H., 1927. Butanol and acetone from corn: a description of the fermentation process. Ind. Eng. Chem. 19, 46–50. doi:10.1021/ie50205a013.

Köpke, M., Held, C., Hujer, S., Liesegang, H., Wiezer, A., Wollherr, A., Ehrenreich, A., Liebl, W., Gottschalk, G., Dürre, P., 2010. *Clostridium ljungdahlii* represents a microbial production platform based on syngas. Proc. Natl. Acad. Sci. USA 107, 13087–13092. doi:10.1073/pnas.1004716107.

Köpke, M., Mihalcea, C., Liew, F., Tizard, J.H., Ali, M.S., Conolly, J.J., Al-Sinawi, B., Simpson, S.D., 2011. 2,3-butanediol production by acetogenic bacteria, an alternative route to chemical synthesis, using industrial waste gas. Appl. Environ. Microbiol. 77, 5467–5475. doi:10.1128/AEM.00355-11.

Kovach, A.R., Hoff, K.E., Canty, J.T., Orans, J., Brennan, R.G., 2014. Recognition of U-rich RNA by Hfq from the Gram-positive pathogen *Listeria monocytogenes*. RNA 20, 1548–1559. doi:10.1261/rna.044032.113.

Kumar, M., Gayen, K., 2011. Developments in biobutanol production: new insights. Appl. Energy 88, 1999–2012. doi:10.1016/j.apenergy.2010.12.055.

Kunitz, M., 1950. Crystalline desoxyribonuclease: isolation and general properties spectrophotometric method for the measurement of desoxyribonuclease activity. J. Gen. Physiol. 33, 349–362.

Laemmli, U.K., 1970. Cleavage of structural proteins during the assembly of the head of bacteriophage T4. Nature 227, 680–685.

Lahiry, A., Stimple, S.D., Wood, D.W., Lease, R.A., 2017. Retargeting a dual-acting sRNA for multiple mRNA transcript regulation. ACS Synth. Biol. doi:10.1021/acssynbio.6b00261.

Langmead, B., Salzberg, S.L., 2012. Fast gapped-read alignment with Bowtie 2. Nat. Methods 9, 357–359. doi:10.1038/nmeth.1923.

Lawson, P.A., Citron, D.M., Tyrrell, K.L., Finegold, S.M., 2016. Reclassification of *Clostridium difficile* as *Clostridioides difficile* (Hall and O'Toole 1935) Prévot 1938. Anaerobe 40, 95–99. doi:10.1016/j.anaerobe.2016.06.008.

Le Chatelier, E., Ehrlich, S.D., Jannière, L., 1996. Countertranscript-driven attenuation system of the pAMβ1 *repE* gene. Mol. Microbiol. 20, 1099–1112.

Leang, C., Ueki, T., Nevin, K.P., Lovley, D.R., 2013. A genetic system for *Clostridium ljungdahlii*: a chassis for autotrophic production of biocommodities and a model homoacetogen. Appl. Environ. Microbiol. 79, 1102–1109. doi:10.1128/AEM.02891-12.

Lee, H.-J., Gottesman, S., 2016. sRNA roles in regulating transcriptional regulators: Lrp and SoxS regulation by sRNAs. Nucleic Acids Res. 44, 6907–6923. doi:10.1093/nar/gkw358.

Lee, S.Y., Mermelstein, L.D., Papoutsakis, E.T., 1993. Determination of plasmid copy number and stability in *Clostridium acetobutylicum* ATCC 824. FEMS Microbiol. Lett. 108, 319–323.

Lee, S.Y., Park, J.H., Jang, S.H., Nielsen, L.K., Kim, J., Jung, K.S., 2008. Fermentative butanol production by clostridia. Biotechnol. Bioeng. 101, 209–228. doi:10.1002/bit.22003.

Lee, T., Feig, A.L., 2008. The RNA binding protein Hfq interacts specifically with tRNAs. RNA 14, 514–523. doi:10.1261/rna.531408.

Lenz, D.H., Mok, K.C., Lilley, B.N., Kulkarni, R.V., Wingreen, N.S., Bassler, B.L., 2004. The small RNA chaperone Hfq and multiple small RNAs control quorum sensing in *Vibrio harveyi* and *Vibrio cholerae*. Cell 118, 69–82. doi:10.1016/j.cell.2004.06.009.

Levine, E., Hwa, T., 2008. Small RNAs establish gene expression thresholds. Curr. Opin. Microbiol. 11, 574–579. doi:10.1016/j.mib.2008.09.016.

Levine, E., Zhang, Z., Kuhlman, T., Hwa, T., 2007. Quantitative characteristics of gene regulation by small RNA. PLoS Biol. 5, e229. doi:10.1371/journal.pbio.0050229.

Li, S.K., Ng, P.K., Qin, H., Lau, J.K., Lau, J.P., Tsui, S.K., Chan, T.F., Lau, T.C., 2013. Identification of small RNAs in *Mycobacterium smegmatis* using heterologous Hfq. RNA 19, 74–84. doi:10.1261/rna.034116.112.

Liew, F., Henstra, A.M., Köpke, M., Winzer, K., Simpson, S.D., Minton, N.P., 2017. Metabolic engineering of *Clostridium autoethanogenum* for selective alcohol production. Metab. Eng. doi:10.1016/j.ymben.2017.01.007.

Lingner, J., Keller, W., 1993. 3'-end labeling of RNA with recombinant yeast poly(A) polymerase. Nucleic Acids Res. 21, 2917–2920.

Link, T.M., Valentin-Hansen, P., Brennan, R.G., 2009. Structure of *Escherichia coli* Hfq bound to polyriboadenylate RNA. Proc. Natl. Acad. Sci. USA 106, 19292–19297. doi:10.1073/pnas.0908744106.

Liu, J.M., Camilli, A., 2010. A broadening world of bacterial small RNAs. Curr. Opin. Microbiol. 13, 18–23. doi:10.1016/j.mib.2009.11.004.

Liu, Y., Wu, N., Dong, J., Gao, Y., Zhang, X., Mu, C., Shao, N., Yang, G., 2010. Hfq is a global regulator that controls the pathogenicity of *Staphylococcus aureus*. PLoS One 5, e13069. doi:10.1371/journal.pone.0013069.

Liu, Z., Qiao, K., Tian, L., Zhang, Q., Liu, Z., Li, F., 2015. Spontaneous large-scale autolysis in *Clostridium acetobutylicum* contributes to generation of more spores. Front. Microbiol. 6, 950. doi:10.3389/fmicb.2015.00950.

Ljungdahl, L.G., 1986. The autotrophic pathway of acetate synthesis in acetogenic bacteria. Annu. Rev. Microbiol. 40, 415–450. doi:10.1146/annurev.mi.40.100186.002215.

López-Gomollón, S., 2011. Detecting sRNAs by Northern blotting. Methods Mol. Biol. 732, 25–38. doi:10.1007/978-1-61779-083-6_3.

Lu, P., Zhang, Y., Hu, Y., Francis, M.S., Chen, S., 2014. A cis-encoded sRNA controls the expression of *fabH2* in *Yersinia*. FEBS Lett. 588, 1961–1966. doi:10.1016/j.febslet.2014.04.005.

Lütke-Eversloh, T., Bahl, H., 2011. Metabolic engineering of *Clostridium acetobutylicum*: recent advances to improve butanol production. Curr. Opin. Biotechnol. 22, 634–647. doi:10.1016/j.copbio.2011.01.011.

Majdalani, N., Cunning, C., Sledjeski, D., Elliott, T., Gottesman, S., 1998. DsrA RNA regulates translation of RpoS message by an anti-antisense mechanism, independent of its action as an antisilencer of transcription. Proc. Natl. Acad. Sci. USA 95, 12462–12467.

Mani, M., Chen, C., Amblee, V., Liu, H., Mathur, T., Zwicke, G., Zabad, S., Patel, B., Thakkar, J., Jeffery, C.J., 2015. MoonProt: A database for proteins that are known to moonlight. Nucleic Acids Res. 43, D277–D282. doi:10.1093/nar/gku954.

Massé, E., Escorcia, F.E., Gottesman, S., 2003. Coupled degradation of a small regulatory RNA and its mRNA targets in *Escherichia coli*. Genes Dev. 17, 2374–2383. doi:10.1101/gad.1127103.

Massé, E., Vanderpool, C.K., Gottesman, S., 2005. Effect of RyhB small RNA on global iron use in *Escherichia coli*. J. Bacteriol. 187, 6962–6971. doi:10.1128/JB.187.20.6962-6971.2005.

Matches, J.R., Liston, J., 1974. Mesophilic clostridia in Puget Sound. Can. J. Microbiol. 20, 1–7. doi:10.1139/m74-001.

McDowall, K.J., Lin-Chao, S., Cohen, S.N., 1994. A+U content rather than a particular nucleotide order determines the specificity of RNase E cleavage. J. Biol. Chem. 269, 10790–10796.

McNair, H.M., Miller, J.M., 2009. Basic gas chromatography, 2nd ed. John Wiley & Sons, Hoboken, USA.

Mégroz, M., Kleifeld, O., Wright, A., Powell, D., Harrison, P., Adler, B., Harper, M., Boyce, J.D., 2016. The RNA-binding chaperone Hfq is an important global regulator of gene expression in *Pasteurella multocida* and plays a crucial role in production of a number of virulence factors, including hyaluronic acid capsule. Infect. Immun. 84, 1361–1370. doi:10.1128/IAI.00122-16.

Mermelstein, L.D., Papoutsakis, E.T., 1993. In vivo methylation in *Escherichia coli* by the *Bacillus subtilis* phage Φ3T I methyltransferase to protect plasmids from restriction upon transformation of *Clostridium acetobutylicum* ATCC 824. Appl. Environ. Microbiol. 59, 1077–1081.

Mermelstein, L.D., Welker, N.E., Bennett, G.N., Papoutsakis, E.T., 1992. Expression of cloned homologous fermentative genes in *Clostridium acetobutylicum* ATCC 824. Biotechnol. Nat. Publ. Co. 10, 190–195.

Mesnage, S., Dellarole, M., Baxter, N.J., Rouget, J.-B., Dimitrov, J.D., Wang, N., Fujimoto, Y., Hounslow, A.M., Lacroix-Desmazes, S., Fukase, K., Foster, S.J., Williamson, M.P., 2014. Molecular basis for bacterial peptidoglycan recognition by LysM domains. Nat. Commun. 5. doi:10.1038/ncomms5269.

Messing, J., Gronenborn, B., Müller-Hill, B., Hopschneider, P.H., 1977. Filamentous coliphage M13 as a cloning vehicle: insertion of a *Hin*dII fragment of the *lac* regulatory region in M13 replicative form in vitro. Proc. Natl. Acad. Sci. USA 74, 3642–3646.

Mikulecky, P.J., Kaw, M.K., Brescia, C.C., Takach, J.C., Sledjeski, D.D., Feig, A.L., 2004. *Escherichia coli* Hfq has distinct interaction surfaces for DsrA, *rpoS* and poly(A) RNAs. Nat. Struct. Mol. Biol. 11, 1206–1214. doi:10.1038/nsmb858.

Milner, H.W., Lawrence, N.S., French, C.S., 1950. Colloidal dispersion of chloroplast material. Science 111, 633–634.

Minton, N.P., 2003. Clostridia in cancer therapy. Nat. Rev. Microbiol. 1, 237–242. doi:10.1038/nrmicro777.

Moll, I., Afonyushkin, T., Vytvytska, O., Kaberdin, V.R., Bläsi, U., 2003. Coincident Hfq binding and RNase E cleavage sites on mRNA and small regulatory RNAs. RNA 9, 1308–1314.

Møller, T., Franch, T., Højrup, P., Keene, D.R., Bächinger, H.P., Brennan, R.G., Valentin-Hansen, P., 2002. Hfq: a bacterial Sm-like protein that mediates RNA-RNA interaction. Mol. Cell 9, 23–30.

Molongoski, J.J., Klug, M.J., 1976. Characterization of anaerobic heterotrophic bacteria isolated from freshwater lake sediments. Appl. Environ. Microbiol. 31, 83–90.

Monot, F., Martin, J.R., Petitdemange, H., Gay, R., 1982. Acetone and butanol production by *Clostridium acetobutylicum* in a synthetic medium. Appl. Environ. Microbiol. 44, 1318–1324.

Morita, T., El-Kazzaz, W., Tanaka, Y., Inada, T., Aiba, H., 2003. Accumulation of glucose 6-phosphate or fructose 6-phosphate is responsible for destabilization of glucose transporter mRNA in *Escherichia coli*. J. Biol. Chem. 278, 15608–15614. doi:10.1074/jbc.M300177200.

Morita, T., Kawamoto, H., Mizota, T., Inada, T., Aiba, H., 2004. Enolase in the RNA degradosome plays a crucial role in the rapid decay of glucose transporter mRNA in the response to phosphosugar stress in *Escherichia coli*. Mol. Microbiol. 54, 1063–1075. doi:10.1111/j.1365-2958.2004.04329.x.

Morita, T., Maki, K., Aiba, H., 2005. RNase E-based ribonucleoprotein complexes: Mechanical basis of mRNA destabilization mediated by bacterial noncoding RNAs. Genes Dev. 19, 2176–2186. doi:10.1101/gad.1330405.

Mortazavi, A., Williams, B.A., McCue, K., Schaeffer, L., Wold, B., 2008. Mapping and quantifying mammalian transcriptomes by RNA-Seq. Nat. Methods 5, 621–628. doi:10.1038/nmeth.1226.

Mullis, K., Faloona, F., Scharf, S., Saiki, R., Horn, G., Erlich, H., 1986. Specific enzymatic amplification of DNA in vitro: the polymerase chain reaction. Cold Spring Harb. Symp. Quant. Biol. 51, 263–273.

Muto, A., Ushida, C., Himeno, H., 1998. A bacterial RNA that functions as both a tRNA and an mRNA. Trends Biochem. Sci. 23, 25–29.

Na, D., Yoo, S.M., Chung, H., Park, H., Park, J.H., Lee, S.Y., 2013. Metabolic engineering of *Escherichia coli* using synthetic small regulatory RNAs. Nat. Biotechnol. 31, 170–174. doi:10.1038/nbt.2461.

Ndaba, B., Chiyanzu, I., Marx, S., 2015. n-Butanol derived from biochemical and chemical routes: a review. Biotechnol. Rep. 8, 1–9. doi:10.1016/j.btre.2015.08.001.

Nguyen, N.P., Linder, S., Flitsch, S.K., Schiel-Bengelsdorf, B., Dürre, P., Soucaille, P., 2016. Cap0037, a novel global regulator of *Clostridium acetobutylicum* metabolism. mBio 7, e01218-16. doi:10.1128/mBio.01218-16.

Nielsen, J.S., Lei, L.K., Ebersbach, T., Olsen, A.S., Klitgaard, J.K., Valentin-Hansen, P., Kallipolitis, B.H., 2010. Defining a role for Hfq in Gram-positive bacteria: evidence for Hfq-dependent antisense regulation in *Listeria monocytogenes*. Nucleic Acids Res. 38, 907–919. doi:10.1093/nar/gkp1081.

Nölling, J., Breton, G., Omelchenko, M.V., Makarova, K.S., Zeng, Q., Gibson, R., Lee, H.M., Dubois, J., Qiu, D., Hitti, J., GTC Sequencing Center Production, Finishing, and Bioinformatics Teams, Wolf, Y.I., Tatusov, R.L., Sabathe, F., Doucette-Stamm, L., Soucaille, P., Daly, M.J., Bennett, G.N., Koonin, E.V., Smith, D.R., 2001. Genome sequence and comparative analysis of the solvent-producing bacterium *Clostridium acetobutylicum*. J. Bacteriol. 183, 4823–4838. doi:10.1128/JB.183.16.4823-4838.2001.

Noyer-Weidner, M., Jentsch, S., Kupsch, J., Bergbauer, M., Trautner, T.A., 1985. DNA methyltransferase genes of *Bacillus subtilis* phages: structural relatedness and gene expression. Gene 35, 143–150.

Noyer-Weidner, M., Jentsch, S., Pawlek, B., Günthert, U., Trautner, T.A., 1983. Restriction and modification in *Bacillus subtilis*: DNA methylation potential of the related bacteriophages Z, SPR, SP beta, Φ3T, and rho 11. J. Virol. 46, 446–453.

Nuyts, S., Van Mellaert, L., Barbé, S., Lammertyn, E., Theys, J., Landuyt, W., Bosmans, E., Lambin, P., Anné, J., 2001. Insertion or deletion of the Cheo box modifies radiation inducibility of *Clostridium* promoters. Appl. Environ. Microbiol. 67, 4464–4470.

Oliva, G., Sahr, T., Rolando, M., Knoth, M., Buchrieser, C., 2017. A unique cis-encoded small noncoding RNA is regulating *Legionella pneumophila* Hfq expression in a life cycle-dependent manner. mBio 8, e02182-16. doi:10.1128/mBio.02182-16.

Olsen, A.S., Møller-Jensen, J., Brennan, R.G., Valentin-Hansen, P., 2010. C-terminally truncated derivatives of *Escherichia coli* Hfq are proficient in riboregulation. J. Mol. Biol. 404, 173–182. doi:10.1016/j.jmb.2010.09.038.

Opdyke, J.A., Kang, J.-G., Storz, G., 2004. GadY, a small-RNA regulator of acid response genes in *Escherichia coli.* J. Bacteriol. 186, 6698–6705. doi:10.1128/JB.186.20.6698-6705.2004.

Overgaard, M., Johansen, J., Møller-Jensen, J., Valentin-Hansen, P., 2009. Switching off small RNA regulation with trap-mRNA. Mol. Microbiol. 73, 790–800. doi:10.1111/j.1365-2958.2009.06807.x.

Panda, G., Tanwer, P., Ansari, S., Khare, D., Bhatnagar, R., 2015. Regulation and RNA-binding properties of Hfq-like RNA chaperones in *Bacillus anthracis*. Biochim. Biophys. Acta 1850, 1661–1668. doi:10.1016/j.bbagen.2015.03.016

Papenfort, K., Said, N., Welsink, T., Lucchini, S., Hinton, J.C.D., Vogel, J., 2009. Specific and pleiotropic patterns of mRNA regulation by ArcZ, a conserved, Hfq-dependent small RNA. Mol. Microbiol. 74, 139–158. doi:10.1111/j.1365-2958.2009.06857.x.

Papenfort, K., Vanderpool, C.K., 2015. Target activation by regulatory RNAs in bacteria. FEMS Microbiol. Rev. 39, 362–378. doi:10.1093/femsre/fuv016.

Paredes, C.J., Alsaker, K.V., Papoutsakis, E.T., 2005. A comparative genomic view of clostridial sporulation and physiology. Nat. Rev. Microbiol. 3, 969–978. doi:10.1038/nrmicro1288.

Persson, C., Wagner, E.G., Nordström, K., 1990. Control of replication of plasmid R1: Formation of an initial transient complex is rate-limiting for antisense RNA-target RNA pairing. EMBO J. 9, 3777–3785.

Perutka, J., Wang, W., Goerlitz, D., Lambowitz, A.M., 2004. Use of computer-designed group II introns to disrupt *Escherichia coli* DExH/D-box protein and DNA helicase genes. J. Mol. Biol. 336, 421–439.

Petersen, D.J., Cary, J.W., Vanderleyden, J., Bennett, G.N., 1993. Sequence and arrangement of genes encoding enzymes of the acetone-production pathway of *Clostridium acetobutylicum* ATCC 824. Gene 123, 93–97. doi:10.1016/0378-1119(93)90545-E.

Petersen, D.J., Welch, R.W., Rudolph, F.B., Bennett, G.N., 1991. Molecular cloning of an alcohol (butanol) dehydrogenase gene cluster from *Clostridium acetobutylicum* ATCC 824. J. Bacteriol. 173, 1831–1834.

Postic, G., Frapy, E., Dupuis, M., Dubail, I., Livny, J., Charbit, A., Meibom, K.L., 2010. Identification of small RNAs in *Francisella tularensis*. BMC Genomics 11, 625. doi:10.1186/1471-2164-11-625.

Prévost, K., Salvail, H., Desnoyers, G., Jacques, J.-F., Phaneuf, E., Massé, E., 2007. The small RNA RyhB activates the translation of *shiA* mRNA encoding a permease of shikimate, a compound involved in siderophore synthesis. Mol. Microbiol. 64, 1260–1273. doi:10.1111/j.1365-2958.2007.05733.x.

Rabhi, M., Espéli, O., Schwartz, A., Cayrol, B., Rahmouni, A.R., Arluison, V., Boudvillain, M., 2011. The Sm-like RNA chaperone Hfq mediates transcription antitermination at Rho-dependent terminators: Hfq-mediated transcription antitermination. EMBO J. 30, 2805–2816. doi:10.1038/emboj.2011.192.

Ramírez-Nuñez, J., Romero-Medrano, R., Nevárez-Moorillón, G.V., Gutiérrez-Méndez, N., 2011. Effect of pH and salt gradient on the autolysis of *Lactococcus lactis* strains. Braz. J. Microbiol. 42, 1495–1499. doi:10.1590/S1517-838220110004000036.

Ramos, C.G., Grilo, A.M., Sousa, S.A., Feliciano, J.R., da Costa, P.J.P., Leitão, J.H., 2014. Regulation of Hfq mRNA and protein levels in *Escherichia coli* and *Pseudomonas aeruginosa* by the *Burkholderia cenocepacia* MtvR sRNA. PLoS One 9, e98813. doi:10.1371/journal.pone.0098813.

Ravagnani, A., Jennert, K.C., Steiner, E., Grünberg, R., Jefferies, J.R., Wilkinson, S.R., Young, D.I., Tidswell, E.C., Brown, D.P., Youngman, P., Morris, J.G., Young, M., 2000. Spo0A directly controls the switch from acid to solvent production in solvent-forming clostridia. Mol. Microbiol. 37, 1172–1185.

Ren, C., Gu, Y., Wu, Y., Zhang, W., Yang, C., Yang, S., Jiang, W., 2012. Pleiotropic functions of catabolite control protein CcpA in butanol-producing *Clostridium acetobutylicum*. BMC Genomics 13, 349. doi:10.1186/1471-2164-13-349.

Reysenbach, A.L., Ravenscroft, N., Long, S., Jones, D.T., Woods, D.R., 1986. Characterization, biosynthesis, and regulation of granulose in *Clostridium acetobutylicum*. Appl. Environ. Microbiol. 52, 185–190.

Rice, R.W., Sanyal, A.K., Elrod, A.C., Bata, R.M., 1991. Exhaust gas emissions of butanol, ethanol, and methanol-gasoline blends. J. Eng. Gas Turbines Power 113, 377. doi:10.1115/1.2906241.

Robinson, K.E., Orans, J., Kovach, A.R., Link, T.M., Brennan, R.G., 2014. Mapping Hfq-RNA interaction surfaces using tryptophan fluorescence quenching. Nucleic Acids Res. 42, 2736–2749. doi:10.1093/nar/gkt1171.

Robson, R.L., Robson, R.M., Morris, J.G., 1974. The biosynthesis of granulose by *Clostridium pasteurianum*. Biochem. J. 144, 503–511.

Rose, A.H., 1961. Industrial Microbiology. Butterworths, London, UK.

Ross, D., 1961. The acetone-butanol fermentation. Prog. Ind. Microbiol. 3, 71–90.

Ross, J.A., Ellis, M.J., Hossain, S., Haniford, D.B., 2013. Hfq restructures RNA-IN and RNA-OUT and facilitates antisense pairing in the Tn10/IS10 system. RNA 19, 670–684. doi:10.1261/rna.037747.112.

Sabathé, F., Croux, C., Cornillot, E., Soucaille, P., 2002. *amyP*, a reporter gene to study strain degeneration in *Clostridium acetobutylicum* ATCC 824. FEMS Microbiol. Lett. 210, 93–98.

Sagawa, S., Shin, J.-E., Hussein, R., Lim, H.N., 2015. Paradoxical suppression of small RNA activity at high Hfq concentrations due to random-order binding. Nucleic Acids Res. 43, 8502–8515. doi:10.1093/nar/gkv777.

Saramago, M., Bárria, C., dos Santos, R.F., Silva, I.J., Pobre, V., Domingues, S., Andrade, J.M., Viegas, S.C., Arraiano, C.M., 2014. The role of RNases in the regulation of small RNAs. Curr. Opin. Microbiol. 18, 105–115. doi:10.1016/j.mib.2014.02.009.

Sauer, E., Schmidt, S., Weichenrieder, O., 2012. Small RNA binding to the lateral surface of Hfq hexamers and structural rearrangements upon mRNA target recognition. Proc. Natl. Acad. Sci. USA 109, 9396–9401. doi:10.1073/pnas.1202521109.

Sauer, E., Weichenrieder, O., 2011. Structural basis for RNA 3'-end recognition by Hfq. Proc. Natl. Acad. Sci. USA 108, 13065–13070. doi:10.1073/pnas.1103420108.

Schiel, B., 2006. Regulation der Lösungsmittelbildung in *Clostridium acetobutylicum* durch DNA-bindende Proteine. Ph.D. thesis. Ulm University, Germany.

Schiel, B., Nold, N., Dürre, P., 2010. Identification of a small non-coding RNA in *Clostridium acetobutylicum*. Biospektrum Spec. Issue, GRV09, 135.

Schilling, D., Gerischer, U., 2009. The *Acinetobacter baylyi hfq* gene encodes a large protein with an unusual C terminus. J. Bacteriol. 191, 5553–5562. doi:10.1128/JB.00490-09.

Schmidt, W.M., Mueller, M.W., 1999. CapSelect: A highly sensitive method for 5’ CAP-dependent enrichment of full-length cDNA in PCR-mediated analysis of mRNAs. Nucleic Acids Res. 27, e31.

Sharma, C.M., Darfeuille, F., Plantinga, T.H., Vogel, J., 2007. A small RNA regulates multiple ABC transporter mRNAs by targeting C/A-rich elements inside and upstream of ribosome-binding sites. Genes Dev. 21, 2804–2817. doi:10.1101/gad.447207.

Sharma, C.M., Vogel, J., 2009. Experimental approaches for the discovery and characterization of regulatory small RNA. Curr. Opin. Microbiol. 12, 536–546. doi:10.1016/j.mib.2009.07.006.

Shimoni, Y., Friedlander, G., Hetzroni, G., Niv, G., Altuvia, S., Biham, O., Margalit, H., 2007. Regulation of gene expression by small non-coding RNAs: a quantitative view. Mol. Syst. Biol. 3, 138. doi:10.1038/msb4100181.

Sievers, F., Wilm, A., Dineen, D., Gibson, T.J., Karplus, K., Li, W., Lopez, R., McWilliam, H., Remmert, M., Soding, J., Thompson, J.D., Higgins, D.G., 2014. Fast, scalable generation of high-quality protein multiple sequence alignments using Clustal Omega. Mol. Syst. Biol. 7, 539. doi:10.1038/msb.2011.75.

Sillers, R., Al-Hinai, M.A., Papoutsakis, E.T., 2009. Aldehyde-alcohol dehydrogenase and/or thiolase overexpression coupled with CoA transferase downregulation lead to higher alcohol titers and selectivity in *Clostridium acetobutylicum* fermentations. Biotechnol. Bioeng. 102, 38–49. doi:10.1002/bit.22058.

Sittka, A., Lucchini, S., Papenfort, K., Sharma, C.M., Rolle, K., Binnewies, T.T., Hinton, J.C.D., Vogel, J., 2008. Deep sequencing analysis of small noncoding RNA and mRNA targets of the global post-transcriptional regulator, Hfq. PLoS Genet 4. doi:10.1371/journal.pgen.1000163.

Smith, C., Heyne, S., Richter, A.S., Will, S., Backofen, R., 2010. Freiburg RNA Tools: a web server integrating IntaRNA, ExpaRNA and LocaRNA. Nucleic Acids Res. 38, 373–377. doi:10.1093/nar/gkq316.

Smith, L.D., 1975. Common mesophilic anaerobes, including *Clostridium botulinum* and *Clostridium tetani*, in 21 soil specimens. Appl. Microbiol. 29, 590–594.

Snyder, L.R., Dolan, J.W., Kirkland, J.J., 2013. Introduction to modern liquid chromatography, 3rd ed. John Wiley & Sons, Inc, Hoboken, USA.

Sobrero, P., Valverde, C., 2012. The bacterial protein Hfq: much more than a mere RNA-binding factor. Crit. Rev. Microbiol. 38, 276–299. doi:10.3109/1040841X.2012.664540.

Sobrero, P., Valverde, C., 2011. Evidences of autoregulation of *hfq* expression in *Sinorhizobium meliloti* strain 2011. Arch. Microbiol. 193, 629–639. doi:10.1007/s00203-011-0701-1.

Sonnleitner, E., Moll, I., Bläsi, U., 2002. Functional replacement of the *Escherichia coli hfq* gene by the homologue of *Pseudomonas aeruginosa*. Microbiology 148, 883–891. doi:10.1099/00221287-148-3-883.

Sonnleitner, E., Napetschnig, J., Afonyushkin, T., Ecker, K., Vecerek, B., Moll, I., Kaberdin, V.R., Bläsi, U., 2004. Functional effects of variants of the RNA chaperone Hfq. Biochem. Biophys. Res. Commun. 323, 1017–1023. doi:10.1016/j.bbrc.2004.08.190.

Sonnleitner, E., Sorger-Domenigg, T., Madej, M.J., Findeiss, S., Hackermüller, J., Hüttenhofer, A., Stadler, P.F., Bläsi, U., Moll, I., 2008. Detection of small RNAs in *Pseudomonas aeruginosa* by RNomics and structure-based bioinformatic tools. Microbiology 154, 3175–3187. doi:10.1099/mic.0.2008/019703-0.

Soper, T., Mandin, P., Majdalani, N., Gottesman, S., Woodson, S.A., 2010. Positive regulation by small RNAs and the role of Hfq. Proc. Natl. Acad. Sci. USA 107, 9602–9607. doi:10.1073/pnas.1004435107.

Spivey, M.J., 1978. The acetone/butanol/ethanol fermentation. Process Biochem. 13, 2–5.

Sriram, G., Martinez, J.A., McCabe, E.R.B., Liao, J.C., Dipple, K.M., 2005. Single-gene disorders: what role could moonlighting enzymes play? Am. J. Hum. Genet. 76, 911–924. doi:10.1086/430799.

Srivastava, R.A., Schonfeld, G., 1991. Use of riboprobes for Northern blotting analysis. BioTechniques 11, 584-588.

Standfest, T., 2009. Untersuchung der Regulatorproteine CcpA, CodY und Hfq in *Clostridium acetobutylicum*. Diploma thesis. Ulm University, Germany.

Steiner, E., Dago, A.E., Young, D.I., Heap, J.T., Minton, N.P., Hoch, J.A., Young, M., 2011. Multiple orphan histidine kinases interact directly with Spo0A to control the initiation of endospore formation in *Clostridium acetobutylicum*. Mol. Microbiol. 80, 641–654. doi:10.1111/j.1365-2958.2011.07608.x.

Stork, M., Di Lorenzo, M., Welch, T.J., Crosa, J.H., 2007. Transcription termination within the iron transport-biosynthesis operon of *Vibrio anguillarum* requires an antisense RNA. J. Bacteriol. 189, 3479–3488. doi:10.1128/JB.00619-06.

Stougaard, P., Molin, S., Nordström, K., 1981. RNAs involved in copy-number control and incompatibility of plasmid R1. Proc. Natl. Acad. Sci. USA 78, 6008–6012.

Strauch, M.A., Webb, V., Spiegelman, G., Hoch, J.A., 1990. The Spo0A protein of *Bacillus subtilis* is a repressor of the *abrB* gene. Proc. Natl. Acad. Sci. USA 87, 1801–1805.

Strauch, M.A., Trach, K.A., Day, J., Hoch, J.A., 1992. Spo0A activates and represses its own synthesis by binding at its dual promoters. Biochimie 74, 619–626.

Stubben, C.J., Micheva-Viteva, S.N., Shou, Y., Buddenborg, S.K., Dunbar, J.M., Hong-Geller, E., 2014. Differential expression of small RNAs from *Burkholderia thailandensis* in response to varying environmental and stress conditions. BMC Genomics 15, 1–18. doi:10.1186/1471-2164-15-385.

Sun, X., Zhulin, I., Wartell, R.M., 2002. Predicted structure and phyletic distribution of the RNA-binding protein Hfq. Nucleic Acids Res. 30, 3662–3671.

Sutcliffe, S., 2014. Green Biologics funding story. http://www.rushlightevents.com/wp-content/uploads/2014/01/R-Show-14-FCC-Sean-Sutcliffe.pdf. 14th March 2017.

Tatusov, R.L., Koonin, E.V., Lipman, D.J., 1997. A genomic perspective on protein families. Science 278, 631–637.

Thormann, K., Feustel, L., Lorenz, K., Nakotte, S., Dürre, P., 2002. Control of butanol formation in *Clostridium acetobutylicum* by transcriptional activation. J. Bacteriol. 184, 1966–1973. doi:10.1128/JB.184.7.1966-1973.2002.

Thorn, G.J., King, J.R., Jabbari, S., 2013. pH-induced gene regulation of solvent production by *Clostridium acetobutylicum* in continuous culture: parameter estimation and sporulation modelling. Math. Biosci. 241, 149–166. doi:10.1016/j.mbs.2012.11.004.

Tomas, C.A., Alsaker, K.V., Bonarius, H.P.J., Hendriksen, W.T., Yang, H., Beamish, J.A., Paredes, C.J., Papoutsakis, E.T., 2003. DNA array-based transcriptional analysis of asporogenous, nonsolventogenic *Clostridium acetobutylicum* strains SKO1 and M5. J. Bacteriol. 185, 4539–4547.

Towbin, H., Staehelin, T., Gordon, J., 1979. Electrophoretic transfer of proteins from polyacrylamide gels to nitrocellulose sheets: Procedure and some applications. Proc. Natl. Acad. Sci. USA 76, 4350–4354.

Tracy, B.P., Jones, S.W., Papoutsakis, E.T., 2011. Inactivation of σ^E and σ^G in *Clostridium acetobutylicum* illuminates their roles in clostridial-cell-form biogenesis, granulose synthesis, solventogenesis, and spore morphogenesis. J. Bacteriol. 193, 1414–1426. doi:10.1128/JB.01380-10.

Tramonti, A., De Canio, M., De Biase, D., 2008. GadX/GadW-dependent regulation of the *Escherichia coli* acid fitness island: transcriptional control at the *gadY-gadW* divergent promoters and identification of four novel 42 bp GadX/GadW-specific binding sites. Mol. Microbiol. 70, 965-982. doi:10.1111/j.1365-2958.2008.06458.x.

Tran-Betcke, A., Behrens, B., Noyer-Weidner, M., Trautner, T.A., 1986. DNA methyltransferase genes of *Bacillus subtilis* phages: comparison of their nucleotide sequences. Gene 42, 89–96.

Tree, J.J., Granneman, S., McAteer, S.P., Tollervey, D., Gally, D.L., 2014. Identification of bacteriophage-encoded anti-sRNAs in pathogenic *Escherichia coli.* Mol. Cell 55, 199–213. doi:10.1016/j.molcel.2014.05.006.

Tsui, H.C., Leung, H.C., Winkler, M.E., 1994. Characterization of broadly pleiotropic phenotypes caused by an *hfq* insertion mutation in *Escherichia coli* K-12. Mol. Microbiol. 13, 35–49.

Tsui, H.C., Winkler, M.E., 1994. Transcriptional patterns of the *mutL-miaA* superoperon of *Escherichia coli* K-12 suggest a model for posttranscriptional regulation. Biochimie 76, 1168–1177.

Tsui, H.C., Mukherjee, D., Ray, V.A., Sham, L.-T., Feig, A.L., Winkler, M.E., 2010. Identification and characterization of noncoding small RNAs in *Streptococcus pneumoniae* serotype 2 strain D39. J. Bacteriol. 192, 264–279. doi:10.1128/JB.01204-09.

Udekwu, K.I., Darfeuille, F., Vogel, J., Reimegård, J., Holmqvist, E., Wagner, E.G.H., 2005. Hfq-dependent regulation of OmpA synthesis is mediated by an antisense RNA. Genes Dev. 19, 2355–2366. doi:10.1101/gad.354405.

Valentin-Hansen, P., Eriksen, M., Udesen, C., 2004. The bacterial Sm-like protein Hfq: a key player in RNA transactions. Mol. Microbiol. 51, 1525–1533.

Vanderpool, C.K., 2007. Physiological consequences of small RNA-mediated regulation of glucose-phosphate stress. Curr. Opin. Microbiol. 10, 146–151. doi:10.1016/j.mib.2007.03.011.

Vanderpool, C.K., Balasubramanian, D., Lloyd, C.R., 2011. Dual-function RNA regulators in bacteria. Biochimie 93, 1943–1949. doi:10.1016/j.biochi.2011.07.016.

Vanecko, S., Laskowski, M., 1961. Studies of the specificity of deoxyribonuclease I: hydrolysis of chains carrying a monoesterified phosphate on carbon 5'. J. Biol. Chem. 236, 3312–3316.

Vecerek, B., Moll, I., Bläsi, U., 2005. Translational autocontrol of the *Escherichia coli hfq* RNA chaperone gene. RNA 11, 976–984. doi:10.1261/rna.2360205

Vecerek, B., Moll, I., Bläsi, U., 2007. Control of Fur synthesis by the non-coding RNA RyhB and iron-responsive decoding. EMBO J. 26, 965–975. doi:10.1038/sj.emboj.7601553.

Venkataramanan, K.P., Jones, S.W., McCormick, K.P., Kunjeti, S.G., Ralston, M.T., Meyers, B.C., Papoutsakis, E.T., 2013. The *Clostridium* small RNome that responds to stress: the paradigm and importance of toxic metabolite stress in *C. acetobutylicum*. BMC Genomics 14, 849. doi:10.1186/1471-2164-14-849

Venkataramanan, K.P., Min, L., Hou, S., Jones, S.W., Ralston, M.T., Lee, K.H., Papoutsakis, E.T., 2015. Complex and extensive post-transcriptional regulation revealed by integrative proteomic and transcriptomic analysis of metabolite stress response in *Clostridium acetobutylicum*. Biotechnol. Biofuels 8, 81. doi:10.1186/s13068-015-0260-9.

Viegas, S.C., Pfeiffer, V., Sittka, A., Silva, I.J., Vogel, J., Arraiano, C.M., 2007. Characterization of the role of ribonucleases in *Salmonella* small RNA decay. Nucleic Acids Res. 35, 7651–7664. doi:10.1093/nar/gkm916.

Villarejo, M.R., Zabin, I., 1974. Beta-galactosidase from termination and deletion mutant strains. J. Bacteriol. 120, 466–474.

Vogel, J., Luisi, B.F., 2011. Hfq and its constellation of RNA. Nat. Rev. Microbiol. 9, 578–589. doi:10.1038/nrmicro2615.

Vogt, S.L., Raivio, T.L., 2014. Hfq reduces envelope stress by controlling expression of envelope-localized proteins and protein complexes in enteropathogenic *Escherichia coli*. Mol. Microbiol. 92, 681–697. doi:10.1111/mmi.12581.

Vrentas, C., Ghirlando, R., Keefer, A., Hu, Z., Tomczak, A., Gittis, A.G., Murthi, A., Garboczi, D.N., Gottesman, S., Leppla, S.H., 2015. Hfqs in *Bacillus anthracis*: role of protein sequence variation in the structure and function of proteins in the Hfq family. Protein Sci. 24, 1808–1819. doi:10.1002/pro.2773.

Wagner, E.G.H., Altuvia, S., Romby, P., 2002. Antisense RNAs in bacteria and their genetic elements. Adv. Genet. 46, 361–398.

Wagner, E.G.H., Vogel, J., 2003. Noncoding RNAs encoded by bacterial chromosomes, chap. 17, p. 242-258, in: Barciszewski, J., Erdmann, V.A. (Eds.), Non-coding RNAs: Molecular biology and molecular medicine. Landes Bioscience, Georgetown, USA.

Wallace, D.M., 1987. Precipitation of nucleic acids. Methods Enzymol. 152, 41–48.

Walter, K.A., Bennett, G.N., Papoutsakis, E.T., 1992. Molecular characterization of two *Clostridium acetobutylicum* ATCC 824 butanol dehydrogenase isozyme genes. J. Bacteriol. 174, 7149–7158.

Wang, J., Rennie, W., Liu, C., Carmack, C.S., Prévost, K., Caron, M.-P., Massé, E., Ding, Y., Wade, J.T., 2015. Identification of bacterial sRNA regulatory targets using ribosome profiling. Nucleic Acids Res. 43, 10308–10320. doi:10.1093/nar/gkv1158.

Wassarman, K.M., 2007. 6S RNA: a regulator of transcription. Mol. Microbiol. 65, 1425–1431. doi:10.1111/j.1365-2958.2007.05894.x.

Wassarman, K.M., Storz, G., 2000. 6S RNA regulates *E. coli* RNA polymerase activity. Cell 101, 613–623.

Waters, L.S., Storz, G., 2009. Regulatory RNAs in bacteria. Cell 136, 615–628. doi:10.1016/j.cell.2009.01.043.

Weiss, B., Jacquemin-Sablon, A., Live, T.R., Fareed, G.C., Richardson, C.C., 1968. Enzymatic breakage and joining of deoxyribonucleic acid. J. Biol. Chem. 243, 4543–4555.

Wiesenborn, D.P., Rudolph, F.B., Papoutsakis, E.T., 1988. Thiolase from *Clostridium acetobutylicum* ATCC 824 and its role in the synthesis of acids and solvents. Appl. Environ. Microbiol. 54, 2717–2722.

Wietzke, M., Bahl, H., 2012. The redox-sensing protein Rex, a transcriptional regulator of solventogenesis in *Clostridium acetobutylicum*. Appl. Microbiol. Biotechnol. 96, 749–761. doi:10.1007/s00253-012-4112-2.

Wilms, I., Möller, P., Stock, A.M., Gurski, R., Lai, E.M., Narberhaus, F., 2012. Hfq influences multiple transport systems and virulence in the plant pathogen *Agrobacterium tumefaciens*. J. Bacteriol. 194, 5209–5217. doi:10.1128/JB.00510-12.

Wilusz, C.J., Wilusz, J., 2005. Eukaryotic Lsm proteins: lessons from bacteria. Nat. Struct. Mol. Biol. 12, 1031–1036. doi:10.1038/nsmb1037.

Winzer, K., Lorenz, K., Zickner, B., Dürre, P., 2000. Differential regulation of two thiolase genes from *Clostridium acetobutylicum* DSM 792. J. Mol. Microbiol. Biotechnol. 2, 531–541.

Yang, G., Wang, L., Wang, Y., Li, P., Zhu, J., Qiu, S., Hao, R., Wu, Z., Li, W., Song, H., 2015. Hfq regulates acid tolerance and virulence by responding to acid stress in *Shigella flexneri*. Res. Microbiol. 166, 476–485. doi:10.1016/j.resmic.2015.06.007.

Yang, S., Pelletier, D.A., Lu, T.Y.S., Brown, S.D., 2010. The *Zymomonas mobilis* regulator Hfq contributes to tolerance against multiple lignocellulosic pretreatment inhibitors. BMC Microbiol. 10, 135. doi:10.1186/1471-2180-10-135

Yoo, M., Croux, C., Meynial-Salles, I., Soucaille, P., 2016. Elucidation of the roles of *adhE1* and *adhE2* in the primary metabolism of *Clostridium acetobutylicum* by combining in-frame gene deletion and a quantitative system-scale approach. Biotechnol. Biofuels 9, 92. doi:10.1186/s13068-016-0507-0.

Yutin, N., Galperin, M.Y., 2013. A genomic update on clostridial phylogeny: Gram-negative spore formers and other misplaced clostridia: Genomics update. Environ. Microbiol. 15, 2631-2641. doi:10.1111/1462-2920.12173.

Zhang, L., Nie, X., Ravcheev, D.A., Rodionov, D.A., Sheng, J., Gu, Y., Yang, S., Jiang, W., Yang, C., 2014. Redox-responsive repressor Rex modulates alcohol production and oxidative stress tolerance in *Clostridium acetobutylicum*. J. Bacteriol. 196, 3949–3963. doi:10.1128/JB.02037-14.

Zimmermann, T., 2013. Untersuchungen zur Butanolbildung von *Hyperthermus butylicus* und *Clostridium acetobutylicum*. Ph.D. thesis. Ulm University, Germany.

Zuker, M., 2003. Mfold web server for nucleic acid folding and hybridization prediction. Nucleic Acids Res. 31, 3406–3415.

Zverlov, V.V., Berezina, O., Velikodvorskaya, G.A., Schwarz, W.H., 2006. Bacterial acetone and butanol production by industrial fermentation in the Soviet Union: use of hydrolyzed agricultural waste for biorefinery. Appl. Microbiol. Biotechnol. 71, 587–597. doi:10.1007/s00253-006-0445-z.

8 Supplement

A

*Nde*I
CATATGTATATCATCATCTGTTTTCCATCACTTTCAAGTATTACCGTAAAACTATCAAATCCCTTAACACTACCTCTCATCTGA

AATCCATTTGTCAAATGAATTGCAACAGGTATCTTATTCTTTCTCGCACTATTTAAAAATATATCCTGCAAATTATTTGTTGAC

start codon *hfq* terminator *hfq* *Sca*I
TTGTTATTCATGATACTCACCCTCCGTTTATTTTACATAGTATAAGAAAAGTAGGCAAGTTTTTTTATTGCCTAGTACT

B

*Nde*I
CATATGTATATCATCATCTGTTTTCCATCACTTTCAAGTATTACCGTAAAACTATCAAATCCCTTAACACTACCTCTCATCTGA

AATCCATTTGTCAAATGAATTGCAACAGGTATCTTATTCTTTCTCGCACTATTTAAAAATATATCCTGCAAATTATTTGTTGAC

start codon *hfq* terminator *hfq*
TTGTTATTCATGATACTCACCCTCCGTTTATTTTACATAGTATAAGAAAAGTAGGCAAGTTTTTTTATTGCCTGATCCTTAAAT

-35 -10
GCGATTAAGCTTGGCTGCAGGTCGACGTCAAAATTAAGATATAGCTTCTTTTATGTAGTATTATTTCAGAAGTCTACAAATTAA

solB
GTTTATATTTAGACCCTGGGGTGTAACTATAGTATTTAATATTGGTACTATTAATTAGGGTTATATATACTAGAACTTATCATG

GTAAACATAAATATAAACTCAATTCTATTTATGCTCCTATAAAATTTTATAATATAGGAAAACTGCTAAATGTAAATTATACGT

*Sca*I
TTACATTTAGCAGTTTATTTTAAACCTTCATGAGTACT

Figure 8.1: Detailed sequence information of as_hfq (A) and as_hfq_solB (B). Restriction sites for cloning into the respective vector are underlined. Start codon of *hfq* is indicated by a dotted box and terminator structure is coded in grey. Promoter structure of *solB* is tagged with dotted lines and the sequence of *solB* is doubly underlined.

A

*Hind*III promoter sequence of *E. coli hfq*
AAGCTTGGTTCACTGGCTTGACAGTGAAAAACCAGAACAGGCGCGTGACGAAGTATTACAGGTTGTTGGTGCTATCGCAGGCTG

AATGTGTACAATTGAGACGTATCGTGCGCAATTTTTTCAGAATCGAAAGGTTCAAAGTACAAATAAGCATATAAGGAAAAGAGA

coding sequence of *E. coli hfq*
GAATGGCTAAGGGGCAATCTTTACAAGATCCGTTCCTGAACGCACTGCGTCGGGAACGTGTTCCAGTTTCTATTTATTTGGTGA

ATGGTATTAAGCTGCAAGGGCAAATCGAGTCTTTTGATCAGTTCGTGATCCTGTTGAAAAACACGGTCAGCCAGATGGTTTACA

AGCACGCGATTTCTACTGTTGTCCCGTCTCGCCCGGTTTCTCATCACAGTAACAACGCCGGTGGCGGTACCAGCAGTAACTACC

ATCATGGTAGCAGCGCGCAGAATACTTCCGCGCAACAGGACAGCGAAGAAACCGAATAAGGTTTCGGGCTGTTTTTTTACACGG

*Eag*I
GGCGGCCG

B

*Hind*III promoter sequence of *E. coli hfq*
AAGCTTGGTTCACTGGCTTGACAGTGAAAAACCAGAACAGGCGCGTGACGAAGTATTACAGGTTGTTGGTGCTATCGCAGGCTG

AATGTGTACAATTGAGACGTATCGTGCGCAATTTTTTCAGAATCGAAAGGTTCAAAGTACAAATAAGCATATAAGGAAAAGAGA

coding sequence of *C. acetobutylicum hfq*
GAATGAATAACAAGTCAACAAATAATTTGCAGGATATATTTTTAAATAGTGCGAGAAAGAATAAGATACCTGTTGCAATTCATT

TGACAAATGGATTTCAGATGAGAGGTAGTGTTAAGGGATTTGATAGTTTTACGGTAATACTTGAAAGTGATGGAAAACAGATGA

TGATATATAAACATGCTGTATCCACCATAACTCCTTTAAGACCGATACTATTTAACCAGCCTCAGCAGGATGAAGAATAAATTA

*Eag*I
TAAGAAAAGTAGGCAAGTTTTTTTATTGCCTCTTTTTTCGGCCG

C

*Hind*III promoter sequence of *E. coli hfq*
AAGCTTGGTTCACTGGCTTGACAGTGAAAAACCAGAACAGGCGCGTGACGAAGTATTACAGGTTGTTGGTGCTATCGCAGGCTG

AATGTGTACAATTGAGACGTATCGTGCGCAATTTTTTCAGAATCGAAAGGTTCAAAGTACAAATAAGCATATAAGGAAAAGAGA

*Eag*I
GACGGCCG

Figure 8.2: Detailed sequence information of hfq_ec (A), hfq_cac (B), and pKon (C). Restriction sites for cloning into respective vector are underlined. Promoter sequences are underlined with dotted lines and codon sequence of respective *hfq*s are doubly underlined.

Table 8.1: Results of distinct genes reporting the differential expression in *C. acetobutylicum* [pIMP1_solB] compared to the *C. acetobutylicum* wild type in stationary growth phase.

Locus tag	Gene product description[a]	Log_2(fold change)
CA_C0213	LysM domain-containing protein	4.61
CA_C0383	PTS system cellobiose-specific transporter subunit IIA	5.41
CA_C0384	PTS system cellobiose-specific transporter subunit IIB	4.16
CA_C1695	sporulation sigma factor SigE	2.61
CA_C2237	ADP-glucose pyrophosphorylase	1.63
CA_C2240	glucanotransferase	1.76
CA_C1201	hypothetical protein	-7.41
CA_C1696	sporulation sigma factor SigG	-8.68
CA_C2964	PTS system lactose-specific transporter subunit IIBC	-6.10
CA_C2965	PTS system lactose-specific transporter subunit IIA	-6.75
CA_C2966	lactose phosphotransferase system repressor lacR	-6.93
CA_C3482	permease	-8.31

[a] description based on NCBI database

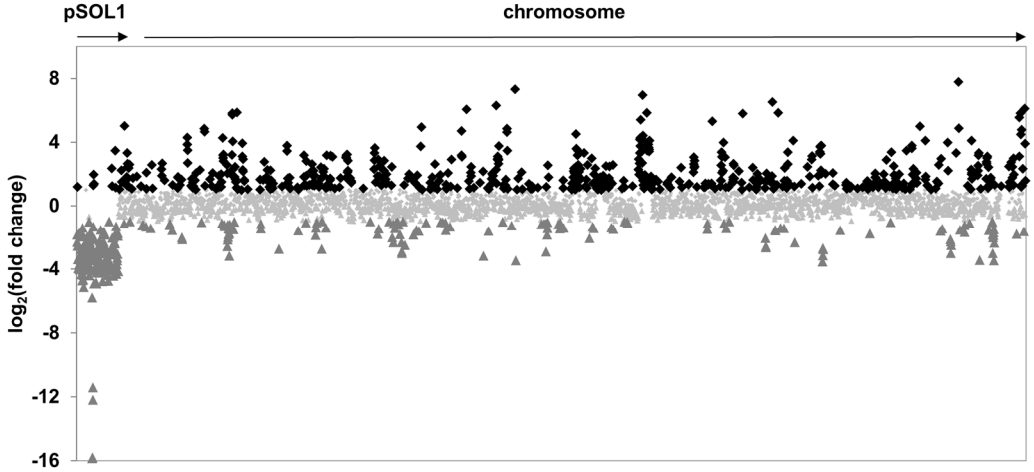

Figure 8.3: Effects of *solB* overexpression on RNA transcriptome level in *C. acetobutylicum* [pIMP1_solB]. Distribution of up- (black) and down-regulated (grey) genes across the megaplasmid pSOL1 and the genome of *C. acetobutylicum* [pIMP1_solB] compared to the *C. acetobutylicum* wild type in exponential growth phase. Faint dots are not regarded as differentially expressed.

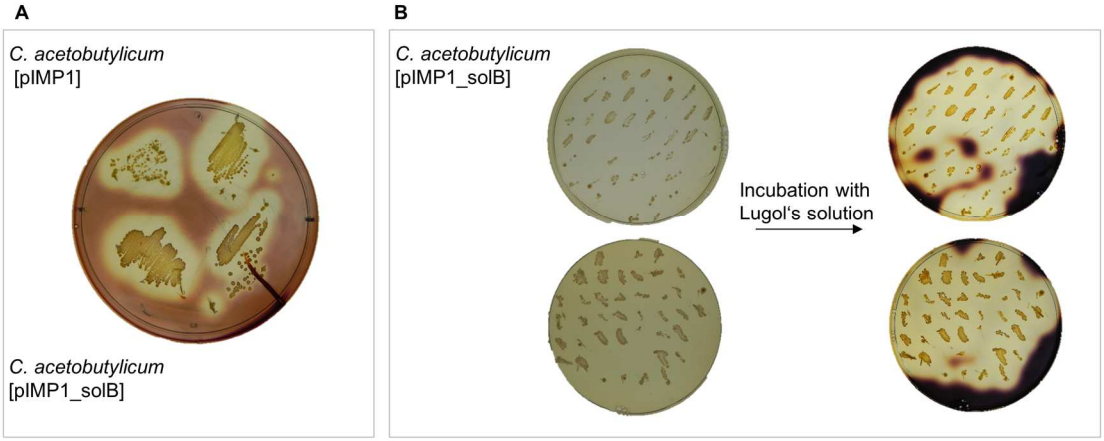

Figure 8.4: (A) Starch agar plates with *C. acetobutylicum* [pIMP1] and *C. acetobutylicum* [pIMP1_solB] were stained with Lugol's solution. (B) Single colonies of *C. acetobutylicum* [pIMP1_solB] were streaked on starch agar plates after transformation. Starch agar plates were stained with Lugol's solution.

Table 8.2: Results of mapped sequences of sequenced RNA from *C. acetobutylicum* [pIMP1_solB], *C. acetobutylicum* Δ*spo0A*, and *C. acetobutylicum* wild type.

C. acetobutylicum	Growth phase	Mapped unique SAM	After RNA removel	Trimmomatic	Total
wild type	exponential	15,292,446	17,687,213	17,974,499	18,532,029
wild type	exponential	18,250,708	19,810,604	20,095,525	20,625,147
wild type	exponential	18,768,055	19,449,165	19,542,559	20,070,680
wild type	stationary	14,915,207	15,956,474	16,474,796	17,100,288
wild type	stationary	2,629,527	12,340,332	18,460,461	18,924,802
wild type	stationary	2,419,819	12,997,652	20,466,650	21,194,826
[pIMP1_solB]	exponential	12,527,060	13,832,768	14,450,706	15,124,408
[pIMP1_solB]	exponential	14,064,293	15,831,417	16,465,894	16,701,686
[pIMP1_solB]	exponential	12,160,786	13,167,940	13,214,568	13,781,378
[pIMP1_solB]	stationary	10,230,012	11,345,225	11,684,966	12,064,516
[pIMP1_solB]	stationary	10,323,640	11,468,967	12,006,667	12,383,068
[pIMP1_solB]	stationary	10,446,717	11,544,130	11,868,951	12,178,578
Δspo0A	exponential	13,237,573	13,979,364	14,216,129	14,445,924
Δspo0A	exponential	9,622,207	10,161,568	10,351,476	10,499,048
Δspo0A	exponential	9,746,065	10,585,680	10,835,887	11,834,338
Δspo0A	stationary	11,702,227	12,367,568	12,669,707	13,067,610
Δspo0A	stationary	13,064,159	13,754,123	14,021,239	14,317,942
Δspo0A	stationary	12,824,950	13,407,049	13,631,645	13,907,754

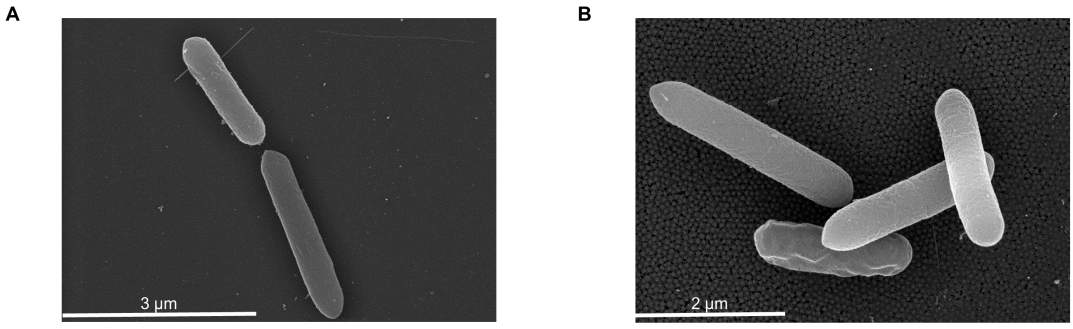

Figure 8.5: Scanning electron microscopy image of of *C. acetobutylicum* wild type (A, scale bar representing 3 µm) and *C. acetobutylicum* [pIMP1_solB] (B, scale bar representing 2 µm) cells growing in clostridial growth medium in stationary growth phase.

*Sfo*I promoter sequence of *ptb-buk*

GGCGCCGCAGGAGGCATAATATCAGCGGCTGTGGATGGAGTTAAGTCAGCAGAAAGTATAATGAGAAAATATAAAATATAAATA

ATTTTCTAAAAAACTTAACTTCATGTGAAAAGTTTGTTAAAATATAAATGAGCACGTTAATCATTTAACATAGATAATTAAATA

coding sequence of *hfq*

GTAAAAGGGAGTGTACGACCAATGAATAACAAGTCAACAAATAATTTGCAGGATATATTTTTAAATAGTGCGAGAAAGAATAAG

ATACCTGTTGCAATTCATTTGACAAATGGATTTCAGATGAGAGGTAGTGTTAAGGGATTTGATAGTTTTACGGTAATACTTGAA

AGTGATGGAAAACAGATGATGATATATAAACATGCTGTATCCACCATAACTCCTTTAAGACCGATACTATTTAACCAGCCTCAG

CAGGATGAAGAATAAATTATAAGAAAAGTAGGCAAGTTTTTTTATTGCCTCTTTTTTGAGTGTGTAATTAAATAAACTCAGGAG

*Sfo*I

GATTACAAGATTTATGCTGGCGCC

Figure 8.6: Detailed sequence information of ptb_hfq. *Sfo*I restriction sites for cloning into the respective vector are underlined. The *ptb-buk* promoter sequences is underlined with dotted lines and codon sequence of *hfq* is doubly underlined.

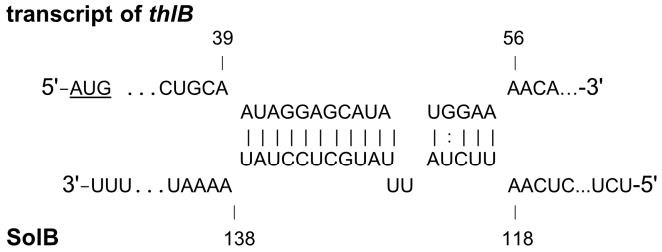

Figure 8.7: Possible interaction sites between the transcript of *thlB* and SolB predicted by IntaRNA and TargetRNA2. Numbers indicate the position from the transcriptional start point of SolB or the position after the start codon (underlined) of the *thlB* transcript. The energy for the binding was calculated with -9.78 kcal/mol.

Table 8.3: Results of mapped sequences on the chromosome (length: 3,940,880 bps) and on the plasmids pIMP1 (length: 4,696 bps) and pIMP1_solB (length: 4941 bps) of sequenced gDNA from *C. acetobutylicum* [pIMP1_solB] and *C. acetobutylicum* [pIMP1].

C. acetobutylicum	Mapped bases on chromsome	Mapped bases on plasmid	Coverage chromosome	Coverage plasmid	Coverage plasmid/ chromsome
[pIMP1_solB]	594,929,078	302,808,678	150.96	61284.90	405.98
[pIMP1_solB]	417,612,033	99,995,024	105.97	20237.81	190.98
[pIMP1_solB]	424,743,054	120,483,649	107.78	24384.47	226.24
[pIMP1]	267,276,444	182,418,351	67.82	38845.48	572.77
[pIMP1]	278,743,520	213,609,809	70.73	45487.61	643.11
[pIMP1]	270,472,639	231,549,975	68.63	49307.92	718.46

9 Acknowledgement

Aus Gründen des Datenschutzes wurde die Danksagung auf den Seiten 152 und 153 entfernt.

10 Curriculum vitae

Aus Gründen des Datenschutzes wurde der Curriculum vitae auf den Seiten 154 und 155 entfernt.

11 Statement

I declare that the present thesis is the result of my own work and that all sources of information and support used for its achievement have been mentioned in the text and in the references. All citations are explicitly identified, all figures contain only the original data and no figure was edited in a way that substantially modified its content. All existing copies of the present thesis are identical regarding their form and content.

Ulm, March 27th, 2017 _____

Elena Riester